



NOVEL ZINC(II) AND CADMIUM(II) COORDINATION POLYMERS
CONTAINING AROMATIC DICARBOXYLATE BRIDGING LIGANDS
AND THEIR APPLICATIONS IN CATALYSIS AND
PHOTOLUMINESCENCE

BY

MISS MATIMON SANGSAWANG

A THESIS SUBMITTED IN PARTIAL FULFILLMENT OF THE REQUIREMENTS
FOR THE DEGREE OF MASTER OF SCIENCE (CHEMISTRY)

DEPARTMENT OF CHEMISTRY
FACULTY OF SCIENCE AND TECHNOLOGY
THAMMASAT UNIVERSITY
ACADEMIC YEAR 2017

COPYRIGHT OF THAMMASAT UNIVERSITY

NOVEL ZINC(II) AND CADMIUM(II) COORDINATION POLYMERS
CONTAINING AROMATIC DICARBOXYLATE BRIDGING LIGANDS
AND THEIR APPLICATIONS IN CATALYSIS AND
PHOTOLUMINESCENCE

BY

MISS MATIMON SANGSAWANG



A THESIS SUBMITTED IN PARTIAL FULFILLMENT OF THE REQUIREMENTS
FOR THE DEGREE OF MASTER OF SCIENCE (CHEMISTRY)

DEPARTMENT OF CHEMISTRY
FACULTY OF SCIENCE AND TECHNOLOGY
THAMMASAT UNIVERSITY
ACADEMIC YEAR 2017

COPYRIGHT OF THAMMASAT UNIVERSITY

THAMMASAT UNIVERSITY
FACULTY OF SCIENCE AND TECHNOLOGY

THESIS

BY

MISS MATIMON SANGSAWANG

ENTITLED

NOVEL ZINC(II) AND CADMIUM(II) COORDINATION POLYMERS CONTAINING AROMATIC
DICARBOXYLATE BRIDGING LIGANDS AND THEIR APPLICATIONS IN CATALYSIS AND
PHOTOLUMINESCENCE

was approved as partial fulfillment of the requirements for
the degree of master of science (chemistry)

on May 7, 2018

Chairman



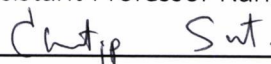
(Assistant Professor Kittipong Chainok, Ph.D.)

Member and Advisor



(Assistant Professor Nanthawat Wannarit, Ph.D.)

Member and Co-advisor



(Assistant Professor Chantip Samart, D.Eng.)

Member



(Assistant Professor Saowanit Saithong, Ph.D.)

Dean



(Associate Professor Somchai Chakhatrakan, Ph.D.)

Thesis Title	NOVEL ZINC(II) AND CADMIUM(II) COORDINATION POLYMERS CONTAINING AROMATIC DICARBOXYLATE BRIDGING LIGANDS AND THEIR APPLICATIONS IN CATALYSIS AND PHOTOLUMINESCENCE
Author	Miss Matimon Sangsawang
Degree	Master of Science (Chemistry)
Department/Faculty/University	Chemistry Faculty of Science and Technology Thammasat University
Thesis Advisor	Assistant Professor Dr. Nanthawat Wannarit
Thesis Co-Advisor	Assistant Professor Dr. Chantip Samart
Academic Year	2017

ABSTRACT

This thesis research concerns about design, synthesis, characterization and properties investigation on the novel zinc(II) and cadmium(II) coordination polymers (CPs) constructing from aromatic dicarboxylate ligands, pyridine-2,6-dicarboxylic acid (2,6-dipicH₂) and benzene-1,3-dicarboxylic acid (1,3-bdcH₂). Three novel CPs have been successfully synthesized, namely [Zn(2,6-dipic)]_n (**1**), {CdNa₂(1,3-bdc)₂(H₂O)₂(DMF)}_n (**2**) and {[Cd₂(1,3-bdc)₂(DMF)]·DMF·2H₂O}_n (**3**). The synthesized compounds have been characterized by using elemental analysis, Fourier transform infrared (FT-IR) spectroscopy, thermogravimetric analysis (TGA), scanning electron microscopy with energy dispersive X-ray spectroscopy (SEM/EDX), powder X-ray diffraction (PXRD) and single-crystal X-ray diffraction (SCXRD) techniques. The structure of compound (**1**) presents interesting 2D coordination network containing three crystallographic independent Zn(II) centers which linked by 2,6-dipic²⁻ ligand. The coordination network of this compound is stabilized by hydrogen bonding interactions between 2D layers. Thermal stability of this

(2)

compound is highly stable to about 450 °C. The catalytic activity of compound (1) for transesterification reaction of phenyl acetate and methanol was investigated by using the optimal reaction condition at 75 °C for 48 h. The result shows that the maximum yield of methyl acetate of 53.50 % was obtained. Moreover, this catalyst can be reused at least 2 cycles without any significant loss of catalytic activity. For compound (2), the crystal structure shows 3D heterobimetallic Cd(II)-Na(I) coordination framework constructing from 1,3-bdc²⁻ bridging ligand. This coordination framework is stabilized by $\pi\cdots\pi$ stacking and hydrogen bonding interactions. The thermal stability of this compound is also stable to 450 °C. Interestingly, the photoluminescence sensing properties of this compound exhibit selectivity for detection of acetone (LOD = 0.024 % v/v). Compound (3) was received from the same synthetic condition as compound (2) which totally different structure. The X-ray structure of compound (3) is 2D coordination network constructing from trinuclear Cd(II) SBUs linked by 1,3-bdc²⁻ ligands. The stabilization of the crystal lattice for this coordination polymer is enhanced by supramolecular interactions, namely hydrogen bonding and CH $\cdots\pi$ interaction between 2D layers.

Keywords: Zinc(II) and cadmium(II) coordination polymers, Aromatic dicarboxylate, Crystal structure, Catalysis, Photoluminescence properties

ACKNOWLEDGEMENTS

I would like to express my deepest and sincere thanks to my thesis advisor, Assistant Professor Dr. Nanthawat Wannarit for his kindness in invaluable guidance, suggestions, encouragement and supporting throughout this research. In addition, the author is also thankful to my thesis co-advisor, Assistant Professor Dr. Chanatip Samart for his beneficial guidance on catalytic study in this thesis. I would like to gratefully acknowledge Professor Dr. Sujitra Youngme, Department of Chemistry, Faculty of Science, Khon Kaen University for many helpful suggestions, chemicals and instrumental supports. I am also grateful to Assistant Professor Dr. Kittipong Chainok, Department of Materials and Textile technology, Faculty of Science and Technology, Thammasat University for his supporting on single-crystal X-ray determination and serving as chairman on this thesis examination. As well as, I am thankful to Assistant Professor Dr. Saowanit Saithong, Department of Chemistry, Faculty of Science, Prince of Songkhla University for serving as member on this thesis examination and also giving me helpful suggestions. I am thankful to Dr. Winya Dungaew, Department of Chemistry, Faculty of Science, Mahasarakham University for helping on powder X-ray diffraction collection. As well as, I also thankful to Dr. Filip Kielar, Department of Chemistry, Faculty of Science, Naresuan University for his supporting and suggesting on solid state photoluminescence investigation. As well as, I am grateful to the Teaching Assistantship (TA) scholarship, Faculty of Science and Technology, Thammasat University (2015). Finally, I am especially thankful to my beloved family for their tender love, entirely care and continuously supports throughout this research as well as to my friends in this research group for their helps during my master degree study.

Miss Matimon Sangsawang

TABLE OF CONTENTS

	Page
ABSTRACT	(1)
ACKNOWLEDGEMENTS	(3)
LIST OF TABLES	(8)
LIST OF FIGURES	(9)
LIST OF ABBREVIATIONS	(16)
CHAPTER 1 INTRODUCTION	1
1.1 Coordination polymers	1
1.2 Factors of the formation of coordination polymers	2
1.2.1 Influence of metal ions	3
1.2.2 Influence of ligands	5
1.2.3 Influence of metal-to-ligand ratio	6
1.2.4 Influence of solvent system	7
1.2.5 Influence of reaction temperature	8
1.2.6 Influence of pH	9
1.3 Carboxylate ligands	10
1.4 Application of Coordination polymers	16
1.4.1 Heterogeneous catalysis	16
1.4.2 Luminescence sensing	18
1.5 Objectives of this research	23
1.6 Scope of this research	23

1.7 Expected results	24
CHAPTER 2 REVIEW OF LITERATURE	25
2.1 One-dimensional Zn(II) and Cd(II) coordination polymers containing aromatic dicarboxylate derivatives	25
2.2 Two-dimensional Zn(II) and Cd(II) coordination polymers containing aromatic dicarboxylate derivatives	38
2.3 Three-dimensional Zn(II) and Cd(II) coordination polymers containing aromatic dicarboxylate derivatives	53
CHAPTER 3 RESEARCH METHODOLOGY	75
3.1 Materials	75
3.1.1 Chemicals	75
3.1.2 Glassware	76
3.1.3 Instrumentation	76
3.2 Method	77
3.2.1 Synthesis	78
3.2.2 Study of catalytic activity of $[\text{Zn}(\text{2,6-dipic})]_n$ (1)	79
3.2.2.1 Tranesterification of phenyl acetate with methanol	79
3.2.2.2 Reusability of catalyst	79
3.2.3 Study of photoluminescence properties of $\{\text{CdNa}_2(\text{1,3-bdc})_2(\text{H}_2\text{O})_2(\text{DMF})\}_n$ (2)	80
3.2.3.1 Solid state photoluminescence study	80
3.2.3.2 Solvent sensing study	80
CHAPTER 4 RESULTS AND DISCUSSION	81
4.1 A novel 2D coordination polymer $[\text{Zn}(\text{2,6-dipic})]_n$ (1)	81

4.1.1 Crystal structure determination	81
4.1.2 Structural description	82
4.1.3 Structural comparison	88
4.1.4 Infrared spectra	91
4.1.5 Powder X-ray diffraction patterns	93
4.1.6 Thermogravimetric analysis	94
4.1.7 Photoluminescence property	95
4.1.8 Catalytic activity	96
4.1.8.1 Effect of reaction temperature	96
4.1.8.2 Effect of reaction time	98
4.1.8.3 Reusability of catalyst	99
4.1.8.4 Possibility of mechanism	101
4.2 A novel 3D coordination polymer $\{CdNa_2(1,3-bdc)_2(H_2O)_2(DMF)\}_n$ (2)	103
4.2.1 Crystal structure determination	103
4.2.2 Structural description	103
4.2.3 Structural comparison	110
4.2.4 Infrared spectra	116
4.2.5 Powder X-ray diffraction patterns	117
4.2.6 Thermogravimetric analysis	118
4.2.7 Scanning electron microscope/Energy-dispersive X-ray spectroscopy	119
4.2.8 Sensing properties	120
4.2.8.1 Solid-state photoluminescence properties	120
4.2.8.2 The photoluminescent sensing for various small organic solvent	122
4.2.8.3 Sensing sensitivity study for acetone	123
4.2.8.4 Sensing selectivity study for acetone	126
4.2.9 Crystal structure of $\{[Cd_2(1,3-bdc)_2(DMF)] \cdot DMF \cdot 2H_2O\}_n$ (3)	127
4.2.9.1 Crystal structure determination	127

4.2.9.2 Structural description	127
4.2.9.3 Structural comparison	132
CHAPTER 5 CONCLUSIONS AND RECOMMENDATIONS	135
5.1 Conclusions	135
5.1.1 A novel 2D coordination polymer $[\text{Zn}(2,6\text{-dipic})]_n$ (1)	135
5.1.2 A novel 3D coordination polymer $\{\text{CdNa}_2(1,3\text{-bdc})_2(\text{H}_2\text{O})_2(\text{DMF})\}_n$ (2)	136
5.2 Recommendations	137
5.2.1 The properties studies of a novel 2D coordination polymer $[\text{Zn}(2,6\text{-dipic})]_n$ (1)	137
5.2.2 The properties studies of a novel 3D coordination polymer $\{\text{CdNa}_2(1,3\text{-bdc})_2(\text{H}_2\text{O})_2(\text{DMF})\}_n$ (2)	137
REFERENCES	139
APPENDICES	152
APPENDIX A THE CATALYTIC STUDY	153
APPENDIX B THE SOLVENT SENSING STUDY	155
APPENDIX C PUBLICATION	160
BIOGRAPHY	165

LIST OF TABLES

Tables	Page
2.1 Summary of previous studies of 1D Zn(II) and Cd(II) coordination polymers containing aromatic dicarboxylate derivatives	63
2.2 Summary of previous studies of 2D Zn(II) and Cd(II) coordination polymers containing aromatic dicarboxylate derivatives CPs	67
2.3 Summary of previous studies of 3D Zn(II) and Cd(II) coordination polymers containing aromatic dicarboxylate derivatives CPs	72
3.1 Chemicals and reagents	75
3.2 Glassware	76
4.1 Crystallographic and refinement data for $[\text{Zn}(2,6\text{-dipic})]_n$ (1)	86
4.2 Selected bond lengths (Å) and angles (°) for $[\text{Zn}(2,6\text{-dipic})]_n$ (1)	87
4.3 Comparison of activities of Zn(II) CPs as catalyst for transesterification reaction of Phenyl acetate and methanol	102
4.4 Crystallographic and refinement data for $\{\text{CdNa}_2(1,3\text{-bdc})_2(\text{H}_2\text{O})_2(\text{DMF})\}_n$ (2)	107
4.5 Selected bond lengths (Å) and angles (°) for $\{\text{CdNa}_2(1,3\text{-bdc})_2(\text{H}_2\text{O})_2(\text{DMF})\}_n$ (2)	108
4.6 Hydrogen bond geometry (Å, °) for $\{\text{CdNa}_2(1,3\text{-bdc})_2(\text{H}_2\text{O})_2(\text{DMF})\}_n$ (2)	109
4.7 Crystallographic and refinement data for $\{[\text{Cd}_2(1,3\text{-bdc})_2(\text{DMF})]\cdot\text{DMF}\cdot 2\text{H}_2\text{O}\}_n$ (3)	130
4.8 Selected bond lengths (Å) and angles (°) for $\{[\text{Cd}_2(1,3\text{-bdc})_2(\text{DMF})]\cdot\text{DMF}\cdot 2\text{H}_2\text{O}\}_n$ (3)	131
4.9 Hydrogen bond geometry (Å, °) for $\{[\text{Cd}_2(1,3\text{-bdc})_2(\text{DMF})]\cdot\text{DMF}\cdot 2\text{H}_2\text{O}\}_n$ (3)	132

LIST OF FIGURES

Figures	Page
1.1 Number of publications and citations per year from 1995-2012 for articles on the topics of “coordination polymers”	2
1.2 Coordination geometries of transition metal ions found in coordination polymers	4
1.3 The example study of influent of metal ions	4
1.4 The example study of influent of ligands	6
1.5 (a) Packing structures of (I-7) and (b) (I-8)	7
1.6 The example study of influent of solvent	8
1.7 Crystal structure of (a) compound (I-12) and (b) compound (I-13)	9
1.8 Crystal structure of (a) compound (I-14) and (b) compound (I-15)	10
1.9 (a) 3D herringbone like structure of (I-16), (b) waved layer and simplified models applied in the topological analysis of (I-18), (c) planar 2D (4,4) network of (I-19) and (d) Molecular structure of three isomer of bdCH_2	14
1.10 (a) Schematic views of compound (I-20) – (I-27) synthesized from different ligands and (b) molecular structure of three isomer of bdCH_2	15
1.11 (a) Unsaturated metal ions and (b) functionalized linkers as catalytic sites	18
1.12 Jablonski diagram displaying schematically the electronic states of the organic linker involved in luminescence phenomena	19
1.13 Packing structure of (I-31) and (b) relative emission intensities of (I-31) observed in different solvents	20
1.14 (a) 2D structure of (I-32), (b) 3D structure of (I-33), (c) Quenching efficiencies of 2.0 % v/v of different organics on the emissions of (I-32) and (d) (I-33)	21

1.15 (a) 3D structure of (I-34) , (b) 3D structure of (I-35) , (c) Quenching efficiency variation of (I-34) and (d) (I-35) dispersed in CH ₃ CN via addition of 2.0 % v/v different organic molecules	22
2.1 (a) Coordination environment of Zn(II) ion and (b) 1D helical chain-like structure of II-1	26
2.2 (a) Coordination environment of Zn(II) ion and (b) 1D zigzag chain-like structure of II-2	27
2.3 (a) The dinuclear unit and (b) 1D chain structure of II-3 extending along the [001] direction. H atoms have been omitted for clarity	27
2.4 (a) Molecular structure of L ¹ , (b) Coordination environment of Zn(II) ion and (c) 1D double chain structure of II-4	28
2.5 (a) Molecular structures of ligands, (b) 1D chain structure with hydrogen bonding to form 2D supramolecular network of II-5 and (c) view of left- and right-handed helical chains of II-6	30
2.6 (a) Molecular structures of L ² and L ³ , (b) 1D double-looped chain of II-7 , (c) 1D chain with loops of II-8 and (d) 1D ladder chains of II-9	31
2.7 (a) Coordination environment around Cd1 and Cd2 and (b) the crystal packing diagram of II-10	33
2.8 (a) Fragment of the zigzag chain in II-11 and (b) fragment of the linear chain in II-12	34
2.9 (a) 1D chain structure of II-13 and (b) 1D chain structure of II-14	35
2.10 (a) Molecular structure of pyim ₂ , (b) 1D chain structure of II-15 showing the dimeric 18-membered macrocycle and (c) 1D chain structure of II-16 with a pendant pyim ₂ ligand	36
2.11 (a) Molecular structure of 4-pyao, (b) fragment of 1D chain structure of II-17 and (c) fragment of 1D chain structure of II-18	37
2.12 (a) Molecular structures of 2,6-dipicOH ₂ , bix, bbi and 4,4'-bpy, (b) 2D brick-wall-like framework of II-19 , (c) 2D herringbone architecture of II-20 and (d) 2D herringbone architecture of II-21	39

- 2.13 (a) 1D chain running along the *c* axis based on 2,6-dipic and Cd ions and (b) 2D infinite layer framework extended in the *bc* plane of **II-22** 40
- 2.14 (a) 2D (4,4) net linked via carboxylate groups along the *c* axis and (b) excitation and emission spectra in the solid state of **II-23** (green) 41
- 2.15 (a) Molecular structure of BITMB, (b) 2D layer and (c) solid-state emission spectrum of **II-24** 42
- 2.16 (a) Molecular structures of L^1 and L^2 , (b) view of the 2D layer of **II-25**, (c) view of the 2D wave-like sheet structure of **II-26** and (d) view of the 2D sheet structure of **II-27** 44
- 2.17 (a) Molecular structures of bpp, 4,4'-bpy, 5-Br-1,3-bdcH₂ and 4-Br-1,3-bdcH₂, (b) view of the 2D layer of **II-28** and (c) view of the 2D layer of **II-29** 45
- 2.18 (a) Molecular structures of L^1 and L^2 , (b) view of the 2D hexagonal nets of **II-30**, (c) view of the 2D hexagonal nets of **II-31**, (d) pleated 2D net of **II-32** and (e) pleated 2D hexagonal net of **II-33** 47
- 2.19 (a) Molecular structures of btb, btp and bth ligands, (b) view of the undulated 2D (4,4) network of **II-34**, (c) view of the undulated 2D (4,4) network of **II-35** and (d) view of the undulated 2D (4,4) network of **II-36** 48
- 2.20 (a) Molecular structures of L^1 ligand, (b) polyhedral view of a single 2D coordination network along [101] plane and (c) solid state PL spectrum of **II-37** (red line) 49

2.21 (a) Molecular structure of pyim ₂ ligand, (b) 2D CP with herringbone pleated network in II-38 showing the 4-connected uninodal net, (c) 2D CP with perpendicular orientation 1D left-handed helix of pyim ₂ ligands (green color) and 1D zigzag chain of 1,4-bdc ²⁻ ligands (pink color) in II-39 and (d) solid state PL spectra of pyim ₂ , II-38 and II-39	51
2.22 (a) Molecular structure of 4-pyao ligand, (b) fragment of the (4,4)-coordination layer in II-40 and (c) solid state PL spectra of II-40 and II-41	52
2.23 (a) Molecular structures of bix and 2,6-dipicOH ₂ ligands, (b) packing of the adjacent framework along the <i>c</i> axis and (c) topological view of the two interpenetrating nets in II-42	53
2.24 (a) Molecular structure of BITMB ligand, (b) 3D porous framework and (c) solid state PL spectrum of II-43	54
2.25 (a) Molecular structure of L ³ ligand, (b) view of the 2-fold interpenetrating framework of II-44 , (c) view of the α -Po network of II-45 and (d) solid state PL spectra of II-44 and II-45	56
2.26 (a) Molecular structures of bpy, bpe and bpp ligands, (b) 2-fold interpenetrating diamond framework of II-46 , (c) 3-fold interpenetrating architecture of II-47 and (d) (3,4)-connected (4·8 ²) (4·8 ² ·10 ³) topology of II-48	57
2.27 (a) Molecular structure of L ² ligand and (b) 3D framework of II-49	58
2.28 (a) Molecular structure of TPOM ligand, (b) 3D framework of II-50 and (c) electric hysteresis loop of II-50 at room temperature	59
2.29 (a) Molecular structure of 4-OH-2,6-dipicH ₂ ligand, (b) 3D framework of II-51 and (c) solid state PL spectra of 4-OH-2,6-dipicH ₂ and II-51	60
2.30 (a) Molecular structures of H ₃ tea and H ₂ dea ligands, (b) 3D framework of II-52 and (c) 3D framework of II-53	62
4.1 View of asymmetric unit of (1) with the atom numbering scheme	82

4.2 Views of Zn(II) chromophores in (1), (a) [Zn(1)N ₂ O ₄], (b) [Zn(2)NO ₄] and (c) [Zn(3)O ₄]	83
4.3 Views of (a) 2D structure and (b) polyhedral displacement of Zn(II) centers of (1)	84
4.4 View of 3D supramolecular framework of (1) via C-H...O interaction between adjacent layers	85
4.5 (a) Coordination environment of Zn(II), (b) μ_3 -coordination mode of HCAM ligand and (c) packing structure of {[Zn(HCAM)]·H ₂ O} view along <i>c</i> axis	89
4.6 (a) Different coordination environments of the Sm ions, (b) μ_3 -coordination mode of 2,6-dipic and (c) packing structure of {[Sm ₂ (2,6-dipic)(ox) ₂ (H ₂ O) ₄]·4(H ₂ O)} _n view along <i>b</i> axis	90
4.7 IR spectra of (a) Zn(NO ₃) ₂ ·4H ₂ O, (b) 2,6-dipicH ₂ and (c) [Zn(2,6-dipic)] _n (1)	91
4.8 PXRD patterns of [Zn(2,6-dipic)] _n (1)	93
4.9 TGA curve of [Zn(2,6-dipic)] _n (1)	94
4.10 Solid state photoluminescent spectra of 2,6-dipicH ₂ (black line) and [Zn(2,6-dipic)] _n (1) (red line)	95
4.11 Plot of methyl acetate yield vs. reaction temperature for the transesterification reaction of phenyl acetate and methanol with (1) for 6 h	97
4.12 Plot of methyl acetate yield vs. reaction time for the transesterification reaction of phenyl acetate and methanol with (1) at 75 °C	98
4.13 Effect of the catalyst recycling on the yield of methyl acetate	99
4.14 PXRD patterns of recovered catalyst	100
4.15 Asymmetric unit of (2) with the atomic-numbering scheme. Displacement ellipsoids are drawn at the 50% probability level.	104
4.16 Coordination mode, μ_5 -1,3-bdc bridging ligands found in (2).	105

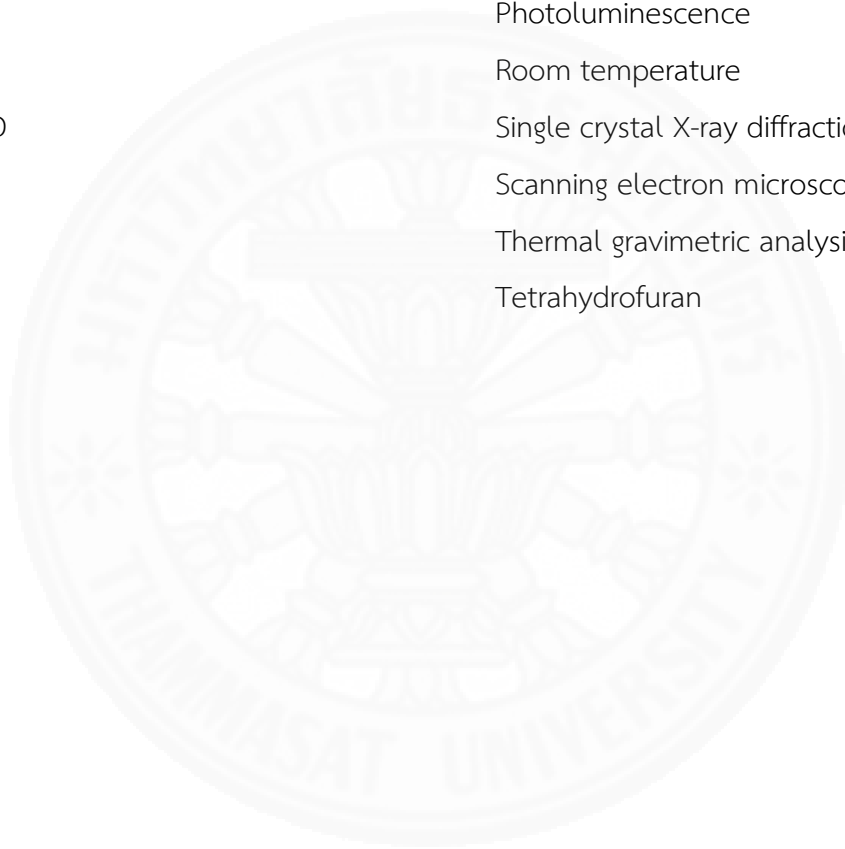
4.17	Perspective view along crystallographic <i>c</i> axis of (a) the three dimensional framework of (2) (coordination polyhedra for Cd(II) and Na(I) are pink and green, respectively) and (b) helical chain-like structure of Cd-Na clusters	105
4.18	Perspective view of three-dimensional framework of (2) (coordination polyhedra for Cd(II) and Na(I) are pink and green, respectively)	106
4.19	(a) μ_4 -coordination mode of 1,3-bdc bridging ligand and (b) packing structure of $\{[\text{CdNa}(1,3\text{-bdc})_2]\cdot[\text{NH}_2(\text{CH}_3)_2]\}$ with dimethylamine templating cations, viewed along the [111] direction	111
4.20	(a) μ_4 -coordination mode of OH-1,3-bdc bridging ligands and (b) Perspective view of the 3D network in $[\text{CdNa}(\text{OH}-1,3\text{-bdc})_2(\text{H}_2\text{O})_2]\cdot 2\text{H}_2\text{O}$ along the <i>c</i> axis	112
4.21	(a) μ_4 -coordination mode of 1,4-bdc bridging ligands and (b) packing structure of $[\text{Zn}_2\text{Na}_2(1,4\text{-bdc})_3\cdot(\text{DMF})_2\cdot(m\text{-H}_2\text{O})_2]$, viewed along the <i>a</i> axis	113
4.22	(a) μ_{10} -coordination mode of 1,2,4-btc bridging ligands and (b) packing structure of $[\text{ZnNa}(1,2,4\text{-btc})]$, viewed along the <i>a</i> axis	114
4.23	(a) μ_5 -coordination mode of ntc bridging ligands and (b) packing structure of $[\text{Cd}_8\text{Na}(\text{ntc})_6(\text{H}_2\text{O})_8]$, viewed along the <i>b</i> axis	115
4.24	IR spectra of (a) $\text{Cd}(\text{NO}_3)_2\cdot 4\text{H}_2\text{O}$, (b) 1,3-H ₂ bdc and (c) $\{\text{CdNa}_2(1,3\text{-bdc})_2(\text{H}_2\text{O})_2(\text{DMF})\}_n$ (2)	116
4.25	PDXRD patterns of $\{\text{CdNa}_2(1,3\text{-bdc})_2(\text{H}_2\text{O})_2(\text{DMF})\}_n$ (2)	117
4.26	TGA curve of $\{\text{CdNa}_2(1,3\text{-bdc})_2(\text{H}_2\text{O})_2(\text{DMF})\}_n$ (2)	118
4.27	SEM image of compound (2)	119
4.28	EDX spectrum of (2)	119
4.29	Solid state photoluminescence spectra of free 1,3-H ₂ bdc ligand and $\{\text{CdNa}_2(1,3\text{-bdc})_2(\text{H}_2\text{O})_2(\text{DMF})\}_n$ (2)	120

4.30 (a) Emission spectra of (2) and (b) relative emission intensities dispersed in various small organic solvents	122
4.31 PL spectra of the dispersed (2) in EtOH in the presence of various concentrations of the acetone and (b) Plot of the PL quenching efficiency of gradual additional amounts of acetone of (2)	123
4.32 Fitting plots of the quenching efficiency of acetone (0 – 0.10 %V) on the emissions of the suspensions of (2) , $\lambda_{\text{ex}} = 300 \text{ nm}$	124
4.33 UV-Vis spectra of various solvent	125
4.34 Quenching efficiency of (2) upon the addition of different organics (red) and subsequent addition of acetone (black), $\lambda_{\text{ex}} = 300 \text{ nm}$.	126
4.35 Coordination environment around the Cd(II) ions in the trinuclear SBU of compound (3)	128
4.36 (a) μ_3 - and (b) μ_4 -coordination modes of 1,3-bdc ²⁻ ligand in (3)	129
4.37 2D framework of compound (3)	129
4.38 (a) Trinuclear SBUs and (b) packing structure of $[\text{H}_2\text{N}(\text{CH}_3)_2]_2[\text{Co}_3(1,3\text{-bdc})_4]\cdot\text{H}_2\text{O}$	133
4.39 (a) Trinuclear SBUs and (b) packing structure of $[\text{Mn}_3(5\text{-py-}1,3\text{-bdc})_2(\text{HCOO})_2(\text{H}_2\text{O})_2]_n$	133
4.40 (a) Trinuclear SBUs and (b) packing structure of $[\text{Mn}_3(5\text{-ID-}1,3\text{-bdc})_3(\text{DMA})(\text{H}_2\text{O})_2]_n \cdot n[(\text{H}_2\text{O})(\text{DMA})]$	134

LIST OF ABBREVIATIONS

Symbols/Abbreviations	Terms
Å	Angstrom
°C	Degree Celsius
%v/v	Volume/Volume percent
1D	One-dimensional
2D	Two-dimensional
3D	Three-dimensional
1,3-bdcH ₂	1,3-benzenedicarboxylic acid
2,6-dipicH ₂	2,6-pyridinedicarboxylic acid
4,4'-bpy	4,4'-bipyridine
AC	Acetone
Cat.	Catalyst
CHN	Carbon Hydrogen Nitrogen
CPs	Coordination polymers
DCM	Dichloromethane
DMF	<i>N,N</i> -Dimethylformamide
DMSO	Dimethyl sulfoxide
EDS	Energy dispersive spectroscopy
EtOH	Ethanol
FID	Flame ionization detector
FTIR	Fourier transform infrared spectroscopy
GC	Gas chromatography
h	Hour
LMCT	Ligand to metal charge transfer
MeOH	Methanol
MLCT	Metal to ligand charge transfer

ml	Milliliter
mmol	Millimole
NaOH	Sodium hydroxide
nm	Nanometer
PA	Phenyl acetate
PDXRD	Powder X-ray diffraction
PL	Photoluminescence
RT	Room temperature
SCXRD	Single crystal X-ray diffraction
SEM	Scanning electron microscope
TGA	Thermal gravimetric analysis
THF	Tetrahydrofuran



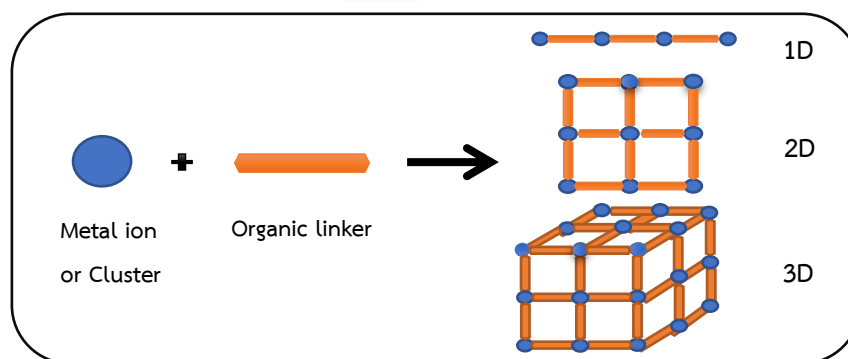
CHAPTER 1

INTRODUCTION

This chapter presents an introduction to coordination polymers (CPs) in the points of general information, influent factors, chemistry of d^{10} transition metals and carboxylate ligands and applications concerning to this study. In addition, the objective, scope and limitation of this research are described.

1.1 Coordination polymers

The term “*coordination polymers*” (CPs) was first mentioned by Shibata, Y. [1] to explain dimers and trimers of various cobalt(II) ammine nitrates in 1916. Later, this term was employed by Bailar, J. C. [2] to compare organic polymers with those inorganic compounds which can be considered as polymeric species in 1964. In 2013, the definition of CPs was provided as “a coordination compound with repeating coordination entities extending in 1, 2, or 3 dimensions” by Batten and coworkers [3]. Generally, coordination polymers consist of two mainly components, namely metal centers or clusters and organic linkers, which are connected together via coordinated covalent bond, the donation of a lone pair of electrons from the organic ligand as a Lewis base to the metal center as a Lewis acid, generating one-, two- and three-dimensional structures [4] as shown in Scheme 1.1.



Scheme 1.1 Formation of coordination polymers

Nowadays, the field of CPs is one of the most popular areas. The number of publications describing their synthesis, structures, characterization and applications has rapidly increased [5] as shown in Figure 1.1. Coordination polymers have attracted great attention not only for their interesting structural diversity, but also for their potential applications in many areas such as gas sorption and separation [6-12], energy storage and conversion [13-16], drug delivery [17-20], catalysis [21-27] and luminescence sensing [28-33].

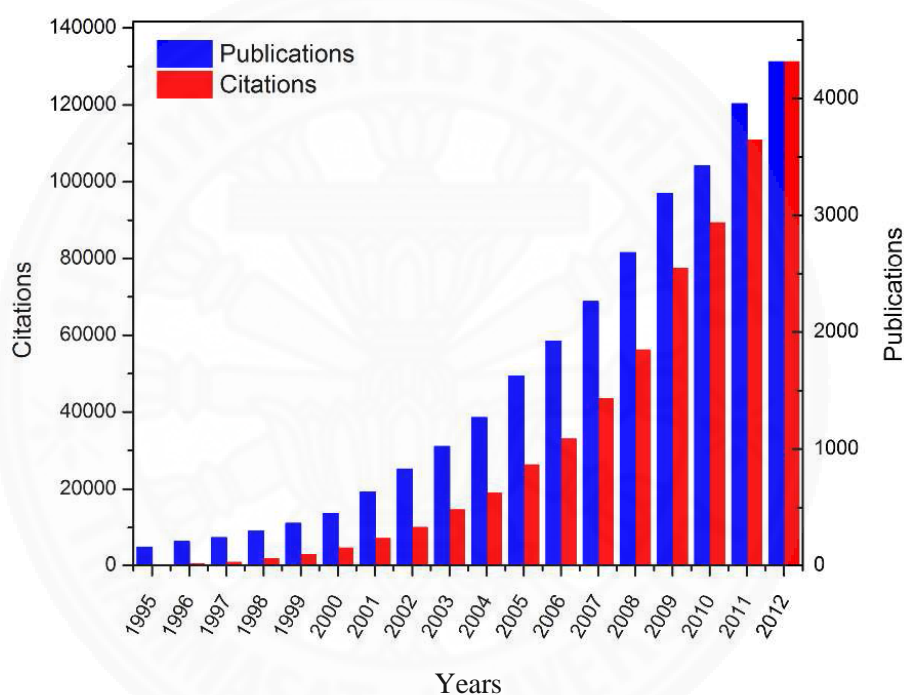


Figure 1.1 Number of publications and citations per year from 1995-2012 for articles on the topics of “coordination polymers” [5]

1.2 Factors of the formation of coordination polymers

The ability to control the structural dimensionality of CPs depends on the combination of several factors, such as the coordination geometry of the metal ion, the chemical structure of the ligand, the metal-to-ligand ratio, solvent system, temperature, pH value, and so on [34]. The descriptions of these factors are given following.

1.2.1 Influence of metal ions

The metal ions and their oxidation states influence on the topologies and properties of CPs. Several types of metal ions such as alkaline, alkaline earth, lanthanide and transition metals have been used to be choices of design and synthesis of CPs [35]. Especially, transition metal are often employed in the construction of CPs because their electronic structures and coordination numbers, giving rise to various geometries namely linear, T- or Y-shaped, tetrahedral, square-planar, square-pyramidal, trigonal-bipyramidal, octahedral and trigonal-prismatic geometries [36], as shown in Figure 1.2. Among *d*-transition metal ions, transition metal ions with d^{10} configuration has been attracted great attention as metal centers for the construction of luminescent CPs because of enhanced emissions arising from $\pi^*-\pi$ transitions within a rigid ligand [37]. The example study of influence of metal ions in CPs has been investigated by Song and coworkers in 2009 [38]. They had successfully synthesized six metal-benzoate with 4,4'-bpy co-ligand compounds using various metal ions as shown in Figure 1.3. Because of the difference in coordination geometries of metal ions, the crystal structures of these compounds show diverse structural features, namely ladder, helical, chain containing paddle-wheel units, zigzag to 2D sheet. It is clear that selection of suitable metal ions can control the coordination geometry of each metal ion to form different crystal structures.

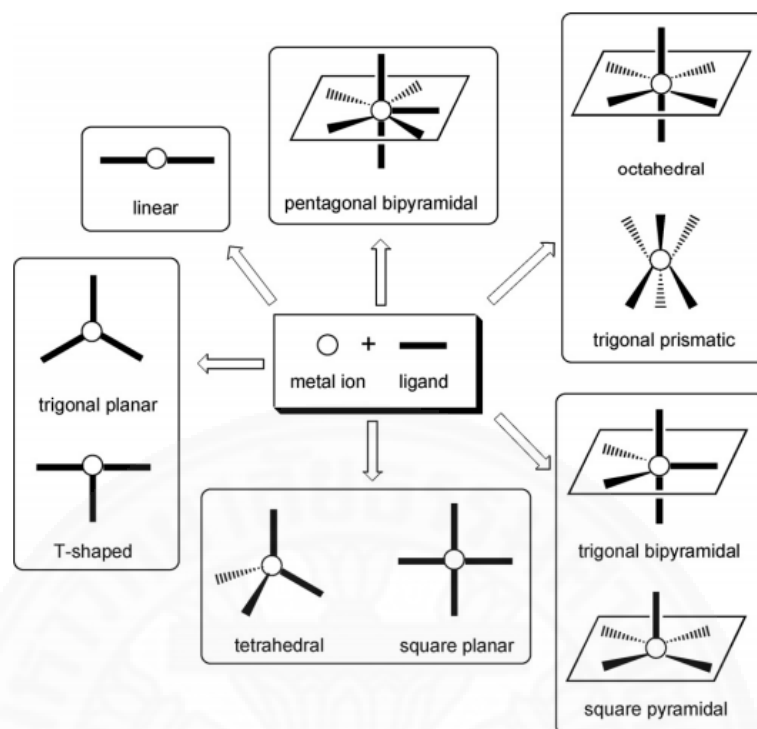


Figure 1.2 Coordination geometries of transition metal ions found in CPs [36]

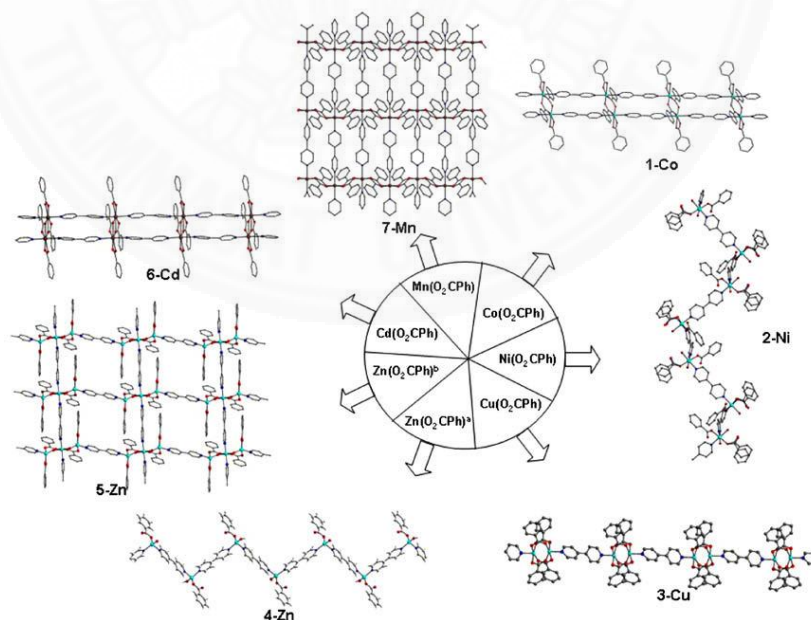


Figure 1.3 Views of the effect of metal ion types on the construction of CPs [38].

1.2.2 Influence of ligands

The configuration, rigidity, substituent and coordination modes of organic ligands have an important effect on the final structures. The organic ligands can be divided into three types namely, rigid, semi-rigid and flexible ligands [39]. In addition, there are also three categories of ligands according to their charge namely neutral, anionic and cationic, [40] as shown in Figure 1.4. Among them, the organic ligand molecules are also containing oxygen- or nitrogen-donor atoms within the functional groups [41]. The *N*-donors organic ligands mainly come from compounds with coordination groups such as pyridine, imidazole, triazole, tetrazole and so on. The *O*-donors organic ligands come from groups such as $-\text{OH}$, $-\text{COOH}$, $-\text{SO}_3\text{H}$, or $-\text{PO}_3\text{H}$. The example of the studies of the influence of nature of the organic ligands has been reported by Zheng and coworkers in 2001 [42]. They synthesized a series of Ag-hmt CPs (hmt = hexamethylene-tetramine) with different carboxylate co-ligands including 4-hydroxybenzoic acid (Hhba), 4-aminobenzoic acid (Haba), 4,4'-biphenyldicarboxylic acid (H_2bac), isonicotinic acid (Hina), benzenesulfinic acid (Hbsa) and 1,4-butanedioic acid (H_2bda). The synthesized compounds show variation of structures. The monocarboxylate co-ligands generated 1D zigzag CPs, while dicarboxylate ligands linked the zigzag chains into ladder like structure. The isonicotinate ligand with two binding sites coordinated to Ag(I) ions to furnish 2D grid network. Benzenesulfinate and 1,4-butanedioate ligands formed double-chain-like CPs. This work suggested that the structural diversity of CPs is mainly dependent on the nature and coordination properties of the organic ligands used.

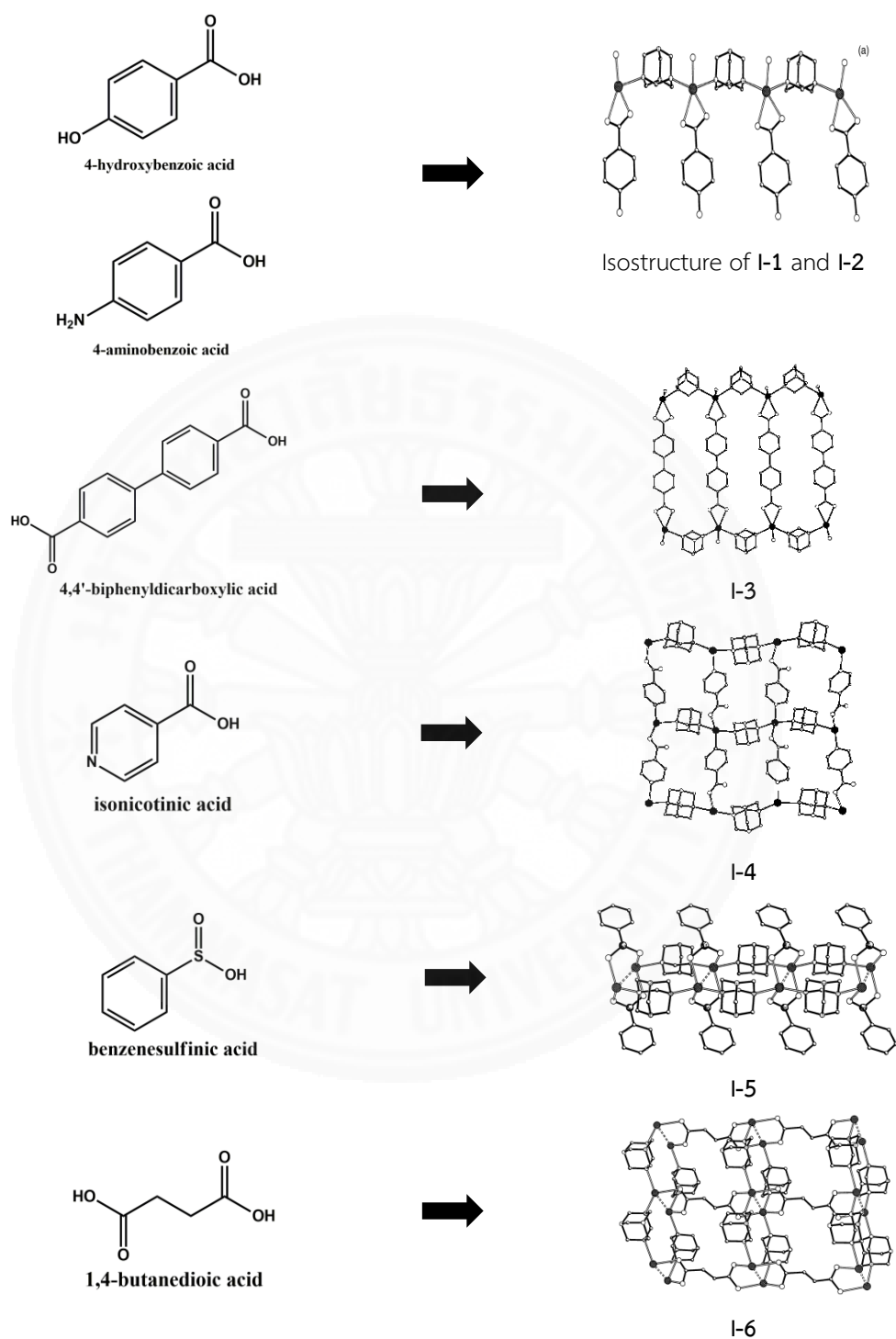


Figure 1.4 The illustration of the effect of organic ligand types on the construction of CPs [42]

1.2.3 Influence of metal-to-ligand ratio

Metal-to-ligand ratio is also important factor for the synthesis of CPs because the structure of CPs sometime depends on the stoichiometry of reactants. For example, Liu and coworkers [43] have studied the metal-to-ligand ratio influences the structure of CPs by using 2,4'-biphenyldicarboxylic acid (2,4'-bpdc) and bis(imidazole) ligands (bimb) to react with Co(II) ions in different mole ratio. Two CPs, $[\text{Co}(2,4'\text{-bpdc})(\text{bimb})(\text{H}_2\text{O})]\cdot 2\text{H}_2\text{O}$ (**I-7**) and $[\text{Co}_2(2,4'\text{-bpdc})_2(\text{bimb})_3(\text{H}_2\text{O})_2]\cdot \text{H}_2\text{O}$ (**I-8**) were obtained by incorporating the starting materials (Co(II): 2,4'-bpdc: bimb) in a molar ratio of 1:1:2 and 2:2.5:5, respectively. Compound (**I-7**) was obtained in a molar ratio of 1:1:2 that could give a 3D network with CdSO_4 -type topology, while compound (**I-8**) displays a 4-connected 6^6 network by increasing the metal to ligand ratio to 2:2.5:5 as shown in Figure 1.5.

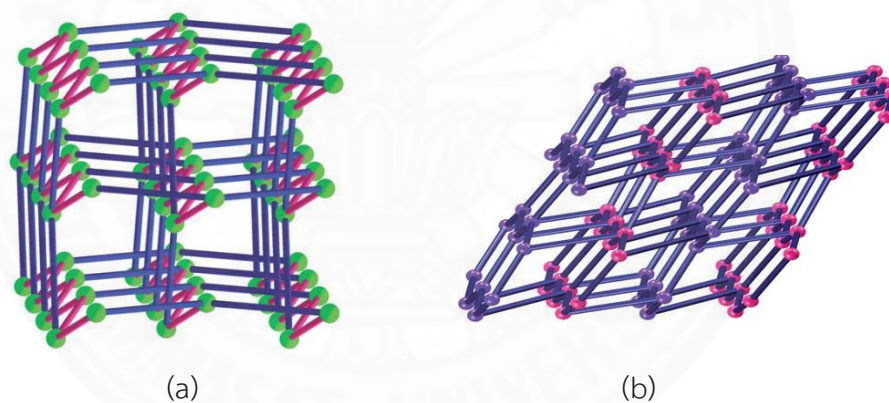


Figure 1.5 3D molecular network of (a) compound (**I-7**) and (b) (**I-8**) [43]

1.2.4 Influence of solvent system

The selection of suitable solvents is directly or indirectly influences to coordination framework topologies. Solvent sometime can participate in the complexation reactions like the ligand or influences the overall frameworks. The structural diversity of CPs may be due to the different size and the solubilizing ability of the solvent molecules. Banerjee and co-worker [44] have reported solvent influences onto the structure of CPs, $\{[\text{Cd}_3(\text{BPT})_2(\text{DMF})_2]\cdot 2\text{H}_2\text{O}\}$ (**I-9**), $[\text{Cd}_3(\text{BPT})_2(\text{DMA})_2]$

(I-10) and $[(\text{CH}_3\text{CH}_2)_2\text{NH}_2][\text{Cd}(\text{BPT})\cdot 2\text{H}_2\text{O}]$ (I-11) by the reaction of biphenyl tricarboxylic acid (H_3BPT) and $\text{Cd}(\text{II})$ ions with three different solvents namely *N,N*-dimethylformamide (DMF), *N,N*-Dimethylacetamide (DMA) and diethyl-formamide (DEF). Both of compounds (I-9) and (I-10) have 3D coordination frameworks in which the DMF molecules acts as a bridging linker in compound (I-9) and the DMA molecules as a terminated coordination solvent in compound (I-10). The structure of compound (I-11) shows a 2D (6,3) honeycomb type net with protonated diethylamine cation which decomposed from DEF inducing the formation of this type structure. The summarized result of this work is depicted in Figure 1.6.

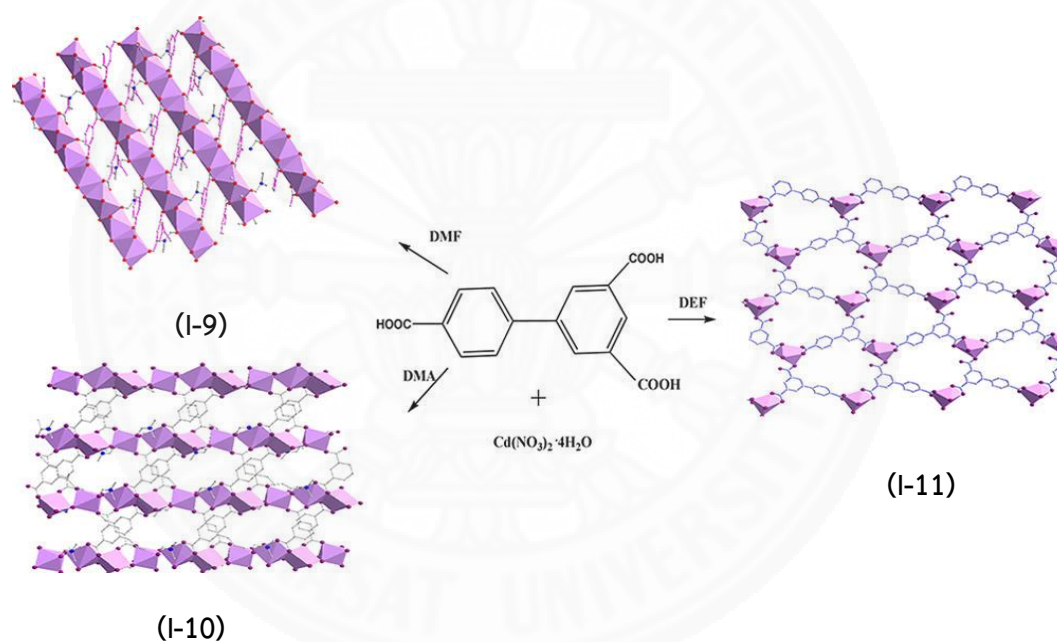


Figure 1.6 The example study of influent of solvent [44]

1.2.5 Influence of reaction temperature

The reaction temperature is also an important factor in the construction of CPs based on many reasons. Firstly, the reaction temperature affects the solubility of the organic ligand. Secondly, flexible organic ligands have the potential to adopt different conformations under different temperatures. Finally, the reaction temperature may play a significant role in tuning the coordination mode of

organic ligands, especially the carboxylate ligand [45]. The example study of the influence of reaction temperature has been reported by Zhang and coworkers [46] in 2009. They have successfully synthesized two CPs, $[(\text{Cu}(\text{L}))_2]$ (**I-12**) and $\{[\text{Cu}_2(\text{L})_2][\text{CH}_3\text{CN}]_3\}_n$ (**I-13**) by the reaction of CuI and 2,3-bis(ter-butylthiomethyl)quinoxaline at room temperature for (**I-12**) and 0°C for (**I-13**). Compound (**I-12**) presents discrete dinuclear molecule, while compound (**I-13**) show 1D chain-like structure (Figure 1.7). This result shows that varying reaction temperatures can affect to adjust the structural formation of CPs.

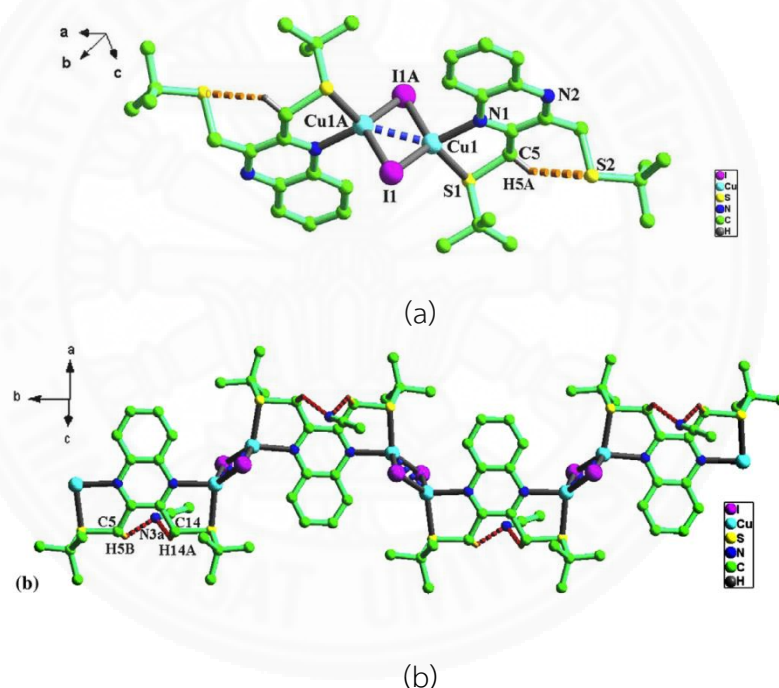


Figure 1.7 Crystal structure of (a) compound (**I-12**) and (b) compound (**I-13**) [46]

1.2.6 Influence of pH

It is well known that the crystallization process is highly influenced by the acidity/basicity of the reaction media. The pH value of the reaction is one of a crucial external factor which has a remarkable influence on the construction of CPs. Yuan and co-worker [47] have studied that how pH value of the reaction influences the structure of CPs. They have successfully synthesized two CPs, $[\text{Cd}_2(\text{ctpy})_4]_n \cdot 2n\text{H}_2\text{O}$

(**I-14**) and $[\text{Cd}_2(\text{ctpy})_2(\text{ox})]_n$ (**I-15**) by using $\text{CdCl}_2 \cdot 2.5\text{H}_2\text{O}$, 4-carboxy 4,2':6',4"-terpyridine (Hctpy) and oxalic acid (H_2ox) with adjust the pH values. Crystal structures of compounds (**I-14**) and (**I-15**) were obtained at pH 7.5 and 5.5 respectively. It is clear that oxalate does not appear in (**I-14**). Oxalic acid may act as a medium for the formation of (**I-15**) at higher pH value leading to 3D interpenetrating framework as shown in Figure 1.8(a), while it is coordinated with Cd(II) atom in (**I-15**) leading to a (4,5)-connected 3D structure (Figure 1.8(b)) at lower pH value. It indicates that the differences in pH values lead to the distinction of the CPs structures.

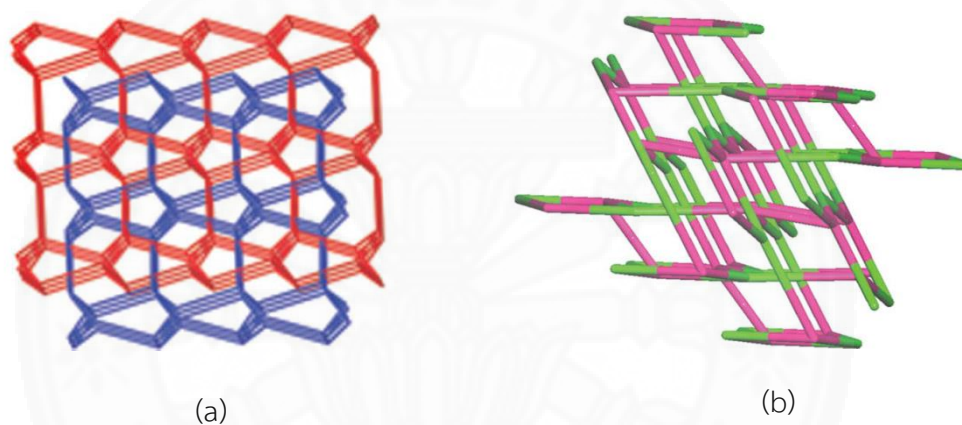


Figure 1.8 Crystal structure of (a) compound (**I-14**) and (b) compound (**I-15**) [47]

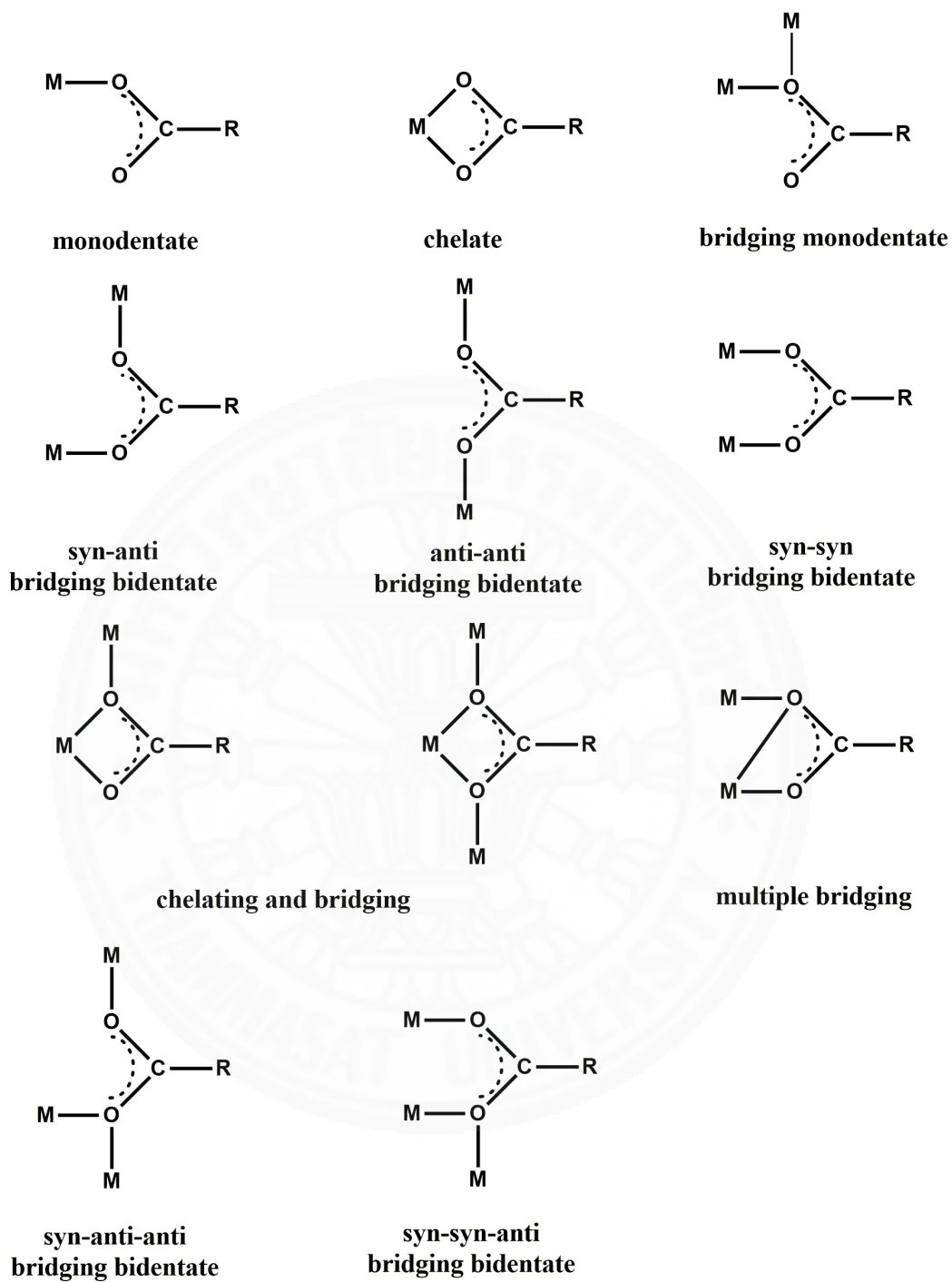
1.3 Carboxylate ligands

The selection of organic ligands containing suitable coordination sites linked by a spacer with specific positional orientation is especially important to the construction of CPs. The most attractive organic ligands are carboxylate derivatives because of their strong coordination ability and versatile coordination modes such as terminal monodentate, bridging bidentate or chelate [48]. This type of ligand can support to gain the diverse structures and topologies of designed CPs. The variety of coordination mode of carboxylate ligand is shown in Scheme 1.2. Among polycarboxylate ligands, dicarboxylates ligands are widely employed for synthesis of

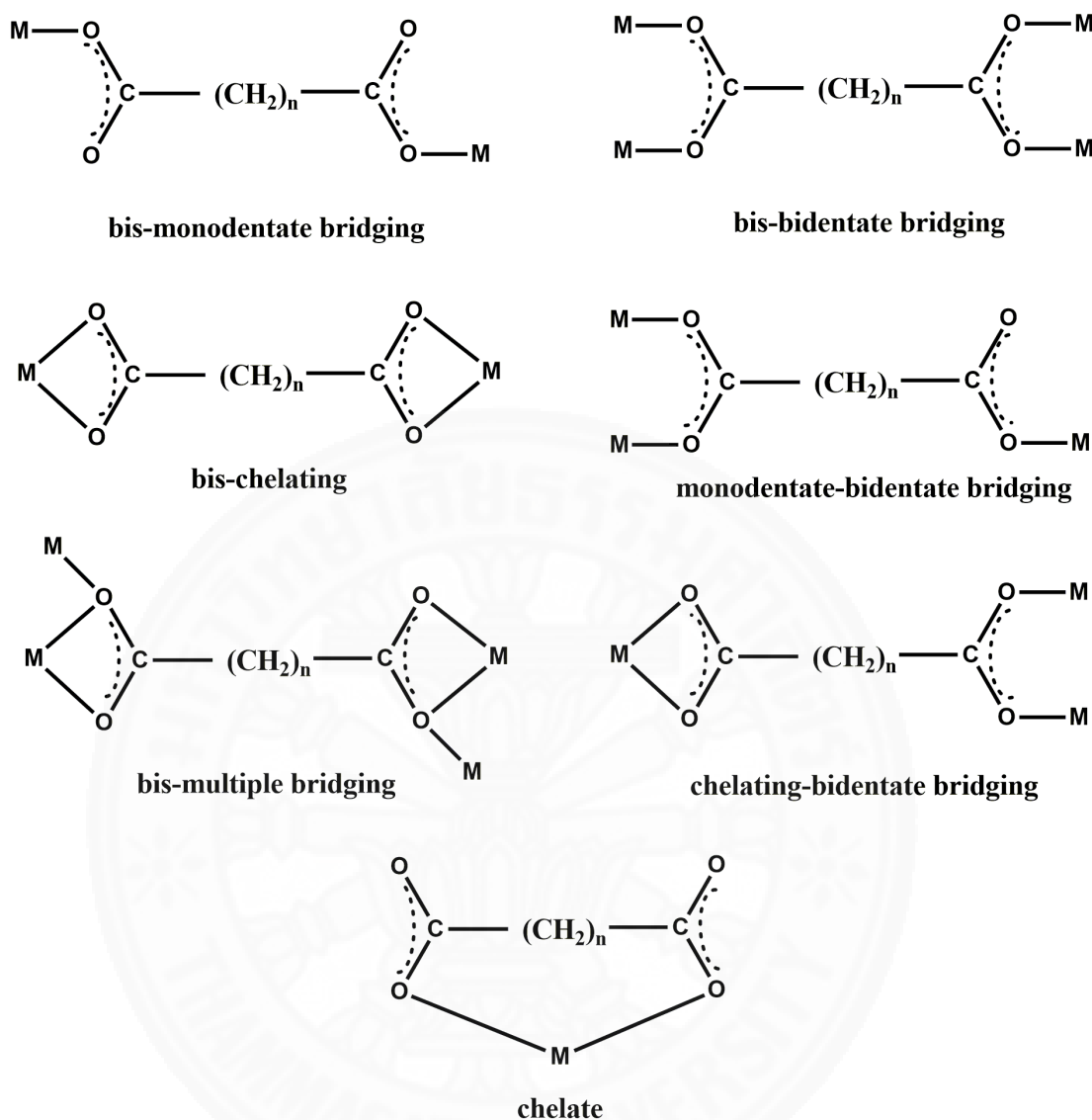
CPs. The coordination modes found for dicarboxylate ligand could be presented in Scheme 1.3 [49].

Within dicarboxylate ligands, the rigid aromatic (such as benzene and pyridine ring) dicarboxylates are interesting to select for the synthesis of CPs. Moreover, the differences in an angle of spacer of dicarboxylates groups to *ortho*-, *meta*- and *para*- positions can be support the construction of a varieties coordination polymer's topologies. The example of this ligand's family such as 1,2-benzenedicarboxylic acid, 1,3-benzenedicarboxylic acid, 1,4-benzenedicarboxylic acid and 2,6-pyridinedicarboxylic acid. There are several research that use these ligands to synthesis new CPs [50,51].





Scheme 1.2 Coordination modes of carboxylate ligand [48]



Scheme 1.3 Coordination modes in dicarboxylate ligand [49]

In 2011, Zhang and coworkers [50] reported four new Zn(II)/Cd(II) coordination polymers, $[\text{Zn}(1,2\text{-bdc})(\text{bth})_{0.5}(\text{H}_2\text{O})]_n$ (**I-16**), $[\text{Cd}(1,2\text{-bdc})(\text{bth})_{0.5}(\text{H}_2\text{O})]_n$ (**I-17**), $[\text{Zn}(1,3\text{-bdc})(\text{bth})]_n$ (**I-18**), and $[\text{Cd}(1,4\text{-bdc})(\text{bth})(\text{H}_2\text{O})_2]_n$ (**I-19**). They used three isomers of bdCH_2 as bridging ligands and 1,6-bis(triazol)hexane (bth) as co-ligand to synthesis these CPs. Both **I-16** and **I-17** are iso-structural, featuring two binodal architectures: $(6^3)(6^5 \cdot 8)$ topology in terms of 1,2-bdc and Zn(II)/Cd(II) as three- and four-connected nodes as shown in Figure 1.9(a). Compound **I-18** exhibits a 2D (4,4) network with the Zn \cdots Zn \cdots Zn angle of 57.84° , while **I-19** displays planar 2D (4,4)

network. A structural comparison of these compounds indicates that the dicarboxylate building blocks with different dispositions of the carboxyl site play significant role in controlling the structural diversity.

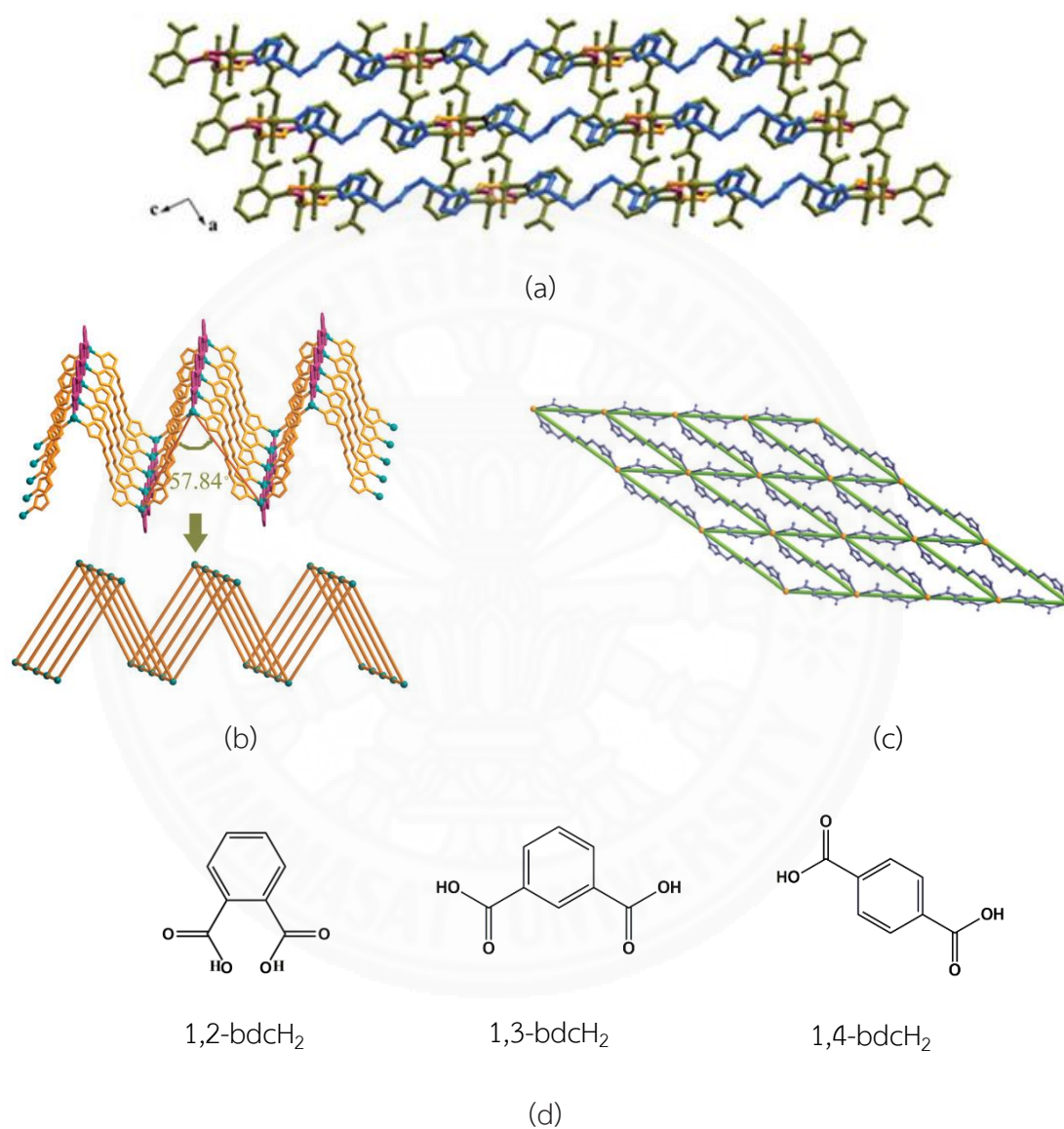


Figure 1.9 (a) 3D herringbone like structure of (I-16), (b) waved layer and simplified models applied in the topological analysis of (I-18), (c) planar 2D (4,4) network of (I-19) and (d) Molecular structure of three isomer of bdch₂ [50]

In 2012, Cheng and coworkers [51] reported eight new Zn(II)/Cd(II) coordination polymers, $[\text{Zn}(1,2\text{-bdc})(\text{L}^2)]_n$ (**I-20**), $[\text{Zn}_2(1,3\text{-bdc})_2(\text{L}^2)(\text{H}_2\text{O})_2]_n$ (**I-21**), $[\text{Zn}_2(1,4\text{-bdc})_2(\text{L}^1)(\text{H}_2\text{O})_2]_n$ (**I-22**), $\{[\text{Zn}_2(1,2\text{-bdc})_2(\text{L}^3)(\text{H}_2\text{O})_2] \cdot 2\text{H}_2\text{O}\}_n$ (**I-23**), $\{[\text{Cd}(1,2\text{-bdc})(\text{L}^2)(\text{H}_2\text{O})] \cdot \text{H}_2\text{O}\}_n$ (**I-24**), $[\text{Cd}_2(1,3\text{-bdc})_2(\text{L}^2)(\text{H}_2\text{O})_4]_n$ (**I-25**), $\{[\text{Cd}_2(1,4\text{-bdc})_2(\text{L}^2)](\text{H}_2\text{O})_3\}_n$ (**I-26**) and $[\text{Cd}_2(1,4\text{-bdc})_2(\text{L}^1)(\text{H}_2\text{O})_2]_n$ (**I-27**). They used three isomers of bdcH_2 as bridging ligands and three isomeric *N,N'*-di(2-pyridyl)adipoamide (L^1), *N,N'*-di(3-pyridyl)adipoamide (L^2) and *N,N'*-di(4-pyridyl)adipoamide (L^3) as co-ligands to construct these CPs. Compounds **I-20**, **I-23**, and **I-24** form 1D double-looped chain, 1D chain with loops and 2D layer with loops, respectively, and **I-19** exhibits a 1D ladder chain. Compound **I-15** shows rare 3-fold interpenetrated hcb layers, whereas compounds **I-22** and **I-27** forms planar and undulated hcb layers, respectively. Compound **I-26** shows a 3D self-penetrating net. From these results, the structural types of these Zn(II) and Cd(II) coordination polymers are thus subjected to the changes of the donor atom positions of the dicarboxylate ligand.

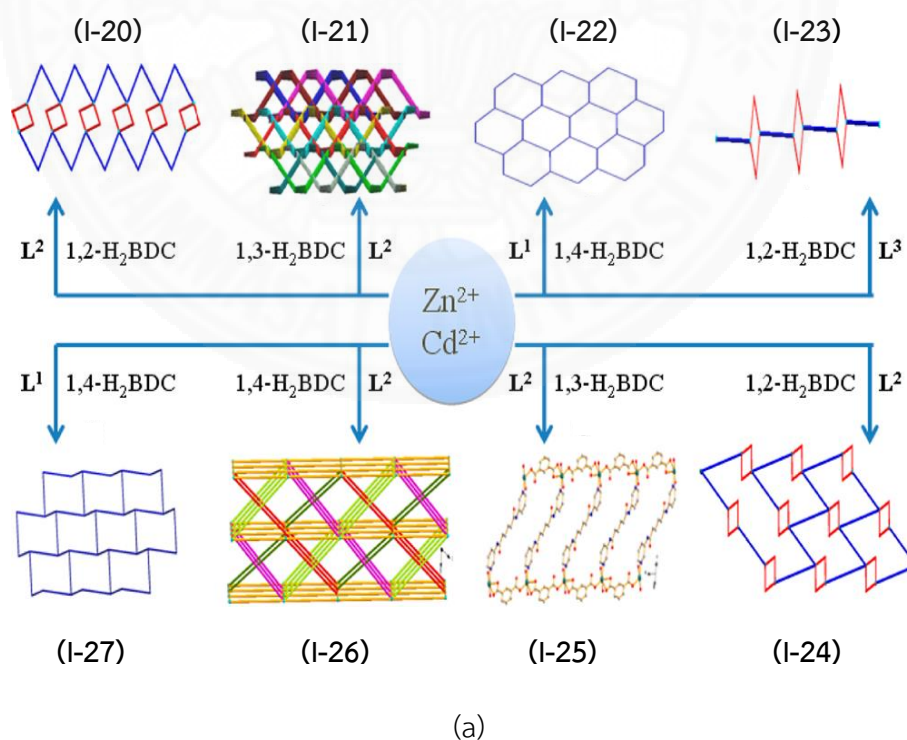


Figure 1.10 (a) Schematic views of compound (**I-20**) – (**I-27**) synthesized from different ligands and (b) molecular structure of three isomer of bdcH_2 [51]

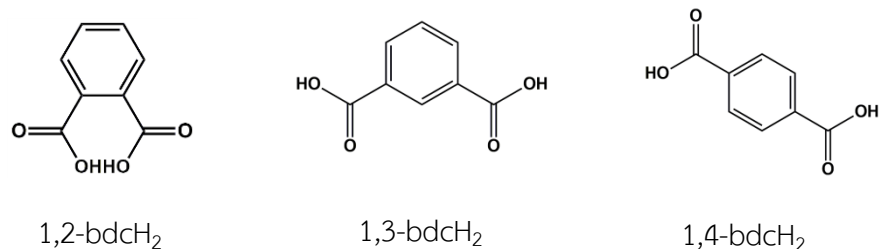


Figure 1.10 (a) Schematic views of compound (I-20) – (I-27) synthesized from different ligands and (b) molecular structure of three isomer of bdch_2 [51] (Cont.)

From previous studies, the large numbers of CPs containing aromatic dicarboxylate ligands have been prepared and properties studied. However, the studies of CPs containing dicarboxylate derivatives are still limited. In this research, we focused on aromatic dicarboxylate ligand, namely pyridine-2,6-dicarboxylic acid ($2,6\text{-dipicH}_2$) and benzene-1,3-dicarboxylic acid ($1,3\text{-bdch}_2$) were used as bridging ligand to synthesize the novel CPs with studies of various factors on the synthesis.

1.4 Application of coordination polymers

Coordination polymers (CPs) continue to be of current interest due to the combination of the individual properties associated with inorganic and organic components. Many researchers have been studied for their rich structural chemistry and potential applications in many areas, including gas sorption and separation [6-12], energy storage and conversion [13-16], drug delivery [17-20], catalysis [21-27] and luminescence sensing [28-33]. In this thesis, we focused on heterogeneous catalysis and luminescence sensing. Details of both applications are described below.

1.4.1 Heterogeneous catalysis

Catalysis is a significant tool for efficiently and selectively making and breaking chemical bonds that are important for converting some chemicals into more valuable products. Recently, the field of CPs as heterogeneous catalysts has

rapidly expanded due to their wide chemical versatility and modifiability [52]. Catalytically active sites can initially be present in an inorganic component or the organic linker of the framework. The representation of this concept is shown in Figure 1.11 [53]. As an example of the first approach of the open metal sites, Hwang and coworkers [54] reported a new 2D Zn(II) coordination polymer, $[\text{Zn}(\text{glu})(\mu\text{-bpe})]\cdot 2\text{H}_2\text{O}$ (**I-28**), which able to catalyze the transesterification reaction of various esters by the 4-coordinated unsaturated Zn(II) ions in the framework. Recently, Wani and coworkers [55] also reported a new 1D Zn(II) coordination polymers, $[\text{Zn}(\text{TPPZ})(\text{HCCB})]_n\cdot \text{DMF}\cdot \text{H}_2\text{O}$ (**I-29**), which can catalyze the transformation of esters and alcohols to produce the corresponding transesterification products with high yield. The second approach is functionalizing the organic linker and using the linker as the catalytic site, Kitagawa and coworkers [56] reported the new 3D coordination polymer with the formula $\{[\text{Cd}(4\text{-btapa})_2(\text{NO}_3)_2]\cdot 6\text{H}_2\text{O}\cdot 2\text{DMF}\}_n$ (**I-30**) where 4-btapa = 1,3,5-benzene tricarboxylic acid tris[*N*-(4-pyridyl)amide]. This compound is able to catalyze the Knoevenagel condensation of benzaldehyde and malononitrile with a good yield because of the containing of effective amide groups can be considered to exhibit a sufficient catalytic activity with base property. Moreover, the introduction of ions of catalytically active transition metals into the framework of the synthesized CPs can formally be considered a post-synthetic modification as well [53].

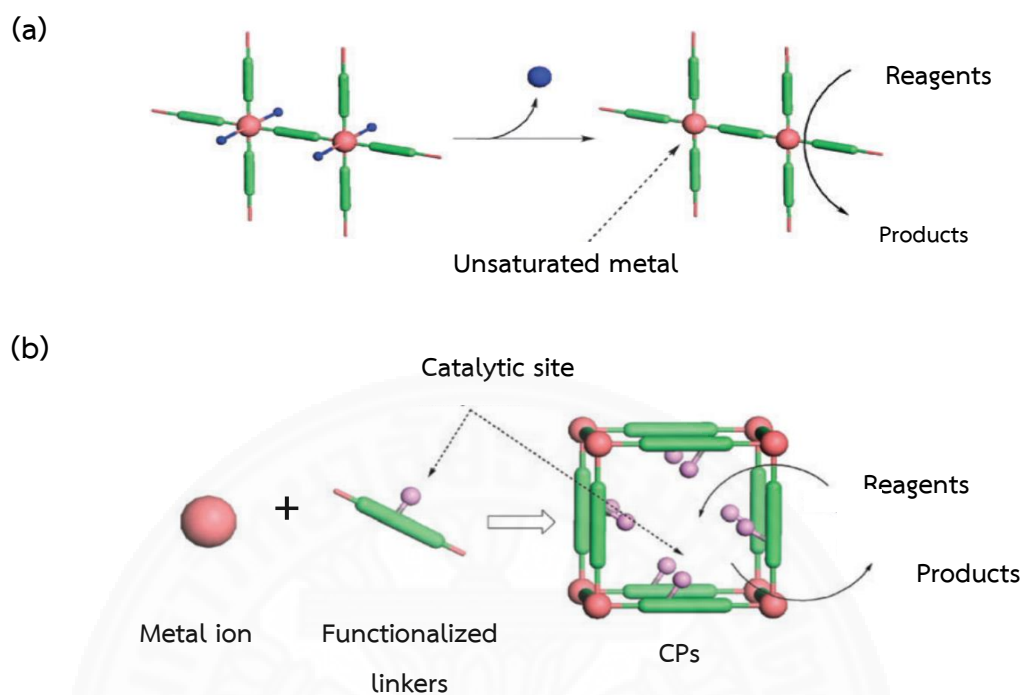


Figure 1.11 (a) Unsaturated metal ions and (b) functionalized linkers as catalytic sites

[53]

1.4.2 Luminescent sensing

Luminescence can be defined as the emission of light upon absorption of energy under the condition that the energy source is not heat based, which refers to incandescence. There are two basic types of luminescence namely fluorescence and Phosphorescence. The fluorescence concerns about the emission of light after absorption of a photon of light at a different wavelength. The emitted light is usually at a longer wavelength (lower energy) than the absorbed light. This phenomenon was observed by George Stokes in 1852 [57]. While the phosphorescence is the spin-forbidden radiates transition from the triplet state T_1 to ground state S_0 . These phosphorescent lifetimes can last from several seconds to hours.

Organic linkers with aromatic moieties or π -conjugated system and rigid molecular backbone in CPs are commonly used in the construction of

luminescence CPs. As the organic fluorophores are fixed in an ordered arrangement and in close proximity with one another in a CPs structure, the nature of their intermolecular communication can be altered resulting in photoemissions that are different from their free form [57]. Ligand to metal charge transfer (LMCT) and metal to ligand charge transfer (MLCT) are also common among d^{10} transition metal based CPs. LMCT is often observed in Zn(II) and Cd(II) compounds [58,59], while MLCT is generally seen in Cu(I) and Ag(I) compounds [60].

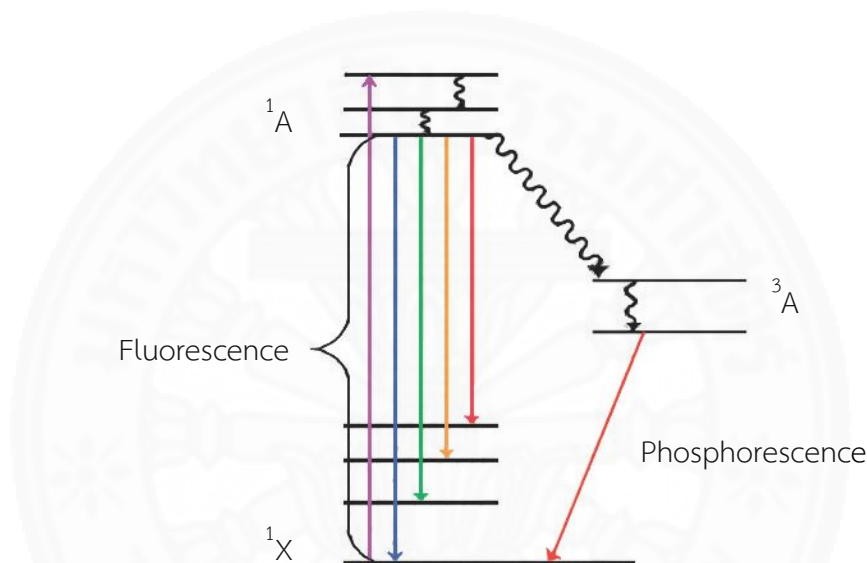


Figure 1.12 Jablonski diagram displaying schematically the electronic states of the organic linker involved in luminescence phenomena [57]

The most luminescent spectra observed for CPs is quenching signal. Many researchers have reported novel luminescence coordination polymers which are able to sense small organic molecules in liquid phase. The selected interesting works are described.

In 2013, Rachuri and coworkers [61] reported a new Cd(II) coordination polymer, $\{[Cd(H_2O)_4(4\text{-BPDB})][BPDC]\}_n$ (**I-31**) where 4-BPDB = 1,3-bis(1,2,4-triazol-1-ylmethyl)-2,4,6-trimethylbenzene and H_2BPDC = 4,4'-biphenyldicarboxylic acid. The PL results present emission intensity of acetonitrile suspension of (**I-31**) is selectively and efficiently quenched in presence of acetone comparing to other

common organic solvents. These results show potential application of this compound as a luminescent sensing material for the detection of acetone.

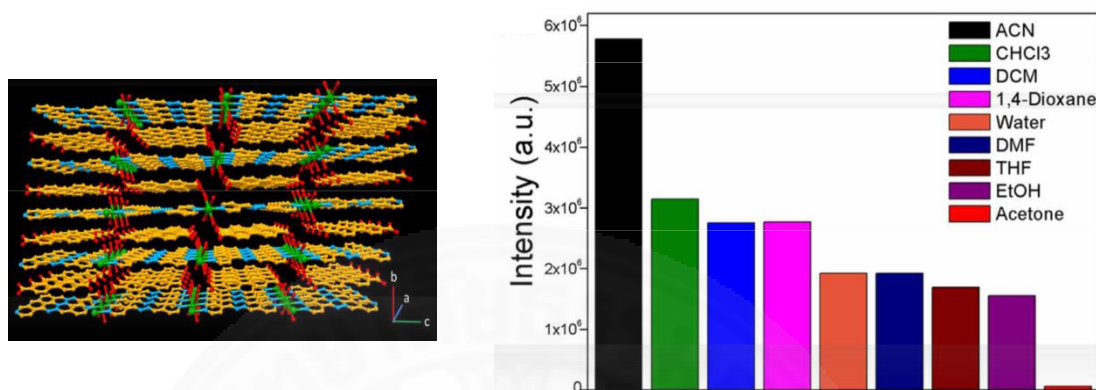


Figure 1.13 Packing structure of (I-31) and (b) relative emission intensities of (I-31) observed in different solvents [61]

In 2014, Li and coworkers [62] reported two Cd(II) coordination polymers, $[\text{Cd}(\text{Tipb})(1,4\text{-bdc})_{0.5}(\text{H}_2\text{O})(\text{NO}_3)] \cdot (\text{DMF})_x(\text{H}_2\text{O})_y$ (**I-32**) and $[\text{Cd}(\text{Tipb})(1,3\text{-bdc})] \cdot (\text{DMF})_x(\text{H}_2\text{O})_y$ (**I-33**) synthesized from a fluorescent ligand, 2,4,6-tris[4-(1*H*-imidazole-1-yl)]-benzene (Tipb). Both compounds show the selective luminescence quenching for acetone as shown in Figure 1.13. The detection limits of (**I-32**) and (**I-33**) were calculated to be 0.084 and 0.075 % v/v, respectively.

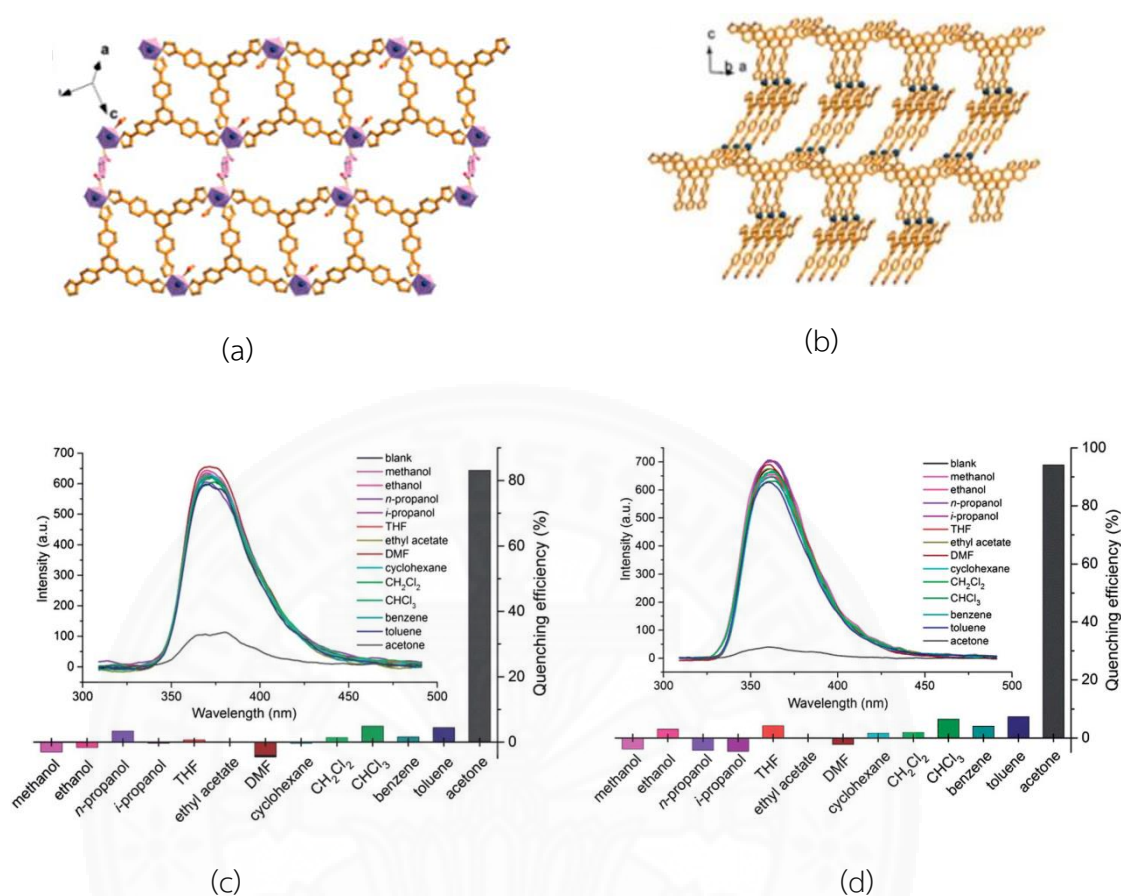


Figure 1.14 (a) 2D structure of (I-32), (b) 3D structure of (I-33), (c) Quenching efficiencies of 2.0 % v/v of different organics on the emissions of (I-32) and (d) (I-33)

[62]

In 2016, Li and coworkers [63] reported two Cd(II) coordination polymers, $[\text{Cd}_3(\text{tib})_2(\text{BTB})_2] \cdot 3\text{DEF} \cdot 4.5\text{H}_2\text{O}$ (I-34) and $[\text{Cd}_3(\text{tib})_2(\text{BTB})_2(\text{DMA})_2(\text{H}_2\text{O})_2] \cdot 2\text{DMA} \cdot 8\text{H}_2\text{O}$ (I-35) where tib = 1,3,5-tris(1-imidazolyl)benzene and H₃BTB = 4,4',4''-benzene-1,3,5-triyl-tribenzoic acid. Both compounds show selectivity for detection of acetone as presented in Figure 1.15.

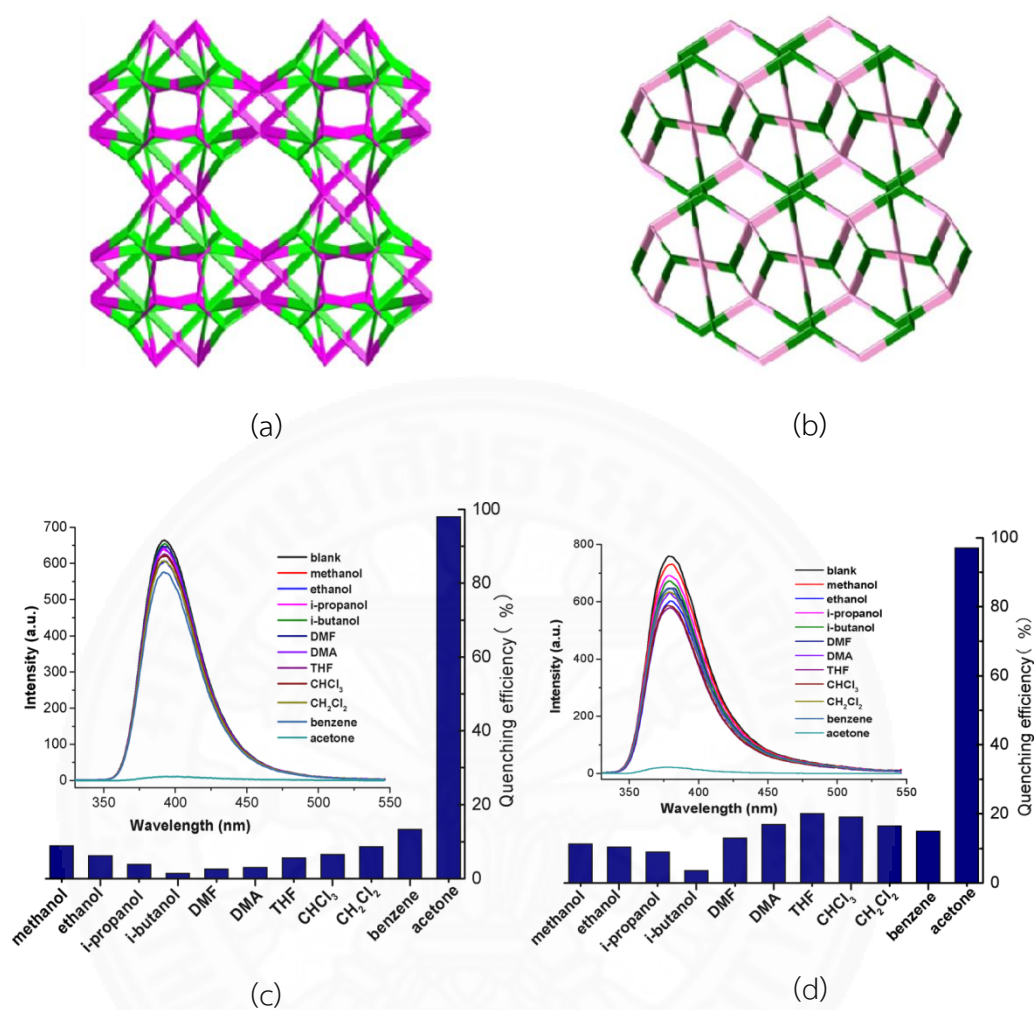


Figure 1.15 (a) 3D structure of (I-34), (b) 3D structure of (I-35), (c) Quenching efficiency variation of (I-34) and (d) (I-35) dispersed in CH₃CN via addition of 2.0 % v/v different organic molecules [63]

1.5 Research objective

1.5.1 To design and synthesize novel coordination polymers by using selected d^{10} transition metal ions namely Zn(II) and Cd(II) ions and aromatic dicarboxylate ligand, namely pyridine-2,6-dicarboxylic acid (2,6-dipicH₂) and benzene-1,3-dicarboxylic acid (1,3-bdch₂) as the bridging ligands.

1.5.2 To characterize the synthesized coordination polymers by using Fourier-transform infrared spectroscopy technique, elemental analysis, energy dispersive spectroscopy and powder X-ray diffraction technique.

1.5.3 To study the crystal structure of synthesized coordination polymers by using single crystal X-ray diffraction technique.

1.5.4 To study the physical properties of synthesized coordination polymers namely thermal stability and luminescent properties.

1.5.5 To study the properties of synthesized coordination polymers namely catalytic and sensing properties.

1.6 limitation of study

1.6.1 Novel coordination polymers have designed and synthesized by using d^{10} transition metal ions namely Zn(II) and Cd(II) ions as a metal center and aromatic dicarboxylate ligand namely pyridine-2,6-dicarboxylic acid (2,6-dipicH₂) and benzene-1,3-dicarboxylic acid (1,3-bdch₂) as the bridging ligands.

1.6.2 The synthetic parameters, namely mole ratio and solvents have been studied.

1.6.3 The FT-IR, elemental analysis and PDXRD techniques have been applied to identify the composition and determine the sample purity of synthesized coordination polymers, respectively

1.6.4 The single crystal X-ray diffraction technique has been applied to study the crystal structures of synthesized coordination polymers.

1.6.5 The thermal stability of synthesized coordination polymers have been studied by using thermogravimetric analysis (TGA).

1.6.6 The solid state photoluminescence property of synthesized coordination polymers comparing to that of their free ligands have been investigated by using fluorescence spectroscopy.

1.6.7 The catalytic activities and the sensing behaviors of synthesized coordination polymers have been examined.

1.7 Expected results

1.7.1 Novel coordination polymers containing aromatic dicarboxylate bridging ligands namely pyridine-2,6-dicarboxylic acid (2,6-dipicH₂) and benzene-1,3-dicarboxylic acid (1,3-bdcH₂) have been successfully synthesized.

1.7.2 The crystal structures of all synthesized coordination polymers have been studied.

1.7.3 The properties of synthesized coordination polymers have been investigated.

1.7.4 The relationship between the crystal structure and properties of synthesized coordination polymers has been studied.

CHAPTER 2

REVIEW OF LITERATURE

This chapter presents the previous studies which related to the multidimensional Zn(II) or Cd(II) coordination polymers constructed from aromatic dicarboxylate derivatives. The details of the synthetic method, crystal structure and their properties are reported and summarized regarding to degree of dimensional structures, as following.

2.1 One-dimensional Zn(II) and Cd(II) containing aromatic dicarboxylate derivatives CPs

In 2005, Wen and coworkers [64] reported a new 1D coordination polymer, $[\text{Zn}(2,6\text{-dipicO})(\text{H}_2\text{O})_2]_n$ (**II-1**) prepared from the reaction of $\text{Zn}(\text{NO}_3)_2 \cdot 6\text{H}_2\text{O}$, pyridine-2,6-dicarboxylic acid *N*-oxide (2,6-dipicOH₂) and triethylamine in the ratio of 1:1:2 by hydrothermal method. This compound crystallizes in a noncentrosymmetric space group $I4_1cd$. The coordination geometry of Zn(II) center is a slightly distorted octahedron as shown in Figure 2.1(a). Each carboxylate group is coordinated to Zn(II) atom in a monodentate mode. The remarkably structural feature of this compound is possesses a one-dimensional helical chain-like structure with 4_1 helices along the *c*-axis with a pitch of 10.090 Å (Figure 2.1 (b)). The nearest Zn...Zn separation of the adjacent helical chains is 7.635 Å. Each helical chain is further extended by hydrogen bonding interactions, generating a 3D supramolecular framework. Moreover, the solid state luminescence property of this compound was investigated. The PL spectrum of this compound showed the strong fluorescent emission spectrum at 417 nm with excitation at 342 nm.

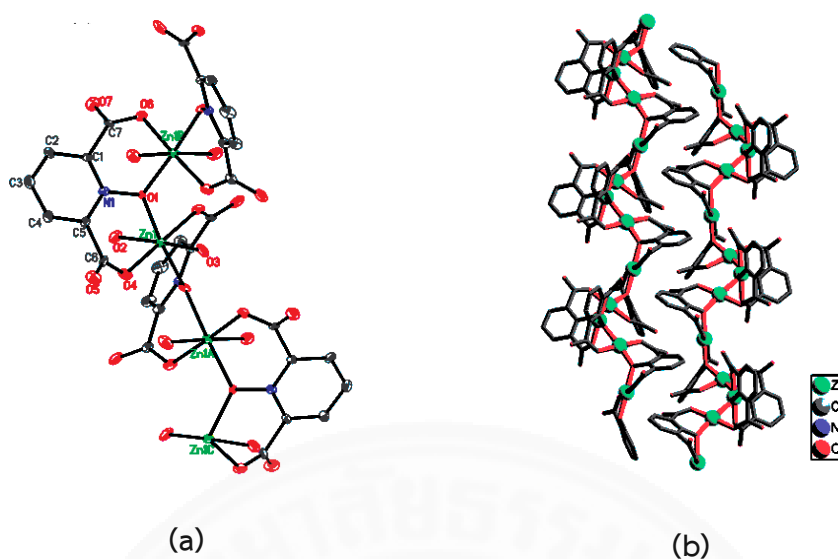


Figure 2.1 (a) Coordination environment of Zn(II) ion and (b) 1D helical chain-like structure of II-1 [64]

In 2006, Gao and coworkers [65] successfully synthesized a new 1D coordination polymer, $\{[\text{Zn}(\text{2,6-dipic})(\text{H}_2\text{O})_{1.5}]\}_n$ (II-2), by the reaction of 0.2 mmol of ZnSO_4 with 0.2 mmol of pyridine-2,6-dicarboxylic acid (2,6-dipicH₂) with mixed solvents of water and ethanol under solvothermal conditions. In the structure of this compound, the Zn(II) ion is six coordinated with octahedral geometry as presented in Figure 2.2(a). The Zn(II) ions are linked through alternative single and double oxygen bridges of 2,6-dipic²⁻ to form a 1D zigzag chain as shown in Figure 2.2(b) with Zn...Zn distances of 3.699 and 3.346 Å. Each 1D chain connects four other chains by hydrogen bonding between coordinated water molecules and oxygen atoms of 2,6-dipic²⁻, resulting a 3D supramolecular network. Furthermore, the solid state luminescence property of this compound was studied. The PL spectrum of this compound showed the strong fluorescent emission spectrum at 543 nm with excitation at 388 nm.

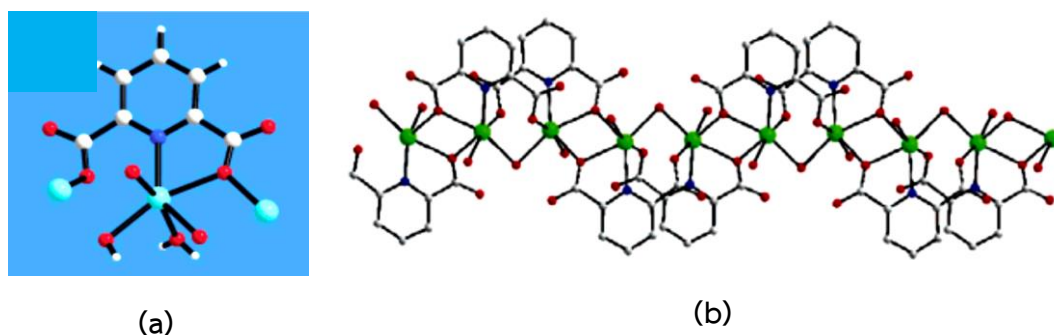


Figure 2.2 (a) Coordination environment of Zn(II) ion and (b) 1D zigzag chain-like structure of II-2 [65]

In 2007, Wu and coworkers [66] reported a 1D coordination polymer, $[\text{Cd}_2(2,6\text{-dipic})_2(\text{CH}_3\text{OH})_2(\text{H}_2\text{O})]_n$ (II-3), synthesized by using layer diffusion method of CdCl_2 and pyridine-2,6-dicarboxylic acid (2,6-dipicH₂) in the ratio of 1:1 by using water and methanol as solvents. This compound crystallizes in orthorhombic space group *Pbcn*. The coordination environment of Cd(II) ion could be described as a pentagonal bipyramid in which the axial positions are occupied by two O atoms from carboxylate and methanol, respectively. Two adjacent Cd(II) ions are linked by a pair of carboxylate O atoms from two 2,6-dipic²⁻ ligands to give a dinuclear unit with a Cd...Cd separation of 3.4064(5) Å (Figure 2.3(a)). These dinuclear units are interconnected via bridging carboxylate O atoms to form a 1D chain structure extending along the [001] direction as presented in Figure 2.3 (b).

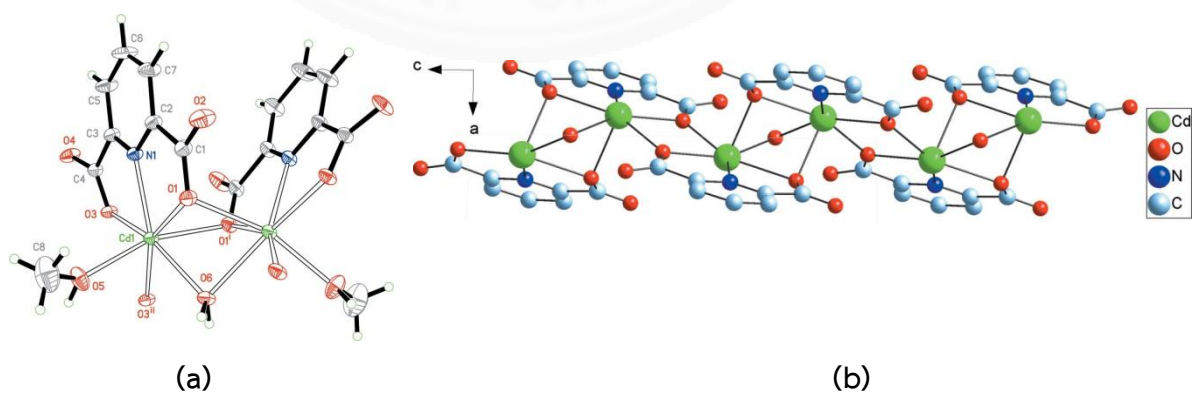


Figure 2.3 (a) The dinuclear unit and (b) 1D chain structure of II-3 extending along the [001] direction. H atoms have been omitted for clarity [66].

In 2010, Liu and coworkers [67] reported a new 1D coordination polymer, formulated as $[\text{Zn}_2(1,3\text{-bdc})_2(\text{L}^1)] \cdot 2\text{H}_2\text{O}$ (**II-4**) where L^1 is 1,1'-(1,4-butanediyl)-bis[2-(2-pyridyl)benzimidazole] (Figure 2.4(a)). This compound synthesized from the solvothermal reaction of $\text{Zn}(\text{OAc})_2 \cdot 2\text{H}_2\text{O}$, benzene-1,3-dicarboxylic acid ($1,3\text{-bdcH}_2$) and L^1 in the ratio of 2:2:1 with water and methanol solvents. Their structures have been determined by single crystal X-ray diffraction analysis and further characterized by various techniques. In this compound, $\text{Zn}(\text{II})$ ion is six-coordinated by four carboxylate oxygen atoms from three $1,3\text{-bdc}^{2-}$ and two nitrogen atoms from L^1 , showing a distorted octahedral coordination geometry as shown in Figure 2.4 (b). Two carboxylate groups of $1,3\text{-bdc}^{2-}$ show bidentate chelating and bidentate bridging coordination modes, respectively. Each $1,3\text{-bdc}^{2-}$ links three $\text{Zn}(\text{II})$ ions to form a 1D double chain (Figure 2.4 (c)). The chains are further extended into 2D layers via $\pi - \pi$ interactions between pyridyl rings from adjacent chains.

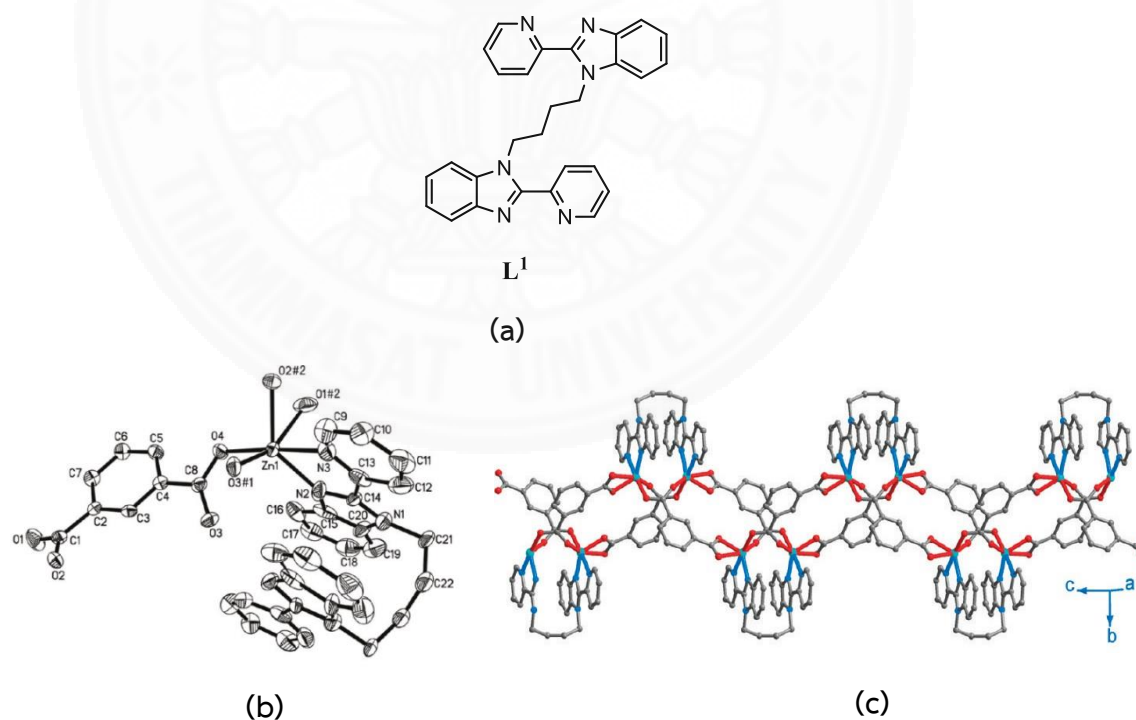


Figure 2.4 (a) Molecular structure of L^1 , (b) Coordination environment of $\text{Zn}(\text{II})$ ion and (c) 1D double chain structure of **II-4** [67].

In 2011, Ma and coworkers [68] synthesized Zn(II) and Cd(II) coordination polymers, namely $[\text{Zn}(5\text{-Br-1,3-bdc})(\text{bpa})(\text{H}_2\text{O})]_n$ (**II-5**) and $[\text{Zn}(4\text{-Br-1,3-bdc})(\text{bpa})(\text{H}_2\text{O})]_n$ (**II-6**) by using hydrothermal reaction of $\text{Zn}(\text{OAc})_2 \cdot 4\text{H}_2\text{O}$, 4-bromo- or 5-bromo-1,3-benzenedicarboxylic acid (4-Br-1,3-bdcH₂ or 5-Br-1,3-bdcH₂) together with 1,2-bis(4-pyridyl)ethane (bpa). The molecular structures of these ligands are shown in Figure 2.5 (a). The crystal structures of both compounds have been studied. The Zn(II) ion in compound **II-5** adopt a distorted trigonal bipyramidal geometry. Each Zn(II) ions are bridged by the 5-Br-1,3-bdc²⁻ ligands to form 1D chains, which are further connected by the hydrogen bonds to form a 2D supramolecular layer. The adjacent 2D networks are parallel and arranged in an ABAB stacking sequence as presented in Figure 2.5(b). For compound **II-6**, the Zn(II) ion is four coordinated to form a tetrahedral geometry. Each 4-Br-1,3-bdc²⁻ links the adjacent Zn(II) ions to form a 1D chain structure. The 1D chain is further connected through the hydrogen bonds to generate a 2D supramolecular network in which the adjacent channels show alternating chirality as shown in Figure 2.5(c).

In 2012, Cheng and coworkers [51] synthesized 1D Zn(II) and Cd(II) coordination polymers, $[\text{Zn}(1,2\text{-bdc})(\text{L}^2)]_n$ (**II-7**), $\{[\text{Zn}_2(1,2\text{-bdc})_2(\text{L}^3)(\text{H}_2\text{O})_2] \cdot 2\text{H}_2\text{O}\}_n$, (**II-8**) and $[\text{Cd}_2(1,3\text{-bdc})_2(\text{L}^2)(\text{H}_2\text{O})_4]_n$ (**II-9**), by the reaction of Zn(II) or Cd(II) salts, benzene-1,2-dicarboxylic acid (1,2-bdcH₂) or benzene-1,3-dicarboxylic acid (1,3-bdcH₂) together with *N,N'*-di(3-pyridyl)adipoamide (L²) or *N,N'*-di(4-pyridyl)adipoamide (L³) under hydrothermal conditions. The molecular structures of L² and L³ are shown in Figure 2.6(a). Their structures have been studied by single crystal X-ray diffraction technique. In compound **II-7**, the Zn(II) ion is four coordinated to form distorted tetrahedral geometry. Each Zn(II) ions are bridged by two 1,2-bdc²⁻ ligands to form dinuclear units and the Zn₂ units are linked to each other via the pyridyl nitrogen atoms of the L² ligands to generate a 1D double-looped chain as shown in Figure 2.6(b). In compound **II-8**, the Zn(II) ion adopt a distorted tetragonal geometry. Each Zn(II) atoms are bridged by two 1,2-bdc²⁻ ligands to form dinuclear units, which are linked to each other by the L³ ligands through the pyridyl nitrogen atoms to form 1D chains with loops as presented in Figure 2.6(c). In compound **II-9**, the Cd(II) ion is six-

coordinated to form distorted octahedral geometry. Each Cd(II) ions are bridged by two 1,3-bdc²⁻ ligands and the pyridyl nitrogen atoms of L² ligands to form 1D ladder chain as exhibited in Figure 2.6(d). Moreover, the solid state photoluminescence of all compound were carried out. The PL spectra of compound **II-7**, **II-8** and **II-9** showed the emission spectra at 386, 397 and 415 nm, respectively.

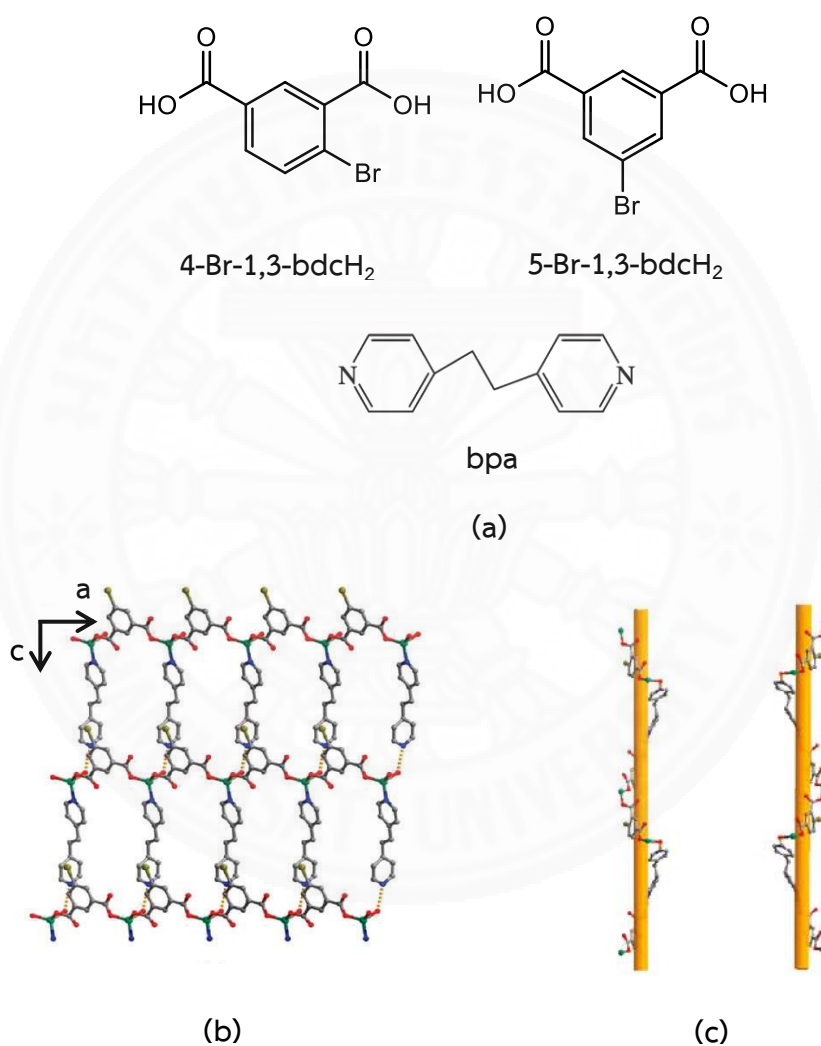


Figure 2.5 (a) Molecular structures of ligands, (b) 1D chain structure with hydrogen bonding to form 2D supramolecular network of **II-5** and (c) view of left- and right-handed helical chains of **II-6** [68].

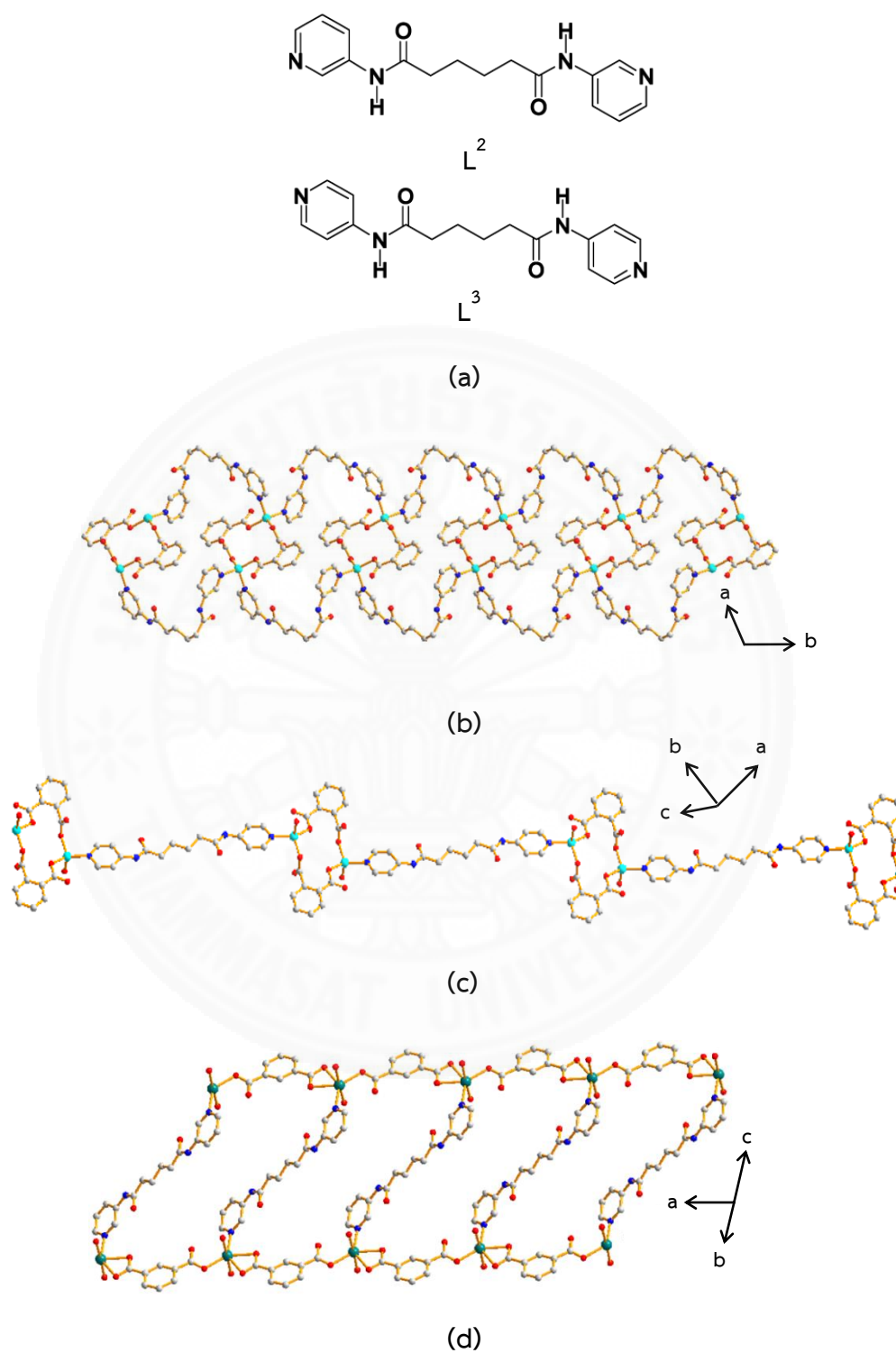


Figure 2.6 (a) Molecular structures of L^2 and L^3 , (b) 1D double-looped chain of **II-7**, (c) 1D chain with loops of **II-8** and (d) 1D ladder chains of **II-9** [51].

In 2013, Sharif and Najafi [69] reported a new 1D Cd(II) coordination polymers, $[\text{Cd}(\text{2,6-dipic})(\text{H}_2\text{O})_{1.5}]_n$ (**II-10**) which obtained from the reaction of 1 mmol $\text{Cd}(\text{NO}_3)_2 \cdot 4\text{H}_2\text{O}$, 1mmol 4-hydroxy-pyridine-2,6-dicarboxylic acid (4-OH-2,6-dipicH₂), 1 mmol pyridine-2,6-dicarboxylic acid (2,6-dipicH₂) and 2 mmol piperazine at 60°C. After allowed the solution mixture to evaporate at room temperature for 3 weeks, the colorless crystals were obtained. The crystal structure showed 4-OH-2,6-dipicH₂ and piperazine were not bonded in the product. This compound consists of two symmetry independent Cd atoms. Both Cd centers are linked to four oxygen and one nitrogen atoms in the equatorial positions and two oxygen atoms in the axial positions resulting to pentagonal bipyramidal geometry. The polymer builds from these dimeric units of **II-10**. The $[\text{CdO}_6\text{N}]$ units (Figure 2.7(a)) share their edges through the equatorial oxygen atoms of their 2,6-dipic²⁻ ligands and form the edge sharing $\text{Cd}_2\text{O}_{10}\text{N}_2$ dimers. Then the carboxylate groups of the 2,6-dipic²⁻ ligands from $\text{Cd1O}_6\text{N}$ and $\text{Cd2O}_6\text{N}$ units are further coordinated to the other $\text{Cd1O}_6\text{N}$ and $\text{Cd2O}_6\text{N}$ units via the axial oxygen atoms and form a 1D helical chain of Cd(II) polymer that runs parallel to the [100] axis as shown in Figure 2.7 (b)). Two CdO_6N pentagonal bipyramidal units with 2,6-dipic²⁻ linkers are connected by a bridging water molecule, which makes the shape look like a pair of pincers. Moreover, there are $\text{C}-\text{O} \cdots \pi$ stacking interactions between the carbonyl groups of the pyridine-2,6-dicarboxylate groups and the pyridine ring of symmetry related. The various hydrogen bonds of type $\text{O}-\text{H} \cdots \text{O}$ and $\text{C}-\text{H} \cdots \text{O}$ are also responsible for the expansion of the structure. Both weak and strong hydrogen bonds with $\text{D} \cdots \text{A}$ distances ranging from 2.613(3) to 3.439(4) Å, are observed in this compound.

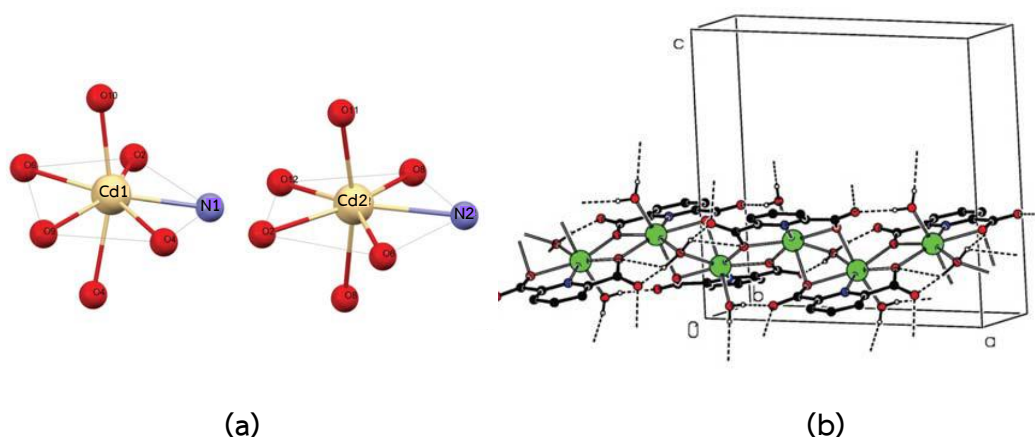


Figure 2.7 (a) Coordination environment around Cd1 and Cd2 and (b) the crystal packing diagram of **II-10** [69]

In 2015, Paraschiv and coworkers [70] reported two new 1D Zn(II) coordination polymers, $[\text{Zn}_2(\text{Htea})_2(1,2\text{-bdc})]_n$ (**II-11**) and $[\text{Zn}(\text{H}_3\text{tris})(1,3\text{-bdc})(\text{CH}_3\text{OH})]_n$ (**II-12**), where H_3tea = triethanolamine, H_3tris = tris(hydroxymethyl)aminomethane, $1,2\text{-bdcH}_2$ = 1,2-benzenedicarboxylic acid and $1,3\text{-bdcH}_2$ = 1,3-benzenedicarboxylic acid. These compounds were synthesized by solvothermal method in the presence of methanol. Their crystal structures of these compounds have been studied. Compound **II-11** has two crystallographically independent Zn(II) ions. The Zn1 atom is five-coordinated, displaying slightly distorted trigonal bipyramidal geometry. The Zn2 atom exhibits a tetrahedral geometry. Each Zn(II) atoms are linked via one *syn-syn* carboxylato and two alkoxo bridges, generating zigzag chains running along the crystallographic *c* axis as presented in Figure 2.8(a). The chains are further connected through hydrogen bonds established between the protonated OH groups from the Htea^{2-} molecules and the uncoordinated oxygen atoms of the $1,2\text{-bdc}^{2-}$ ligands. For compound **II-12**, the reaction of Zn(II) ion, H_3tris , and $1,3\text{-bdcH}_2$ under solvothermal condition led to the formation of a 1D coordination polymer $[\text{Zn}(\text{H}_3\text{tris})(1,3\text{-bdc})(\text{CH}_3\text{OH})]_n$, in which the bridging $1,3\text{-bdc}^{2-}$ ligands link $[\text{Zn}(\text{H}_3\text{tris})(\text{CH}_3\text{OH})]^{2+}$ nodes. Two carboxylato groups belonging to $1,3\text{-bdc}^{2-}$ show different coordination modes: bidentate chelating and monodentate. The Zn(II) center is six-coordinated with a strongly distorted octahedral geometry. The linear

chains run along the crystallographic *a* axis (Figure 2.8(b)). They are further connected *via* hydrogen bonds between the uncoordinated OH groups from the H₃tris molecules and two carboxylato oxygen atoms from an adjacent chain, resulting in layers parallel to the crystallographic *ab* plane. These layers are interconnected into a complex noncovalent 3D network through strong hydrogen bonds involving the uncoordinated OH groups of the H₃tris ligand with the coordinated ones and also with the oxygen atoms from the methanol ligands.

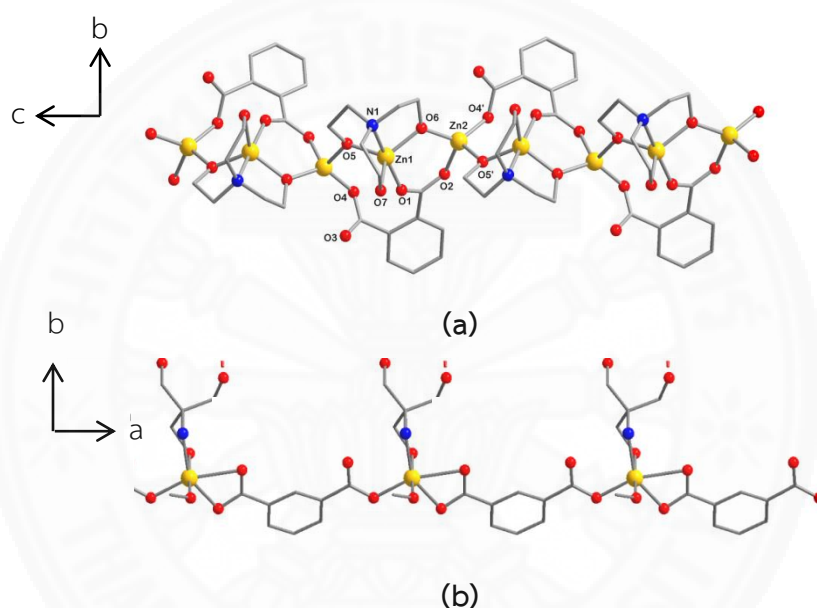


Figure 2.8 (a) Fragment of the zigzag chain in **II-11** and (b) fragment of the linear chain in **II-12** [70]

In 2015, Wang and coworkers [71] reported two new 1D Cd(II) coordination polymers, $[\text{Cd}_2(2,6\text{-dipic})_2(\text{H}_2\text{O})_3]_n$ (**II-13**) and $\{[\text{Cd}_2(4\text{-OH-}2,6\text{-dipic})_2(\text{H}_2\text{O})_4] \cdot 3\text{H}_2\text{O}\}_n$ (**II-14**) where 4-OH-2,6-dipicH₂ = 4-hydroxypyridine-2,6-dicarboxylic acid. These compounds were synthesized by hydrothermal method. The crystal structure of compound **II-13** has two crystallographically independent Cd(II) ions. Both Cd1 and Cd2 are seven-coordinate in distorted pentagonal bipyramidal geometry. 2,6-dipic²⁻ anions are chelated one Cd(II) and bridged another two Cd(II) ions to form a Cd₂O₂ grid. The Cd₂O₂ grids are linked by three bridging $\mu_2\text{-O}$ atoms to

construct a 1D chain as presented in Figure 2.9 (a). Furthermore, each 1D chain further connects three other chains via hydrogen bonding interactions to generate the 3D supramolecular packing structure. In compound **II-14**, there are two crystallographically independent Cd(II) ions. Both Cd1 and Cd2 are close to distorted pentagonal bipyramidal geometry. All hydroxyl groups in 4-OH-2,6-dipic²⁻ are uncoordinated and this ligands have two types of coordination mode. Two Cd1 ions are connected by two μ_2 -O2 and O2A of carboxylate group to form a Cd₂O₂ grid, while a similar Cd₂O₂ grid is constructed by Cd2 ions. Those grids are bridged alternately by μ_2 -O_c of carboxylate group to form a 1D chain structure as shown in Figure 2.9 (b). In addition, each 1D chain is surrounded by four other 1D chains via hydrogen bonds. As a result, a 3D supramolecular packing structure is formed.

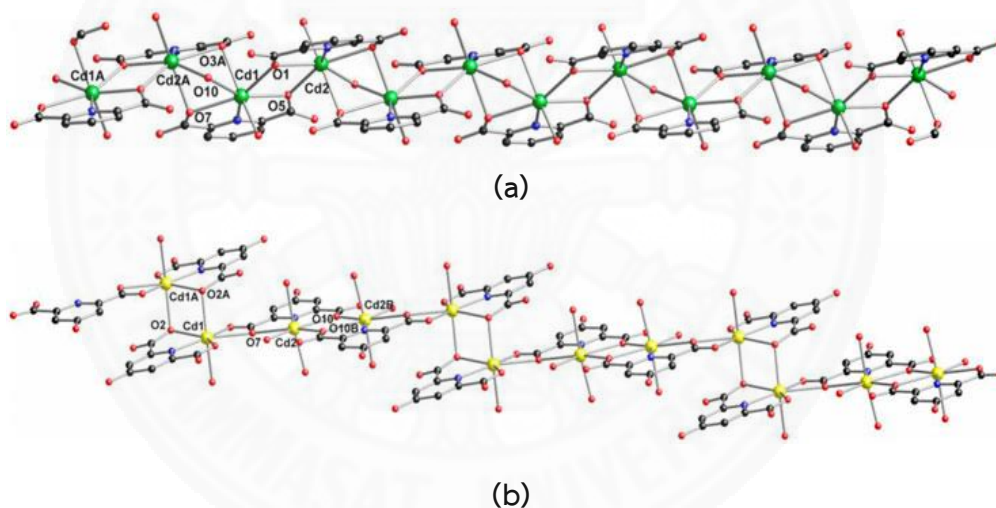


Figure 2.9 (a) 1D chain structure of **II-13** and (b) 1D chain structure of **II-14** [71]

In 2016, Tripathi and coworkers [72] reported two new 1D Zn(II) and Cd(II) coordination polymers, $\{[\text{Zn}_2(\text{pyim}_2)_2(1,3\text{-bdc})_2]\cdot(\text{DMF})_4\}_n$ (**II-15**) and $\{[\text{Cd}(\text{pyim}_2)(\text{p-BDC})(\text{H}_2\text{O})]\cdot(\text{H}_2\text{O})_2\}_n$ (**II-16**) where $\text{pyim}_2 = 2,6\text{-bis}(\text{imidazol-1-yl})\text{pyridine}$ (Figure 2.10(a)). These compounds were synthesized by using layers diffusion method in the ratio of metal: pyim_2 : bdcH_2 is 1:2:1 with DMF and methanol solvents. The X-ray diffraction study exhibits that each Zn(II) ion in compound **II-15** is located in a tetrahedral environment with the ZnN_2O_4 unit. The 1,3- bdc^{2-} anion is coordinated to the Zn(II)

center in the η^1 mode, therefore linking two Zn(II) ions, which are further connected through the pym_2 ligand to form a loop structure. As a result, two Zn(II) ions form a dimeric 18-membered macrocycle composed of one pym_2 and one $1,3\text{-bdc}^{2-}$ ligand, which further coordinate to another macrocycle to generate the 1D chain as shown in Figure 2.10 (b). In addition, the stability of 1D chain is provided through $\text{CH}\cdots\text{O}$, $\text{CH}\cdots\pi$ and $\pi\text{-}\pi$ interactions, resulting to a 2D supramolecular arrangement. In compound **II-16**, Cd(II) ion displays a distorted pentagonal bipyramidal geometry with a CdN_2O_5 unit. The $1,4\text{-bdc}^{2-}$ units are present in the chelating η^2 mode and connect two Cd(II) ions, generating a 1D chain structure as presented in Figure 2.10 (c). Further stabilization of 1D chain is provided through $\text{C-H}\cdots\pi$, $\pi\text{-}\pi$, hydrogen bond and $\text{CH}\cdots\text{O}$ interactions, which together interconnect two adjacent 1D chains. In addition, one of the lattice water molecules acts as a bridge between two independent 1D chains and interacts with one of the 1D chains through hydrogen bonding and to the other 1D chain via $\text{CH}\cdots\text{O}$ interactions, leading to a 2D supramolecular structure. Moreover, the solid state photoluminescence of all compound were investigated. The PL spectra of compound **II-15** and **II-16** exhibited the emission spectra at 360 and 348 nm, respectively.

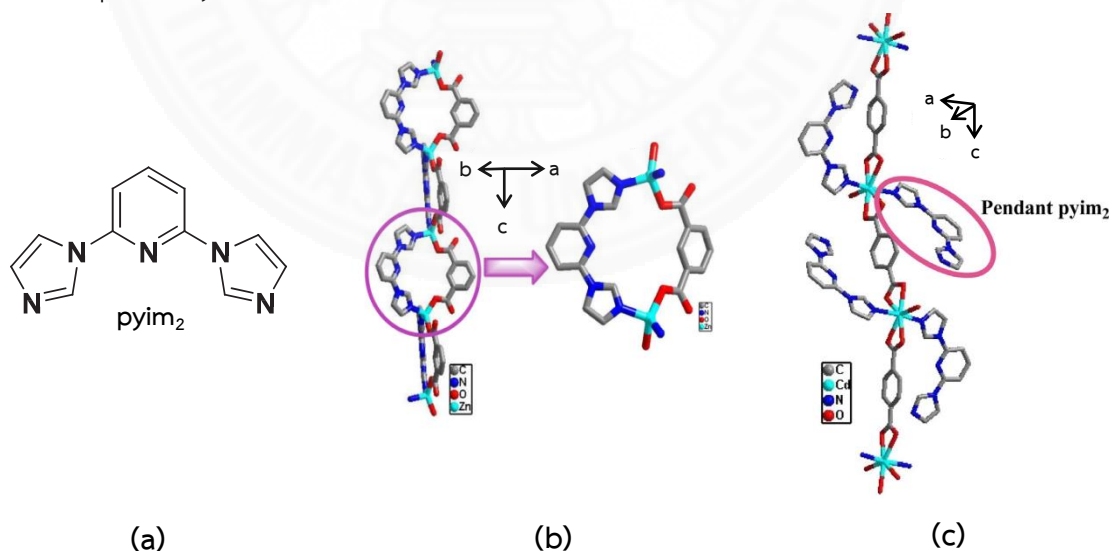


Figure 2.10 (a) Molecular structure of pym_2 , (b) 1D chain structure of **II-15** showing the dimeric 18-membered macrocycle and (c) 1D chain structure of **II-16** with a pendant pym_2 ligand [72]

In 2017, Croitor and coworkers [73] reported two new 1D Cd(II) coordination polymers, $\{[\text{Cd}(1,3\text{-bdc})(4\text{-pyao})(\text{H}_2\text{O})_2]\cdot\text{DMF}\cdot\text{H}_2\text{O}\}_n$ (**II-17**) and $\{[\text{Cd}(1,4\text{-bdc})(4\text{-pyao})_2(\text{H}_2\text{O})]\cdot\text{DMF}\}_n$ (**II-18**) where 4-pyao = pyridine-4-aldoxime (Figure 2.11(a)). Both compounds were synthesized by direct method in the presence of methanol, water and DMF solvent. The Cd(II) center in compound **II-17** adopt the CdNO_6 pentagonal bipyramidal geometry. Consequently, an extension of these Cd(II) nodes results in the formation of a 1D translational chain running along the *c* axis as shown in Figure 2.11 (b). These 1D chains are further interconnected by interlayer hydrogen-bonds between the water ligands and carboxylate groups to generate a 2D hydrogen-bonded network. In compound **II-18**, each Cd(II) ion is seven coordinated, showing a distorted pentagonal bipyramidal geometry. The 1,4-bdc²⁻ anion acts in the *bis*-bidentate chelating mode. The zigzag-like chains are further interlinked by $\text{OH}\cdots\text{O}$ hydrogen bonds between the 4-pyao and water ligands and carboxylate groups to afford a 3D supramolecular framework.

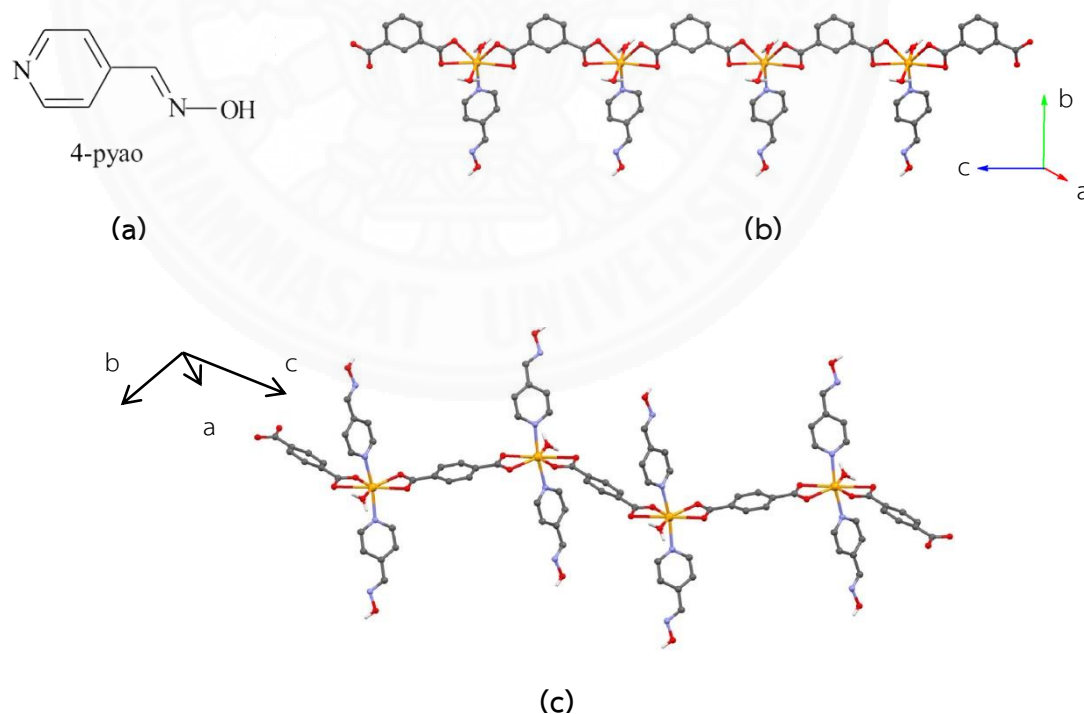


Figure 2.11 (a) Molecular structure of 4-pyao, (b) fragment of 1D chain structure of **II-17** and (c) fragment of 1D chain structure of **II-18** [72]

2.2 Two-dimensional Zn(II) and Cd(II) containing aromatic dicarboxylate derivatives CPs

In 2005, Wen and coworkers [64] successfully synthesized and structurally characterized three novel 2D Zn(II) coordination polymers, $\{[\text{Zn}_2(2,6\text{-dipicO})_2(4,4'\text{-bpy})_2(\text{H}_2\text{O})_2]\cdot 3\text{H}_2\text{O}\}_n$ (**II-19**), $[\text{Zn}(2,6\text{-dipicO})(\text{bix})]_n$ (**II-20**) and $\{[\text{Zn}(2,6\text{-dipicO})(\text{bbi})]\cdot 0.5\text{H}_2\text{O}\}_n$ (**II-21**) when 2,6-dipicOH₂ = pyridine-2,6-dicarboxylic acid *N*-oxide, 4,4'-bpy = 4,4'-bipyridine, bix = 1,4-bis(imidazol-1-ylmethyl)benzene and bbi = 1,1'-(1,4-butanediyl)bis(imidazole). The molecular structures of these ligands are shown in Figure 2.12(a). These structures were synthesized by hydrothermal method. The X-ray diffraction study displays that each Zn(II) center in compound **II-19** exhibits a distorted octahedron geometry. This compound is an infinite chiral 2D brick wall-like layer structure in the *ac* plane built from achiral components, which is composed of $\{\text{Zn}_2(2,6\text{-dipicO})_2\}$ dimer units and 4,4'-bpy linkages, with 2₁ helices running along the *c* axis as shown in Figure 2.12(b). The free water molecules are included between the layers, and the layers are stacked in an -ABAB- sequence along the *b* axis with strong interlayer hydrogen-bond interactions by the coordinated and free water molecules linking the carboxylic acid moieties, thus generating the construction of a 3D host-guest network. For compounds **II-20** and **II-21**, each crystallographically unique Zn(II) metal center in a less-common distorted trigonal bipyramidal geometry, $\{\text{ZnN}_2\text{O}_3\}$. The fully deprotonated 2,6-dipicO²⁻ anions act as effective tridentate bridging ligands linking the Zn(II) centers by monodentate carboxylate and *N*-oxide groups. It is noteworthy that the repetition of the $\{\text{ZnN}_2\text{O}_3\}$ metallic structural motif of **II-20** generates an infinite 2D herringbone architecture extended in the *ac* plane as presented in Figure 2.12(c). The resulting 2D structure is cross-linked by weaker hydrogen-bond interactions between C-H groups from a bix ligand and uncoordinated carboxylate or *N*-oxide oxygen atoms, thus producing a 3D supramolecular framework. Interestingly, there is a 34-membered metallocycle in the 2D layer developed in the *ab* plane for compound **II-21** as displayed in Figure 2.12(d). Lattice water molecules are also included between the layers, and the

relatively weaker $O_{\text{water}}-H\cdots N$ and $C-H\cdots O_{\text{carboxylate}}$ hydrogen bonds complete the final 3D supramolecular framework.

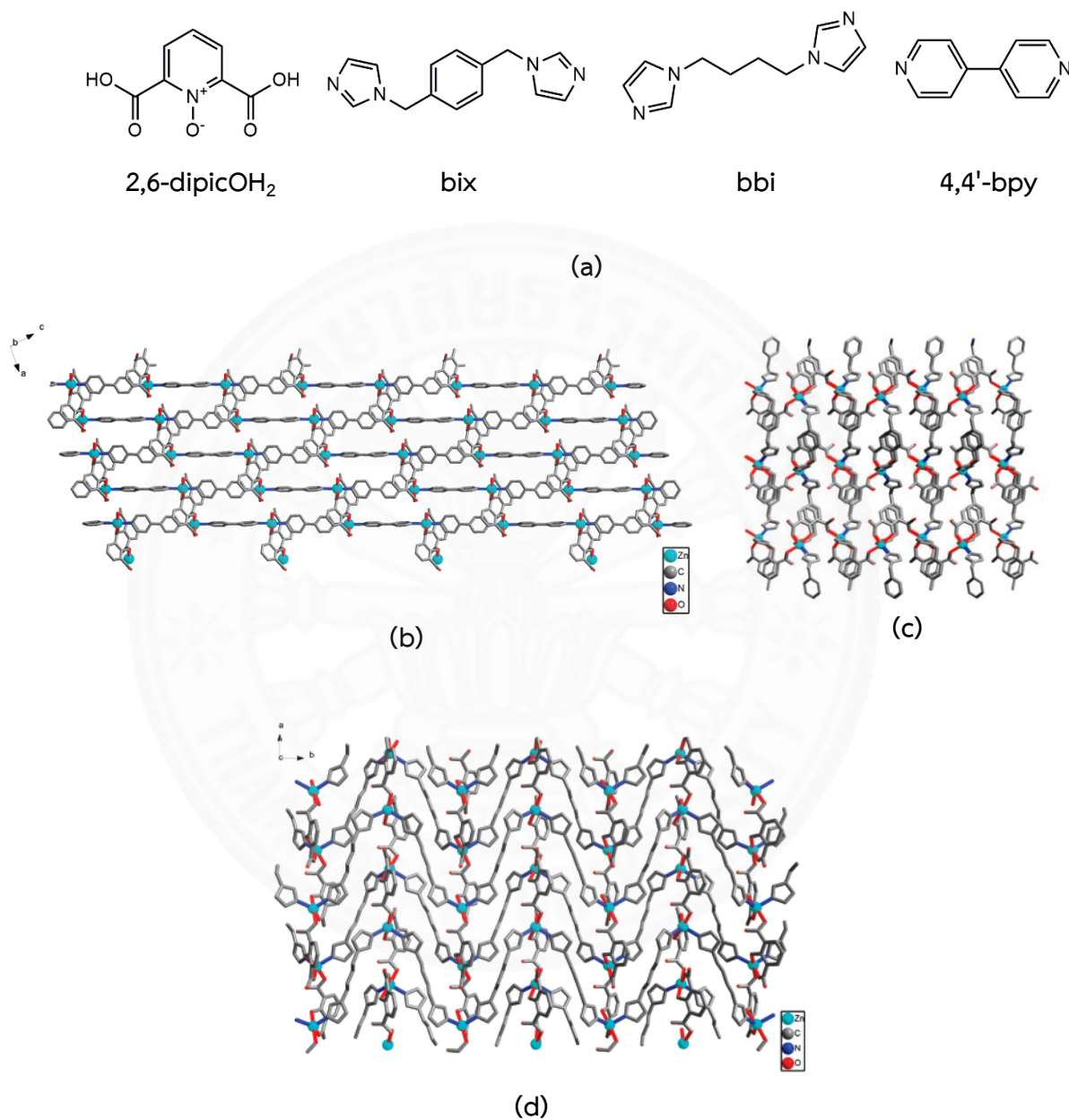


Figure 2.12 (a) Molecular structures of 2,6-dipicOH₂, bix, bbi and 4,4'-bpy, (b) 2D brick-wall-like framework of **II-19**, (c) 2D herringbone architecture of **II-20** and (d) 2D herringbone architecture of **II-21** [64]

In 2006, Wen and coworkers [74] successfully synthesized a novel 2D Cd(II) coordination polymer, $[\text{Cd}_2(\mu_2\text{-OH}_2)(2,6\text{-dipic})_2(\text{bix})]_n$ (**II-22**) (bix=1,4-bis(imidazol-1-yl)methyl) benzene) by the reaction of $\text{CdCl}_2 \cdot 2\text{H}_2\text{O}$, 2,6-dipicH₂, bix and NaOH in the ratio of 1:1:1:2 under hydrothermal condition. The crystal structure of this compound has two crystallographically Cd(II) centers, Cd1 is in a distorted pentagonal bipyramidal geometry which is completed by one bix nitrogen atom and one carboxylate oxygen atom occupying the apical positions, while the basal plane is completed by three oxygen atoms and one nitrogen atom from two different 2,6-dipic²⁻ ligands, as well as one aqua ligand, Cd2 is surrounded by four carboxylate oxygen from three inequivalent 2,6-dipic²⁻ ligands, two nitrogens from one 2,6-dipic²⁻, one bix, and one coordinated water molecule, also in a highly distorted pentagonal bipyramidal geometry. The 2,6-dipic²⁻ ligand acts as a triconnector by the bimonodentate carboxylate and pyridyl N group. Cd1 atoms and Cd2 atoms are bridged by three $\mu_2\text{-O}$ bridges from two separate carboxylate moieties and one aqua to form dimer units, which are further interconnected by another two carboxylate oxygen bridges to generate a 1D chain running along the *c* axis as shown in Figure 2.13(a). Progression of the 1D chain via bix along the *b* axis produces a 2D infinite layer framework as illustrated in Figure 2.13(b). The resulting 2D structure is cross-linked by hydrogen-bond interactions between C-H groups from bix and uncoordinated carboxylate oxygen atoms, thus producing a 3D supramolecular framework.

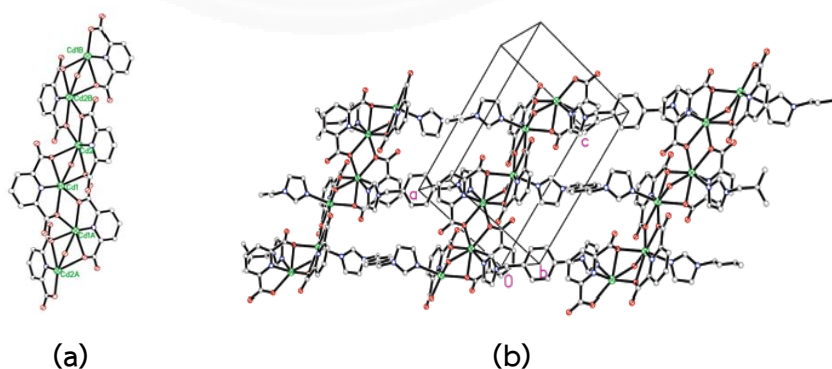


Figure 2.13 (a) 1D chain running along the *c* axis based on 2,6- dipic and Cd ions and (b) 2D infinite layer framework extended in the *bc* plane of **II-22** [74]

In 2006, Gao and coworkers [65] reported a new 2D Zn(II) coordination polymer, $\{[\text{Zn}(4\text{-OH-2,6-dipic})]\cdot\text{H}_2\text{O}\}_n$ (**II-23**) where 4-OH-2,6-dipicH₂ = 4-hydroxypyridine-2,6-dicarboxylic acid. This compound was synthesized by the reaction mixture of ZnSO₄ (0.2 mmol), 4-OH-2,6-dipicH₂ (0.2 mmol), H₂O and ethanol under solvothermal condition. The crystal structure of this compound reveals that the Zn(II) ion is five coordinated with a distorted trigonal bipyramidal geometry. Each Zn(II) atom are connected together via four 4-OH-2,6-dipic²⁻ molecules to form a 2D grid with a (4,4) network, which give two kind of Zn...Zn distances (4.979 and 5.315 Å) as shown in Figure 2.14(a). The hydroxyl oxygen atoms in 4-OH-2,6-dipic²⁻ do not coordinate to the Zn(II) centers, which direct the formation of hydrogen bonds with water molecules. The hydrogen bonds between carboxylate O atoms or OH groups and water molecules connect the 2D coordination sheets to form a 3D supramolecular structure. The 2D coordination sheets pack in an ABAB sequence along the *c* axis with channels of the approximated dimensions 5 × 5 Å². Moreover, the solid state luminescence property of this compound was investigated. The PL spectrum of this compound exhibited the strong fluorescent emission spectrum at 543 nm while excitation at 388 nm as presented in Figure 2.14(b).

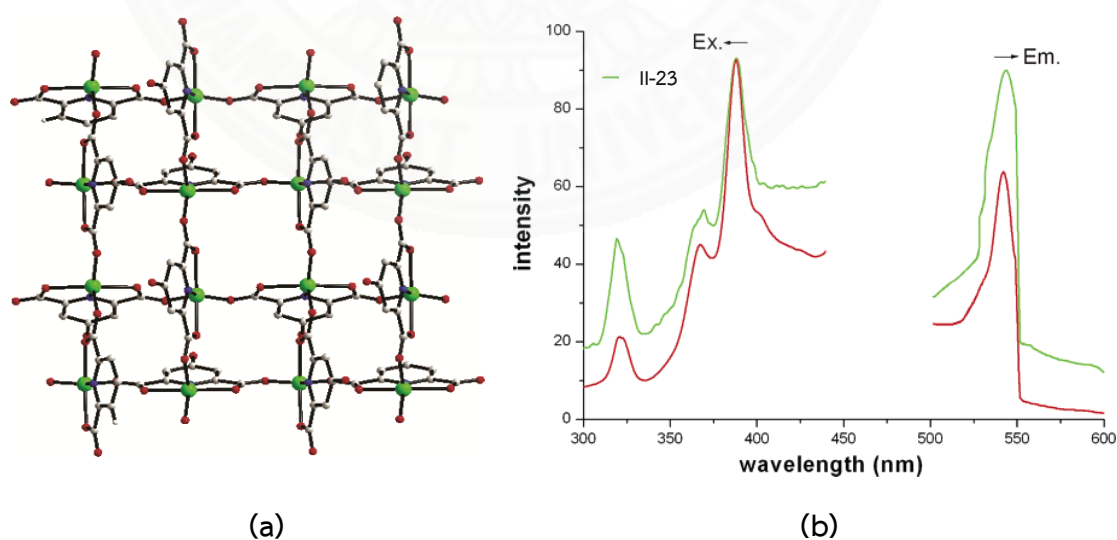


Figure 2.14 (a) 2D (4,4) net linked via carboxylate groups along the *c* axis and (b) excitation and emission spectra in the solid state of **II-23** (green) [65]

In 2010, He and coworkers [75] successfully synthesized and crystal structure studied a new 2D Zn(II) coordination polymer, $[\text{Zn}(\text{BITMB})(1,3\text{-bdc})\cdot 3\text{H}_2\text{O}]_n$ (**II-24**) (where BITMB = 1,3-bis(imidazol-1-ylmethyl)-2,4,6-trimethylbenzene and $1,3\text{-bdcH}_2 = 1,3\text{-benzenedicarboxylic acid}$), by the reaction mixture of $\text{Zn}(\text{NO}_3)_2\cdot 6\text{H}_2\text{O}$, $1,3\text{-bdcH}_2$, BITMB, DMF, EtOH and H_2O under solvothermal condition. The molecular structure of BITMB is shown in Figure 2.15(a). The result shows that the central Zn(II) ion adopts a tetrahedral geometry and is coordinated by two oxygen atoms from different $1,3\text{-bdc}^{2-}$ ligands and two nitrogen atoms from different BITMB ligands. Two BITMB ligands link two Zn(II) ions to generate a 24-membered macrometallocycle. Both carboxylate groups of $1,3\text{-bdc}^{2-}$ adopts a bidentate bridging mode to link two Zn(II) ions. Thus, every $1,3\text{-bdc}^{2-}$ ligand links two macrometallocycle subunits and each macrometallocycle subunit attaches to four $1,3\text{-bdc}^{2-}$ ligands, resulting to the formation of a 2D layer as presented in Figure 2.15(b). Furthermore, the solid state luminescence property of this compound was carried out. The PL spectrum of this compound exhibited the strong fluorescent emission spectrum at 460 and 548 nm while excitation at 250 nm as shown in Figure 2.15(c).

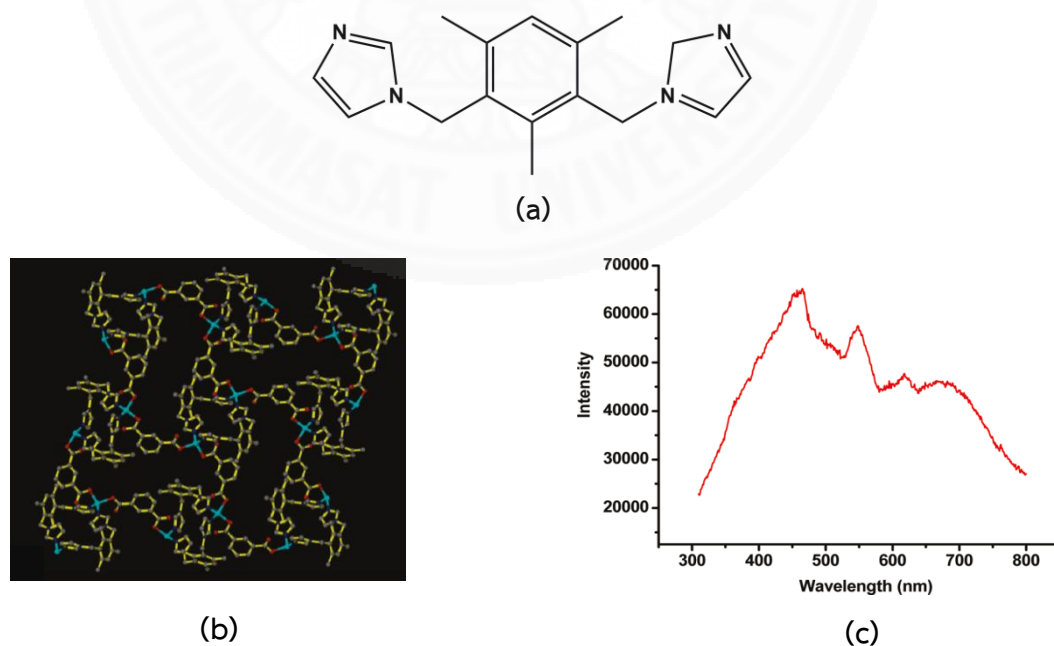


Figure 2.15 (a) Molecular structure of BITMB, (b) 2D layer and (c) solid-state emission spectrum of **II-24** [75]

In 2010, Liu and coworkers [67] reported three new 2D Zn(II) coordination polymers, $[\text{Zn}_2(1,4\text{-bdc})_2(\text{L}^1)(\text{H}_2\text{O})_2]_n$ (**II-25**), $[\text{Zn}_2(1,3\text{-bdc})_2(\text{L}^2)] \cdot 2.25\text{H}_2\text{O}$ (**II-26**) and $[\text{Zn}_2(1,4\text{-bdc})_2(\text{L}^2)] \cdot \text{CH}_3\text{OH}$ (**II-27**) where $\text{L}^1 = 1,1'-(1,4\text{-butanediyl})\text{bis}[2-(2\text{-pyridyl})\text{benzimidazole}]$, $\text{L}^2 = 1,1'-(1,6\text{-hexanediyl})\text{bis}[2-(2\text{-pyridyl})\text{benzimidazole}]$. The molecular structures of L^1 and L^2 are shown in Figure 2.16(a). These compounds were synthesized by solvothermal method in the presence of water and methanol. Their crystal structures have been studied. The results exhibit that the Zn(II) center in compound **II-25** is five coordinated with a trigonal bipyramidal geometry. The carboxylate groups of the $1,4\text{-bdc}^{2-}$ anion exhibit the *bis*-monodentate coordination mode. In this mode, the $1,4\text{-bdc}^{2-}$ anions link the Zn(II) ions to give a 1D zigzag chain. The adjacent chains are further bridged by L^2 ligands to form a 2D layer as shown in Figure 2.16(b). For compound **II-26**, the Zn(II) center displays a distorted tetrahedral geometry. Each $1,3\text{-bdc}^{2-}$ coordinates to two Zn(II) ions with two carboxylate groups adopting *bis*-monodentate coordination modes. The adjacent Zn(II) atoms are bridged by the $1,3\text{-bdc}^{2-}$ ligands to form 1D chains, which are further connected by L^2 ligands to generate a 2D wave-like layer as presented in Figure 2.16(c). For compound **II-27**, the Zn(II) atom shows an octahedral coordination geometry with $[\text{ZnO}_4\text{N}_2]$. The $1,4\text{-bdc}^{2-}$ anions bridge adjacent Zn(II) atoms in the bidentate chelating modes to generate a 1D zigzag chain, which is further connected by L^2 ligands to form a 2D (6,3) sheet as illustrated in Figure 2.16(d).

In 2011, Ma and coworkers [68] successfully synthesized Zn(II) and Cd(II) coordination polymers, $\{[\text{Zn}_2(5\text{-Br-}1,3\text{-bdc})_2(4,4'\text{-bpy})(\text{H}_2\text{O})] \cdot 2\text{H}_2\text{O}\}_n$ (**II-28**) and $\{[\text{Cd}(4\text{-Br-}1,3\text{-bdc})(\text{bpp})]\}_n$ (**II-29**) by hydrothermal reactions based on 4-bromo- or 5-bromo-1,3-benzenedicarboxylic acid ($4\text{-Br-}1,3\text{-bdcH}_2$ or $5\text{-Br-}1,3\text{-bdcH}_2$) and different dipyridyl types co-ligands, 4,4'-bipyridyl (4,4'-bpy) and 1,3-di(4-pyridyl)propane (bpp). The molecular structures of these ligands are shown in Figure 2.17(a). Their crystal structures were studied. The results exhibit that the Zn(II) center in compound **II-28** is four coordinated with a tetragonal geometry. Each Zn(II) ions are bridged by the $5\text{-Br-}1,3\text{-bdc}^{2-}$ ligands to form a 1D chain and such 1D chains are further linked by the 4,4'-bpy ligand via Zn-N coordination bonds, generating a 2D (6,3) network as shown

in Figure 2.17(b). For compound **II-29**, the Cd(II) center is six-coordinated, adopting a slightly distorted octahedral geometry. The 4-Br-1,3-bdc²⁻ ligands link the Cd(II) ions, generating a 1D chain. Each 1D chains are further connected via the bpp ligands to produce a 2D layer, which can be classified as a (3.5)-connected network with (4²·6) (4²·6⁷·8) topology as presented in Figure 2.17(c).

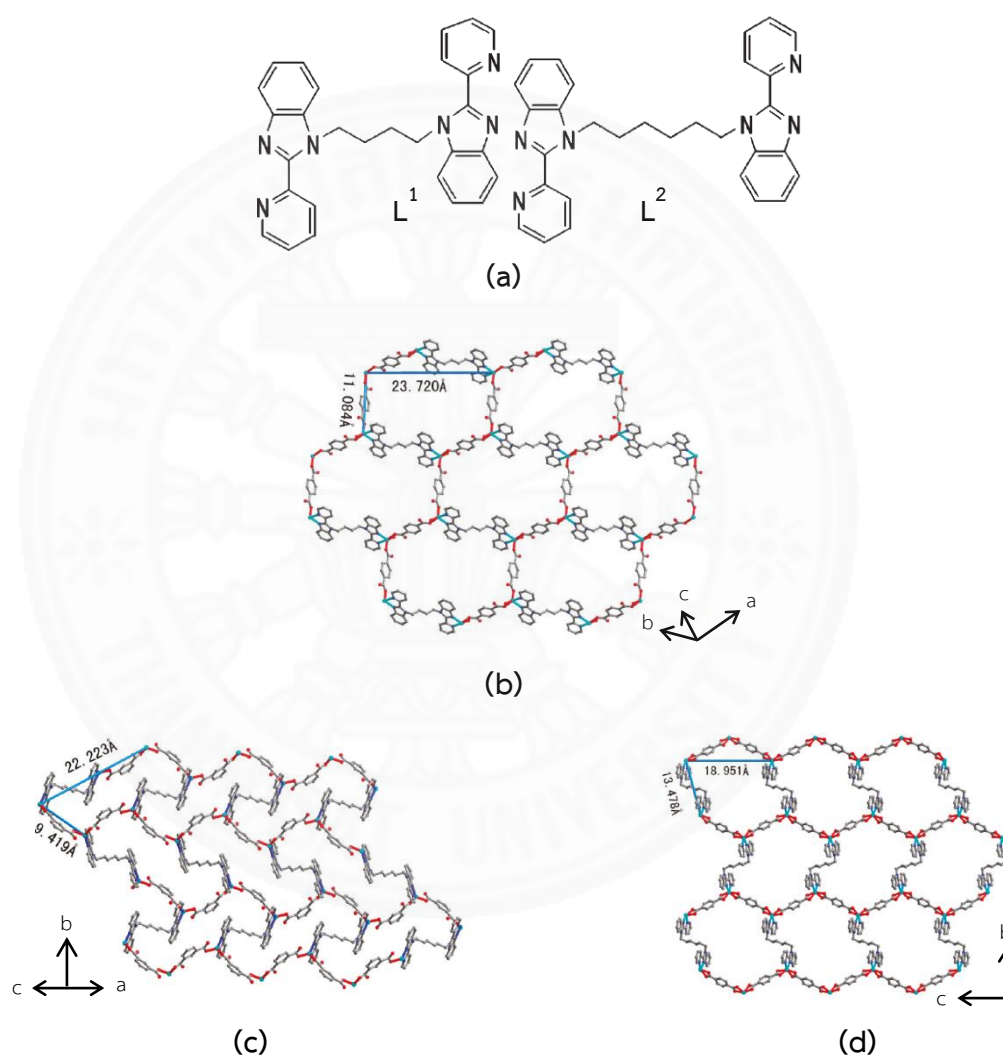


Figure 2.16 (a) Molecular structures of L¹ and L², (b) view of the 2D layer of **II-25**, (c) view of the 2D wave-like sheet structure of **II-26** and (d) view of the 2D sheet structure of **II-27** [67]

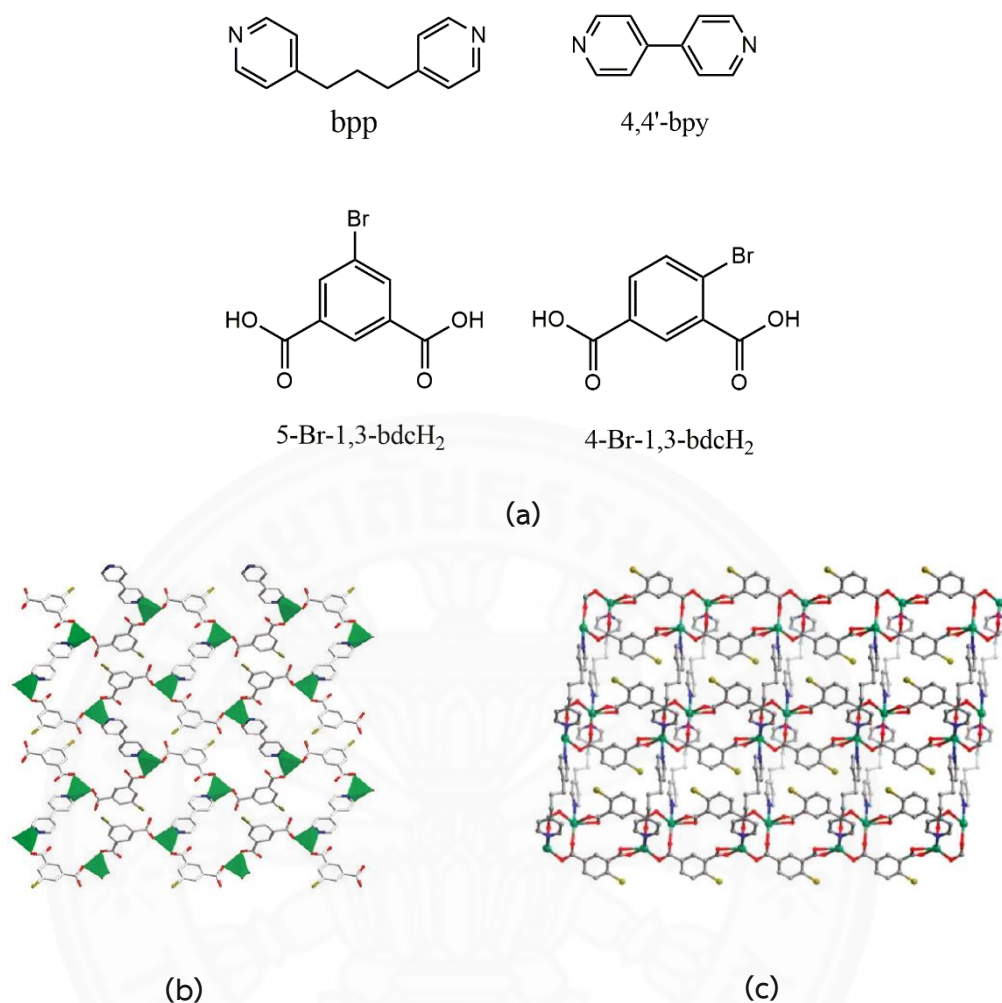


Figure 2.17 (a) Molecular structures of bpp, 4,4'-bpy, 5-Br-1,3-bdcH₂ and 4-Br-1,3-bdcH₂, (b) view of the 2D layer of **II-28** and (c) view of the 2D layer of **II-29** [68]

In 2012, Cheng and coworkers [51] reported four new 2D Zn(II) and Cd(II) coordination polymers containing the flexible dipyridyl amide and the rigid dicarboxylate ligands, [Zn₂(1,3-bdc)₂(L²)(H₂O)₂]_n (**II-30**), [Zn₂(1,4-bdc)₂(L¹)(H₂O)₂]_n (**II-31**), [[Cd(1,2-bdc)(L²)(H₂O)]·H₂O]_n (**II-32**) and [Cd₂(1,4-bdc)₂(L¹)(H₂O)₂]_n (**II-33**), When L¹ = *N,N'*-di(2-pyridyl) adipoamide and L² = *N,N'*-di(3-pyridyl) adipoamide. The molecular structures of L¹ and L² are shown in Figure 2.18(a). These compounds were synthesized by hydrothermal method. Their crystal structures have been studied. The results show that the Zn(II) center in compound **II-30** is four coordinated with a distorted tetrahedral geometry. Each Zn(II) ions are bridged by the L¹ and 1,3-bdc²⁻

ligands to generate highly undulated 2D hexagonal (hcb) layers, which are equivalent and are composed of 62-membered metallocycles as presented in Figure 2.18(b). For compound **II-31**, Zn(II) center is five coordinated with a distorted square pyramidal geometry. Each Zn(II) ions are bridged by the L^1 and $1,4\text{-bdc}^{2-}$ ligands to form planar 2D hexagonal nets (hcb) as shown in Figure 2.18(c). The 2D nets are also interconnected by the hydrogen bonds between the N-H groups of L^1 ligands and carboxylate oxygen of $1,4\text{-bdc}^{2-}$ ligands. For compound **II-32**, Cd(II) center is seven coordinated with a distorted pentagonal bipyramidal geometry. The Cd(II) ions are bridged by the L^2 and the $1,2\text{-bdc}^{2-}$ to form 2D pleated layer with loops as illustrated in Figure 2.18(d). The 2D nets are further connected by the hydrogen bonds between the N-H groups of L^2 ligands and carboxyl oxygen of $1,2\text{-bdc}^{2-}$ ligands. For compound **II-33**, Cd(II) center is six coordinated with a distorted octahedral geometry. The Cd(II) ions are bridged by the L^1 and $1,4\text{-bdc}^{2-}$ ligands to form pleated 2D hexagonal nets (hcb) as shown in Figure 2.18(e). The 2D nets are also interconnected by the hydrogen bonding interactions between the N-H groups of L^1 ligands and carboxyl oxygen of $1,4\text{-bdc}^{2-}$ ligands. Moreover, the solid state luminescence property of these compounds was investigated. The PL spectra of these compounds showed the fluorescent emission spectra at 398, 392, 414 and 387 nm after excitation at 339, 340, 328 and 335 nm for compounds **II-30**, **II-31**, **II-32** and **II-33**, respectively.

In 2013, Zhang and coworkers [76] reported three new 2D Zn(II) and Cd(II) coordination polymers, $[\text{Zn}(5\text{-OH-1,3-bdc})(\text{btb})]\cdot 2\text{H}_2\text{O}$ (**II-34**), $[\text{Cd}(5\text{-OH-1,3-bdc})(\text{btp})(\text{H}_2\text{O})]\cdot 3\text{H}_2\text{O}$ (**II-35**) and $[\text{Cd}(5\text{-OH-1,3-bdc})(\text{bth})_2(\text{H}_2\text{O})]\cdot \text{H}_2\text{O}$ (**II-36**) when btb = 1,4-bis(1,2,4-triazol-1-yl)butane, btp = 1,3-bis(1,2,4-triazol-1-yl)propane, bth = 1,6-bis(1,2,4-triazol-1-yl)hexane (Figure 2.19(a)) and $5\text{-OH-1,3-bdcH}_2 = 5\text{-hydroxy-1,3-benzenedicarboxylic acid}$. These compounds were synthesized by hydrothermal method. Their crystal structures have been studied. The Zn(II) center of compound **II-34** is five coordinated with a distorted bipyramidal coordination geometry. Each 5-OH-1,3-bdc^{2-} ligand acts as a binode in which one carboxylate group is chelating while the other carboxylate group shows monodentate mode, bridging two Zn(II)

atoms in $(k^1)-(k^2)-\mu_2$ mode. Each Zn(II) is coordinated by two btb and two 5-OH-1,3-bdc²⁻ ligands to form a neutral undulated 2D (4,4) network as shown in Figure 2.19(b). For compound **II-35**, Cd(II) ion is eight coordinated and exhibits a distorted pentagonal bipyramidal coordination geometry. Four Cd(II) atoms, two btp, and two 5-OH-1,3-bdc²⁻ ligands generate a $[\text{Cd}_4(\text{btp})_2(5\text{-OH-1,3-bdc})_2]$ unit and extend to form an undulated 2D (4,4) network as presented in Figure 2.19(c). For compound **II-36**, seven-coordinated Cd(II) ion is coordinated by five O atoms from two 5-OH-1,3-bdc²⁻ ligands and one coordinated water, two N atoms from two bth ligands and displays a distorted pentagonal bipyramidal coordination geometry. The ligand 5-OH-1,3-bdc²⁻ shows the bischelating coordination mode, generating a 2D undulated (4,4) net in “ABAB” packing fashion as shown in Figure 2.19(d). Furthermore, compound **II-34** and **II-35** show reversible dehydration-rehydration behaviors with an exposure to water vapor at ambient temperature, indicating their possible potential uses as water absorbents.

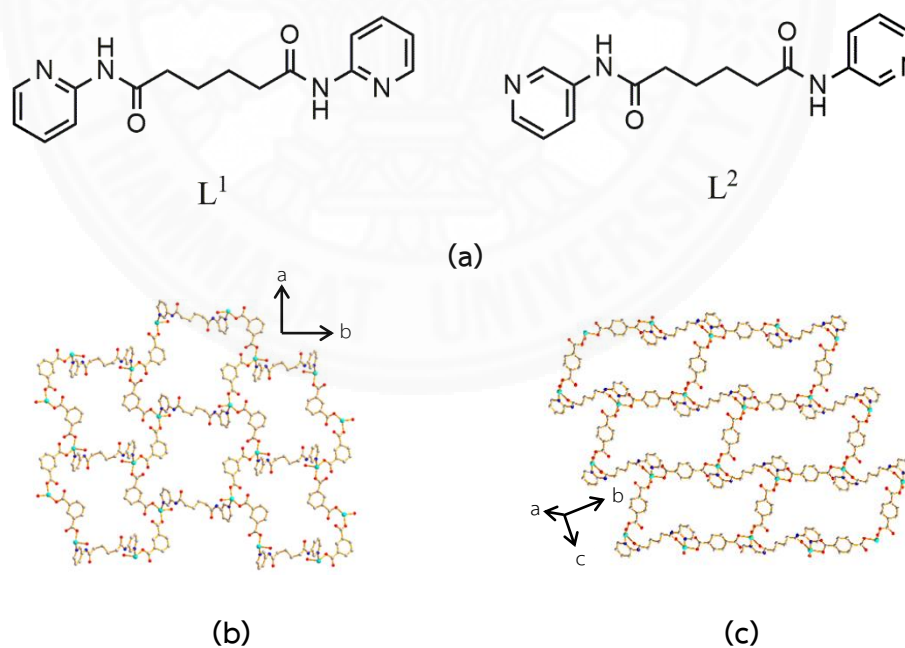


Figure 2.18 (a) Molecular structures of L^1 and L^2 , (b) view of the 2D hexagonal nets of **II-30**, (c) view of the 2D hexagonal nets of **II-31**, (d) pleated 2D net of **II-32** and (e) pleated 2D hexagonal net of **II-33** [51]

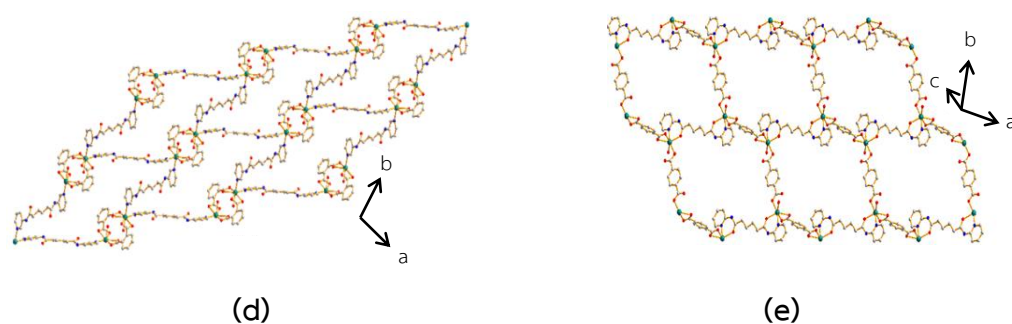


Figure 2.18 (a) Molecular structures of L^1 and L^2 , (b) view of the 2D hexagonal nets of **II-30**, (c) view of the 2D hexagonal nets of **II-31**, (d) pleated 2D net of **II-32** and (e) pleated 2D hexagonal net of **II-33** (cont.) [51]

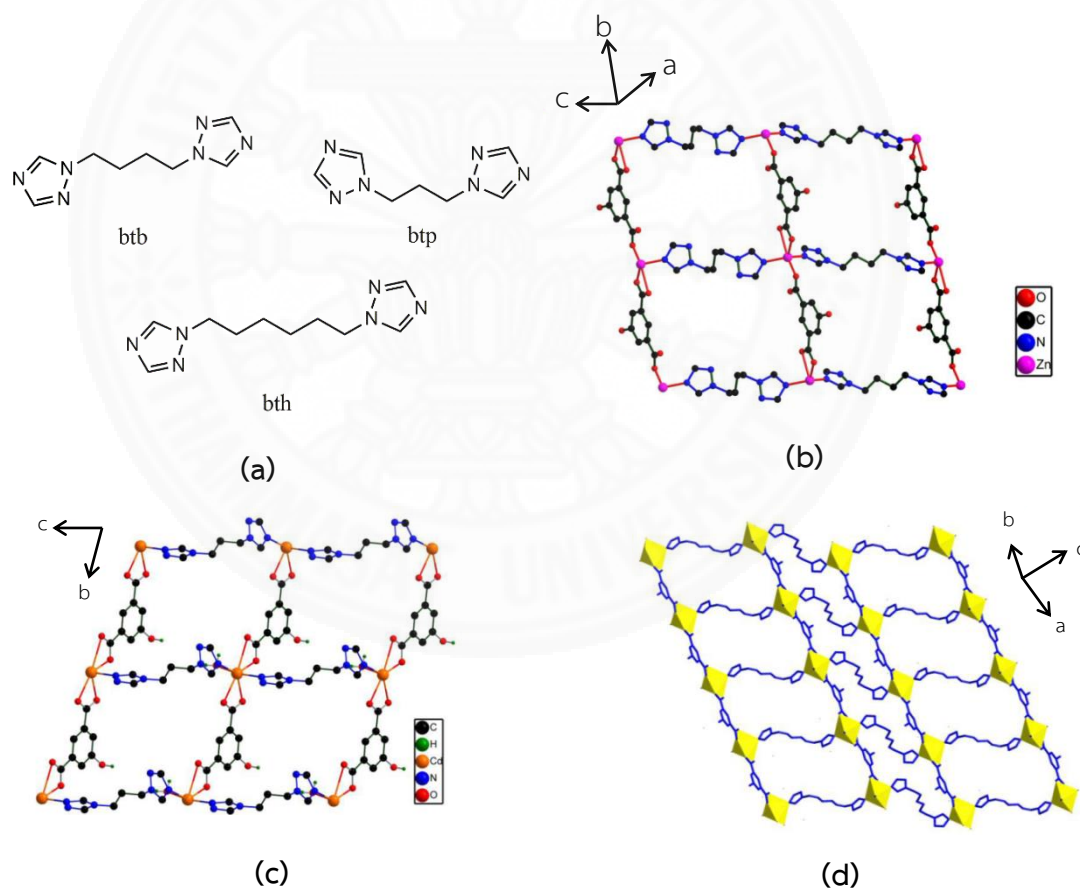


Figure 2.19 (a) Molecular structures of btb, btp and bth ligands, (b) view of the undulated 2D (4,4) network of **II-34**, (c) view of the undulated 2D (4,4) network of **II-35** and (d) view of the undulated 2D (4,4) network of **II-36** [76]

In 2014, Zhang and coworkers [77] reported a new 2D Zn(II) coordination polymer, $\{[\text{Zn}(\text{L}^1)(1,3\text{-bdc})]\}_n$ (**II-37**), when $\text{L}^1 = 4,4'-(2,5\text{-dimethoxy-1,4-phenylene})$. The molecular structure of L^1 is shown in Figure 2.20(a). This compound was synthesized by the reaction mixture of $\text{Zn}(\text{NO}_3)_2 \cdot 6\text{H}_2\text{O}$, L^1 , $1,3\text{-bdcH}_2$, H_2O and DMF under solvothermal condition. The crystal structure has been studied. The results show that Zn(II) center is six-coordinated by four carboxylate oxygen atoms from three different $1,3\text{-bdc}^{2-}$ ligands and two nitrogen atoms belonging to two L^1 ligands. Two carboxyl groups of $1,3\text{-bdc}^{2-}$ adopt two different coordination modes, one adopts bidentate bridging mode to combine two Zn(II) ions, the other adopts bidentate chelating mode to connect one Zn(II) ion. The $1,3\text{-bdc}^{2-}$ ligands link the Zn(II) ions to form a 1D chain. Each 1D chain is further extended via L^1 ligands from nearly perpendicular direction to furnish a 2D layer. From a topological perspective, the 2D layers can be simplified to (4,4) connected **sql** nets with point symbol $\{4^4 \cdot 6^2\}$ as shown in Figure 2.20(b). In addition, the solid state luminescence property of this compound was investigated. As shown in Figure 2.20(c), the PL spectrum of this compound exhibited the fluorescent emission spectrum at 420 nm while excitation at 350 nm.

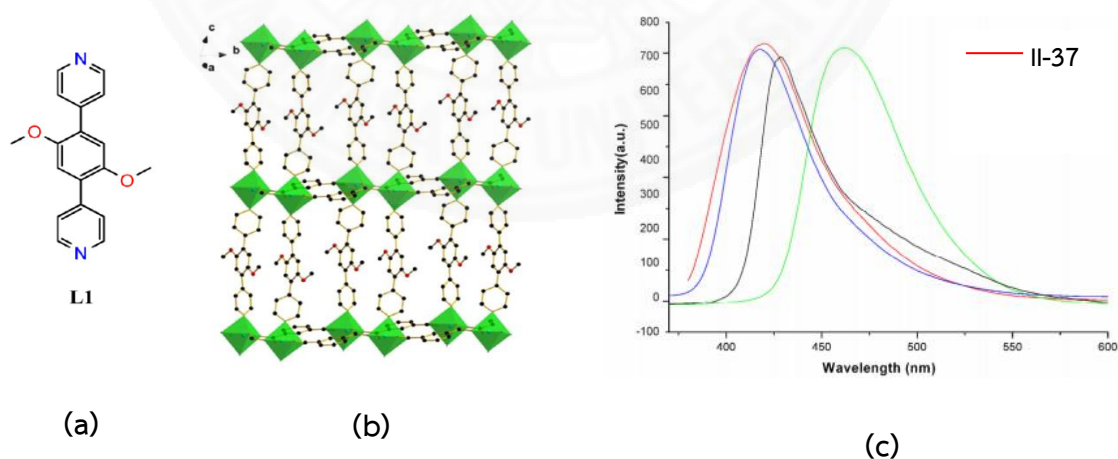


Figure 2.20 (a) Molecular structures of L^1 ligand, (b) polyhedral view of a single 2D coordination network along [101] plane and (c) solid state PL spectrum of **II-37** (red line) [77]

In 2016, Tripathi and coworkers [72] reported two new 2D Zn(II) coordination polymers, $\{[\text{Zn}(\text{pyim}_2)(1,2\text{-bdc})]\cdot(\text{DMF})\cdot(\text{MeOH})\}_n$ (**II-38**) and $\{[\text{Zn}(\text{pyim}_2)(1,4\text{-bdc})]\cdot(\text{DMF})\}_n$ (**II-39**), when $\text{pyim}_2 = 2,6\text{-bis}(\text{imidazol-1-yl})\text{pyridine}$ (Figure 2.21(a)). These compounds were synthesized by the reaction mixture of $\text{Zn}(\text{NO}_3)_2\cdot 6\text{H}_2\text{O}$, $1,2\text{-bdcH}_2$, pyim_2 , MeOH and DMF at room temperature. Structural analysis reveals that compound **II-38** consists of a tetrahedral Zn(II) ion with a ZnN_2O_2 unit coordinated by two oxygen atoms from two different $1,2\text{-bdc}^{2-}$ units in the monodentate η^1 mode and two imidazole nitrogen atoms from two distinct pyim_2 ligands. The $1,2\text{-bdc}^{2-}$ and pyim_2 ligands are further connected to two different Zn(II) units, generate a tetrameric 36-membered macrocycle. This macrocycle is further coordinated to another macrocycle, leading to a 2D herringbone pleated architecture as presented in Figure 2.21(b). For compound **II-39**, Zn(II) center is four coordinated with tetrahedral geometry. The $1,4\text{-bdc}^{2-}$ and pyim_2 ligands are further connected to two different Zn(II) ions, forming a tetrameric 40-membered macrocycle which is further coordinated to another macrocycle leading to a 2D parallel pleated network. The 2D network is composed of left-handed 1D helical chains of pyim_2 ligands running along the c axis, which are further connected to 1D zigzag chains of $1,4\text{-bdc}^{2-}$ ligands running along the b axis and both the 1D chains (helical and zigzag) are oriented perpendicular to each other, resulting in the grid network as shown in Figure 2.21(c). The adjacent 2D bilayers are further connected through $\pi\text{-}\pi$ and $\text{CH}\cdots\text{O}$ interactions forming a 3D supramolecular framework which shows stacking of parallel pleats in an ABAB fashion. Moreover, the solid state luminescence property of both compounds was studied. As presented in Figure 2.21(d), the PL spectra of these compounds exhibited the fluorescent emission spectrum at 398 and 390 nm while excitation at 290 and 320 nm for compound **II-38** and **II-39**, respectively.

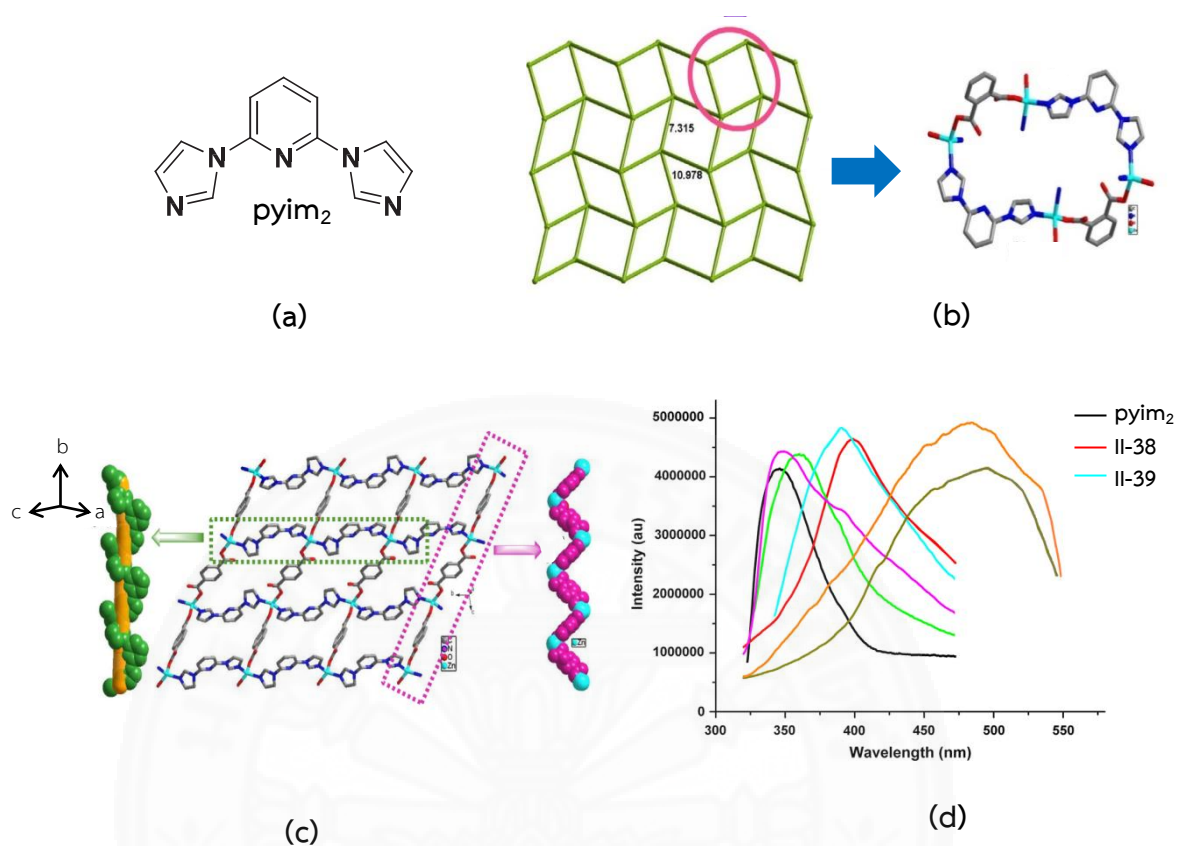


Figure 2.21 (a) Molecular structure of pyim₂ ligand, (b) 2D CP with herringbone pleated network in II-38 showing the 4-connected uninodal net, (c) 2D CP with perpendicular orientation 1D left-handed helix of pyim₂ ligands (green color) and 1D zigzag chain of 1,4-bdc²⁻ ligands (pink color) in II-39 and (d) solid state PL spectra of pyim₂, II-38 and II-39 [72]

In 2017, Croitor and coworkers [73] reported two 2D isostructure coordination polymers, $\{[M(1,4\text{-bdc})(4\text{-pyao})_2]\cdot\text{DMF}\}_n$ for $M = \text{Zn(II)}, \text{Cd(II)}$ (II-40 and II-41) when 4-pyao = pyridine-4-aldoxime (Figure 2.22(a)). These compounds were synthesized by the reaction mixture of $M(\text{CH}_3\text{COO})_2$, 1,4-bdcH₂, 4-pyao, MeOH and DMF at room temperature. Their crystal structures have been determined by single crystal X-ray diffraction. The results shows that the binuclear metal clusters $\{M_2(\text{COO})_2\}$ represent the secondary building unit (SBU) in these compounds. Each metal atom is six coordinated with a N₂O₄ distorted octahedral geometry.

The 1,4-bdc²⁻ linker shows two bridging modes, namely *syn,syn*-bidentate-bridging within the cluster and *bis*-monodentate between the clusters. Each 1,4-bdc²⁻ residue bridges three Zn(II) atoms. Considering the binuclear unit as a single coordination node in the coordination layer, the 2D coordination network has the (3,4) **sql** topology as shown in Figure 2.22(b). It is extended parallel to the *ab* crystallographic plane to form square windows with the linear dimensions 15.443 x 15.443 Å in **II-40** and 15.925 x 15.925 Å in **II-41**. In addition, the solid state luminescence property of both compounds was carried out. In Figure 2.22(c), the solid state PL spectra of these compounds exhibited the fluorescent emission spectra at 404 and 377 nm after excitation at 337 nm for compound **II-40** and **II-41**, respectively.

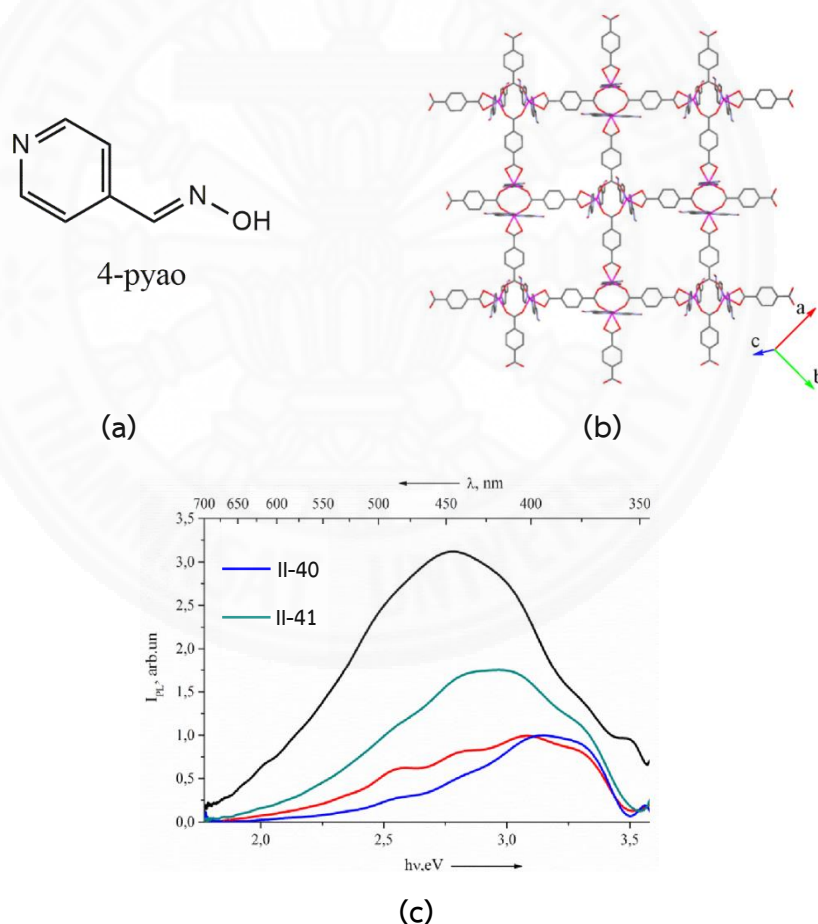


Figure 2.22 (a) Molecular structure of 4-pyao ligand, (b) fragment of the (4,4)-coordination layer in **II-40** and (c) solid state PL spectra of **II-40** and **II-41** [73]

2.3 Three-dimensional Zn(II) and Cd(II) containing aromatic dicarboxylate derivatives CPs

In 2005, Wen and coworkers [64] reported a new 3D Cd(II) coordination polymers, $\{[\text{Cd}(2,6\text{-dipicO})(\text{bix})_{1.5}] \cdot 1.5\text{H}_2\text{O}\}_n$ (**II-42**), when $\text{dipicOH}_2 = \text{pyridine-2,6-dicarboxylic acid } N\text{-oxide}$ and $\text{bix} = 1,4\text{-bis(imidazole-1-ylmethyl) benzene}$. The molecular structure of bix is shown in Figure 2.23(a). This compound was synthesized by the reaction of $\text{CdCl}_2 \cdot 2\text{H}_2\text{O}$, $2,6\text{-dipicOH}_2$ and bix in the ratio of 1:1:1 under hydrothermal condition. The crystal structure has been studied. The geometry of Cd(II) atom shows a distorted hexagonal configuration with a N_3O_3 unit. The structure consists of a 1D wave-like structure with a period equal to the c axis, which is constructed from *cis*- bix and $2,6\text{-dipicO}^{2-}$ ligands. The 1D structure is further connected along a and b axis with the bidentate *trans*- bix spacers occupying the void spaces, generating a 3D porous framework as shown in Figure 2.23(b). Interestingly, the presence of large free voids in the single framework results in the formation of interpenetrations. The channels of **II-42** are filled by another identical framework in a typical 2-fold interpenetration fashion, displaced by the usual half of the length of the unit as presented in Figure 2.23(c). Furthermore, the solid state PL spectrum of this compound showed the fluorescent emission spectrum at 418 nm after excitation at 342 nm.

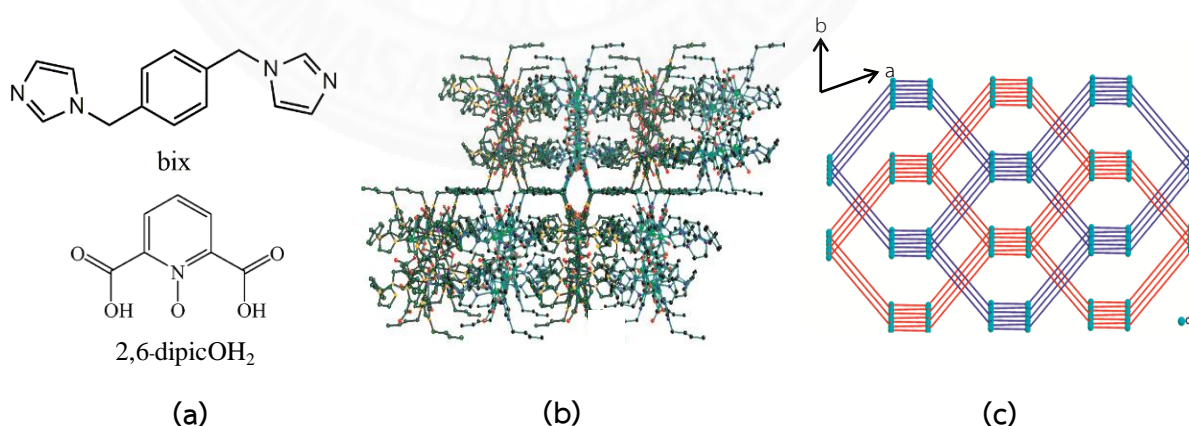


Figure 2.23 (a) Molecular structures of bix and $2,6\text{-dipicOH}_2$ ligands, (b) packing of the adjacent framework along the c axis and (c) topological view of the two interpenetrating nets in **II-42** [64]

In 2010, He and coworkers [75] reported a new 3D Zn(II) coordination polymers, $[\text{Zn}_2(\text{BITMB})_2(1,3\text{-bdCH})_2(1,3\text{-bdC})\cdot\text{H}_2\text{O}]_n$ (**II-43**), when BITMB = 1,3-bis(imidazol-1-ylmethyl)-2,4,6-trimethylbenzene (Figure 2.24(a)). This compound was synthesized by the reaction of $\text{Zn}(\text{NO}_3)_2\cdot 6\text{H}_2\text{O}$, 1,3-bdCH₂ and BITMB in the ratio of 3:3:1 with mixed solvents of H₂O, EtOH and DMF under the solvothermal condition. Single crystal X-ray diffraction reveals that compound **II-43** is a 3D porous framework based on 1D Zn-BITMB chains. Each Zn(II) ion (Zn1, Zn2, and Zn3) adopts a tetrahedral geometry. Zn1, Zn2, and Zn3 ions are connected by BITMB ligands to form two similar 1D zigzag chains. The zigzag chains run in opposite directions along the *b* axis. These chains are further connected by the 1,3-bdc²⁻ ligands through monodentate carboxylate groups coordinating to Zn1 and Zn2, resulting in the formation of a 2D layer. Each 2D layers are further linked by 1,3-bdc²⁻ ligands via the monodentate carboxylate group coordinating to Zn3 ions to complete the tetrahedral geometry of Zn3, producing a 3D porous framework along the *a* axis as shown in Figure 2.24(b). Moreover, the solid state luminescence property of this compound was studied. In Figure 2.24(c), the solid state PL spectrum of this compound exhibited the fluorescent emission spectrum at 460 nm while excitation at 250 nm.

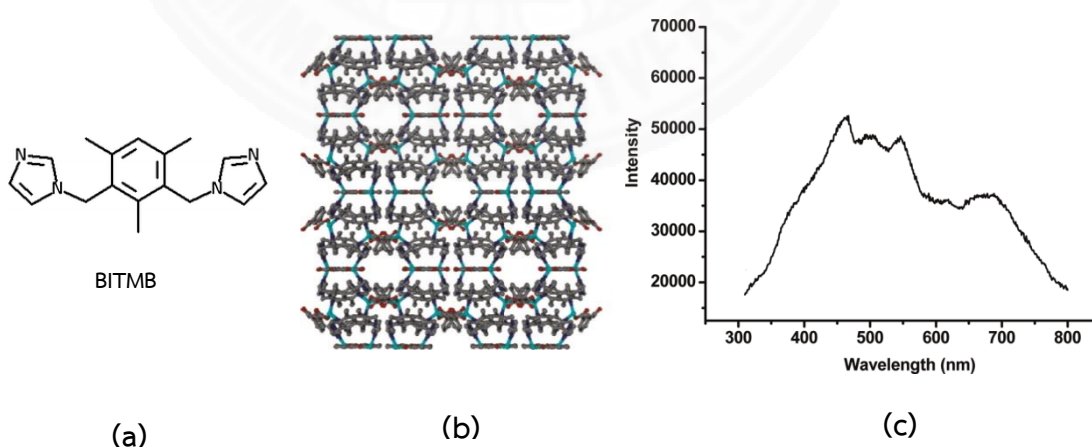


Figure 2.24 (a) Molecular structure of BITMB ligand, (b) 3D porous framework and (c) solid state PL spectrum of **II-43** [75]

In 2010, Liu and coworkers [67] reported two new 3D Zn(II) coordination polymers, $[\text{Zn}_2(1,3\text{-bdc})_2(\text{L}^3)] \cdot 2\text{H}_2\text{O}$ (**II-44**) and $[\text{Zn}_2(1,4\text{-bdc})_2(\text{L}^3)] \cdot 2\text{CH}_3\text{OH}$ (**II-45**) when $\text{L}^3 = 1,1'-(1,10\text{-decanediyl})\text{bis}[2-(2\text{-pyridyl})\text{benzimidazole}]$ (Figure 2.25(a)). These compounds were synthesized by the reaction mixture of $\text{Zn}(\text{COO})_2 \cdot 2\text{H}_2\text{O}$, L^3 , 1,3-bdcH₂ or 1,4-bdcH₂, with mixed solvents of H₂O and MeOH under solvothermal condition. Their structures have been investigated. The results show that compounds **II-44** and **II-45** show 2-fold interpenetrating 3D network structures. For compound **II-44**, Zn(II) center is five coordinated with square-pyramidal geometry. Each 1,3-bdc²⁻ anion coordinates to three Zn(II) atoms in the monodentate and bidentate bridging coordination modes. Two adjacent Zn(II) ions are connected together via bidentate bridging carboxylate groups of two 1,3-bdc²⁻ anions. As a result, two Zn(II) ions and two carboxylate groups constitute a bimetallic $[\text{Zn}_2(\text{CO}_2)_2]$ unit. Each bimetallic unit links four 1,3-bdc²⁻ anions and in turn each 1,3-bdc²⁻ anion links two bimetallic units to give a 2D sheet. The L^3 ligands bridge the adjacent sheets in the bidentate chelating coordination mode to form a 3D structure as shown in Figure 2.25(b). For compound **II-45**, Zn(II) center is five coordinated, displaying a distorted square pyramidal geometry. A part of 1,4-bdc²⁻ anions link the adjacent Zn(II) atoms with the bidentate bridging modes to give a 1D chain structure. In this chain, there are the bimetallic $[\text{Zn}_2(\text{CO}_2)_2]$ units. Furthermore, these chains are connected by another part of the 1,4-bdc²⁻ anions with the *bis*-monodentate modes to form a 2D polymeric sheet. The 3D framework of **II-45** is shown in Figure 2.25(c). The packing modes of compounds **II-44** and **II-45** are very similar. In addition, the solid state PL spectra of both compounds showed the fluorescent emission spectra at 415 and 405 nm while excitation at 356 and 355 nm for compound **II-44** and **II-45**, respectively.

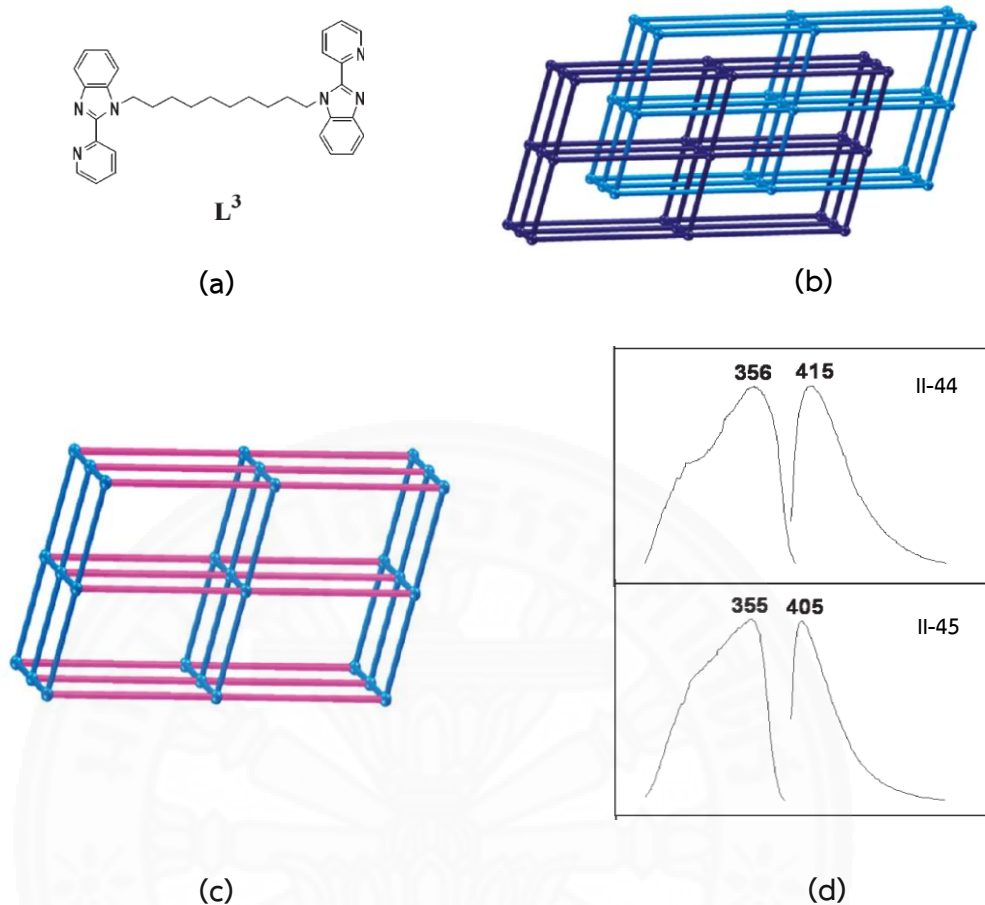


Figure 2.25 (a) Molecular structure of L^3 ligand, (b) view of the 2-fold interpenetrating framework of **II-44**, (c) view of the α -Po network of **II-45** and (d) solid state PL spectra of **II-44** and **II-45** [67]

In 2011, Ma and coworkers [68] reported new 3D Zn(II) and Cd(II) coordination polymers, $\{[\text{Cd}(5\text{-Br-1,3-bdc})(\text{bpp})(\text{H}_2\text{O})]\}_n$ (**II-46**), $\{[\text{Zn}(5\text{-Br-1,3-bdc})(\text{bpe})]\}_n$ (**II-47**) and $\{[\text{Zn}_2(4\text{-Br-1,3-bdc})_2(\text{bpy})]\cdot\text{H}_2\text{O}\}_n$ (**II-48**), when $\text{bpp} = 1,3\text{-di}(4\text{-pyridyl})\text{propane}$, $\text{bpe} = 1,2\text{-di}(4\text{-pyridyl})\text{ethane}$ and $4,4'\text{-bpy} = 4,4'\text{-bipyridyl}$. The molecular structures of these ligands are shown in Figure 2.26(a). These compounds were prepared by reaction mixtures of $\text{M}(\text{COO})_2\cdot 2\text{H}_2\text{O}$, Br-1,3-bdcH_2 and different dipyrindyl-type coligands under hydrothermal condition. Single crystal X-ray diffraction reveals that Cd(II) center in compound **II-46** is six-coordinated, displaying a distorted octahedral geometry. Each Cd(II) ions are linked by the 5-Br-1,3-bdc^{2-} ligands to form

a 1D zigzag chain. Furthermore, these 1D chains are connected by the exobidentate bpp bridges to form a 2-fold interpenetrating 3D framework with the diamond-like topology as shown in Figure 2.26(b). For compound **II-47**, Zn(II) center is four-coordinated with tetrahedral geometry. Each 5-Br-1,3-bdc²⁻ ligand links the adjacent Zn(II) ions to form left-handed and right-handed helical chains. The bpe ligands further connect the 1D chain to form a 3D network as presented in Figure 2.26(c). For compound **II-48**, Zn(II) center is four-coordinated, showing a tetrahedral geometry. The Zn(II) ions are bridged by the 4-Br-1,3-bdc²⁻ ligands to give rise to a 2D network with 4-8² topology. The 2D layers are further connected by the bpy ligands to construct a 3D pillar-layered framework as shown in Figure 2.26(d).

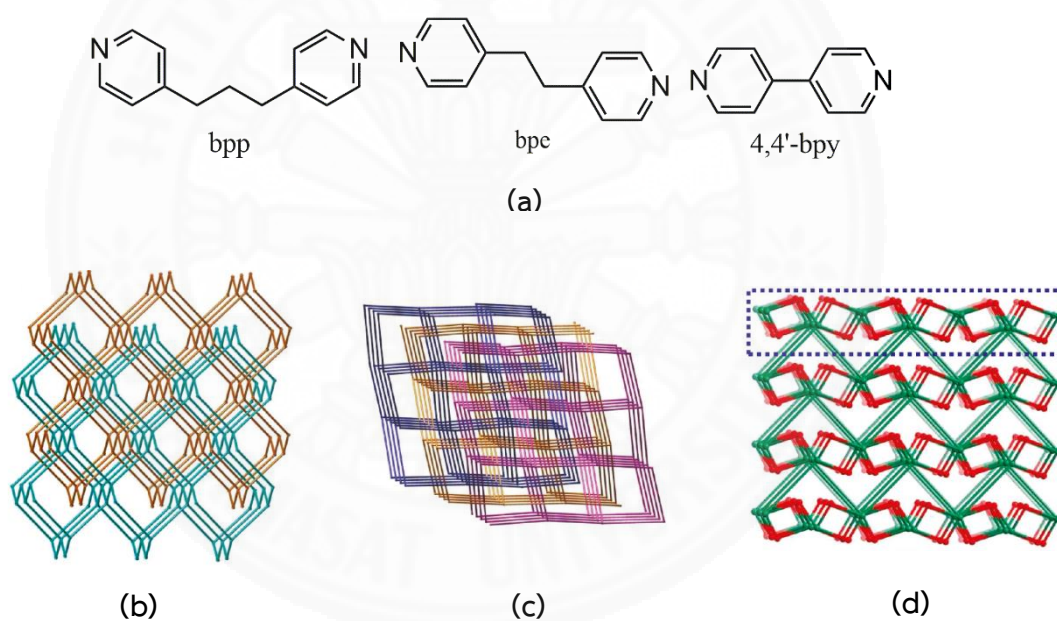


Figure 2.26 (a) Molecular structures of bpe, bpc and bpp ligands, (b) 2-fold interpenetrating diamond framework of **II-46**, (c) 3-fold interpenetrating architecture of **II-47** and (d) (3,4)-connected (4-8²) (4-8² · 10³) topology of **II-48** [68]

In 2012, Cheng and coworkers [51] reported a new 3D Cd(II) coordination polymers, $\{[\text{Cd}_2(1,4\text{-bdc})_2(\text{L}^2)_2] \cdot (\text{H}_2\text{O})_3\}_n$ (**II-49**), when $\text{L}^2 = N,N'$ -di(3-pyridyl)adipoamide (Figure 2.27(a)). This compound was synthesized by the reaction of $\text{Cd}(\text{CH}_3\text{COO})_2 \cdot 2\text{H}_2\text{O}$, 1,4-bdcH₂ and L^2 in the ratio of 1:1:1 under hydrothermal

condition. Their structures have been investigated. The results show that Cd(II) ions are six-coordinated, showing a distorted octahedral geometry. Each Cd(II) ion is bridged by 1,4-bdc²⁻ ligands to generate 2D nets, which are also connected to each other via the pyridyl nitrogen atoms of L² ligands to form a 3D coordination network as shown in Figure 2.27(b). Moreover, the solid state PL spectrum of this compound exhibited the fluorescent emission spectrum at 385 nm while excitation at 325 nm.

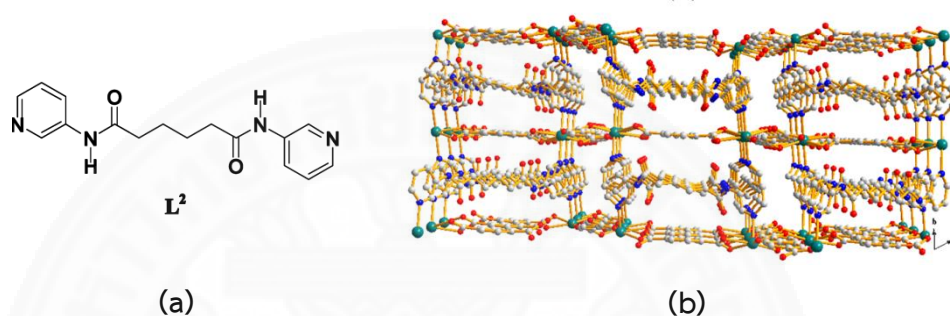


Figure 2.27 (a) Molecular structure of L² ligand and (b) 3D framework of **II-49** [51]

In 2012, Hu and coworkers [78] reported a new 3D Zn(II) coordination polymer, $\{[\text{Zn}_2(\text{TPOM})(5\text{-OH-}1,3\text{-bdc})_2] \cdot (\text{DMF})(\text{H}_2\text{O})_2\}_n$ (**II-50**), when TPOM = tetrakis(4-pyridyloxymethylene)methane (Figure 2.289a)). This compound was synthesized by the reaction of $\text{Zn}(\text{NO}_3)_2 \cdot 6\text{H}_2\text{O}$, 5-OH-bdcH₂ and TPOM in the ratio of 2:2:1 with mixed solvents of H₂O and DMF under solvothermal condition. The crystal structure has been investigated. The results show that Zn(II) ions are four-coordinated and reside in the distorted tetrahedral coordination environment. Each tetrahedral Zn(II) atom coordinates to TPOM ligands to generate an infinitely wave-like 2D network along the *a* axis. The 5-OH-bdc²⁻ anions connect two Zn(II) atoms belonging to different 2D networks to create a 3D framework as shown in Figure 2.28(b). In addition, the electrical hysteresis loop of **II-50** was recorded at room temperature. As presented in Figure 2.28(c), the remnant electric polarization (P_r) is 0.052 $\mu\text{C}/\text{cm}^2$ and electric coercive field (E_c) is 5.755 kV/cm, respectively; saturation of the spontaneous polarization (P_s) is ca. 0.451 $\mu\text{C}/\text{cm}^2$.

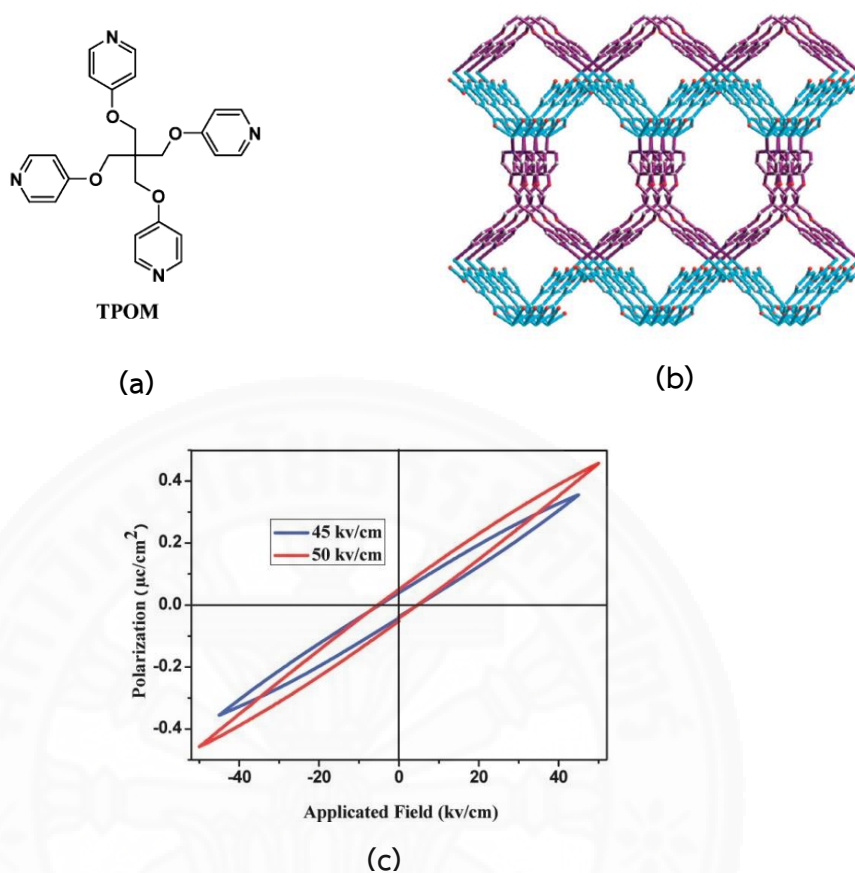


Figure 2.28 (a) Molecular structure of TPOM ligand, (b) 3D framework of **II-50** and (c) electric hysteresis loop of **II-50** at room temperature [78]

In 2013, Lin and coworkers [79] reported a new 3D Cd(II) coordination polymer, $\{Cd_{2.5}(4\text{-OH-}2,6\text{-dipic})(4\text{-OH-}2,6\text{-Hdipic})(H_2O)_7 \cdot 1.5H_2O\}_n$ (**II-51**), when $4\text{-OH-}2,6\text{-dipicH}_2 = 4\text{-hydroxy-}2,6\text{-pyridinedicarboxylic acid}$ (Figure 2.29(a)). This compound was synthesized by the reaction of $CdCl_2 \cdot 2.5H_2O$ and $4\text{-OH-}2,6\text{-dipicH}_2$ at $50\text{ }^\circ\text{C}$, along with little of ammonia added dropwise. The crystal structure has been studied. The results show that Cd1 and Cd2 atoms are both seven-coordinated with distorted pentagonal-bipyramidal geometry, while Cd3 is six-coordinated with a distorted octahedral geometry. All Cd(II) centers are bridged by carboxylate O atoms to form 2D layers, which are further linked by hydroxyl O atoms to form the 3D framework as shown in Figure 2.29(b). Furthermore, the solid state luminescence property of this compound was studied. As presented in Figure 2.29(c), the PL spectrum of this

compound illustrated the fluorescent emission spectrum at 469 nm upon excitation at 370 nm.

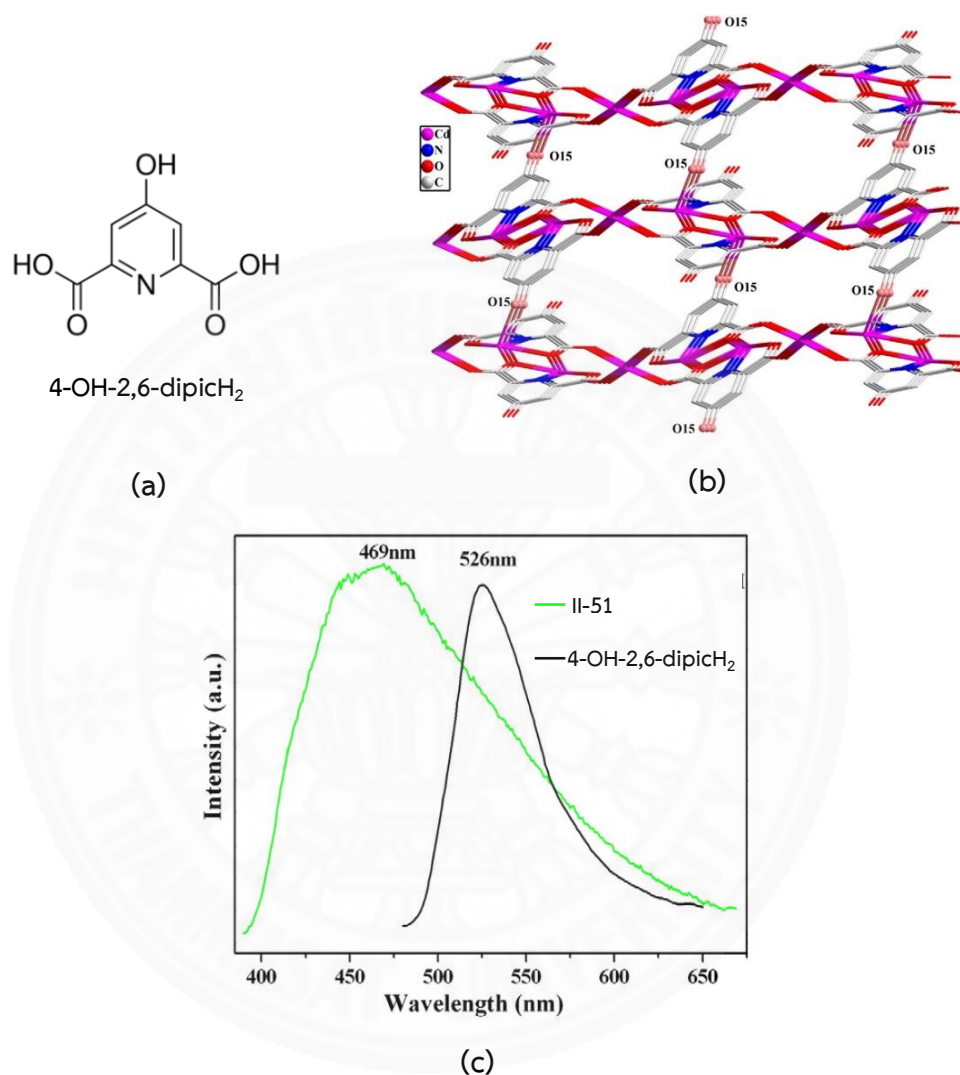


Figure 2.29 (a) Molecular structure of 4-OH-2,6-dipicH₂ ligand, (b) 3D framework of II-51 and (c) solid state PL spectra of 4-OH-2,6-dipicH₂ and II-51 [79]

In 2014, Paraschiv and coworkers [70] reported two new 3D Zn(II) coordination polymers, $\{[\text{Zn}_5(\text{Htea})_2(1,3\text{-bdc})_3(\text{H}_2\text{O})] \cdot 2.6\text{H}_2\text{O}\}_n$ (II-52) and $[\text{Zn}_3(\text{H}_2\text{dea})_2(1,4\text{-bdc})_3]_n$ (II-53), when H₃tea = triethanolamine and H₂dea = diethanolamine. The molecular structures of these ligands are shown in Figure

2.30(a). These compounds were synthesized by the reaction mixtures of $\text{Zn}(\text{NO}_3)_2 \cdot 6\text{H}_2\text{O}$, 1,3- or 1,4-bdc H_2 and H_3tea or H_2dea with mixed solvents of Et_3N and MeOH under solvothermal condition. Single crystal X-ray diffraction exhibits that compound **II-52** consists of five crystallographically independent Zn(II) ions. The formation of a zigzag chain, which construct by alternating $\{\text{Zn}_3\}$ and $\{\text{Zn}_2\}$ secondary building units (SBUs), involving Zn1, Zn2, and Zn3 atoms and Zn4 and Zn5 atoms, respectively. The binuclear and trinuclear SBUs are alternately linked by alkoxo bridges into helicoidal chains running along a axis. Each Htea^{2-} ligand acts as a bridge between three Zn(II) atoms. Both right-handed (P) and left-handed (M) helices are present in the crystal, and they are alternately interconnected by pairs of dicarboxylato bridges, forming in a 3D porous network as shown in Figure 2.30(b). For compound **II-53**, the central Zn1 atom is six coordinated with a nearly perfect octahedral geometry. The H_2dea molecule is not deprotonated and coordinates as a bidentate chelating ligand toward Zn2 ions via the nitrogen atom and one oxygen atom, while the other OH group remains uncoordinated. Two of the carboxylato groups act as bridges in the $\mu_2\text{-}\eta^1:\eta^1$ *syn-syn* mode, while the other one coordinates in a bridging-chelating $\mu_2\text{-}\eta^1:\eta^2$ fashion. The geometry of Zn2 atoms is a distorted octahedron. The 1,4-bdc $^{2-}$ anions link the $\{\text{Zn}_3(\text{H}_2\text{dea})_2\}^{6+}$ nodes into a 3D network as presented in Figure 2.30(c). Furthermore, compound **II-52** was tested as photocatalyst in the photo oxidations reactions of phenol and benzylamine. The results suggest that compound **II-52** proved to be active in the selective photo oxidation of phenol to form hydroquinone and benzylamine to form *N*-benzylidenebenzylamine.

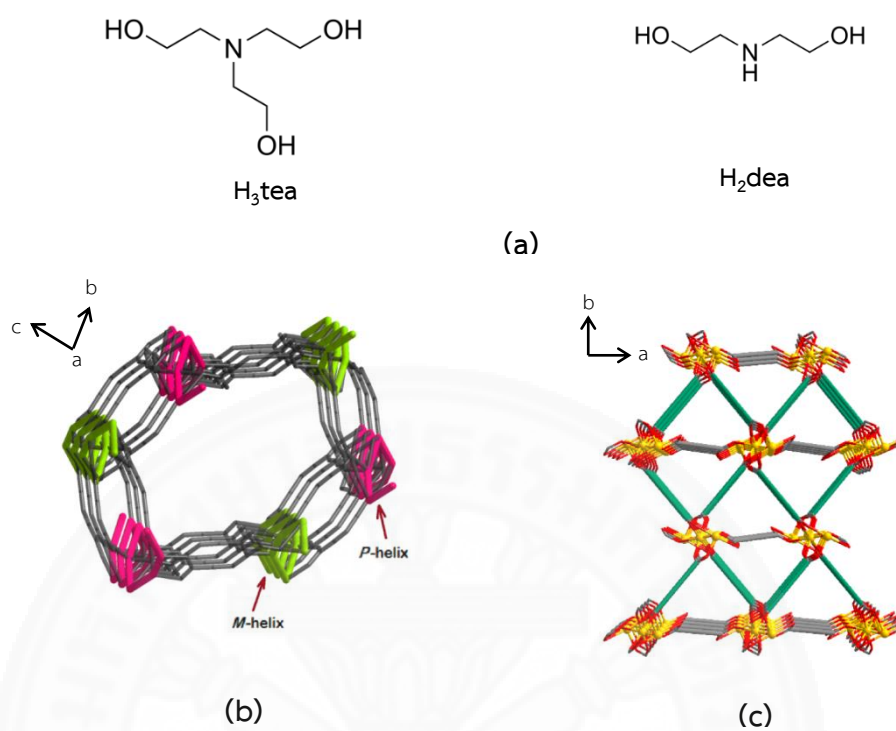


Figure 2.30 (a) Molecular structures of H₃tea and H₂dea ligands, (b) 3D framework of II-52 and (c) 3D framework of II-53 [70]

Table 2.1 Summary of previous studies of 1D Zn(II) and Cd(II) containing aromatic dicarboxylate derivatives CPs

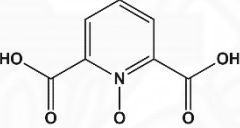
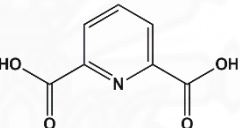
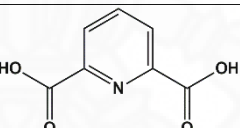
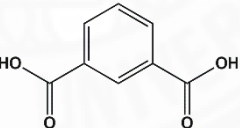
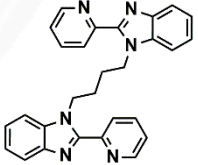
Year	Empirical formula	Synthetic method	Aromatic dicarboxylate derivative	Co-ligand	Topology	[Ref.]
2005	$[\text{Zn}(\text{2,6-dipicO})(\text{H}_2\text{O})_2]_n$	Hydrothermal		-	1D helical chain	[64]
2006	$\{[\text{Zn}(\text{2,6-dipic})(\text{H}_2\text{O})_{1.5}]\}_n$	Solvothermal		-	1D zigzag chain	[65]
2007	$[\text{Cd}_2(\text{2,6-dipic})_2(\text{CH}_3\text{OH})_2(\text{H}_2\text{O})]_n$	Layer diffusion		-	1D chain	[66]
2010	$[\text{Zn}_2(\text{1,3-bdc})_2(\text{L}^1)] \cdot 2\text{H}_2\text{O}$	Solvothermal			1D double chain	[67]

Table 2.1 Summary of previous studies of 1D Zn(II) and Cd(II) containing aromatic dicarboxylate derivatives CPs (cont.)


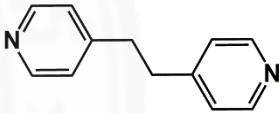
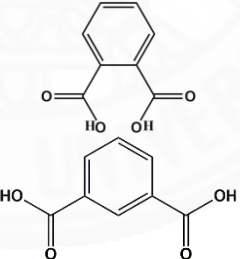
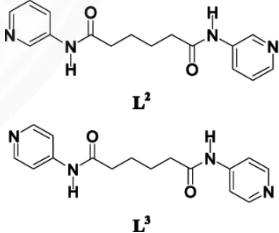
Year	Empirical formula	Synthetic method	Aromatic dicarboxylate derivative	Co-ligand	Topology	Ref.
2011	$[\text{Zn}(5\text{-Br-1,3-bdc})(\text{bpa})(\text{H}_2\text{O})]_n$ $[\text{Zn}(4\text{-Br-1,3-bdc})(\text{bpa})(\text{H}_2\text{O})]_n$	Hydrothermal			1D ladder chain	[68]
2012	$[\text{Zn}(1,2\text{-bdc})(\text{L}^2)]_n$ $\{[\text{Zn}_2(1,2\text{-bdc})_2(\text{L}^3)(\text{H}_2\text{O})_2] \cdot 2\text{H}_2\text{O}\}_n$ $[\text{Cd}_2(1,3\text{-bdc})_2(\text{L}^2)(\text{H}_2\text{O})_4]$	Hydrothermal			1D double-looped chain, 1D chains with loops and 1D ladder chain	[51]

Table 2.1 Summary of previous studies of 1D Zn(II) and Cd(II) containing aromatic dicarboxylate derivatives CPs (cont.)

Year	Empirical formula	Synthetic method	Aromatic dicarboxylate derivative	Co-ligand	Topology	Ref.
2013	$[\text{Cd}(2,6\text{-dipic})(\text{H}_2\text{O})_{1.5}]_n$	Direct method		-	1D helical chain	[69]
2014	$[\text{Zn}_2(\text{Htea})_2(1,2\text{-bdc})]_n$ $[\text{Zn}(\text{H}_3\text{tris})(1,3\text{-bdc})(\text{CH}_3\text{OH})]_n$	Solvothermal			1D zigzag chain 1D linear chain	[70]
2015	$[\text{Cd}_2(2,6\text{-dipic})_2(\text{H}_2\text{O})_3]_n$ $\{[\text{Cd}_2(4\text{-OH-}2,6\text{-dipic})_2(\text{H}_2\text{O})_4] \cdot 3\text{H}_2\text{O}\}_n$	Hydrothermal		-	1D chain 1D chain	[71]

Table 2.1 Summary of previous studies of 1D Zn(II) and Cd(II) containing aromatic dicarboxylate derivatives CPs (cont.)

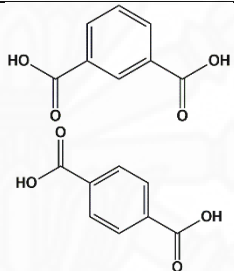
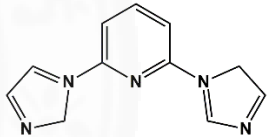
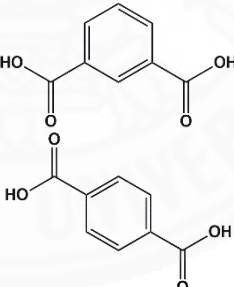
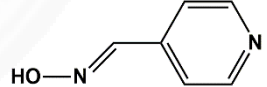
Year	Empirical formula	Synthetic method	Aromatic dicarboxylate derivative	Co-ligand	Topology	Ref.
2016	$\{[\text{Zn}_2(\text{pyim}_2)_2(1,3\text{-bdc})_2]\cdot(\text{DMF})_4\}_n$ $\{[\text{Cd}(\text{pyim}_2)(1,4\text{-bdc})(\text{H}_2\text{O})]\cdot(\text{H}_2\text{O})_2\}_n$	Layers diffusion			1D chain 1D chain	[72]
2017	$\{[\text{Cd}(1,3\text{-bdc})(4\text{-pyao})(\text{H}_2\text{O})_2]\cdot\text{DMF}\cdot\text{H}_2\text{O}\}_n$ $\{[\text{Cd}(1,4\text{-bdc})(4\text{-pyao})_2\cdot(\text{H}_2\text{O})]\cdot\text{DMF}\}_n$	Direct method			1D translational chain and 1D zigzag chain	[73]

Table 2.2 Summary of previous studies of 2D Zn(II) and Cd(II) containing aromatic dicarboxylate derivatives CPs

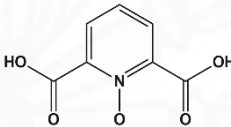
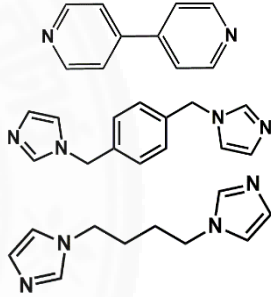
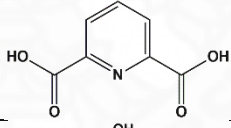
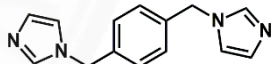
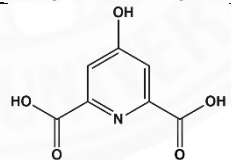
Year	Empirical formula	Synthetic method	Aromatic dicarboxylate derivative	Co-ligand	Topology	Ref.
2005	$\{[\text{Zn}_2(2,6\text{-dipicO})_2(4,4'\text{-bpy})_2(\text{H}_2\text{O})_2]\cdot 3\text{H}_2\text{O}\}_n$ $[\text{Zn}(2,6\text{-dipicO})(\text{bix})]_n$ $\{[\text{Zn}(2,6\text{-dipicO})(\text{bbi})]\cdot 0.5\text{H}_2\text{O}\}_n$	Hydrothermal			2D brick-wall-like structure, 2D herringbone structure and 2D herringbone structure	[64]
2006	$[\text{Cd}_2(\mu_2\text{-OH})_2(2,6\text{-dipic})_2(\text{bix})]_n$	Hydrothermal			2D structure	[74]
2006	$\{[\text{Zn}(4\text{-OH-}2,6\text{-dipic})]\cdot \text{H}_2\text{O}\}_n$	Solvothermal		-	2D (4,4) net	[65]

Table 2.2 Summary of previous studies of 2D Zn(II) and Cd(II) containing aromatic dicarboxylate derivatives CPs (cont.)

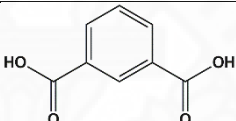
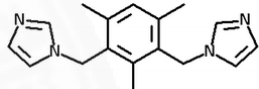
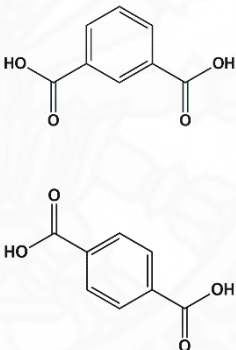
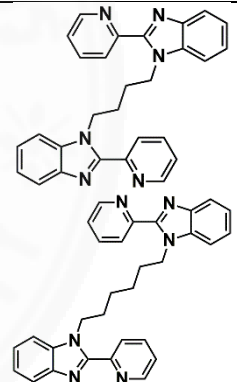
Year	Empirical formula	Synthetic method	Aromatic dicarboxylate derivative	Co-ligand	Topology	Ref.
2010	$[\text{Zn}(\text{BITMB})(1,3\text{-bdc})\cdot 3\text{H}_2\text{O}]_n$	Solvothermal			2D structure	[75]
2010	$[\text{Zn}_2(1,4\text{-bdc})_2(\text{L}^1)(\text{H}_2\text{O})_2]_n$ $[\text{Zn}_2(1,3\text{-bdc})_2(\text{L}^2)]\cdot 2.25\text{H}_2\text{O}$ $[\text{Zn}_2(1,4\text{-bdc})_2(\text{L}^2)]\cdot \text{CH}_3\text{OH}$	Solvothermal			2D layer structure, 2D wavelike sheet structure and 2D sheet structure	[67]

Table 2.2 Summary of previous studies of 2D Zn(II) and Cd(II) containing **aromatic** dicarboxylate derivatives CPs (cont.)


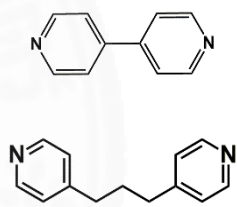
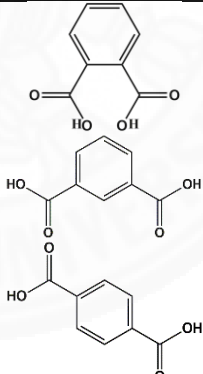
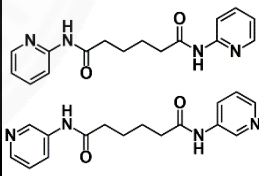
Year	Empirical formula	Synthetic method	Aromatic dicarboxylate derivative	Co-ligand	Topology	Ref.
2011	$\{[\text{Zn}_2(5\text{-Br-1,3-bdc})_2(4,4'\text{-bpy})(\text{H}_2\text{O})]\cdot 2\text{H}_2\text{O}\}_n$ $\{[\text{Cd}(4\text{-Br-1,3-bdc})(\text{bpp})]\}_n$	Hydrothermal			2D (6,3) network and 2D (3.5)- connected network	[68]
2012	$[\text{Zn}_2(1,3\text{-bdc})_2(\text{L}^2)(\text{H}_2\text{O})_2]_n$ $[\text{Zn}_2(1,4\text{-bdc})_2(\text{L}^1)(\text{H}_2\text{O})_2]_n$ $\{[\text{Cd}(1,2\text{-bdc})(\text{L}^2)(\text{H}_2\text{O})]\cdot \text{H}_2\text{O}\}_n$ $[\text{Cd}_2(1,4\text{-bdc})_2(\text{L}^1)(\text{H}_2\text{O})_2]_n$	Hydrothermal			2D hexagonal nets, 2D hexagonal nets, 2D pleated layer and 2D hexagonal nets	[51]

Table 2.2 Summary of previous studies of 2D Zn(II) and Cd(II) containing aromatic dicarboxylate derivatives CPs (cont.)

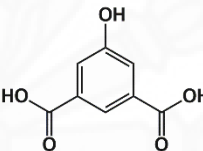
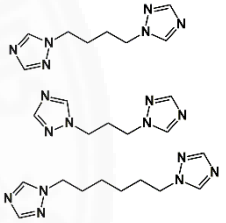
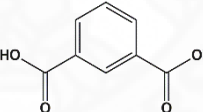
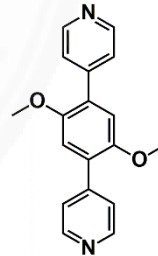
Year	Empirical formula	Synthetic method	Aromatic dicarboxylate derivative	Co-ligand	Topology	Ref.
2013	$[\text{Zn}(5\text{-OH-1,3-bdc})(\text{btb})] \cdot 2\text{H}_2\text{O}$ $[\text{Cd}(5\text{-OH-1,3-bdc})(\text{btp})(\text{H}_2\text{O})] \cdot 3\text{H}_2\text{O}$ $[\text{Cd}(5\text{-OH-1,3-bdc})(\text{bth})_2(\text{H}_2\text{O})] \cdot \text{H}_2\text{O}$	Hydrothermal			2D (4,4) network, 2D (4,4) network and 2D undulated (4,4) net	[76]
2014	$\{[\text{Zn}(\text{L}^1)(1,3\text{-bdc})]\}_n$	Solvothermal			2D (4,4) connected sql nets	[77]

Table 2.2 Summary of previous studies of 2D Zn(II) and Cd(II) containing aromatic dicarboxylate derivatives CPs (cont.)

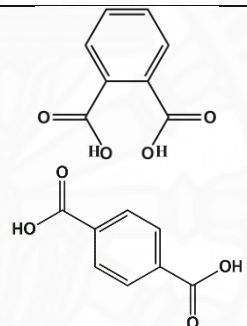
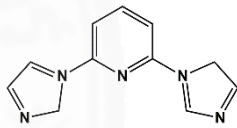
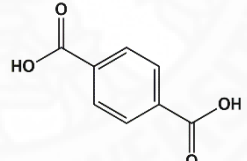
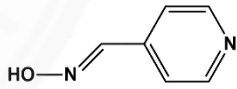
Year	Empirical formula	Synthetic method	Aromatic dicarboxylate derivative	Co-ligand	Topology	Ref.
2016	$\{[\text{Zn}(\text{pyim}_2)(1,2\text{-bdc})]\cdot(\text{DMF})\cdot(\text{MeOH})\}_n$ $\{[\text{Zn}(\text{pyim}_2)(1,4\text{-bdc})]\cdot(\text{DMF})\}_n$	Direct method			2D herringbone pleated structure and 2D parallel pleated network	[72]
2017	$\{[\text{Zn}(1,4\text{-bdc})(4\text{-pyao})_2]\cdot\text{DMF}\}_n$ $\{[\text{Cd}(1,4\text{-bdc})(4\text{-pyao})_2]\cdot\text{DMF}\}_n$	Direct method			2D (4,4) network 2D (4,4) network	[73]

Table 2.3 Summary of previous studies of 3D Zn(II) and Cd(II) containing aromatic dicarboxylate derivatives CPs

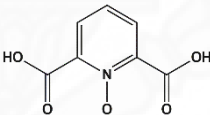
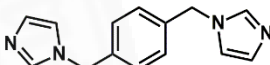
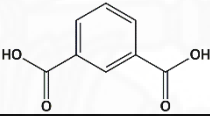
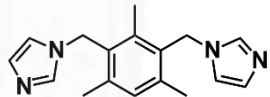
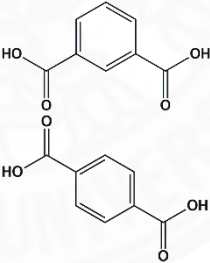
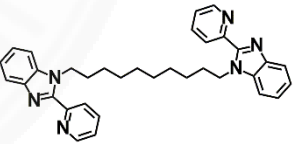
Year	Empirical formula	Synthetic method	Aromatic dicarboxylate derivative	Co-ligand	Topology	Ref.
2005	$\{[\text{Cd}(2,6\text{-dipicO})(\text{bix})_{1,5}] \cdot 1.5\text{H}_2\text{O}\}_n$	Hydrothermal			2-fold interpenetration 3D framework	[64]
2010	$[\text{Zn}_2(\text{BITMB})_2(1,3\text{-bdcH})_2(1,3\text{-bdc}) \cdot \text{H}_2\text{O}]_n$	Solvothermal			3D porous framework	[75]
2010	$[\text{Zn}_2(1,3\text{-bdc})_2(\text{L}^3)] \cdot 2\text{H}_2\text{O}$ $[\text{Zn}_2(1,4\text{-bdc})_2(\text{L}^3)] \cdot 2\text{CH}_3\text{OH}$	Solvothermal			2-fold interpenetrating 3D network and 2-fold interpenetrating 3D network	[67]

Table 2.3 Summary of previous studies of 3D Zn(II) and Cd(II) containing aromatic dicarboxylate derivatives CPs (cont.)

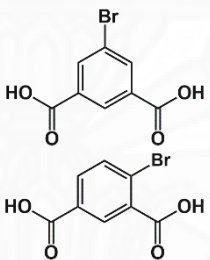
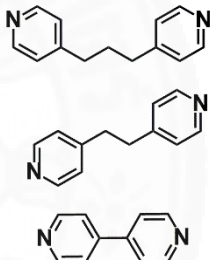
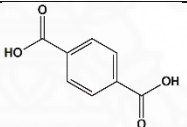
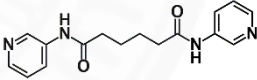
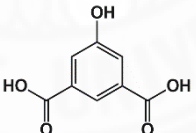
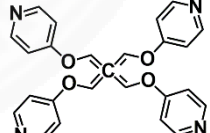
Year	Empirical formula	Synthetic method	Aromatic dicarboxylate derivative	Co-ligand	Topology	Ref.
2011	$\{[\text{Cd}(5\text{-Br-}1,3\text{-bdc})(\text{bpp})(\text{H}_2\text{O})]\}_n$ $\{[\text{Zn}(5\text{-Br-}1,3\text{-bdc})(\text{bpe})]\}_n$ $\{[\text{Zn}_2(4\text{-Br-}1,3\text{-bdc})_2(\text{bpy})]\cdot\text{H}_2\text{O}\}_n$	Hydrothermal			2-fold interpenetrating 3D framework, 3D network and 3D pillar-layered framework	[68]
2012	$\{[\text{Cd}_2(1,4\text{-bdc})_2(\text{L}^2)_2]\cdot(\text{H}_2\text{O})_3\}_n$	Hydrothermal			3D framework	[51]
2012	$\{[\text{Zn}_2(\text{TPOM})(5\text{-OH-}1,3\text{-bdc})_2]\cdot(\text{DMF})(\text{H}_2\text{O})_2\}_n$	Solvothermal			3D framework	[78]

Table 2.3 Summary of previous studies of 3D Zn(II) and Cd(II) containing aromatic dicarboxylate derivatives CPs (cont.)

Year	Empirical formula	Synthetic method	Aromatic dicarboxylate derivative	Co-ligand	Topology	Ref.
2013	$\{\text{Cd}_{2.5}(\text{4-OH-2,6-dipic})-(\text{4-OH-2,6-Hdipic})(\text{H}_2\text{O})_7 \cdot 1.5\text{H}_2\text{O}\}_n$	Direct method		-	3D framework	[79]
2014	$\{[\text{Zn}_5(\text{Htea})_2(1,3\text{-bdc})_3(\text{H}_2\text{O})] \cdot 2.6\text{H}_2\text{O}\}_n$ $[\text{Zn}_3(\text{H}_2\text{dea})_2(1,4\text{-bdc})_3]_n$	Solvothermal			3D porous network 3D framework	[70]

CHAPTER 3

RESEARCH METHODOLOGY

The purpose of this chapter is to present the research methodology. In more details, the author outlines the steps of this research including synthesis method, characterization, crystal structure determination and properties study. Moreover, the list of chemicals, glassware and instruments that used for this thesis were provided.

3.1 Materials

3.1.1. Chemicals

All the chemicals and solvents were commercially purchased and used as received without further purification.

Table 3.1 Chemicals and reagents

Chemicals and reagents	Formula	Mw (g/mol)	% Purity	Company
Zinc nitrate tetrahydrate	$\text{Zn}(\text{NO}_3)_2 \cdot 4\text{H}_2\text{O}$	261.44	98.5	Carlo Erba
Cadmium nitrate tetrahydrate	$\text{Cd}(\text{NO}_3)_2 \cdot 4\text{H}_2\text{O}$	308.48	98.0	Carlo Erba
Pyridine-2,6-dicarboxylic acid	$\text{C}_7\text{H}_5\text{NO}_4$	167.12	99.0	Sigma Aldrich
Benzene-1,3-dicarboxylic acid	$\text{C}_8\text{H}_6\text{O}_4$	163.13	99.0	Acros organic
Sodium hydroxide	NaOH	40.00	98.0	Carlo Erba
Methanol	CH_3OH	32.04	99.9	RCI labscan
Ethanol	$\text{C}_2\text{H}_5\text{OH}$	46.07	99.9	RCI labscan
<i>N,N</i> -Dimethylformamide	$\text{C}_3\text{H}_7\text{NO}$	73.09	99.8	RCI labscan
Acetone	$\text{C}_3\text{H}_6\text{O}$	58.08	99.5	RCI labscan
Dichloromethane	CH_2Cl_2	84.93	99.8	Carlo Erba

Table 3.1 Chemicals and reagents (cont.)

Chemicals and reagents	Formula	Mw (g/mol)	% Purity	Company
Phenyl acetate	C ₈ H ₈ O ₂	136.15	99.0	Acros organic
Methyl acetate	C ₃ H ₆ O ₂	74.08	99.8	Acros organic
Acetonitrile	CH ₃ CN	41.05	99.0	Carlo Erba
Benzene	C ₆ H ₆	78.11	99.8	Carlo Erba
Toluene	C ₇ H ₈	92.14	98.0	RCI labscan
Hexane	C ₆ H ₁₄	86.18	98.0	RCI labscan
Tetrahydrofuran	(CH ₂) ₄ O	72.11	99.5	Carlo Erba
Dimethyl sulfoxide	(CH ₃) ₂ SO	78.13	99.9	Carlo Erba

3.1.2. Glassware

Table 3.2 Glassware

1. Beakers	6. Volumetric flasks
2. Cylinders	7. Droppers
3. Glass funnel	8. Screw auto sampler vial
4. Glass scintillation vial with polyseal cone lined urea caps	9. Quartz cuvette
5. Stirring rod	10. Micropipette

3.1.3 Instrumentation

1. IR spectra were recorded in range of 4000-400 cm⁻¹ on a Perkin Elmer infrared spectrophotometer using a KBr pellet.

2. Elemental analysis (%C, %H and %N) was performed on a 628 series, Leco Corporation CHNS/O Analyzer.

3. SEM images and the corresponding elemental analyses were obtained by a JEOL 7800F SEM, equipped with a RIGAKU ZSX Primus energy dispersive spectroscopy (EDS) accessory.

4. Powder X-ray diffraction pattern were obtained on a Bruker D8 QUEST XRD system at 40 kV and 40 mA in the 2θ range 5-50 degree at room temperature .

5. X-ray crystallographic data of suitable single crystals were collected with a Bruker APEXII D8 QUEST CMOS, using Mo- K_{α} radiation ($\lambda = 0.71073 \text{ \AA}$).

6. Thermogravimetric analysis was performed under nitrogen flow with a heating rate of $10 \text{ }^{\circ}\text{C min}^{-1}$ using a Mettler Toledo SDTA851e analyzer.

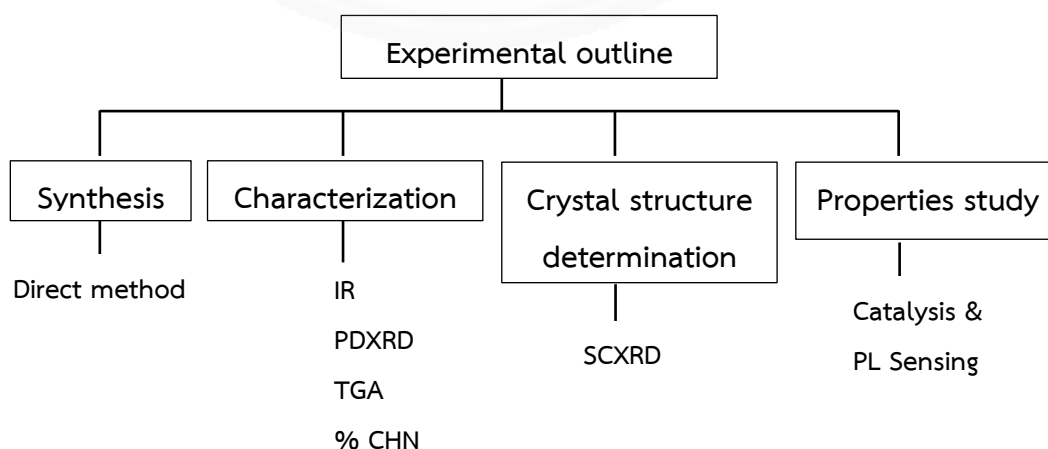
7. The solid state photoluminescence measurements were performed on a Horiba FluoroMax-4 spectrofluorometer at room temperature.

8. The photoluminescent spectra for liquid suspension were recorded on jasco FP-6200 spectrofluorometer.

9. Gas chromatograms were performed on a Shimadzu GC-2010 gas chromatograph system equipped with a FID detector using a 30-m Rtx-Wax column.

3.2 Method

The experimental procedure of this research consists of four steps namely, synthesis, characterization, crystal structure determination and properties study. The experimental outline of this research is shown in Figure 3.1. The details of synthesis for all compounds, catalytic study of (1) and PL sensing study of (2) are described.



Scheme 3.1 Experimental outline of this research

3.2.1 Synthesis

Synthesis of $[\text{Zn}(2,6\text{-dipic})]_n$ (1)

A mixture solution of pyridine-2,6-dicarboxylic acid (1.0 mmol) and NaOH (2.0 mmol) in 10 mL of distilled water was slowly dropped to 5 mL of a methanolic solution of $\text{Zn}(\text{NO}_3)_2 \cdot 4\text{H}_2\text{O}$ (1.0 mmol). The mixture solution was continuously stirred at 60°C for 30 min, resulting in the formation of white precipitate. Then, the mixture solution was filtered and left to evaporate at room temperature. The colorless block-shape crystals of $[\text{Zn}(2,6\text{-dipic})]_n$ (1) suitable for X-ray diffraction technique were obtained within 7 days, yield ca.63 % based on Zn(II) source (*Anal.Calced.* of $\text{C}_{112}\text{H}_{48}\text{N}_{16}\text{O}_{64}\text{Zn}_{16}$: C 36.48; H 1.31; N 6.02 *Found*: C 36.27; H 1.34; N 5.90).

Synthesis of $\{\text{CdNa}_2(1,3\text{-bdc})_2(\text{H}_2\text{O})_2(\text{DMF})\}_n$ (2)

A mixture solution of benzene-1,3-dicarboxylic acid (1.0 mmol) and NaOH (2.0 mmol) in 10 ml of distilled water was slowly dropped to 5 ml of a methanolic solution of $\text{Cd}(\text{NO}_3)_2 \cdot 4\text{H}_2\text{O}$ (1.0 mmol). The mixture solution was stirred at 60°C for 30 min, resulting in the formation of white precipitate. Then, 10 ml of DMF were added. Consequently, the mixture solution was continuously stirred and heated until a completely clear solution was obtained and filtered. This solution was allowed to slowly evaporate in the air. After 3 days, the colorless block-shape crystals of $\{\text{CdNa}_2(1,3\text{-bdc})_2(\text{H}_2\text{O})_2(\text{DMF})\}_n$ (2) suitable for X-ray diffraction technique were obtained, yield ca.76 % based on Cd(II) source (*Anal. Calced.* of $\text{C}_{19}\text{H}_{19}\text{CdNNa}_2\text{O}_{11}$: C 38.31; H 3.21; N 2.35 *Found*: C 38.36; H 3.26; N 2.33).

Synthesis of $\{[\text{Cd}_2(1,3\text{-bdc})_2(\text{DMF})] \cdot \text{DMF} \cdot 2\text{H}_2\text{O}\}$ (3)

The single crystal of this compound was obtained by using the same synthetic condition of compound (2). The crystal structure of (3) is determined by using the single crystal X-ray diffraction technique. However, this compound could not be repeated. In this thesis, only the structural feature of this compound is described in chapter 4.

3.2.2 Study of catalytic activity of [Zn(2,6-dipic)]_n (1)

3.2.2.1 Transesterification of phenyl acetate with methanol

The catalytic activity of synthesized coordination polymers (1) for the transesterification reaction of phenyl acetate and methanol was investigated. The reaction was designed by performing in a glass scintillation vial with polyseal cone lined urea caps. A solution of 10 mmol of phenyl acetate in 60 mmol of methanol was used in the presence of 0.05 g/g (5 mass % PA) of (1). To study the influence of temperature and time, the reactions were studied with different temperatures and time in range of RT-100 °C and 6-60 h, respectively for suitable conditions. After reaction, the reaction mixture was quenched by placing in an ice bath. Then, the solid catalyst was separated by filtration, while the filtrate was collected and diluted with dichloromethane, and the total volume of the solution was made up to 10 ml. This solution was subjected to quantitative GC analysis and the yield of the reaction was calculated. All reaction samples were run at least three times, and the average yields are reported here.

3.2.2.2 Reusability of the catalyst

The reusability of catalyst (1) for the transesterification of phenyl acetate with methanol was investigated. Phenyl acetate (10 mmol), methanol (60 mmol), and catalyst (5 mass % PA) were used. Each reaction batch, the mixture solution was heated and continuously stirred at 75 °C for 48 hours. After reaction completed, the reaction mixture was quenched by placing it in an ice bath. The reaction mixture was filtered. The liquid phase was analyzed by GC, while the solid catalyst was washed with methanol, dried at 85 °C for 10 hours, and reused directly as a catalyst for the next run under the same conditions.

3.2.3 Study of photoluminescence properties of $\{\text{CdNa}_2(1,3\text{-bdc})_2 \cdot (\text{H}_2\text{O})_2(\text{DMF})\}_n$ (2)

3.2.3.1 Solid state photoluminescence study

The solid state photoluminescence spectra of free 1,3-bdcH₂ ligand and compound (2) were recorded at room temperature with the excitation at 305 nm and emission range of 320 – 580 nm.

3.2.3.2 Solvent sensing study

The solvent sensing property of (2) was studied in the liquid suspension with various types of organic solvents namely, ethanol (EtOH), methanol (MeOH), dichloromethane (DCM), acetone (AC), benzene, tetrahydrofuran (THF), toluene, hexane and dimethyl sulfoxide (DMSO). The amount of 2 mg of finely ground fresh sample (2) was added to 3 ml different organic solvents without any activation. Consequently, the liquid suspension was allowed to ultrasonicate for 30 minutes, and then aged for 2 days to produce the stable suspensions. The fluorescent emission was recorded upon excitation at 300 nm. The fluorescence quenching efficiency was calculated based on $(1 - I/I_0) \times 100\%$, where I_0 and I are the fluorescence intensities before and after the addition of acetone respectively.

CHAPTER 4

RESULTS AND DISCUSSION

This chapter is presented about the results and discussion about crystal structure determination, crystal structure description and characterization by various techniques namely Fourier transform infrared spectroscopy, powder X-ray diffraction, thermogravimetric analysis, energy dispersive X-ray spectroscopy, solid-state photoluminescence spectroscopy of two novel coordination polymers namely $[Zn(2,6-dipic)]_n$ (**1**) and $\{CdNa_2(1,3-bdc)_2(H_2O)_2(DMF)\}_n$ (**2**) and the structural description of $\{Cd_2(1,3-bdc)_2(DMF)\} \cdot DMF \cdot 2H_2O$ (**3**). Moreover, the results of catalytic properties of (**1**) and solvent sensing properties of (**2**) are presented, respectively.

4.1 A novel 2D coordination polymer $[Zn(2,6-dipic)]_n$ (**1**)

4.1.1 Crystal structure determination

In order to determine the crystal structure of $[Zn(2,6-dipic)]_n$ (**1**), the selected crystal was inspected with microscope to ensure that no visible defects. Consequently, the selected crystal was attached to a glass fiber which was fastened to brass pin. Finally, the pin containing the crystal was mounted onto a goniometer head and placed onto the diffractometer.

The intensity data was collected on a single crystal of size $0.125 \times 0.119 \times 0.027 \text{ mm}^3$ at 293 K. Reflection data of this compound were collected on a 4 K Bruker SMART APEX CCD area detector diffractometer using *SMART* program [80]. The reflections were integrated using *SAINTE* program [81] and intensity data were corrected for Lorentz and polarization effects. Empirical absorption corrections were applied with *SADABS* program [82]. The structures were solved and refined by the Bruker *SHELXTL* program [83]. C-bound H atom were positioned geometrically, with $C-H = 0.93 \text{ \AA}$, and include as riding atoms, with $U_{iso}(H) = 1.2 U_{eq}(C)$.

4.1.2 Structural description

In compound $[\text{Zn}(2,6\text{-dipic})]_n$ (**1**), the zinc metal ions were in the +2 oxidation state and 2,6-dipicH₂ ligands were fully deprotonated for balance the charge of the compound.

The reaction of 2,6-dipicH₂ with $\text{Zn}(\text{NO}_3)_2 \cdot 4\text{H}_2\text{O}$ in the presence of NaOH leads to the formation of novel 2D coordination polymers, $[\text{Zn}(2,6\text{-dipic})]_n$ (**1**). Compound (**1**) was crystallized in monoclinic system space group *C2/c*. As shown in Figure 4.1, the asymmetric unit of this compound consists of three independent Zn(II) ions and two 2,6-dipic²⁻ ions. The Zn(2) and Zn(3) ions are occupied in centrosymmetric position with site occupancy of 0.5.

Crystallographic and refinement data are presented in Table 4.1. The selected bond lengths (Å) and angles (°) are listed in Table 4.2.

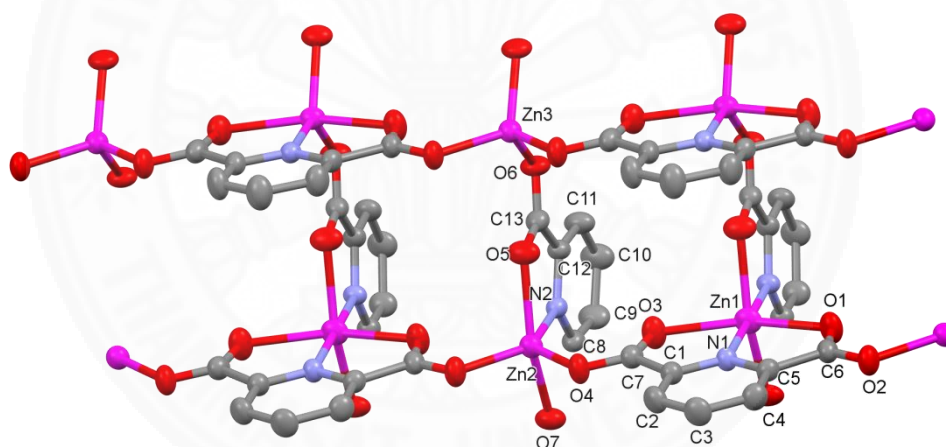


Figure 4.1 View of asymmetric unit of (**1**) with the atom numbering scheme

The molecular structure of $[\text{Zn}(2,6\text{-dipic})]_n$ (**1**) comprises of three crystallographic independent Zn(II) centers which are connected together by dipic²⁻ bridging ligands. Zn(1) ion is six coordinated by two dipic²⁻ ligands, four oxygen atoms of two different dipic²⁻ ligands in the basal plane with bond distance in range of 2.189(2) – 2.192(2) Å and two nitrogen atoms occupying the axial sites (1.996 Å), constructing a distorted octahedral geometry with $[\text{ZnN}_2\text{O}_4]$ chromophore as shown in Figure 4.2(a). This type of chromophore was found in mononuclear bis(dipic)

transition metal complexes [84,85]. For the molecular plane between two coordinated dipic ligand of Zn(1) chromophore presents almost perfectly perpendicular $92.97(9)^\circ$. Zn(2) ion is five coordinated by two oxygen atoms and one nitrogen atom from a dipic²⁻ ligand with bond distance of 2.031(2) – 2.196(2) Å and two oxygen (O2 and O4) atoms of carboxylate group from the other two adjacent dipic²⁻ bridging ligands (1.966(2) – 1.971(2) Å) as shown in Figure 4.2(b) generating a distorted trigonal bipyramidal geometry. While, Zn(3) ion is four coordinated by four oxygen atoms from different carboxylate groups of four different dipic bridges which coordinate to Zn(2) ions as shown in Figure 4.2(c).

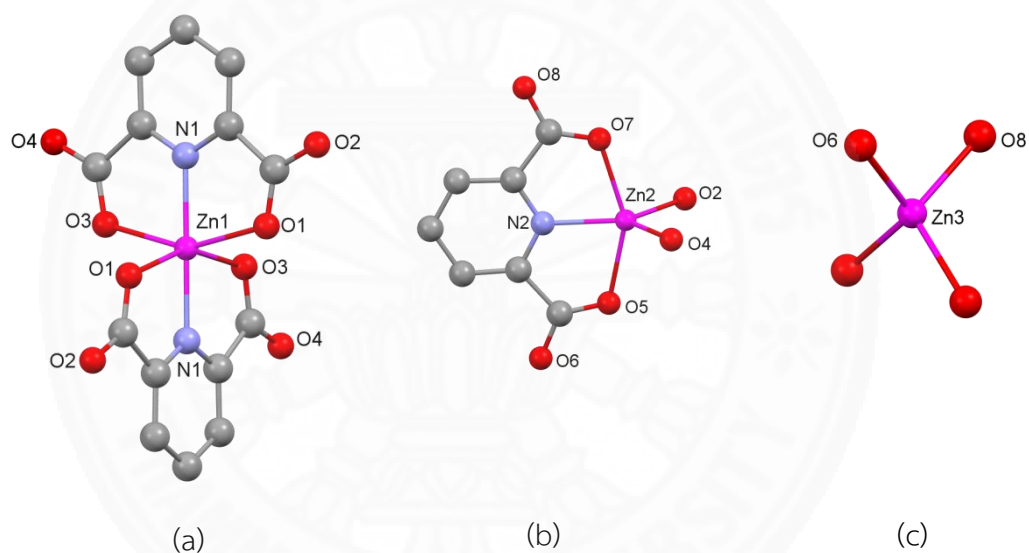


Figure 4.2 Views of Zn(II) chromophores in (1), (a) $[\text{Zn}(1)\text{N}_2\text{O}_4]$, (b) $[\text{Zn}(2)\text{NO}_4]$ and (c) $[\text{Zn}(3)\text{O}_4]$

Interestingly, all Zn(II) centers in the molecular structure of **(1)** are linked together by oxygen atoms of dicarboxylato groups in *syn-anti* bridging mode with the alternating Zn(1) and Zn(2) sites and the alternating Zn(2) and Zn(3) nodes, generating 2D network with (4,4) topology coordination framework in the crystallographic *ab* plane. The distances between zinc centers were 5.079(1), 5.111(1), 7.052(1) and 7.316(1) Å for Zn(1)···Zn(2), Zn(2)···Zn(3), Zn(1)···Zn(3) and Zn(2)···Zn(2), respectively. The polyhedra displacement of Zn(II) centers in two-dimensional network are represented in Figure 4.3

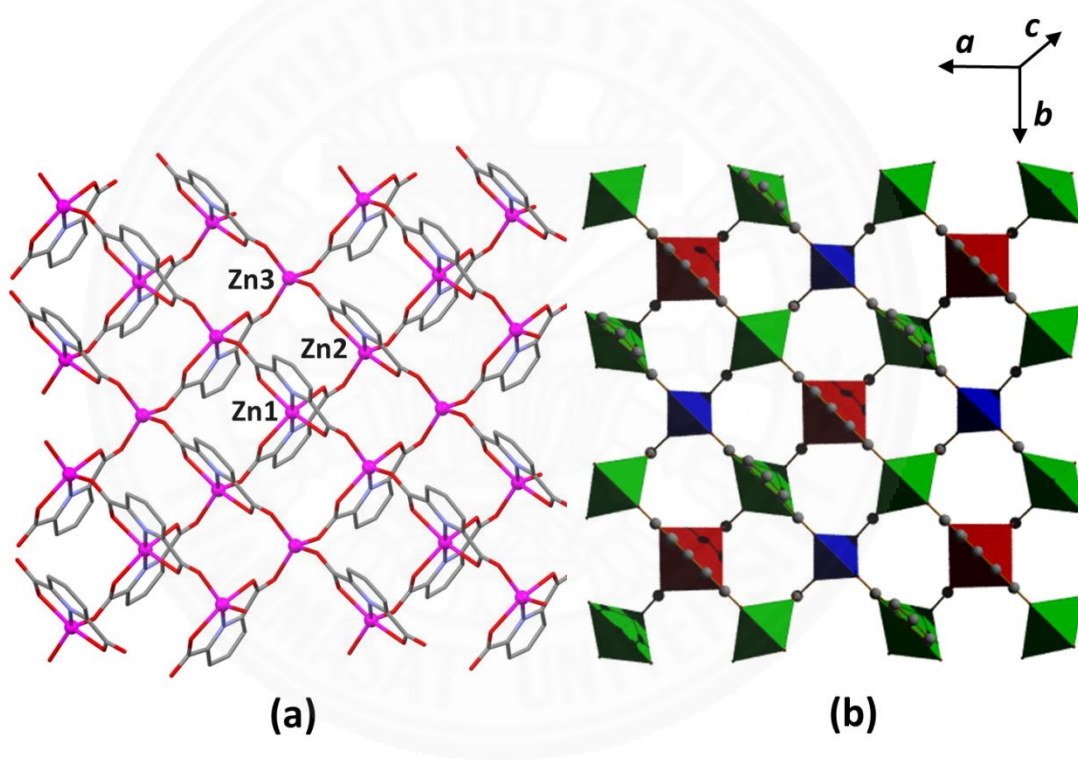


Figure 4.3 Views of (a) 2D structure and (b) polyhedral displacement of Zn(II) centers of **(1)**

Furthermore, the crystal structure of **(1)** is stabilized by hydrogen bonding interaction between adjacent 2D layers by C(3)-H(3) on pyridine ring of dipic ligand which coordinate to Zn(1) ion and O(5) of carboxylate group on dipic ligand which coordinate to Zn(2) [C3-H3···O5^{vii}, D-H 0.93 Å, H···A 2.25 Å, D···A 3.133(4) Å, D-H-

A 158° ; symmetry code $vii = -x+1, -y+2, -z+1$, resulting 3D supramolecular framework as shown in Figure 4.4.

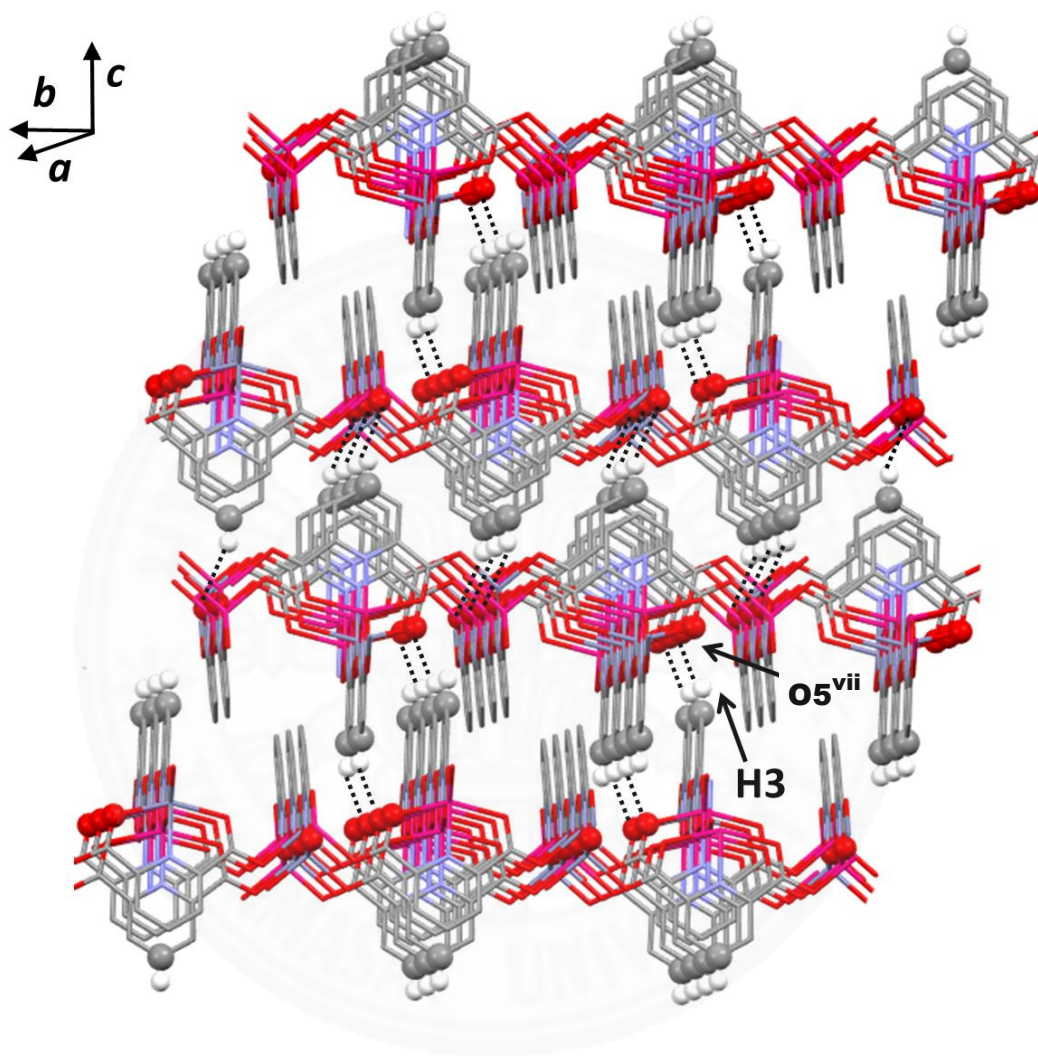


Figure 4.4 View of 3D supramolecular framework of (1) via C-H...O interaction between adjacent layers [C3-H3...O5^{vii}, D-H 0.93 Å, H...A 2.25 Å, D...A 3.133(4) Å, D-H-A 158° ; symmetry code $vii = -x+1, -y+2, -z+1$]

Table 4.1 Crystallographic and refinement data for [Zn(2,6-dipic)]_n (1)

Empirical formula	C ₁₄ H ₆ N ₂ O ₈ Zn ₂	
Formula weight	460.99	
Temperature/K	293	
Crystal system	monoclinic	
Space group	C2/c	
Unit cell dimensions	a/Å	14.0658(12)
	b/Å	14.0971(12)
	c/Å	16.6752(14)
	α/°	90
	β/°	100.6855(18)
	γ/°	90
Volume/Å ³	3249.1(5)	
Z	8	
Density (calculated) g.cm ³	1.8847	
Absorption coefficient (μ)/mm ⁻¹	3.001	
F(000)	1829.9	
Crystal size/mm ³	0.13 x 0.12 x 0.03	
2θ range for data collection/°	4.12 – 56.1	
Index ranges	-18 ≤ h ≤ 18, -18 ≤ k ≤ 18, -21 ≤ l ≤ 22	
Reflections collected	16685	
Independent reflections	3942[R _{int} = 0.0386, R _{sigma} = 0.0362]	
Data/restraints/parameters	3942/0/235	
Goodness-of-fit on F ²	1.035	
Final R indexes [I > 2σ(I)]	R ₁ = 0.0388, wR ₂ = 0.0857	
Final R indexes [all data]	R ₁ = 0.0603, wR ₂ = 0.0944	
Largest diff. peak/hole/eÅ ⁻³	0.58, -0.36	

$$R = \frac{\sum ||F_o| - |F_c||}{\sum |F_o|}, R_w = \left[\frac{\sum w \{ |F_o| - |F_c| \}^2}{\sum |F_o|^2} \right]^{1/2}$$

Table 4.2 Selected bond lengths (Å) and angles (°) for compound (1)

Bond lengths (Å)			
Zn(1)-N(1 ^{iv})	1.996(2)	Zn(2)-N(5)	2.031(2)
Zn(1)-N(1)	1.996(2)	Zn(2)-O(8 ⁱ)	1.971(2)
Zn(1)-O(5)	2.189(2)	Zn(2)-O(9)	2.196(2)
Zn(1)-O(5 ^{iv})	2.189(2)	Zn(3)-O(2 ⁱⁱ)	1.978(2)
Zn(1)-O(10 ^{iv})	2.192(2)	Zn(3)-O(2 ⁱⁱⁱ)	1.978(2)
Zn(1)-O(10)	2.192(2)	Zn(3)-O(1 ^{iv})	1.984(2)
Zn(2)-O(3)	1.996(2)	Zn(3)-O(1)	1.984(2)
Zn(2)-O(4)	2.165(2)		
Bond angle (°)			
N(1)-Zn(1)-N(1 ^{iv})	178.68(13)	N(5)-Zn(2)-O(3)	132.95(9)
O(5)-Zn(1)-N(1)	76.89(8)	N(5)-Zn(2)-O(4)	76.49(8)
O(5)-Zn(1)-N(1 ^{iv})	104.05(8)	O(8 ⁱ)-Zn(2)-O(3)	98.51(8)
O(5 ^{iv})-Zn(1)-N(1)	104.05(8)	O(8 ⁱ)-Zn(2)-O(4)	98.95(9)
O(5 ^{iv})-Zn(1)-N(1 ^{iv})	76.89(8)	O(8 ⁱ)-Zn(2)-N(5)	128.55(9)
O(5 ^{iv})-Zn(1)-O(5)	93.15(12)	O(9)-Zn(2)-O(3)	99.27(9)
O(10)-Zn(1)-N(1)	76.89(8)	O(9)-Zn(2)-O(4)	151.80(8)
O(10 ^{iv})-Zn(1)-N(1)	102.18(8)	O(9)-Zn(2)-N(5)	75.33(8)
O(10)-Zn(1)-N(1 ^{iv})	102.18(8)	O(9)-Zn(2)-O(8 ⁱ)	99.27(9)
O(10 ^{iv})-Zn(1)-N(1 ^{iv})	76.89(8)	O(2 ⁱⁱ)-Zn(3)-O(2 ⁱⁱⁱ)	114.27(13)
O(10 ^{iv})-Zn(1)-O(5 ^{iv})	153.77(7)	O(1)-Zn(3)-O(2 ⁱⁱⁱ)	97.54(8)
O(10)-Zn(1)-O(5)	153.77(7)	O(1 ^{iv})-Zn(3)-O(2 ⁱⁱⁱ)	115.72(9)
O(10)-Zn(1)-O(5 ^{iv})	92.97(9)	O(1 ^{iv})-Zn(3)-O(2 ⁱⁱ)	97.54(8)
O(10 ^{iv})-Zn(1)-O(5)	92.97(9)	O(1)-Zn(3)-O(2 ⁱⁱ)	115.72(9)
O(10)-Zn(1)-O(10 ^{iv})	92.72(12)	O(1)-Zn(3)-O(1 ^{iv})	117.24(12)
O(4)-Zn(2)-O(3)	99.10(9)		

Symmetry codes: ⁱ 1-x,+y,1/2-z; ⁱⁱ -x,+y,1/2-z; ⁱⁱⁱ 1/2+x,-1/2+y,+z; ^{iv} 1/2-x,1/2+y,1/2-z; ^v -1/2+x,1/2+y,+z; ^{vi} 1/2-x,-1/2+y,1/2-z

4.1.3 Structural comparison

To the best of our knowledge of structure closely related to compound (1), only the two-dimensional (4,4) grid network $\{[\text{Zn}(\text{HCAM})]\cdot\text{H}_2\text{O}\}$ has been reported by Gao and coworkers in 2006 [65]. This compound crystallized in the tetragonal space group $P-42_1c$. The Zn(II) ion is five-coordinated with a distorted trigonal bipyramidal geometry (Figure 4.5(a)). As shown in Figure 4.5(b), Zn(II) ions are connected together through four HCAM molecules with μ_3 -coordination mode to generate a 2D grid with a (4,4) network, which give two kind of Zn...Zn distances (4.979 and 5.315 Å). In comparison, compound (1) consists of three crystallographic independent Zn(II) centers. All Zn(II) centers of (1) were linked together by 2,6-dipic ligands with μ_3 -coordination mode, generating 2D network with (4,4) topology coordination framework. The distances between Zn centers were 5.079(1), 5.111(1), 7.052(1) and 7.316(1) Å for Zn(1)...Zn(2), Zn(2)...Zn(3), Zn(1)...Zn(3) and Zn(2)...Zn(2), respectively.

Another related two-dimensional (4,4) grid network coordination frameworks containing pyridine dicarboxylate ligands has been published, $\{[\text{Sm}_2(2,6\text{-dipic})(\text{ox})_2(\text{H}_2\text{O})_4]\cdot 4(\text{H}_2\text{O})\}_n$ (2,6-dipicH₂ = 2,6-pyridinedicarboxylic acid and oxH₂ = oxalic acid) [86]. This compound crystallized in the triclinic space group $P-1$. The Sm(II) ion have two types of coordination environments (Figure 4.6a). Sm1 is ten-coordinated, whereas Sm2 is nine-coordinated with a tricapped trigonal prism geometry. In Figure 4.6(b), Sm1 and Sm2 atoms are alternately arrayed by carboxylate bridges of dipic and ox bridging ligand and generate a tetranuclear homometallic Sm₄ square unit with 12-membered Sm₄C₂O₆ motifs. The rhombic Sm₄ metallic species as a building blocks are further connected by carboxylate O atoms to assemble into an infinite 2D grid with a (4,4) network. The distances between Sm1 and Sm2 atoms are 5.013(5) and 6.405(6) Å.

From the structural data of two related compounds above, it is found that both compound present 2D network which dipic derivatives presents μ_3 -coordination mode to link the metal centers.

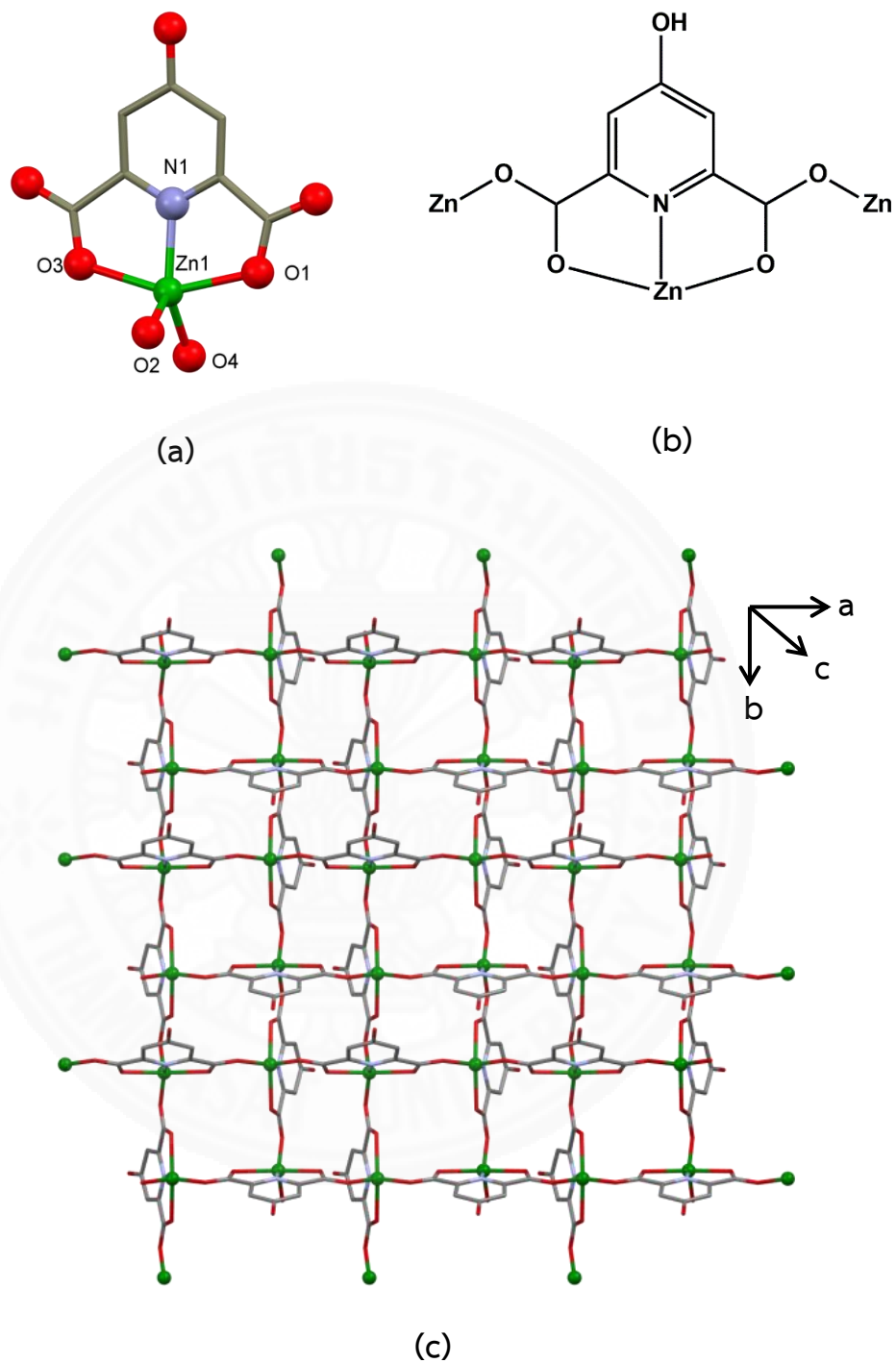


Figure 4.5 (a) Coordination environment of Zn(II), (b) μ_3 -coordination mode of HCAM ligand and (c) packing structure of $\{[Zn(HCAM)] \cdot H_2O\}$ view along c axis [65]

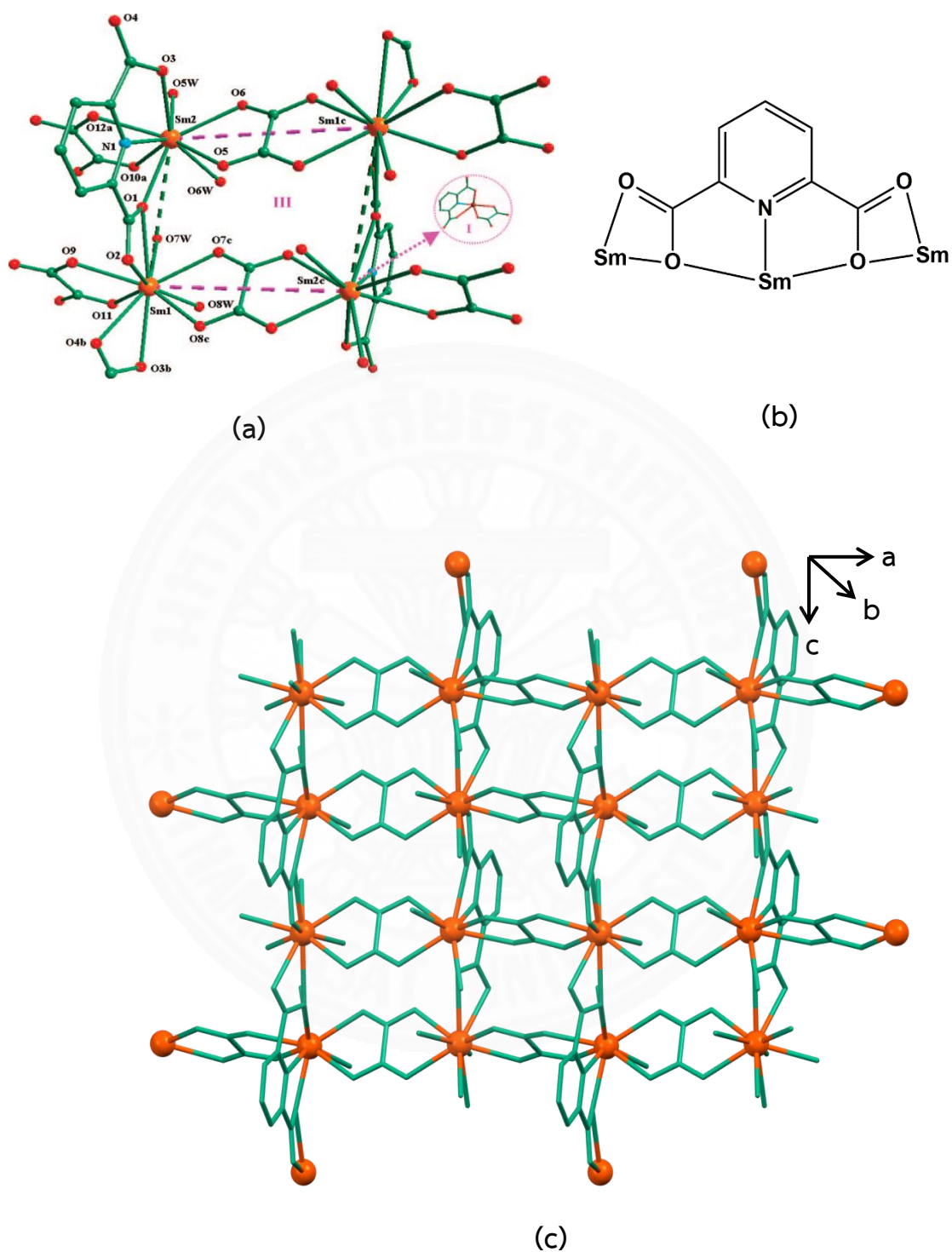


Figure 4.6 (a) Different coordination environments of the Sm ions, (b) μ_3 -coordination mode of 2,6-dipic and (c) packing structure of $\{[\text{Sm}_2(2,6\text{-dipic})(\text{ox})_2(\text{H}_2\text{O})_4] \cdot 4(\text{H}_2\text{O})\}_n$ view along b axis [86]

4.1.4 Infrared spectra

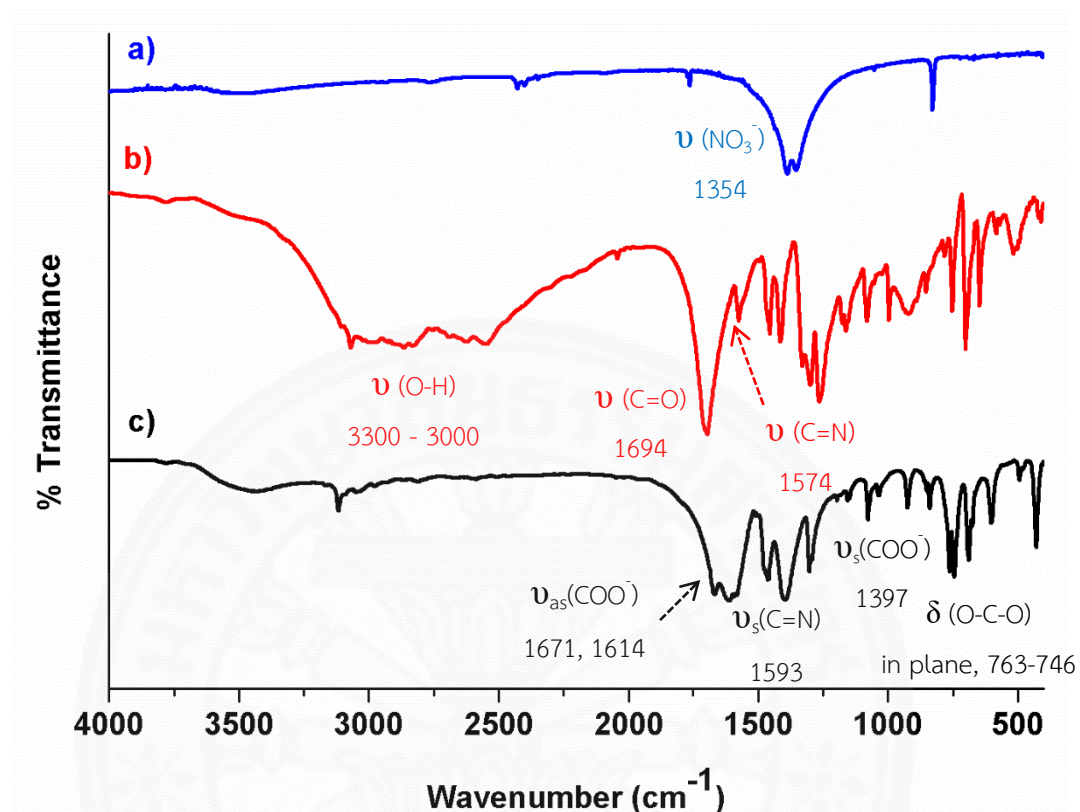
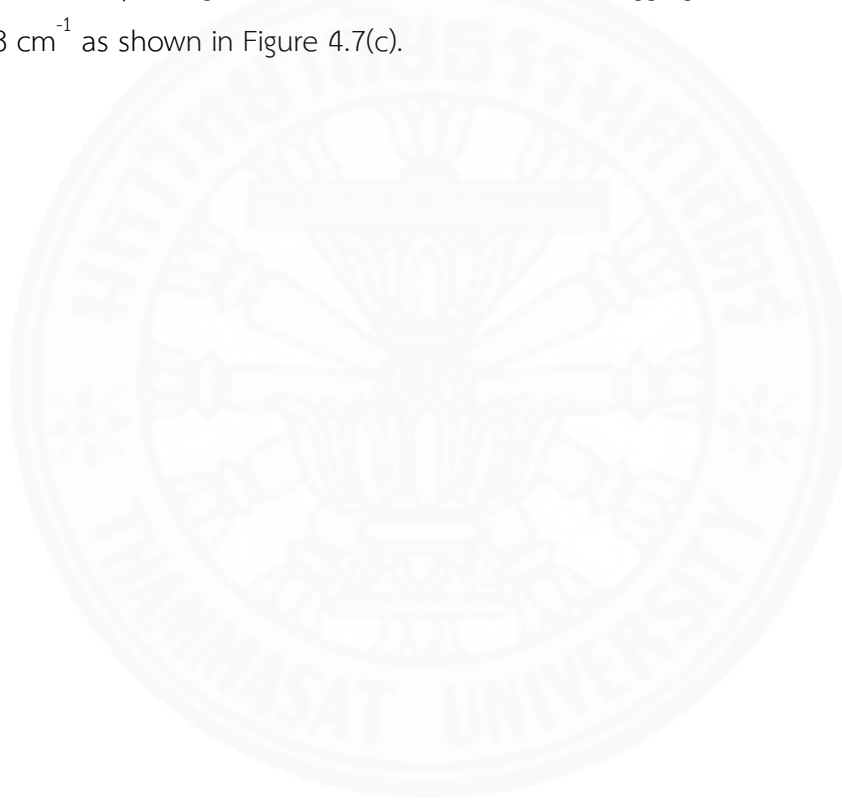


Figure 4.7 IR spectra of (a) $\text{Zn}(\text{NO}_3)_2 \cdot 4\text{H}_2\text{O}$, (b) 2,6-dipicH₂ and (c) $[\text{Zn}(2,6\text{-dipic})]_n$ (**1**)

To investigate the existence of the component in (**1**) by using the identification of the functional groups of synthesized coordination polymer, $[\text{Zn}(2,6\text{-dipic})]_n$ (**1**) and comparing with that of reactants, the FT-IR spectra of $\text{Zn}(\text{NO}_3)_2 \cdot 4\text{H}_2\text{O}$, 2,6-dipicH₂ and (**1**) were recorded in range of 4000 - 400 cm^{-1} on a Perkin Elmer infrared spectrophotometer using a KBr pellet.

The FT-IR spectrum of $\text{Zn}(\text{NO}_3)_2 \cdot 4\text{H}_2\text{O}$ was displayed the characteristic absorption peak of NO_3^- group at 1354 cm^{-1} as shown in Figure 4.7(a). In Figure 4.7(b), FT-IR spectrum of 2,6-dipicH₂ was exhibited very broad bands at 3000-3300 cm^{-1} . This band results from the O-H stretching of the carboxylic groups. The absorption peak at 1694 cm^{-1} was assigned to the absorption of C=O groups of carboxylate group. The characteristic band at 1574 cm^{-1} was assigned to the absorption of C=N groups in pyridine ring. For IR spectrum of (**1**), the absorption peak

of nitrate group was not found, confirming the nitrate group was disappeared in (1). The broad absorption peak of O-H stretching in carboxylic acid group was not presented, proving the carboxylic acid was fully deprotonated. The existence of strong bands in the 1671 and 1614 cm^{-1} were attributed to the asymmetric stretching vibration and 1397 cm^{-1} was assigned to symmetric stretching vibration of COO^- group, accounting for the presence of dipic [71,87]. The weak peak at 1593 cm^{-1} was assigned to the absorption of C=N group of dipic. The $\delta(\text{O-C-O})$ in plane deformation vibrations of dipic ring occurs at 763-746 cm^{-1} and wagging vibrations of pyridine ring at 688 cm^{-1} as shown in Figure 4.7(c).



4.1.4 Powder X-ray diffraction patterns

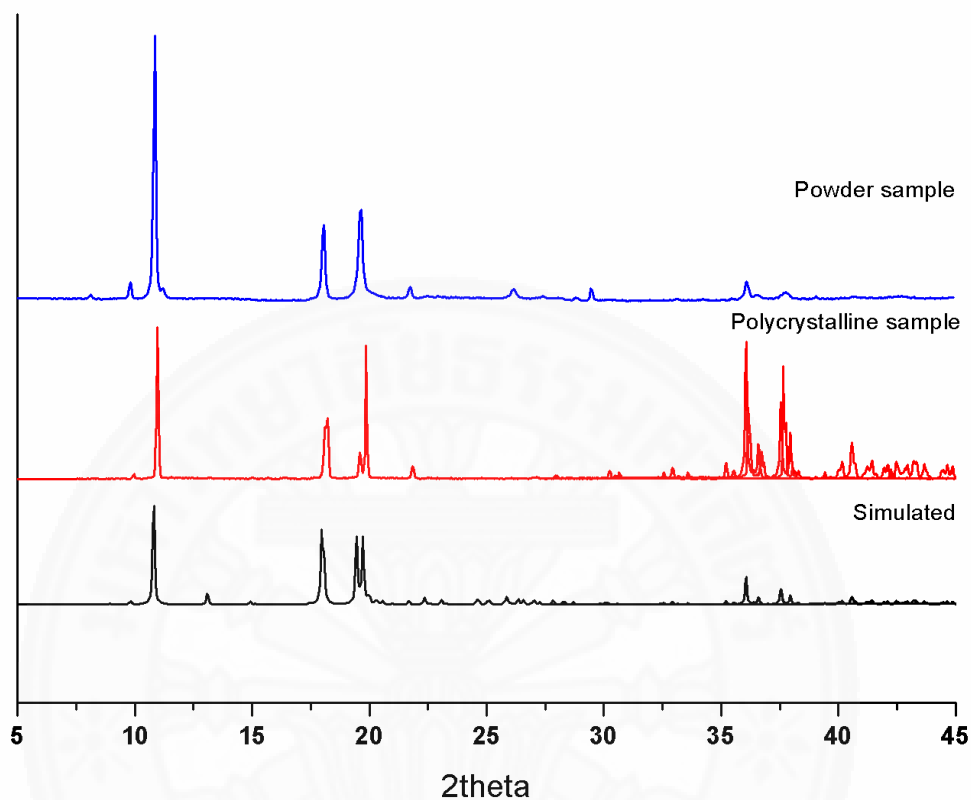


Figure 4.8 PDXRD patterns of $[Zn(2,6-dipic)]_n$ (1)

To confirm the phase purity of bulk solid sample in powder and polycrystalline forms by using powder X-ray diffraction (PDXRD) technique. The powder X-ray diffraction patterns for simulated and as-synthesized in both forms were shown in Figure 4.8. The peak positions and intensities of all patterns were matched well with those observed in the simulated patterns generated from single-crystal diffraction data, confirming both forms are purify and repeatable.

4.1.6 Thermogravimetric analysis

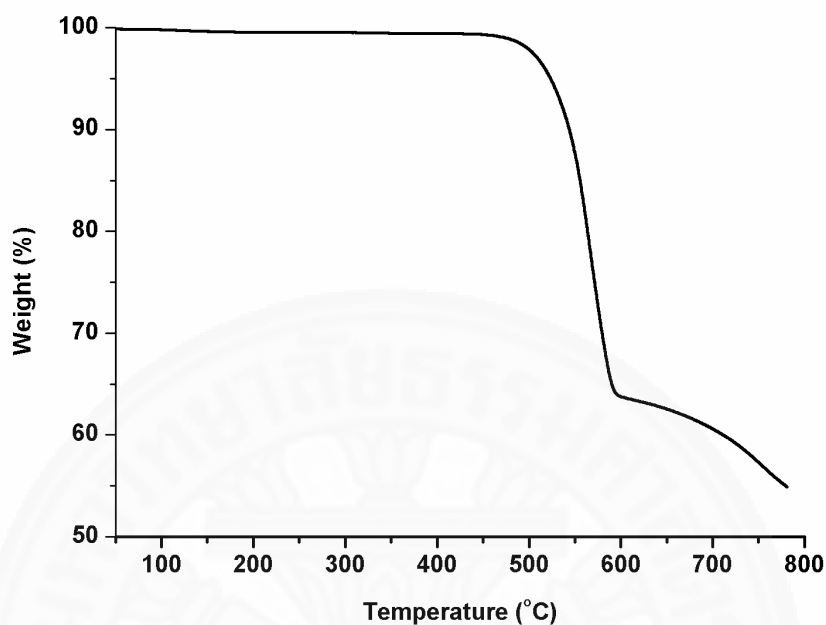


Figure 4.9 TGA curve of [Zn(2,6-dipic)]_n (1)

To study the thermal stability of (1), thermogravimetric analysis of [Zn(2,6-dipic)]_n (1) was investigated by thermogravimetric measurement which performed from room temperature to 800 °C under nitrogen atmosphere. In Figure 4.9, the thermogravimetric analysis curve shows that the structure of (1) is highly stable at high temperature to about 450 °C. The TGA curve exhibits the first decomposition of the framework after 450 °C. The main weight loss (35.16 wt %) reveals that the framework was started to collapse with the loss of a dipic molecule per formula. Furthermore, the weight loss was found at temperature higher than 600 °C which could be attributed to the formation of ZnO as the final product [64].

4.1.7 Photoluminescence property

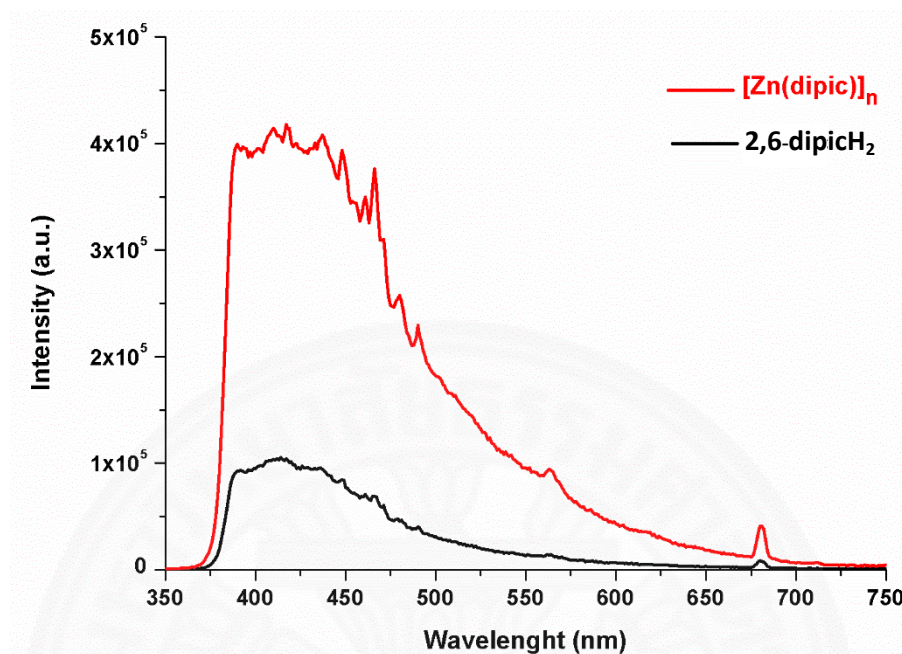
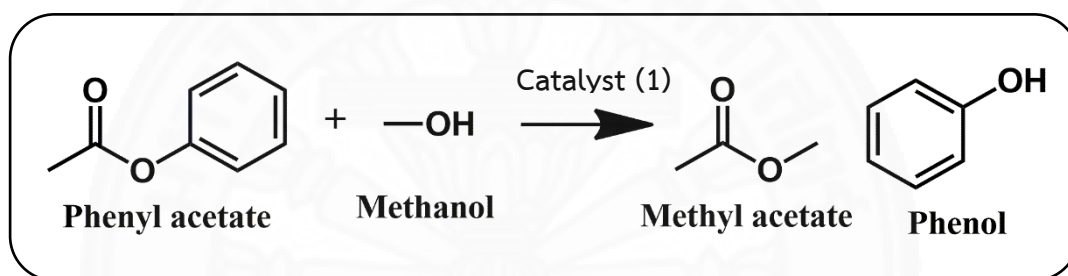


Figure 4.10 Solid state photoluminescent spectra of 2,6-dipicH₂ (black line) and [Zn(2,6-dipic)]_n (**1**) (red line)

Coordination polymers constructed from d^{10} -metal ions and conjugated aromatic linkers were known to be potential luminescent materials [57-60]. Therefore, the solid state photoluminescence properties of free 2,6-dipicH₂ ligand and [Zn(2,6-dipic)]_n (**1**) were investigated and performed by using a Horiba FluoroMax-4 spectrofluorometer at room temperature. Figure 4.10 presents the solid photoluminescent spectra of 2,6-dipicH₂ and (**1**) under excitation at 340 nm. The solid state photoluminescent spectrum of free 2,6-dipicH₂ ligand was exhibited the emission peak at 414 nm. While the photoluminescent spectrum of (**1**) presents the fluorescence enhancement and intense emission bands which observed at 417 nm, which may be attributed to ligand to metal charge transfer (LMCT) band [58,59]. The results indicate that compound (**1**) could be a good candidate for use as a luminescent material.

4.1.8 Catalytic activity

From crystal structural data analysis, compound (1) contains unsaturated metal sites on Zn₂ and Zn₃ which can be expected to be the active sites for the interesting organic reaction. Therefore, the potential catalytic activity of compound (1) was preliminary tested with selected transesterification reaction of phenyl acetate and methanol. In order to achieve optimal reaction conditions for the maximum methyl acetate yields, the reaction temperature and reaction time were studied. Moreover, the reusability of catalyst was also tested. The diagram of transesterification reaction is shown in scheme 4.1



Scheme 4.1 Transesterification of phenyl acetate and methanol

4.1.8.1 Effect of reaction temperature

The effect of reaction temperature on the methyl acetate yield (%) was designed and investigated by varying the reaction temperature in a range of room temperature, 50, 65, 75, 85 and 100 °C. While, the reactant concentrations, amount of catalyst and reaction time were fixed constant for all reaction temperature in which using a phenyl acetate (PA) concentration of 10 mmol, methanol concentration of 60 mmol, catalyst amount of 5 mass % PA and reaction time of 6 h.

In Figure 4.11, the result shows that when increasing reaction temperature from room temperature to 75 °C, the methyl acetate yield was enhanced from 2.76 – 35.59 %. Further increasing the reaction temperature up to 85 and 100 °C, the methyl acetate yield were reduced to 20.33 and 16.25 %, respectively. This result indicated that the maximum yield of methyl acetate were

obtained at 75 °C. The decrease of methyl acetate yield at reaction temperatures higher than 75 °C occurred because those temperature are above the boiling point of methanol. Therefore, methanol is mostly in vapor form cause to reducing the conversion of reactants.

Meanwhile, to compare the obtained methyl acetate yield from the reaction that without catalyst and reaction with catalyst in each temperature, the reaction without catalyst was simultaneously study. In Figure 4.11, the yellow bar show methyl acetate yield of the reaction without catalyst which is lower than methyl acetate yield from the reaction with catalyst in blue bar. This result indicated that the existence of catalyst can improve the methyl acetate yield in this reaction.

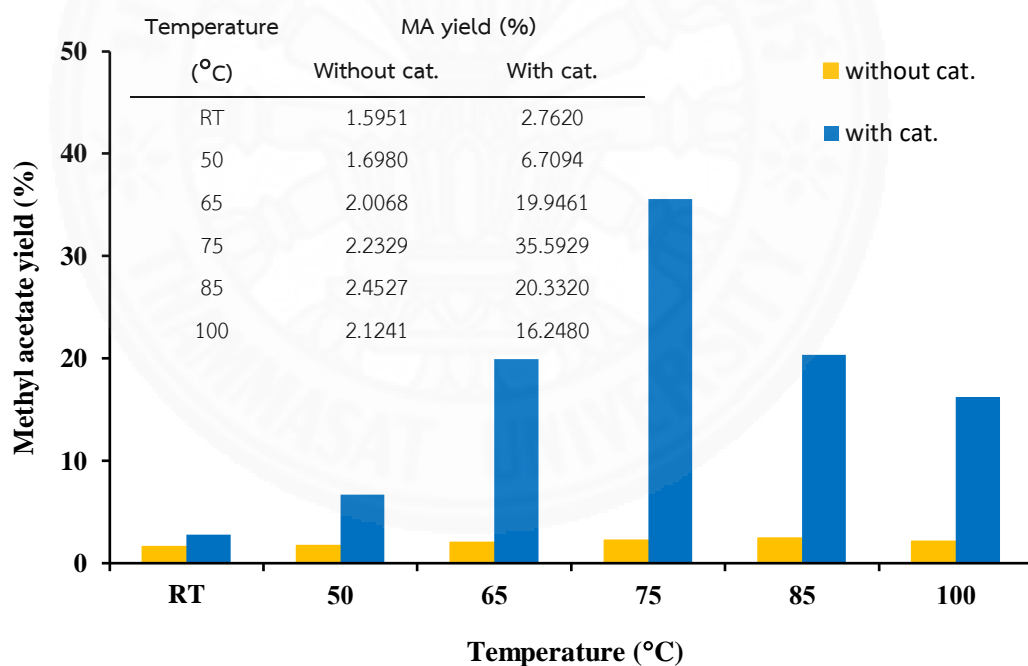


Figure 4.11 Plot of methyl acetate yield vs. reaction temperature for the transesterification reaction of phenyl acetate and methanol with (1) for 6 h

4.1.8.2 Effect of reaction time

The effect of reaction time on the methyl acetate yield (%) was also studied. The reaction was carried out by varying the reaction time in a range of 6, 12, 24, 48 and 60 h. Whereas, the reactant concentrations, catalyst amount and reaction temperature were kept constant which using a phenyl acetate (PA) concentration of 10 mmol, methanol concentration of 60 mmol, catalyst amount of 5 mass % PA and reaction temperature of 75 °C.

In Figure 4.12, it was found that when the reaction time was increased from 6 to 48 h, the methyl acetate yield increased from 35.59 % to 53.49 %. Further increasing the reaction time to 60 h reduced the methyl acetate yield (%) to 48.96 %. Therefore, the reaction approached equilibrium at 48 h under these conditions. From the obtained results, it can be indicated that 48 h was the optimal reaction time.

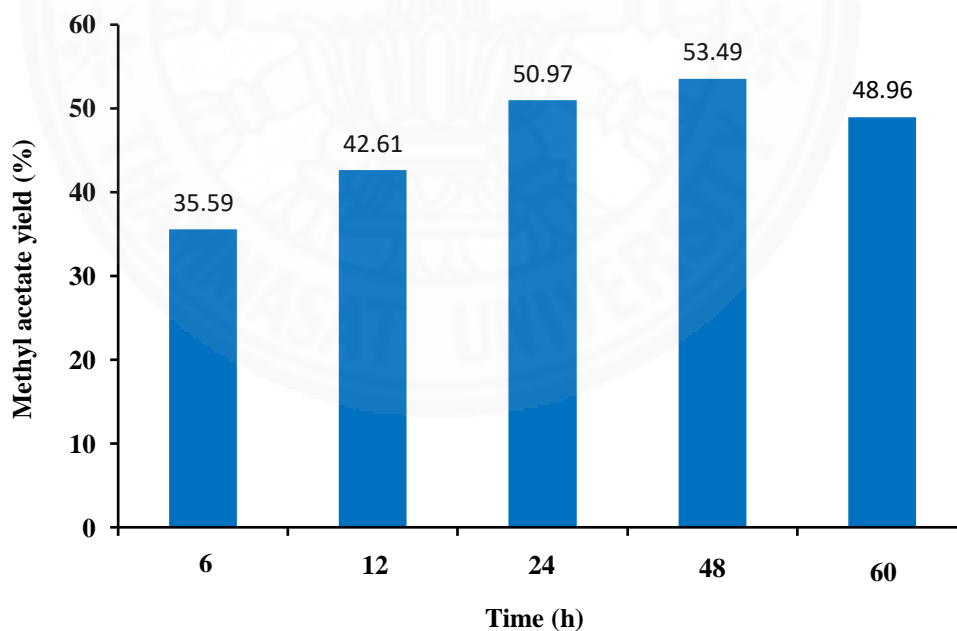


Figure 4.12 Plot of methyl acetate yield vs. reaction time for the transesterification reaction of phenyl acetate and methanol with (1) at 75 °C

4.1.8.3 Reusability of catalyst

Lastly, the reusability of catalyst was also studied. The reaction was carried out under the optimal conditions (75 °C for 48 h with a 1:6 molar ratio of PA: methanol). After the reaction completed, the catalyst was recovered by filtration, thoroughly washed with methanol and dried at 85 °C for 10 h before reusing it in subsequent transesterification process.

In Figure 4.13, it was observed that the methyl acetate yield reduced each cycle by ≤ 3.7 yield % after two cycles. From the obtained results, it can be explained that compound (1) showed good reusability without any significant loss of catalytic activity.

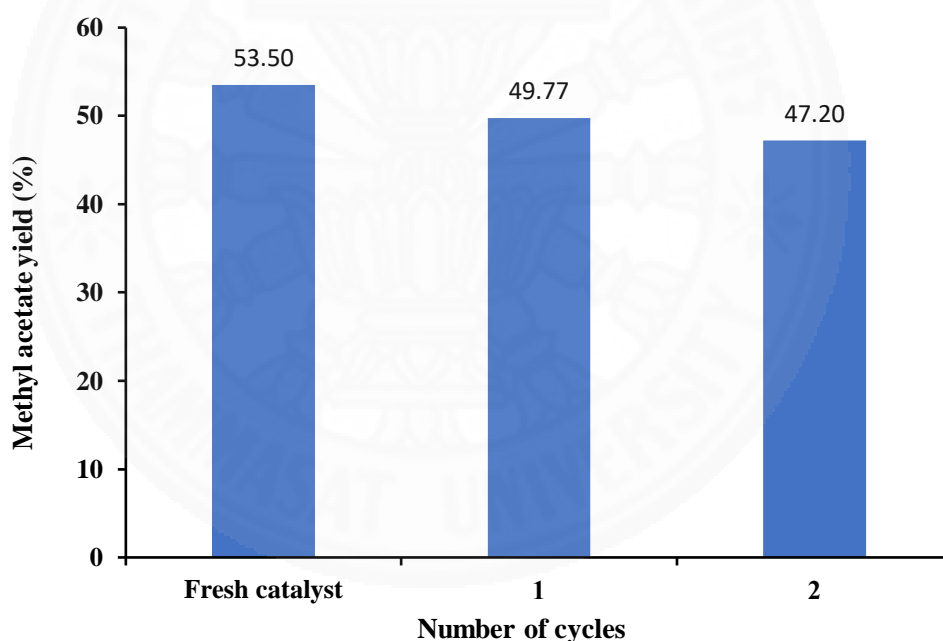


Figure 4.13 Effect of the catalyst recycling on the yield of methyl acetate

After reusing process, the stability of the catalyst was observed by powder X-ray diffraction (PXRD) technique. In Figure 4.14, it was observed that the PXRD patterns of recovered catalyst still match well with those of

fresh catalyst. Hence, compound (1) showed stable heterogeneous catalyst for this transesterification reaction.

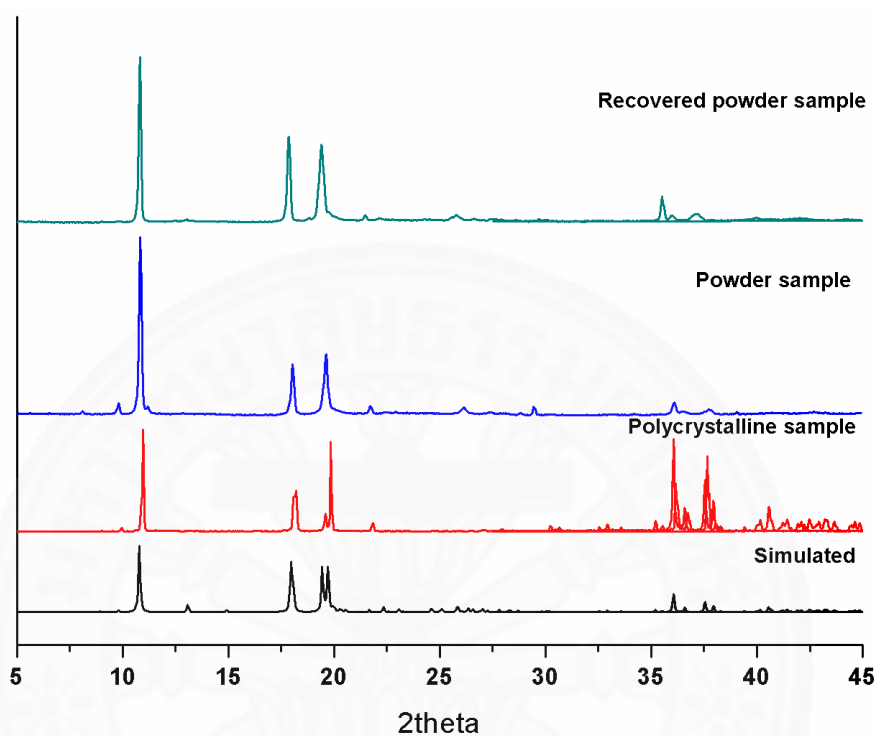
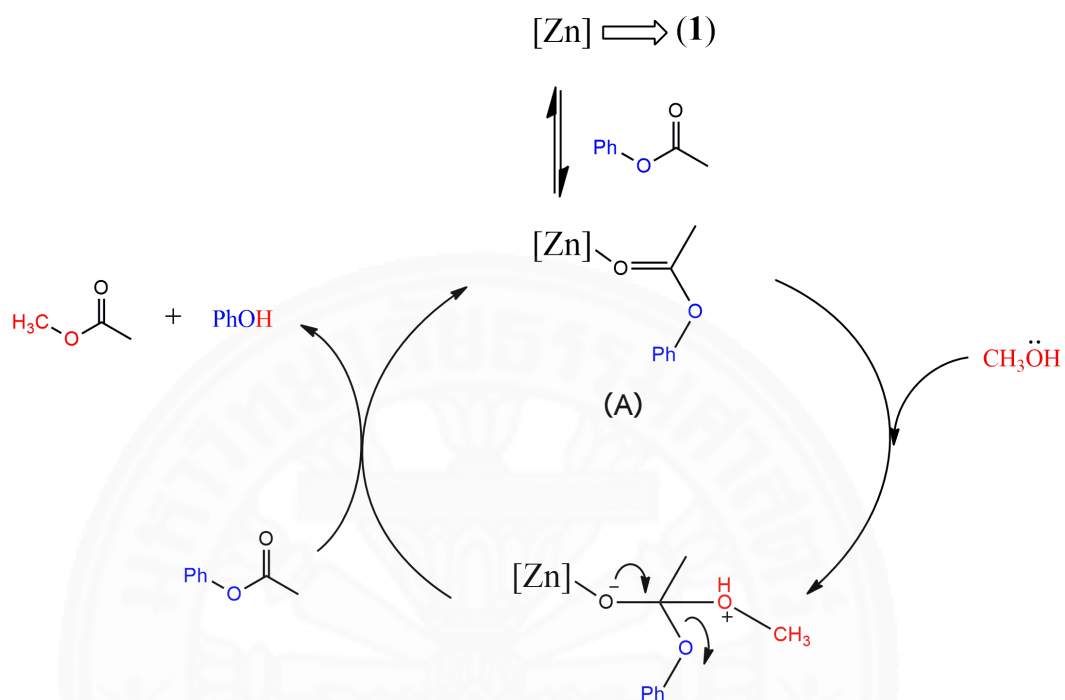


Figure 4.14 PDXRD patterns of recovered catalyst

In summary, these results may represent an excellent starting point for the development of a new simple synthetic method to produce the novel coordination polymer that might be efficiently used as heterogeneous catalysts.

4.1.8.4 Possibility of mechanism



Scheme 4.2 Proposed catalytic cycle for the transesterification reaction catalyzed by compound (1)

The mechanism of metal catalyzed transesterification may involve an electrophilic activation of the carbon center of the carbonyl moiety by binding of the metal to the carbonyl oxygen [88,89]. Based on this idea, a possible transesterification mechanism in this catalyst system can be proposed as shown in Scheme 4.2. At the first step, the carbonyl oxygen of the substrate phenyl acetate binds to the unsaturated Zn atom (Zn^{2+} and Zn^{3+}) to give adduct (A). Then, the nucleophile methanol would attack the carbon atom of the carbonyl moiety of the adduct (A) to produce the product methyl acetate.

According to the previous reports, there are several Zn(II) CPs related to compound (1) had been studied for catalytic activities of transesterification reaction focusing on the reaction of phenyl acetate and methanol. These reported Zn(II) CPs present various type of topology such as 1D, 2D and 3D frameworks. Their optimum reaction conditions and yield of product have been summarized in Table 4.3

Table 4.3 Catalytic activities of previously reported Zn(II) CPs for transesterification reaction of phenyl acetate and methanol

Catalyst	Reaction Condition	Yield (%)	[Ref.]
[Zn(2,6-dipic)] _n (1)	75 °C, 48 h	53.5	This work
[Zn(NO ₃)(H ₂ O) ₂ (btp) ₂] _n ⁺	RT, 120 h	100	[90]
[Zn ₃ (OH) ₃ {(NC ₅ H ₄) ₂ C ₃ H ₆ } ₃][NO ₃] ₃ ·8.67H ₂ O	RT, 17 h	100	[91]
[Zn ₆ (OH) ₈ {(NC ₅ H ₄) ₂ C ₃ H ₆ } ₄](OTf) ₄ ·3H ₂ O	RT, 72 h	100	[91]
[Zn(Hdpa)(H ₂ O) ₂ (SO ₄) _n]	RT, 17 days	100	[92]
[Zn(Hdpa)(Br) ₂] _n	RT, 120 h	100	[92]
[Zn(Hdpa)(Cl) ₂] _n	RT, 96 h	100	[92]
[Zn(glu)(μ-bpe)]·2H ₂ O	50 °C, 120 h	100	[54]
[Zn ₂ (MeO-dfp)(O ₂ CMe) ₂](O ₂ CMe) ₂ ·2H ₂ O	50 °C, 20 h	100	[93]
[Zn ₂ (Me-dfp)(O ₂ CMe) ₂](O ₂ CMe) ₂ ·2H ₂ O	50 °C, 20 h	52	[93]
[Zn ₂ (CO ₂ Et-dfp)(O ₂ CMe) ₂](O ₂ CMe) ₂ ·3H ₂ O	50 °C, 20 h	38	[93]
[Zn ₂ (Br-dfp)(O ₂ CMe) ₂](O ₂ CMe) ₂ ·H ₂ O	50 °C, 20 h	74	[93]

Note : btp = (2,6-bis(*N*-1,2,4-triazolyl)pyridine) ; Hdpa = 2,2'-dipyridylamine ; H₂glu = glutaric acid ; bpe = 1,2-bis(4-pyridyl)ethylene) ; dfp = 2,6-bis((*E*)-(1,3-dihydroxy-2-(hydroxymethyl)propan-2-ylimino)methyl)phenol

4.2 A novel 3D coordination polymer $\{\text{CdNa}_2(1,3\text{-bdc})_2(\text{H}_2\text{O})_2(\text{DMF})\}_n$ (**2**)

4.2.1 Crystal structure determination

The intensity data of (**2**) were collected on a single crystal of size $0.35 \times 0.21 \times 0.16 \text{ mm}^3$ at 296.15 K. Reflection data of this compound were collected on a Bruker APEXII D8 QUEST CMOS diffractometer [94]. The reflections were integrated using *SAINIT* program [94] and intensity data were corrected for Lorentz and polarization effects. Empirical absorption corrections were applied with *SADABS* program [94]. The structures were solved and refined by the *SHELXT* program [95]. All hydrogen atoms except those of water molecules were geometrically generated and isotropically refined using a riding model, with $\text{C-H} = 0.93 \text{ \AA}$ and $U_{\text{iso}}(\text{H}) = 1.2U_{\text{eq}}(\text{C})$. The coordinated DMF molecule was found to be disordered with two set of sites with a refined occupancy ratio of 0.382(10) and 0.618(10).

4.2.2 Structural description of $\{\text{CdNa}_2(1,3\text{-bdc})_2(\text{H}_2\text{O})_2(\text{DMF})\}_n$ (**2**)

Compound (**2**) crystallizes in the tetragonal crystal system with $P4_3$ space group. Crystallographic and refinement data was presented in Table 4.4. The selected bond lengths (\AA) and angles ($^\circ$) were listed in Table 4.5.

The asymmetric unit of (**2**) consists of one Cd(II) ion, two crystallographically independent Na(I) ions, two 1,3-bdc²⁻ ligands, two coordinated water molecules and one coordinated DMF molecules, as shown in Figure 4.15.

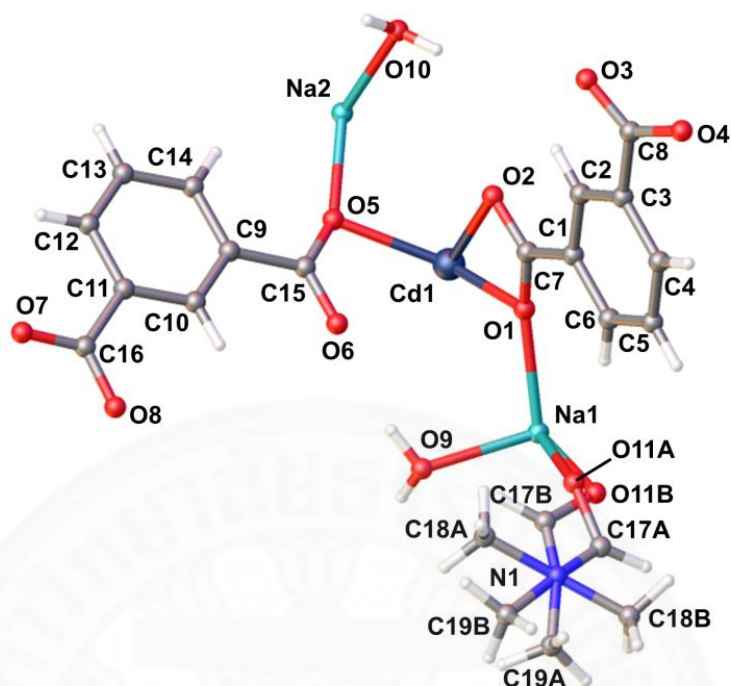


Figure 4.15 Asymmetric unit of (2) with the atomic-numbering scheme. Displacement ellipsoids are drawn at the 50% probability level.

Each Cd(II) ion is coordinated by seven carboxylate oxygen atoms from four different 1,3-bdc²⁻ ligands with the Cd-O bond distances range between 2.301 (3) and 2.555 (3) Å as presented in Table 4.5. The Na1 ion is surrounded by three carboxylate oxygen atoms of three different 1,3-bdc²⁻ ligands, one oxygen atom from water molecule, and one DMF molecule with the Na-O bond distances ranging between 2.304 (7) and 2.498 (11) Å, while the Na2 ion adopts a five-coordinate [4+1] coordination with four oxygen atoms from three different 1,3-bdc²⁻ ligands and one oxygen atom from water molecule. The Na-O bond distances are in the range of 2.275 (5) - 2.354 (8) Å. Figure 4.16 shows the coordination modes of the 1,3-bdc²⁻ ligand in compound (2). The 1,3-bdc²⁻ molecule is fully deprotonated and coordinated to the Cd(II) and Na(I) ions in a μ_5 -coordination mode, generating a one-dimensional heterobimetallic chain running parallel to the *c* axis.

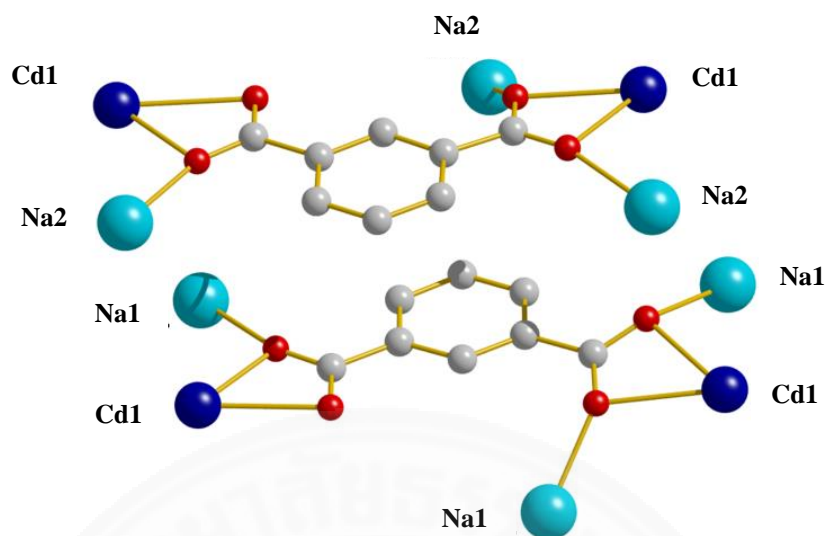


Figure 4.16 Coordination mode, μ_5 -1,3-bdc bridging ligands found in (2). All hydrogen atoms are omitted for clarity.

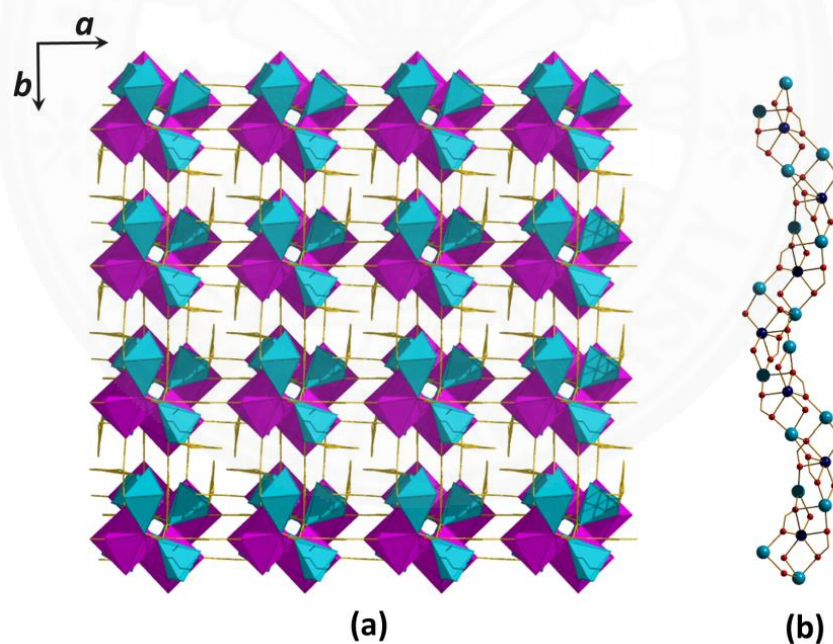


Figure 4.17 Perspective view along crystallographic c axis of (a) the three dimensional framework of (2) (coordination polyhedra for Cd(II) and Na(I) are pink and green, respectively) and (b) helical chain-like structure of Cd-Na clusters (dark blue = Cd, blue = Na and red = O).

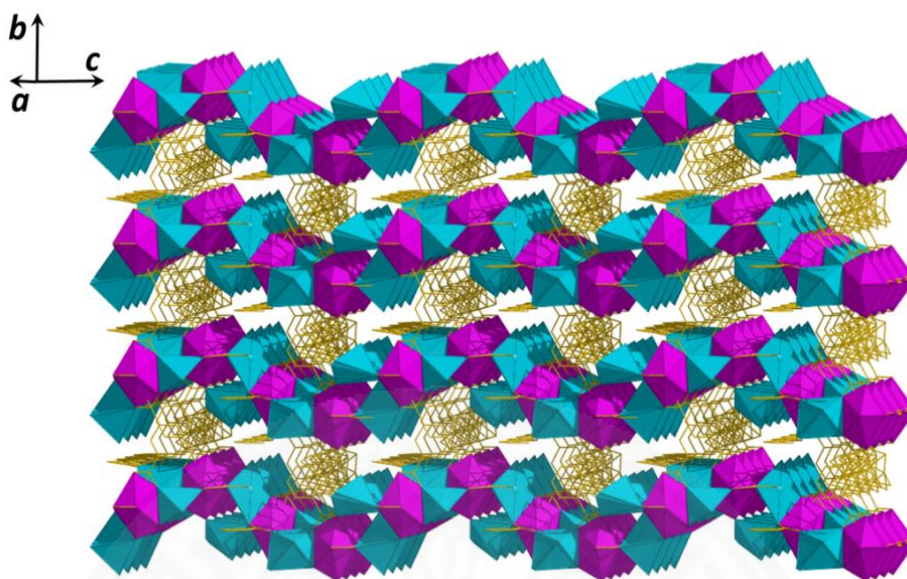


Figure 4.18 Perspective view of three-dimensional framework of **(2)** (coordination polyhedra for Cd(II) and Na(I) are pink and green, respectively).

All hydrogen atoms are omitted for clarity.

Each chain is further linked to neighboring chains through the 1,3-bdc²⁻ ligands in the *a*- and *b*-axis directions, leading to an interesting 3D framework structure (Figure 4.17 and 4.18). The coordinated water and DMF molecules adopt a monodentate coordination mode and serve as a terminal pendant ligand pointing inside the channels.

In the crystal of **(2)**, classical O-H...O hydrogen bonds and aromatic π - π stacking interactions are observed and these interactions presumably help to stabilize the frameworks. All water molecules are shown to act as O-H...O hydrogen bond donors towards the carboxylate groups of the 1,3-bdc²⁻ ligands (Table 4.6). The π - π stacking interactions are between symmetry-related aromatic rings of the 1,3-bdc ligands with a Cg1...Cg2ⁱⁱⁱ distance of 3.588 (3) Å (Symmetry code: (iii) $-y, x, z-1/4$) and a dihedral angle of 3.8 (4)^o [Cg1 and Cg2 are the centroids of the C1-C6 and C9-C14 rings, respectively].

Table 4.4 Crystallographic and refinement data for compound (2)

Empirical formula		$C_{19}H_{19}NCdNa_2O_{11}$
Formula weight		595.73
Temperature/K		296.15
Crystal system		Tetragonal
Space group		$P4_3$
Unit cell dimensions	$a/\text{\AA}$	10.1437(8)
	$b/\text{\AA}$	10.1437(8)
	$c/\text{\AA}$	21.4664(15)
	$\alpha/^\circ$	90
	$\beta/^\circ$	90
	$\gamma/^\circ$	90
Volume/ \AA^3		2208.8(4)
Z		4
Density (calculated) g.cm^{-3}		1.791
Absorption coefficient (μ)/ mm^{-1}		1.090
F(000)		1192.0
Crystal size/ mm^3		0.35 x 0.21 x 0.16
2θ range for data collection/ $^\circ$		5.526 – 57.43
Index ranges		$-13 \leq h \leq 13, -12 \leq k \leq 13, -28 \leq l \leq 29$
Reflections collected		56814
Independent reflections		5708 [$R_{\text{int}} = 0.0740, R_{\text{sigma}} = 0.0366$]
Data/restraints/parameters		5708/160/351
Goodness-of-fit on F^2		1.034
Final R indexes [$I \geq 2\sigma(I)$]		$R_1 = 0.0274, wR_2 = 0.0651$
Final R indexes [all data]		$R_1 = 0.0318, wR_2 = 0.0666$
Largest diff. peak/hole/ $\text{e}\text{\AA}^{-3}$		0.52, -0.45
Flack parameter		0.080(13)

$$R = \frac{\sum ||F_o| - |F_c||}{\sum |F_o|}, R_w = \left[\frac{\sum w \{ |F_o| - |F_c| \}^2}{\sum |F_o|^2} \right]^{1/2}$$

Table 4.5 Selected bond lengths (Å) and angles (°) for compound (2)

Bond lengths (Å)			
Cd(1)-O(1)	2.301(3)	Na(1)-O(4 ⁱ)	2.442(5)
Cd(1)-O(2)	2.556(3)	Na(1)-O(9)	2.303(7)
Cd(1)-O(3 ⁱ)	2.495(3)	Na(1)-O(11B)	2.497(11)
Cd(1)-O(4 ⁱ)	2.385(3)	Na(1)-O(11A)	2.475(19)
Cd(1)-O(5)	2.284(4)	Na(2)-O(4 ^v)	2.655(4)
Cd(1)-O(7 ⁱⁱ)	2.396(3)	Na(2)-O(5)	2.277(5)
Cd(1)-O(8 ⁱⁱ)	2.472(3)	Na(2)-O(7 ⁱⁱ)	2.281(4)
Na(1)-Na(2 ⁱⁱⁱ)	3.915(6)	Na(2)-O(8 ^{vi})	2.275(5)
Na(1)-O(1)	2.368(5)	Na(2)-O(10)	2.355(8)
Na(1)-O(3 ^{iv})	2.338(5)		
Symmetry codes: ⁱ +x,-1+y,+z; ⁱⁱ -1+x,+y,+z; ⁱⁱⁱ -y,+x,-1/4+z; ^{iv} 1-y,+x,-1/4+z; ^v -1+y,-x,1/4+z; ^{vi} +y,1-x,1/4+z			
Bond angle (°)			
O(1)-Cd(1)-O(2)	53.14(14)	O(7 ⁱⁱ)-Cd(1)-O(3 ⁱ)	93.99(14)
O(1)-Cd(1)-O(3 ⁱ)	131.60(14)	O(7 ⁱⁱ)-Cd(1)-O(8 ⁱⁱ)	53.57(13)
O(1)-Cd(1)-O(4 ⁱ)	80.31(12)	O(8 ⁱⁱ)-Cd(1)-O(2)	93.07(11)
O(1)-Cd(1)-O(7 ⁱⁱ)	125.93(12)	O(8 ⁱⁱ)-Cd(1)-O(3 ⁱ)	91.93(10)
O(1)-Cd(1)-O(8 ⁱⁱ)	92.03(13)	O(1)-Na(1)-Na(2 ⁱⁱⁱ)	77.98(11)
O(3 ⁱ)-Cd(1)-O(2)	172.97(16)	O(1)-Na(1)-O(4 ⁱ)	77.82(16)
O(4 ⁱ)-Cd(1)-O(2)	132.62(15)	O(1)-Na(1)-O(11B)	104.0(4)
O(4 ⁱ)-Cd(1)-O(3 ⁱ)	53.38(12)	O(1)-Na(1)-O(11A)	97.3(6)
O(4 ⁱ)-Cd(1)-O(7 ⁱⁱ)	122.40(12)	O(3 ^{iv})-Na(1)-Na(2 ⁱⁱⁱ)	77.95(14)
O(4 ⁱ)-Cd(1)-O(8 ⁱⁱ)	78.81(13)	O(3 ^{iv})-Na(1)-O(1)	151.0(2)
O(5)-Cd(1)-O(1)	125.67(14)	O(3 ^{iv})-Na(1)-O(4 ⁱ)	94.58(15)
O(5)-Cd(1)-O(2)	90.34(16)	O(3 ^{iv})-Na(1)-O(11B)	83.0(3)
O(5)-Cd(1)-O(3 ⁱ)	82.64(15)	O(3 ^{iv})-Na(1)-O(11A)	93.2(6)
O(5)-Cd(1)-O(4 ⁱ)	128.83(14)	O(4 ⁱ)-Na(1)-Na(2 ⁱⁱⁱ)	41.85(10)

Bond angle (°) (cont.)

O(5)-Cd(1)-O(7 ⁱⁱ)	80.40(12)	O(4 ⁱ)-Na(1)-O(11B)	177.5(4)
O(5)-Cd(1)-O(8 ⁱⁱ)	133.24(16)	O(4 ⁱ)-Na(1)-O(11A)	171.2(8)
O(7 ⁱⁱ)-Cd(1)-O(2)	85.03(14)	O(9)-Na(1)-Na(2 ⁱⁱⁱ)	130.1(2)
O(9)-Na(1)-O(1)	95.8(2)	O(5)-Na(2)-O(10)	104.5(2)
O(9)-Na(1)-O(3 ^{iv})	122.0(2)	O(7 ⁱⁱ)-Na(2)-Cd(1 ^v)	133.30(13)
O(9)-Na(1)-O(4 ⁱ)	88.3(2)	O(7 ⁱⁱ)-Na(2)-Na(1 ^v)	92.35(12)
O(9)-Na(1)-O(11B)	93.2(4)	O(7 ⁱⁱ)-Na(2)-O(4 ^{vi})	94.98(14)
O(9)-Na(1)-O(11A)	84.9(9)	O(7 ⁱⁱ)-Na(2)-O(10)	80.5(2)
O(11A)-Na(1)-Na(2 ⁱⁱⁱ)	144.8(9)	O(8 ^{vii})-Na(2)-Cd(1 ^v)	38.83(8)
Cd(1 ^v)-Na(2)-Na(1 ^v)	55.94(7)	O(8 ^{vii})-Na(2)-Na(1 ^v)	89.00(13)
O(4 ^{vi})-Na(2)-Cd(1 ^v)	38.59(8)	O(8 ^{vii})-Na(2)-O(4 ^{vi})	77.01(13)
O(4 ^{vi})-Na(2)-Na(1 ^v)	37.87(11)	O(8 ^{vii})-Na(2)-O(5)	110.18(16)
O(5)-Na(2)-Cd(1 ^v)	102.07(15)	O(8 ^{vii})-Na(2)-O(7 ⁱⁱ)	164.92(18)
O(5)-Na(2)-Na(1 ^v)	57.70(13)	O(8 ^{vii})-Na(2)-O(10)	102.3(2)
O(5)-Na(2)-O(4 ^{vi})	95.46(19)	O(10)-Na(2)-Cd(1 ^v)	139.3(2)
O(5)-Na(2)-O(7 ⁱⁱ)	83.03(17)	O(10)-Na(2)-Na(1 ^v)	161.75(19)
O(10)-Na(2)-O(4 ^{vi})	158.7(2)		

Symmetry codes: ⁱ +x,-1+y,+z; ⁱⁱ -1+x,+y,+z; ⁱⁱⁱ -y,+x,-1/4+z; ^{iv} 1-y,+x,-1/4+z; ^v +y,-x,1/4+z;
^{vi} -1+y,-x,1/4+z; ^{vii} +y,1-x,1/4+z; ^{viii} +x,1+y,+z; ^{ix} -y,1+x,-1/4+z; ^x 1+x,+y,+z

Table 4.6 Hydrogen bond geometry (Å, °) for compound (2)

<i>D</i> -H... <i>A</i>	<i>D</i> -H	H... <i>A</i>	<i>D</i> ... <i>A</i>	<i>D</i> -H... <i>A</i>
O9-H9B...O6	0.90	2.22	3.074(8)	159
O10-H10B...O6 ^{vii}	0.86	2.29	3.073(8)	152

Symmetry code: (vii) y, -x+1, z+1/4.

4.2.3 Structural comparison

To the best of our knowledge of structure closely related to compound (2), only the three-dimensional coordination framework $\{[\text{CdNa}(1,3\text{-bdc})_2]\cdot[\text{NH}_2(\text{CH}_3)_2]\}$ has been reported by Che and coworkers in 2007 [96]. This compound crystallized in the centrosymmetric space group $C2/c$. The Cd(II) and Na(I) centers are linked by a 1,3-bdc ligand in a μ_4 -coordination mode (Figure 4.19 (a)). The DMF solvent decomposes under solvothermal synthesis, with the construction of a 3D coordination framework with open channels containing $\text{NH}_2(\text{CH}_3)_2$ molecules as shown in Figure 4.19 (b). In comparison, compound (2) contains coordinated H_2O and DMF molecules projecting into the framework channels. Other related three-dimensional heterobimetallic d^{10} -Na(I) coordination frameworks containing benzene polycarboxylate ligands have been published, such as $[\text{CdNa}(\text{OH}-1,3\text{-bdc})_2(\text{H}_2\text{O})_2]\cdot 2\text{H}_2\text{O}$ where $\text{OH}-1,3\text{-bdcH}_2 = 5\text{-hydroxy-benzene-1,3-dicarboxylic acid}$ [97], $[\text{Zn}_2\text{Na}_2(1,4\text{-bdc})_3\cdot(\text{DMF})_2\cdot(\text{H}_2\text{O})_2]$ where $1,4\text{-bdcH}_2 = \text{benzene-1,4-dicarboxylic acid}$ [98], $[\text{ZnNa}(1,2,4\text{-btc})]$ where $1,2,4\text{-btc} = 1,2,4\text{-benzenetricarboxylate}$ [99] and $[\text{Cd}_8\text{Na}(\text{ntc})_6(\text{H}_2\text{O})_8]$ where $\text{ntcH}_3 = 5\text{-nitrobenzene-1,2,3-tricarboxylic acid}$ [100]. The three dimensional coordination framework topologies of these compounds are the result of the construction of different types of metal centers, geometries and carboxylate ligand derivatives. It is found that the carboxylate ligand derivatives in the structure of these related compounds almost exhibit a μ_4 -coordination mode as presented in Figure 4.20(a) and 4.21(a).

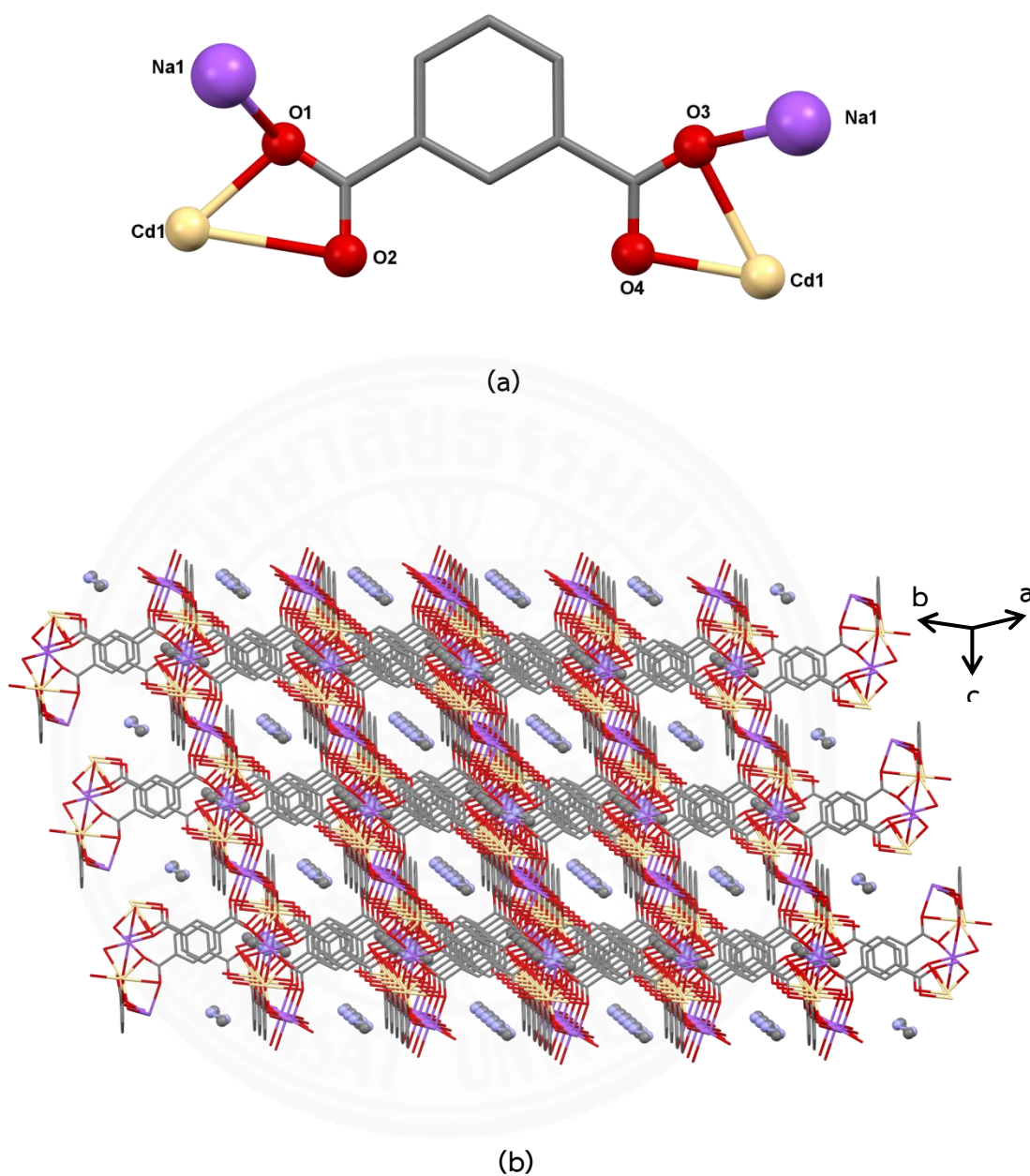
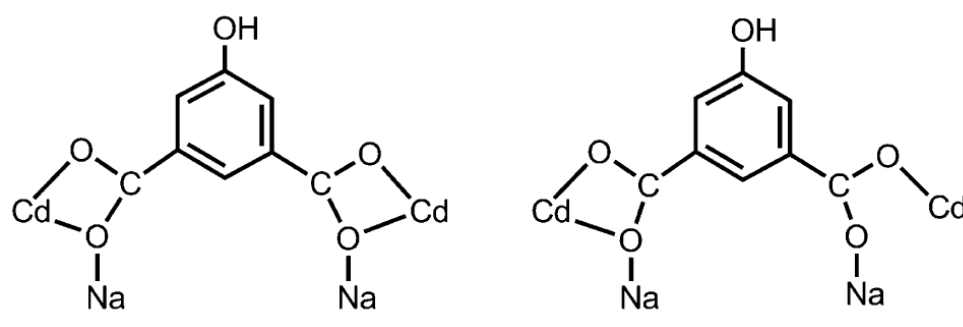
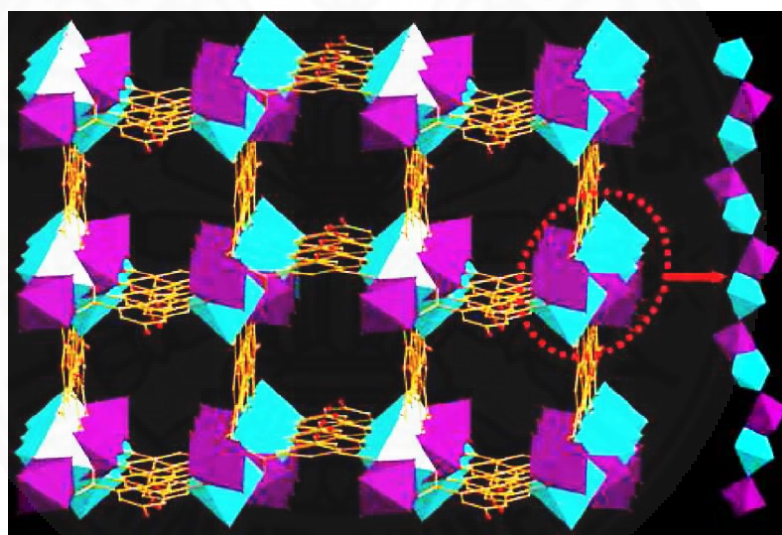


Figure 4.19 (a) μ_4 -coordination mode of 1,3-bdc bridging ligand and (b) packing structure of $\{[CdNa(1,3-bdc)_2] \cdot [NH_2(CH_3)_2]\}$ with dimethylamine templating cations, viewed along the [111] direction [96]



(a)



(b)

Figure 4.20 (a) μ_4 -coordination mode of OH-1,3-bdc bridging ligands and (b) Perspective view of the 3D network in $[\text{CdNa}(\text{OH-1,3-bdc})(\text{H}_2\text{O})_2] \cdot 2\text{H}_2\text{O}$ along the c axis [97]

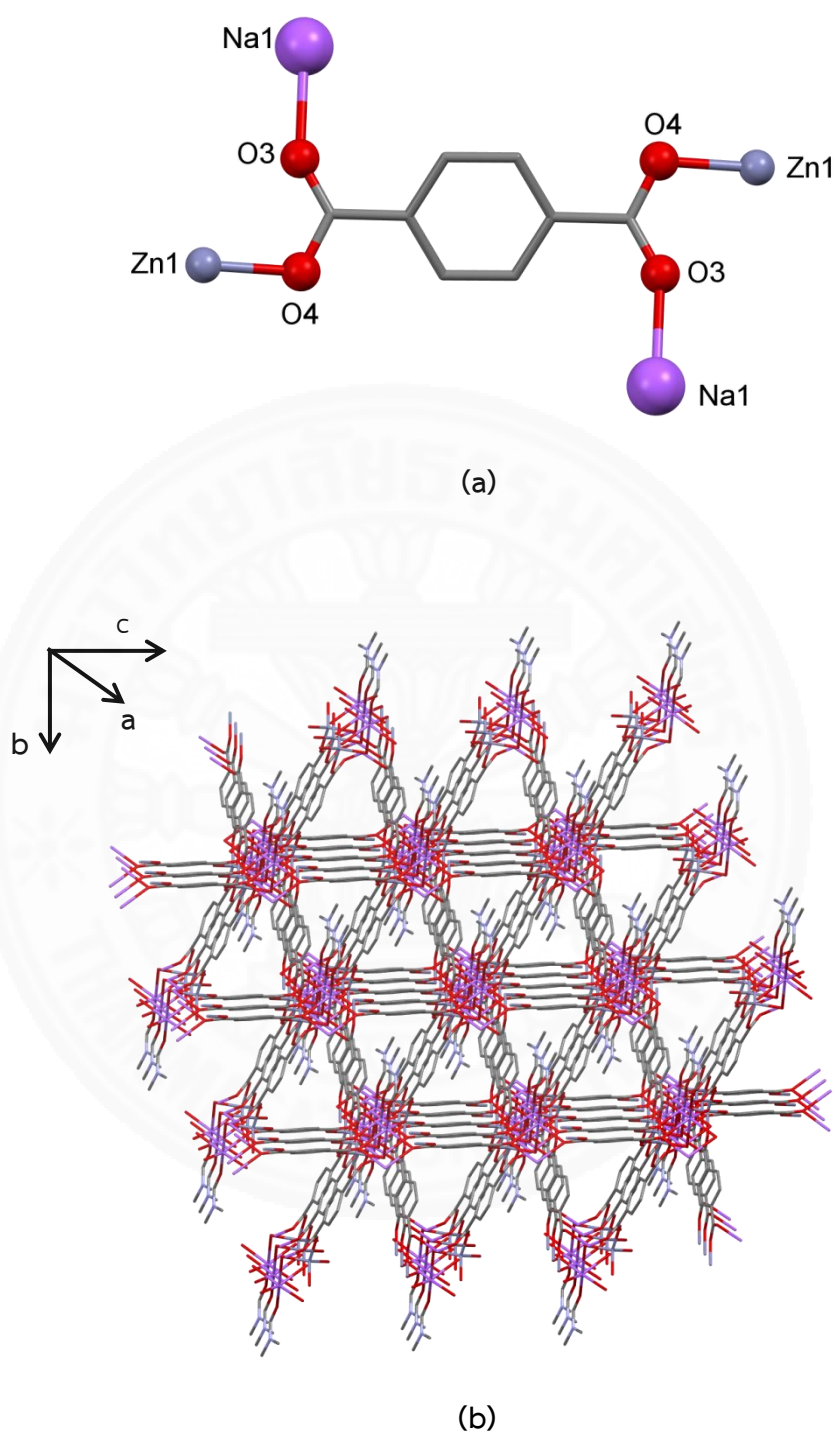


Figure 4.21 (a) μ_4 -coordination mode of 1,4-bdc bridging ligands and (b) packing structure of $[\text{Zn}_2\text{Na}_2(1,4\text{-bdc})_3(\text{DMF})_2(\text{H}_2\text{O})_2]$, viewed along the a axis [98]

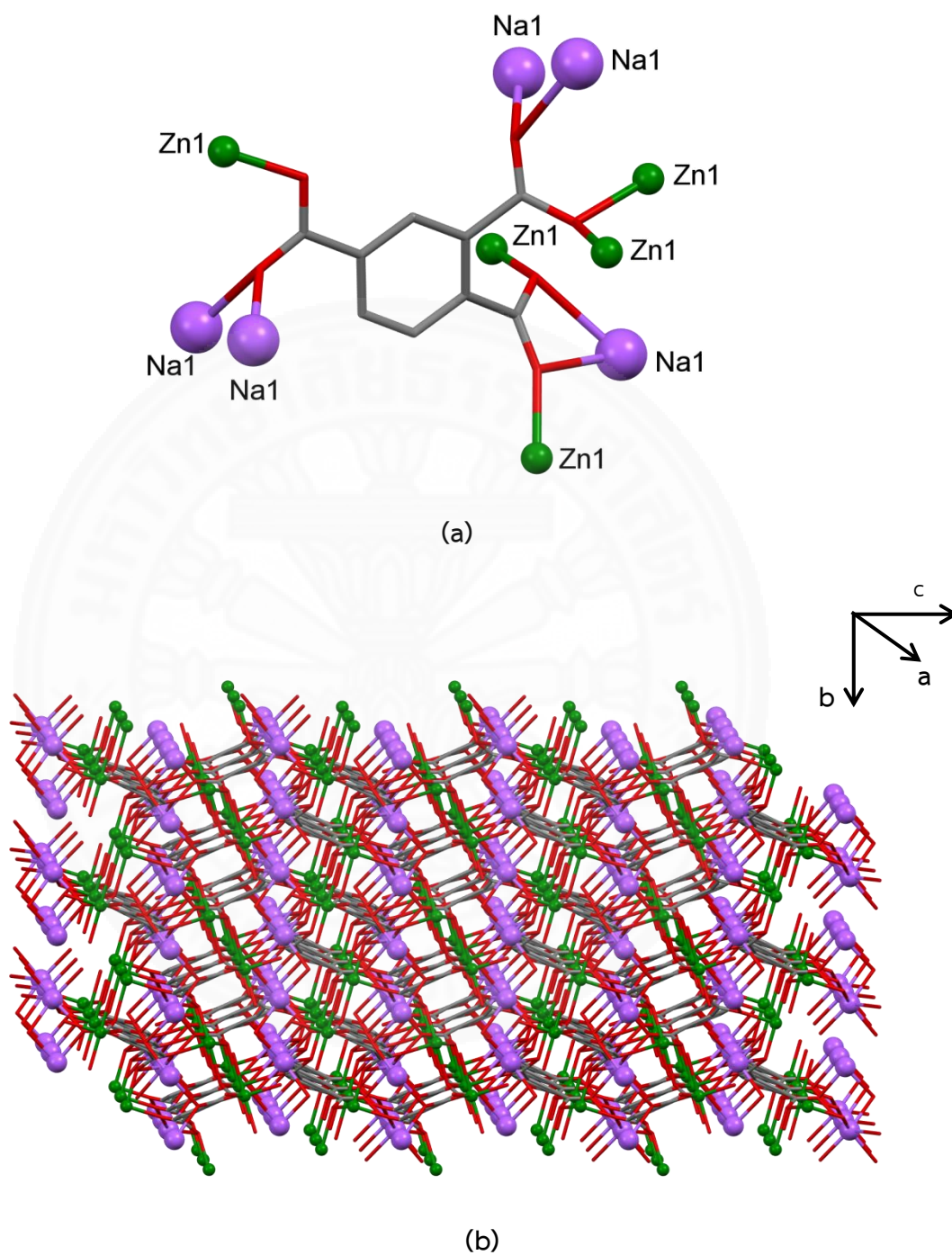


Figure 4.22 (a) μ_{10} -coordination mode of 1,2,4-btc bridging ligands and (b) packing structure of [ZnNa(1,2,4-btc)], viewed along the *a* axis [99]

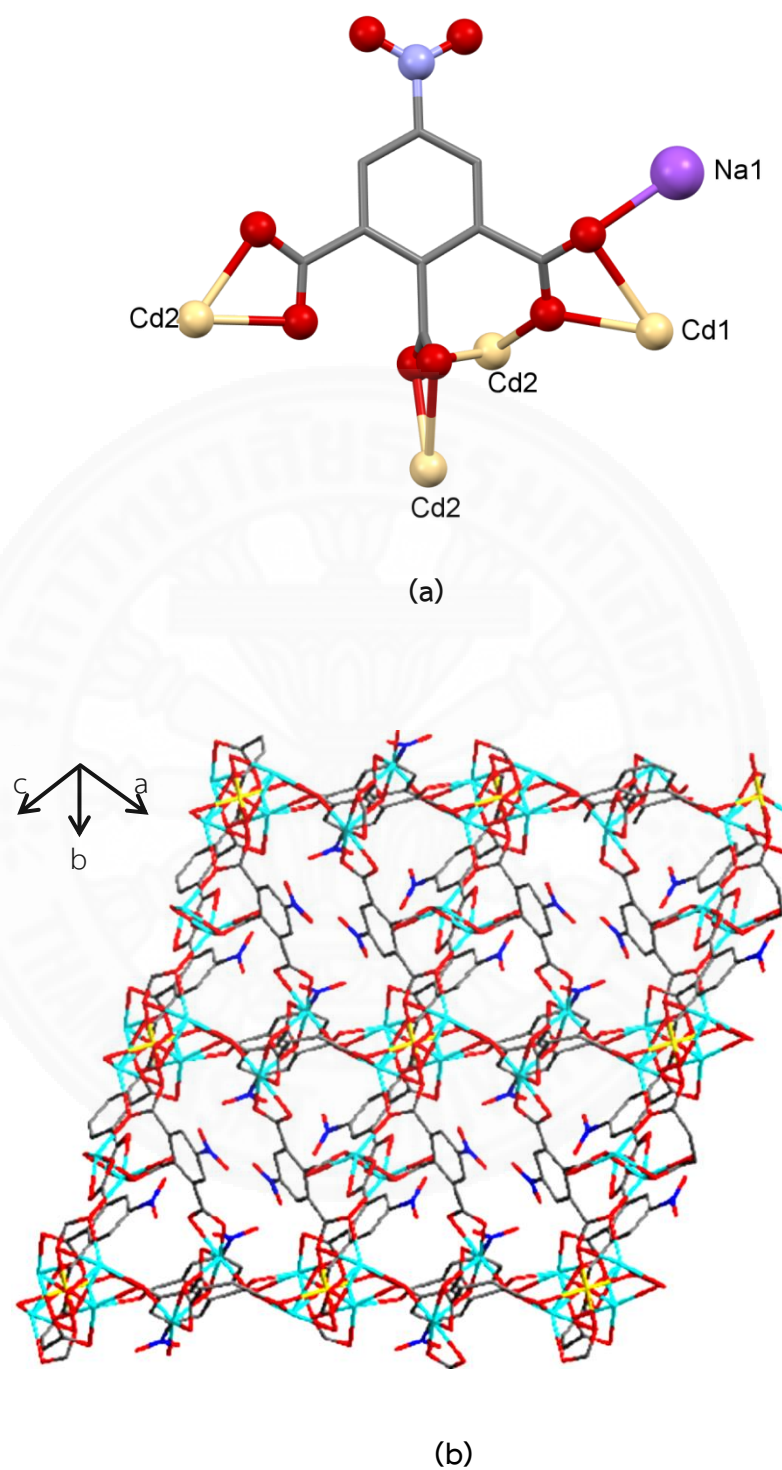


Figure 4.23 (a) μ_5 -coordination mode of ntc bridging ligands and (b) packing structure of $[\text{Cd}_8\text{Na}(\text{ntc})_6(\text{H}_2\text{O})_8]$, viewed along the b axis [100]

4.2.4 Infrared spectra

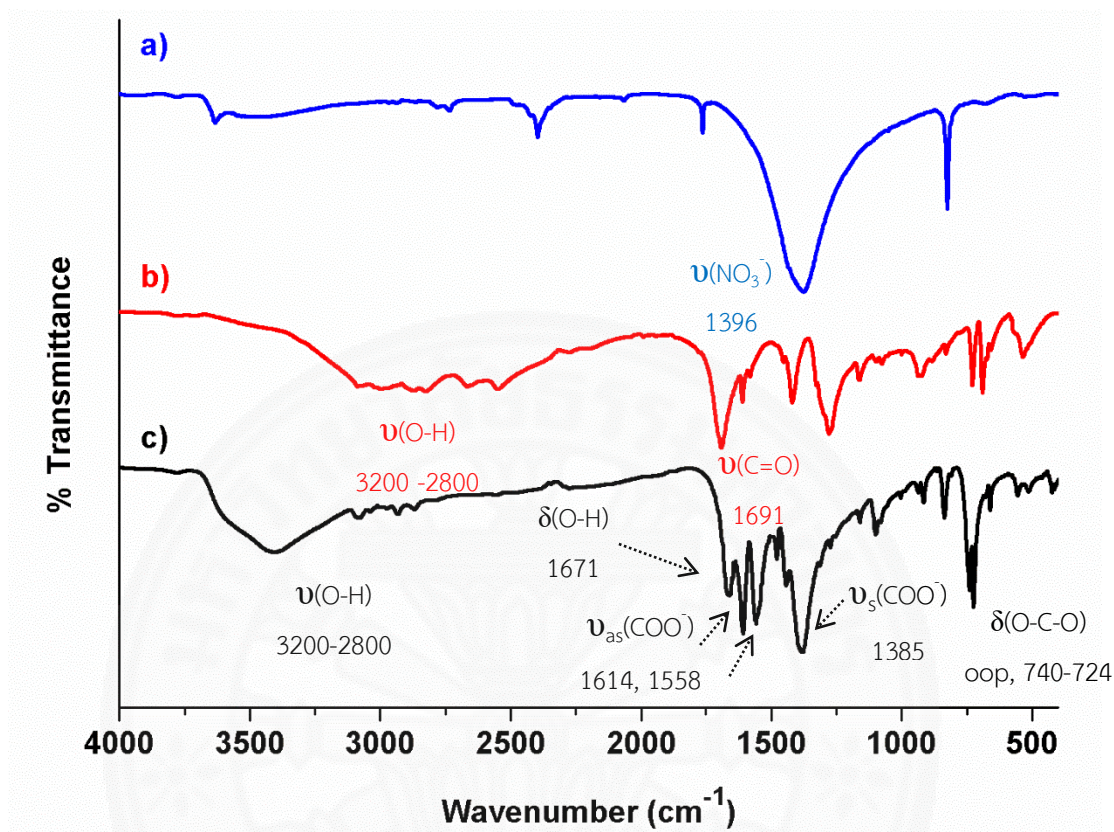


Figure 4.24 IR spectra of (a) $\text{Cd}(\text{NO}_3)_2 \cdot 4\text{H}_2\text{O}$, (b) 1,3-bdcH₂ and (c) $\{\text{CdNa}_2(1,3\text{-bdc})_2(\text{H}_2\text{O})_2(\text{DMF})\}_n$ (**2**)

To investigate the existence of the component in (**2**) by using the identification of the functional groups of synthesized coordination polymer, $\{\text{CdNa}_2(1,3\text{-bdc})_2(\text{H}_2\text{O})_2(\text{DMF})\}_n$ (**2**) and compare with that of reactants, the FT-IR spectra of $\text{Cd}(\text{NO}_3)_2 \cdot 4\text{H}_2\text{O}$, 1,3-H₂bdc and (**2**) were performed in range 4000 - 400 cm^{-1} on a Perkin Elmer infrared spectrophotometer using a KBr pellet.

The FT-IR spectrum of $\text{Cd}(\text{NO}_3)_2 \cdot 4\text{H}_2\text{O}$ was revealed the characteristic absorption peak of NO_3^- group at 1396 cm^{-1} as presented in Figure 4.24a. In Figure 4.24b, FT-IR spectrum of 1,3-bdcH₂ was exhibited very broad bands at 3200-2800 cm^{-1} . This band results from the O-H stretching of the carboxylic groups. The characteristic band at 1691 cm^{-1} was assigned to the absorption of C=O groups.

For IR spectrum of (2), the absorption peak of nitrate group was not found, confirming the nitrate group was disappeared in (2). The broad absorption peak of O-H stretching in carboxylic acid group was not presented, indicating the carboxylic acid was fully deprotonated. The existence of strong bands in the 1614 and 1558 cm^{-1} were attributed to the asymmetric stretching vibration and 1385 cm^{-1} was assigned to symmetric stretching vibration of COO^- group, confirming for the presence of bdc ligands [97]. The absorption peak at 1671 cm^{-1} was assigned to the bending vibration of O-H of coordinated water molecules. The $\delta(\text{O-C-O})$ out of plane vibration of bdc ring occurs at 740-724 cm^{-1} as shown in Figure 4.24c.

4.2.5 Powder X-ray diffraction patterns

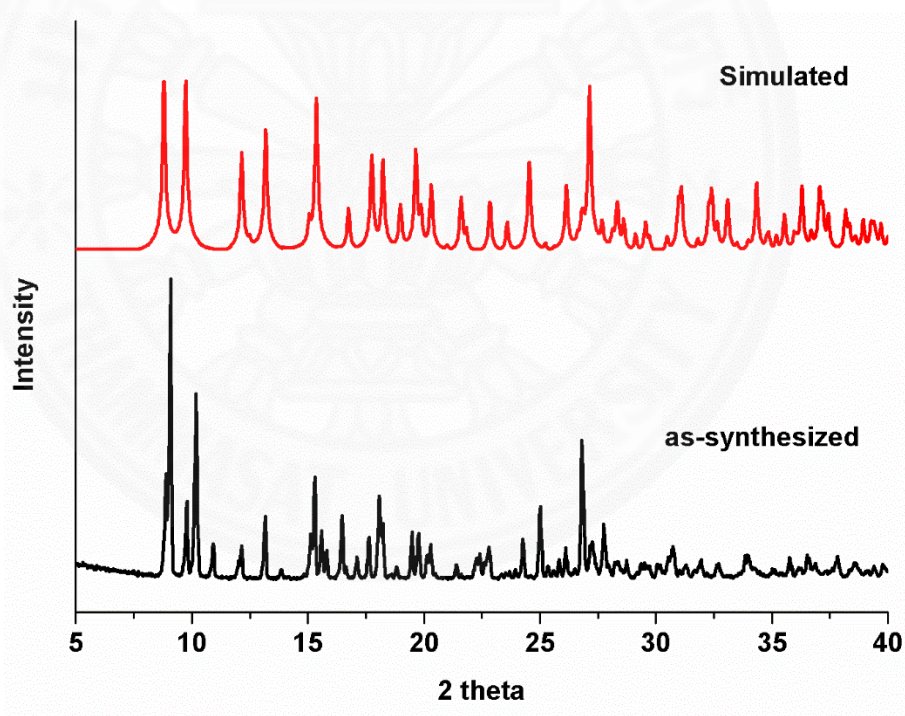


Figure 4.25 PDXRD patterns of $\{\text{CdNa}_2(1,3\text{-bdc})_2(\text{H}_2\text{O})_2(\text{DMF})\}_n$ (2)

To confirm the phase purity of bulk solid sample, the powder X-ray diffraction (PDXRD) data was collected. The simulated and as-synthesized powder X-ray diffraction pattern for compound (2) was shown in Figure 4.25. The peak positions

and intensities presented in the experimental patterns were in good agreement with the corresponding simulated one generated from single-crystal diffraction data, indicating the phase purity of the bulk compound.

4.2.6 Thermogravimetric analysis

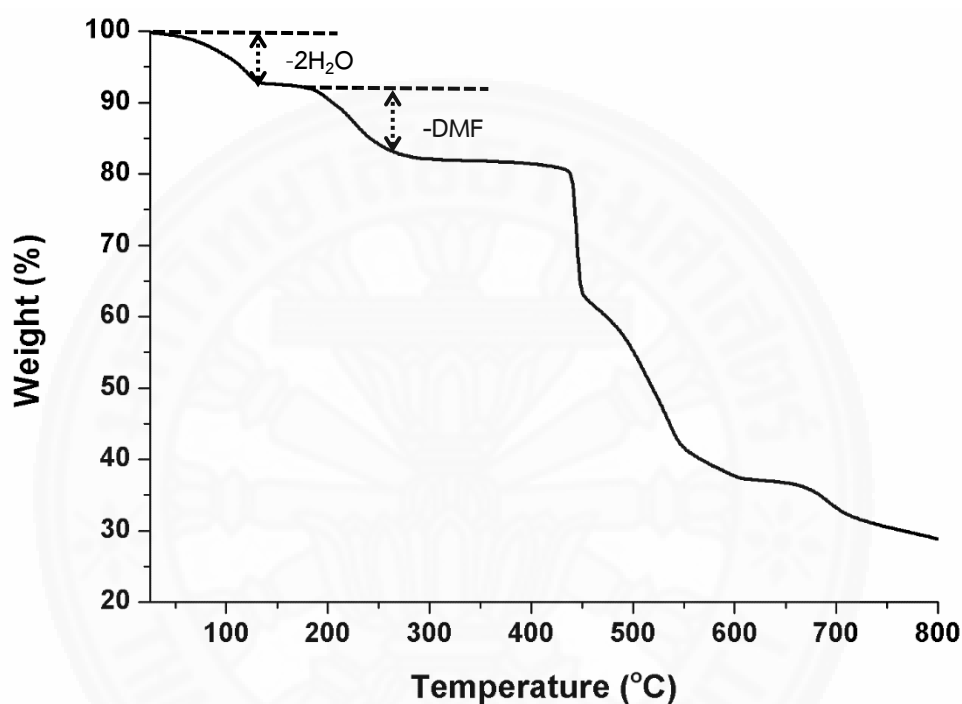


Figure 4.26 TGA curve of $\{\text{CdNa}_2(1,3\text{-bdc})_2(\text{H}_2\text{O})_2(\text{DMF})\}_n$ (**2**)

To study the thermal stability of compound (**2**), thermogravimetric measurement was carried out in the range 25 – 800 °C under a nitrogen atmosphere and the result was shown in Figure 4.26. The TGA curve indicated that the first weight loss of 7.32 % (calculated 6.04 %) from 25 to 130 °C was observed, corresponding to the removal of two coordinated water molecules. In the second step, a weight loss of 10.74 % (calculated 12.27 %) was observed in the temperature range of 130 – 300 °C, suggesting the loss of coordinated DMF molecules. Compound (**2**) was thermally stable up to *ca* 450 °C. The framework was started to collapse with the

loss of a bdc molecule per formula. Moreover, the remaining species was gradually decomposed to metal oxide at the temperature higher than 450 °C.

4.2.7 Scanning electron microscope /Energy-dispersive X-ray spectroscopy

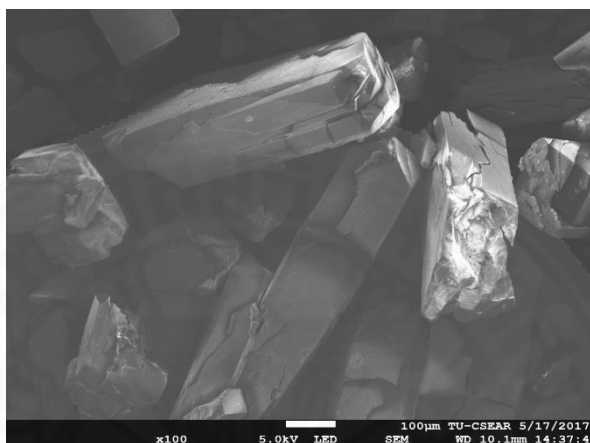


Figure 4.27 SEM image of compound 2

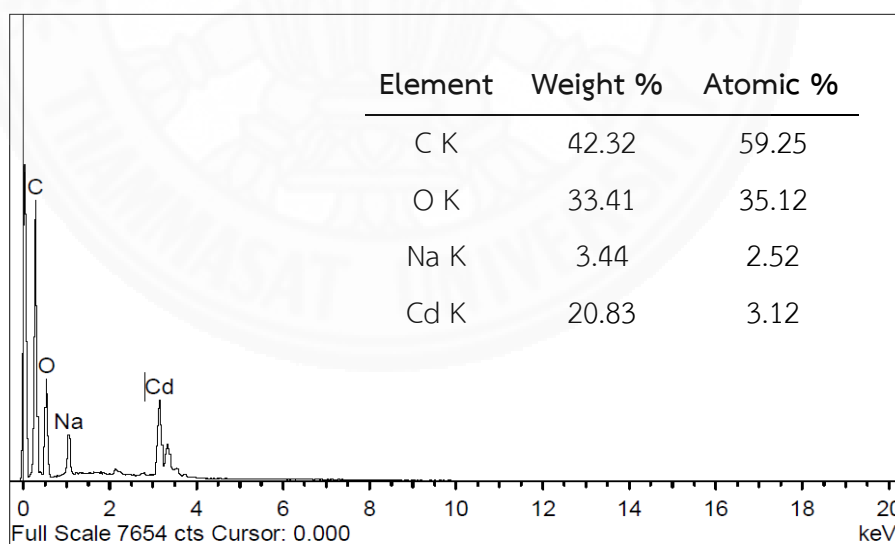


Figure 4.28 EDX spectrum of (2)

From the crystal structural data analysis, compound (2) consists of Na ions. To confirm the presence of Na ions in this framework, the SEM-EDX measurement was carried out. The scanning electron microscope (SEM) was used to

determine the morphology of (2). As shown in Figure 4.27, the SEM image shows a block shape crystal of (2). Subsequently, the elemental composition was studied by energy-dispersive X-ray spectroscopy (EDX). The resulting EDX spectrum (Figure 4.28) reveals the amount of each element contained in this compound. Moreover, It can be confirmed the presence of Na ions in this framework.

4.2.8 Sensing properties

4.2.8.1 Solid state photoluminescence properties

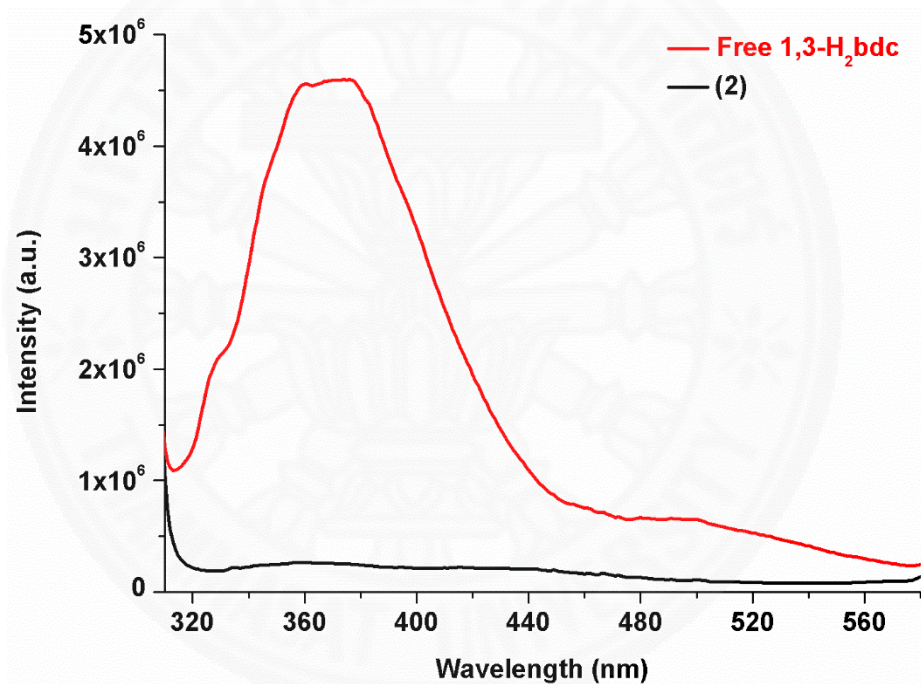


Figure 4.29 Solid state photoluminescence spectra of free 1,3-bdcH₂ ligand and {CdNa₂(1,3-bdc)₂(H₂O)₂(DMF)_n (2)

Coordination polymers constructed from d^{10} -metal ions and conjugated aromatic linkers were known to be potential luminescent materials [57-60]. Therefore, the solid-state photoluminescence properties of free 1,3-bdcH₂ ligand and (2) were investigated and carried out by using a Horiba FluoroMax-4 spectrofluorometer at room temperature. The solid photoluminescence of 1,3-bdcH₂ and (2)

under excitation at 305 nm is presented in Figure 4.29. The emission spectrum of free 1,3-bdcH₂ ligand was displayed at 362 nm, while that of **(2)** presents the fluorescence quenching. This quenching phenomenon may be occurred from the conjugated part in crystalline framework of **(2)** are well separated by Cd(II) and Na(I) ions to avoid the typical face-to-face π - π interactions of this type of large planar aromatic molecules [57].



4.2.8.2 The photoluminescent sensing for various small organic solvents

Photoluminescent sensing properties in liquid suspension of compound (2) in various organic solvents were studied. Interestingly, the results revealed that compound (2) shows emission spectra in presence of different solvent. Homogenous suspension of (2) was prepared by immersing 2 mg of finely ground fresh sample to 3 ml different organic solvents without any activation. Consequently, the liquid suspension was treated by ultrasonic dispersion for 30 minutes, and then aged for 2 days to produce the stable suspensions. The fluorescent emission was carried out upon excitation at 300 nm. The various small organic solvents such as acetone (AC), dimethylsulfoxide (DMSO), dichloromethane (DCM), ethanol (EtOH), methanol (MeOH), benzene, toluene, hexane and tetrahydrofuran (THF) had been selected to test for this experiment.

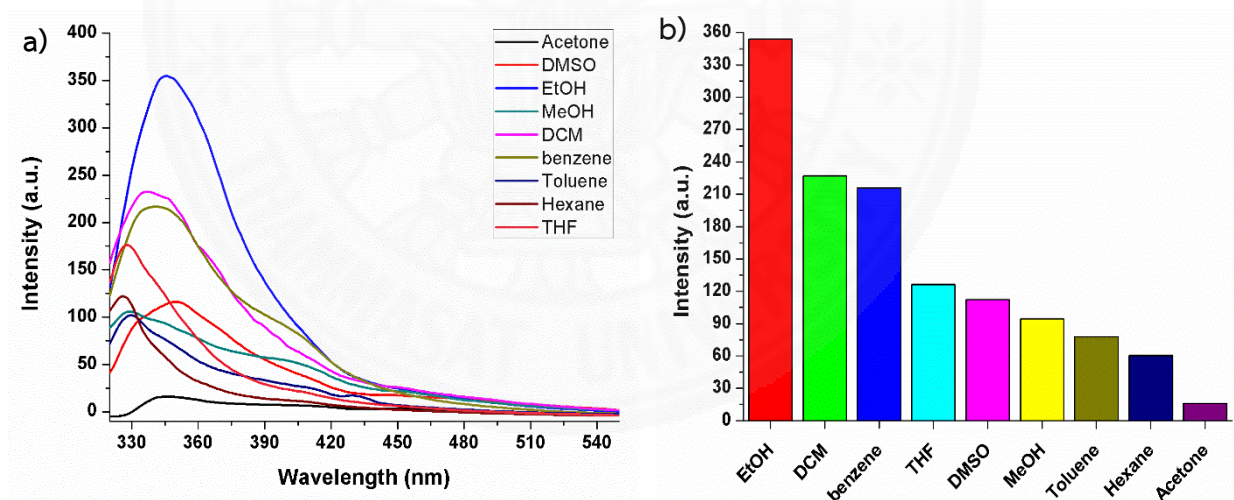


Figure 4.30 (a) Emission spectra of (2) and (b) relative emission intensities dispersed in various small organic solvents

In Figure 4.30, among the selected small organic solvents, suspension of (2) in ethanol exhibited strongest emission and acetone exhibited highest quenching. Therefore, ethanol was used as the suspension medium for study in the next step of other experiments.

4.2.8.3 Sensing sensitivity study for acetone

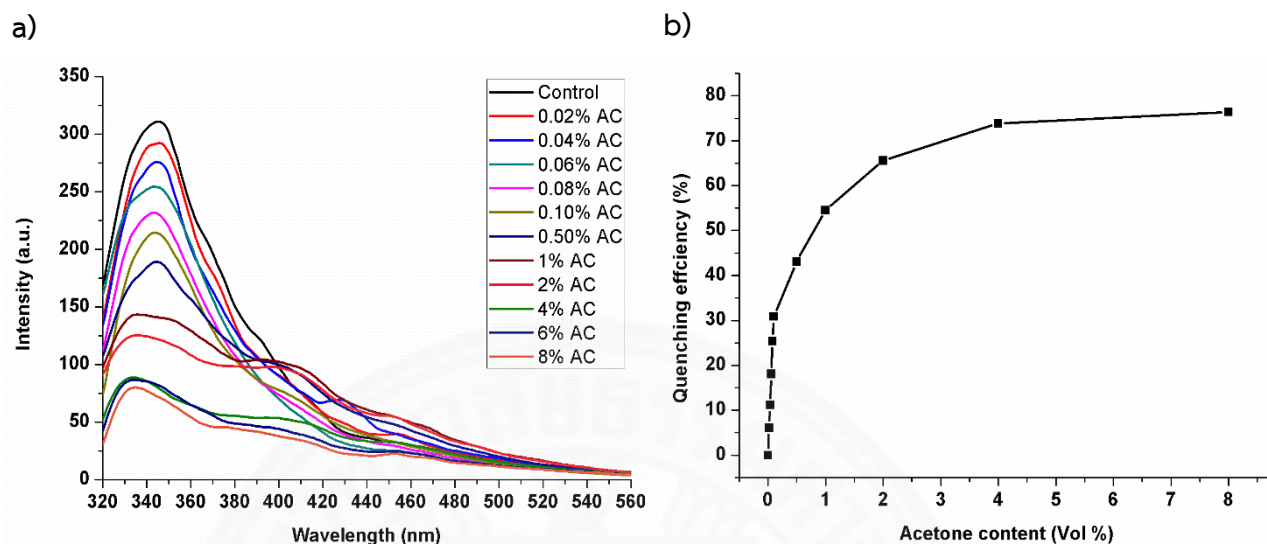


Figure 4.31 (a) PL spectra of the dispersed (**2**) in EtOH in the presence of various concentrations of the acetone and (b) Plot of the PL quenching efficiency of gradual additional amounts of acetone of compound **2**.

To study the photoluminescent sensing sensitivity of compound (**2**) in acetone, a batch of suspension (**2**) dispersed in ethanol with gradually increasing acetone contents in range of 0.02 – 8.00 % v/v was prepared to record the emission spectra. A gradual decrease of the fluorescence intensity was observed upon the addition of acetone content to the ethanol suspension of (**2**) (Figure 4.31a).

As illustrated in Figure 4.31b, the fluorescence quenching efficiency drastically increased within low concentration of acetone (0 - 0.10 % v/v). A good linear correlation ($R^2 = 0.997$) of fitting plot between the quenching efficiency and the acetone content was obtained. From the slopes of the fitting lines, the detection limit was calculated (calculated by using $3\sigma/m$, m: slope, σ : SD) to be 0.024 % v/v or 240 ppm (Figure 4.32)

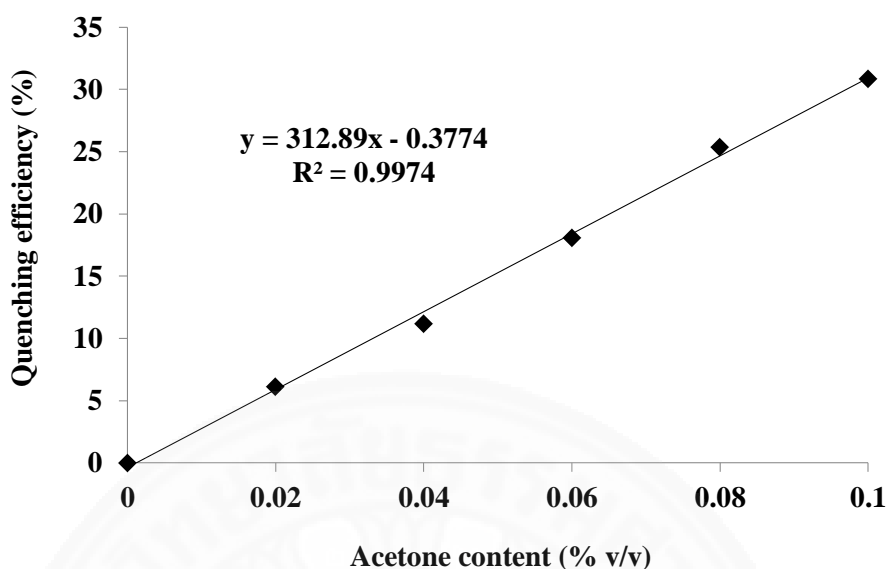


Figure 4.32 Fitting plots of the quenching efficiency of acetone (0 - 0.10 % v/v) on the emissions of the suspensions of compound (2), $\lambda_{\text{ex}} = 300$ nm.

The physical interaction of the solute and solvent plays an important role in both fluorescence enhancing and quenching effects of small solvent molecules. The observed fluorescence quenching effect may be attributed to the interactions between the framework and small organic molecules. The quenching mechanism is due to a competition of adsorption of the light source energy between the excited CPs and acetone molecules adsorbed on the surface of the CPs particles. The energy absorbed by the organic ligands in CPs is transferred to acetone molecules, resulting in a decrease in the luminescence intensity [101,102]. To further support this mechanism, we have examined the UV-Vis absorption spectra of acetone and other tested organic solvents (Figure 4.33). It was found that the absorption spectrum of acetone (230 – 340 nm) overlaps with the emission peak of suspension of compound (2) in ethanol (310 – 420 nm), which possible enhance the energy transfer in acetone sensing systems. In contrast, other tested organic solvents do not have absorption above 280 nm.

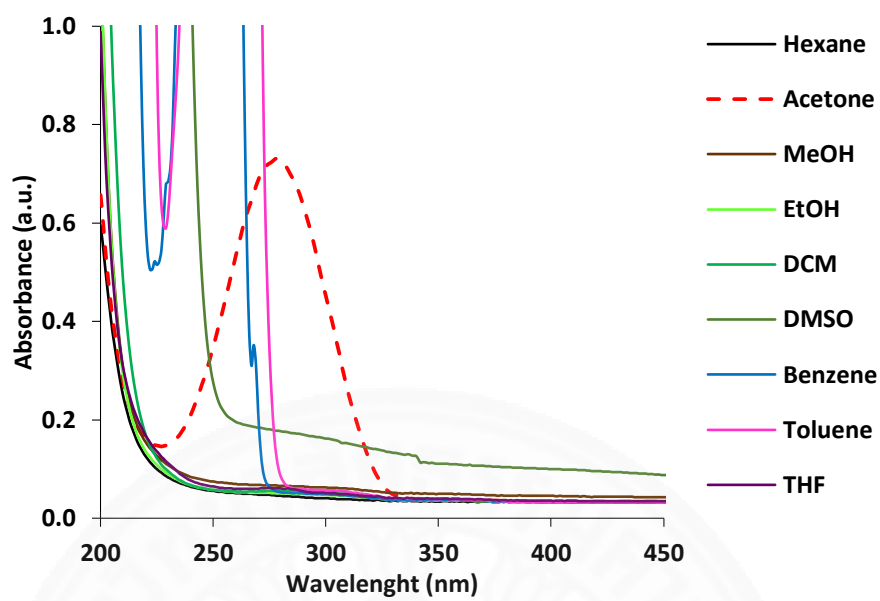


Figure 4.33 UV-Vis spectra of small organic solvents

4.2.8.4 Sensing selectivity study for acetone

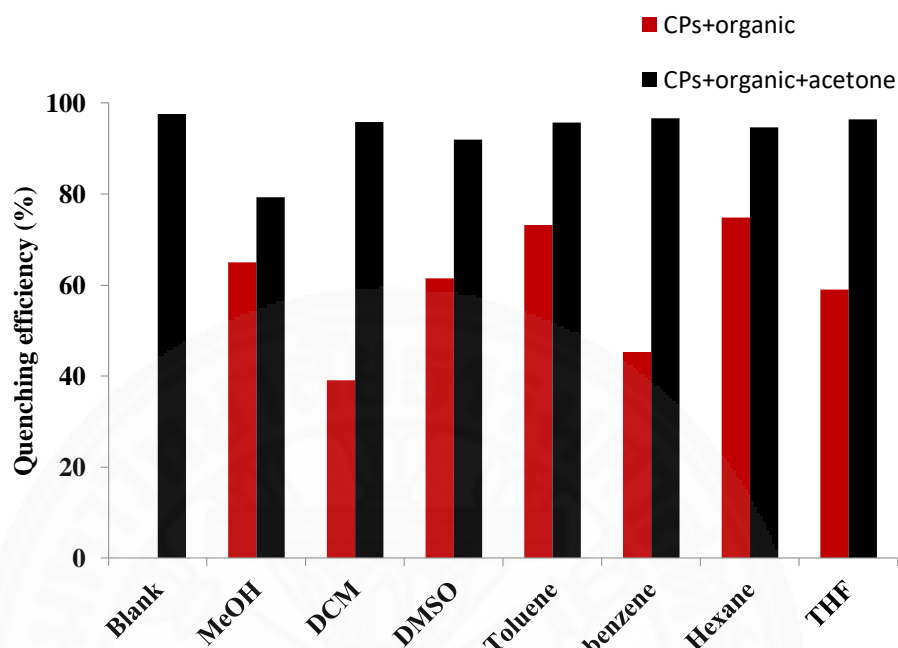


Figure 4.34 Quenching efficiency of (2) upon the addition of different organics (red) and subsequent addition of acetone (black), $\lambda_{\text{ex}} = 300 \text{ nm}$.

Furthermore, the anti-interference ability of (2) against other small organic solvents such as methanol (MeOH), dichloromethane (DCM), dimethylsulfoxide (DMSO), toluene, benzene, hexane and tetrahydrofuran (THF) was also investigated by introducing these other organic solvents and acetone into the ethanol suspension and the quenching efficiency were evaluated by using the formula $[(1-I/I_0) \times 100]$ whereas I is the maximum fluorescence intensity of (2) in ethanol with an addition of organics solvent, while I_0 is that of (2) dispersed in pure ethanol. The result shows that the influence of the mixing other organic solvent has been weak affected on the luminescence intensity of (2) (Figure 4.34). Hence compound (2) presents the good acetone photoluminescent sensing.

4.2.9 Crystal structure of $\{[\text{Cd}_2(1,3\text{-bdc})_2(\text{DMF})]\cdot\text{DMF}\cdot 2\text{H}_2\text{O}\}_n$ (**3**)

4.2.9.1 Crystal structural determination

The intensity data of (**3**) were collected on a single crystal of size $0.35 \times 0.12 \times 0.05 \text{ mm}^3$ at 293 K. Reflection data of this compound were collected on a Bruker APEXII D8 QUEST CMOS diffractometer [94]. The reflections were integrated using *SAINTE* program [94] and intensity data were corrected for Lorentz and polarization effects. Empirical absorption corrections were applied with *SADABS* program [94]. The structures were solved and refined by the *SHELXT* program [95]. All hydrogen atoms except those of water molecules were geometrically generated and isotropically refined using a riding model, with $\text{C-H} = 0.93 \text{ \AA}$ and $U_{\text{iso}}(\text{H}) = 1.2U_{\text{eq}}(\text{C})$. The coordinated DMF molecule was found to be disordered with two set of sites with a refined occupancy ratio of 0.50 and 0.50. The hydrogen atom of two lattice water molecules could be not located.

4.2.9.2 Structural description

There is a new coordination polymer, $\{[\text{Cd}_2(1,3\text{-bdc})_2(\text{DMF})]\cdot\text{DMF}\cdot 2\text{H}_2\text{O}\}_n$ (**3**) was prepared by using the same synthetic of compound (**2**). However, this compound could not be repeated. In this thesis, the structural description of this compound are included and reported as the following.

Compound $\{[\text{Cd}_2(1,3\text{-bdc})_2(\text{DMF})]\cdot\text{DMF}\cdot 2\text{H}_2\text{O}\}_n$ (**3**) crystallizes in the triclinic system with *P*-1 space group. Crystallographic and refinement data was presented in Table 4.7. The selected bond lengths (\AA) and angles ($^\circ$) were listed in Table 4.8.

The structure of this compound is composed of the trinuclear Cd SBUs which there are two crystallographically independent Cd(II) ions, Cd2 center connected together by 1,3-bdc²⁻ bridging ligands. In trinuclear SBUs, two Cd1 atoms on the side position are coordinated by five oxygen atom from four distinct 1,3-bdc²⁻ ligands [$\text{Cd-O} = 2.194(2) - 2.499(2) \text{ \AA}$] and one oxygen atom from terminally coordinated DMF molecule [$\text{Cd-O} = 2.381(7) \text{ \AA}$], forming a distorted octahedral geometry. The Cd2 atom is in the middle position which locate on the

centrosymmetry inversion, also shows octahedrally coordinated by six oxygen atoms from six 1,3-bdc²⁻ ligands [Cd-O = 2.209(2) - 2.373(2) Å] as presented in Figure 4.35.

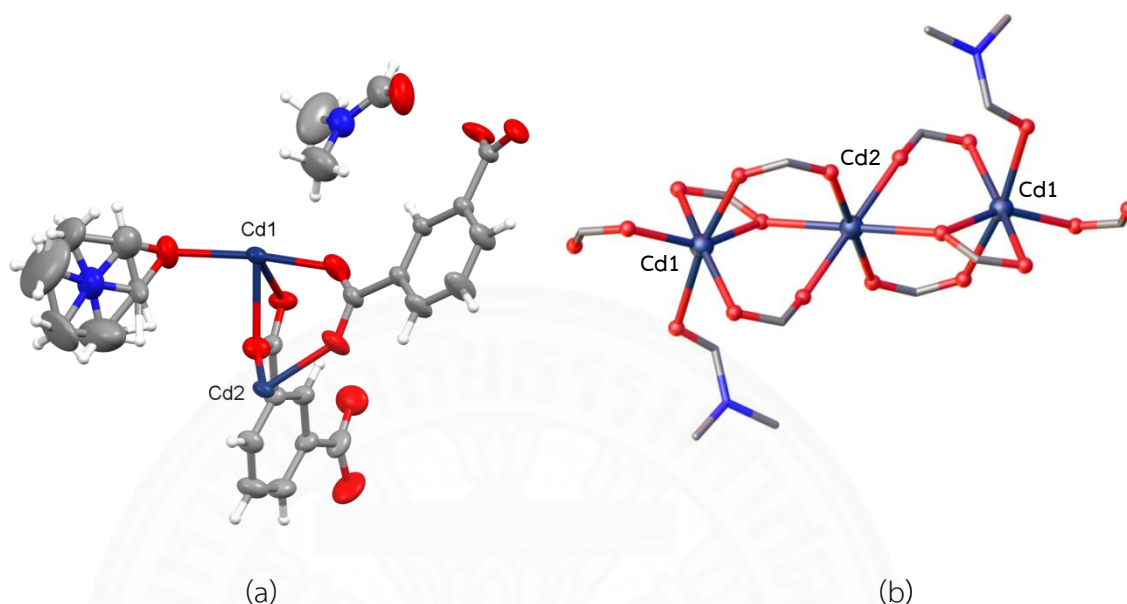


Figure 4.35 (a) Asymmetric unit and (b) Coordination environment around the Cd(II) ions in the trinuclear SBU of (**3**)

The fully deprotonated carboxylate groups of the 1,3-bdc²⁻ ligand adopt μ_3 - and μ_4 -coordination modes as shown in Figure 4.36. Cd2 in central position and Cd1 in terminal position in one SBU are bridged by two carboxyl groups in bidentate mode and one carboxyl group in bridging chelate mode with Cd-Cd distances of 3.756 Å. Furthermore, each trinuclear SBU is further connected together via 1,3-bdc²⁻ ligand in *a* and *c* axis to form 2D frameworks as shown in Figure 4.37. The coordination network of compound (**3**) is stabilized by hydrogen bonding (Table 4.9) and CH \cdots π interaction between 2D layers, resulting 3D supramolecular framework.

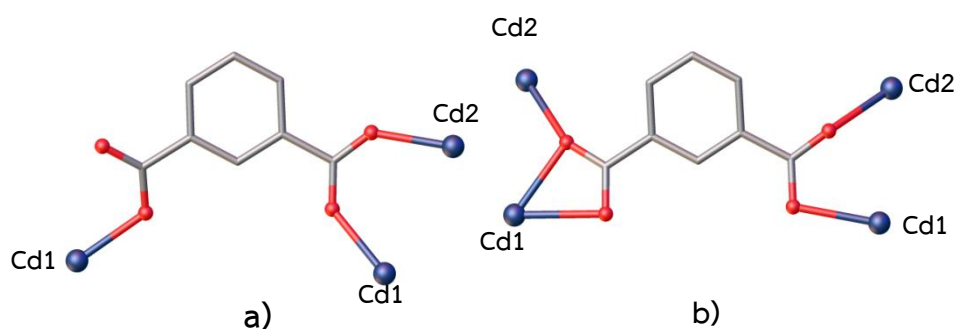


Figure 4.36 (a) μ_3 - and (b) μ_4 -coordination modes of 1,3-bdc²⁻ ligand in (3)

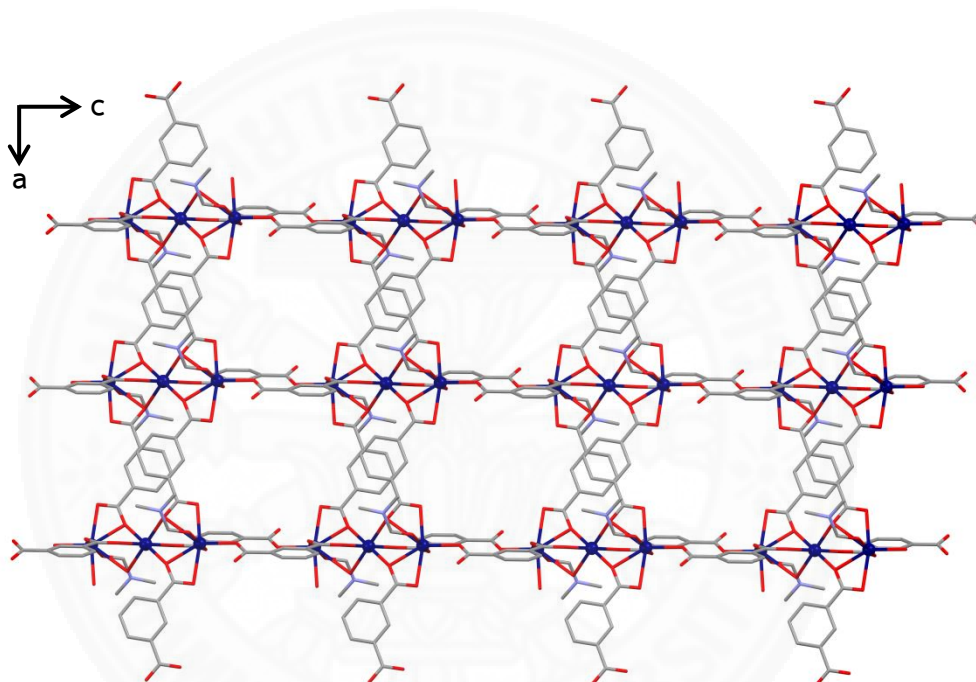


Figure 4.37 2D framework of compound (3)

Hydrogen atoms and lattice DMF and waters molecules are omitted for clarity.

Table 4.7 Crystallographic and refinement data for compound (3)

Empirical formula	C ₄₄ H ₄₄ Cd ₃ N ₄ O ₂₄	
Formula weight	1392.96	
Temperature/K	293 (2)	
Crystal system	Triclinic	
Space group	P-1	
Unit cell dimensions	a/Å	9.859(3)
	b/Å	11.752(4)
	c/Å	13.309(4)
	α/°	109.672(9)
	β/°	95.979(9)
	γ/°	112.548(9)
Volume/Å ³	1291.9(7)	
Z	1	
Density (calculated) g.cm ³	1.735	
Absorption coefficient (μ)/mm ⁻¹	1.311	
F(000)	672	
Crystal size/mm ³	0.35 × 0.12 × 0.05	
2θ range for data collection/°	5.46 – 56.52	
Index ranges	-13 ≤ h ≤ 13, -15 ≤ k ≤ 15, -17 ≤ l ≤ 17	
Reflections collected	49152	
Independent reflections	6389[R _{int} = 0.0420, R _{sigma} = 0.0272]	
Data/restraints/parameters	6389/0/373	
Goodness-of-fit on F ²	1.079	
Final R indexes [I >= 2σ(I)]	R ₁ = 0.0448, wR ₂ = 0.1267	
Final R indexes [all data]	R ₁ = 0.0500, wR ₂ = 0.1306	
Largest diff. peak/hole/eÅ ⁻³	2.747, -0.865	

$$R = \frac{\sum ||F_o| - |F_c||}{\sum |F_o|}, R_w = \frac{[\sum w \{ |F_o| - |F_c| \}^2 / |F_o|^{2.1/2}]^{1/2}}$$

Table 4.8 Selected bond lengths (Å) and angles (°) for compound (3)

Bond lengths (Å)			
Cd(1)-O(1)	2.499(2)	Cd(2)-O(2 ⁱⁱⁱ)	2.373(2)
Cd(1)-O(2)	2.348(2)	Cd(2)-O(2)	2.373(2)
Cd(1)-O(5)	2.267(3)	Cd(2)-O(6)	2.209(2)
Cd(1)-O(4 ⁱ)	2.352(3)	Cd(2)-O(6 ⁱⁱⁱ)	2.209(2)
Cd(1)-O(7 ⁱⁱ)	2.194(2)	Cd(2)-O(3 ^{iv})	2.277(3)
Cd(1)-O(9A)	2.381(7)	Cd(2)-O(3 ⁱ)	2.277(3)
Cd(1)-O(9B)	2.387(12)		
Symmetry codes: ⁱ -1+x,+y,+z; ⁱⁱ 1-x,1-y,1-z; ⁱⁱⁱ 1-x,1-y,-z; ^{iv} 2-x,1-y,-z; ^v 1+x,+y,+z			
Bond angle (°)			
O(2)-Cd(1)-O(1)	53.41(7)	O(9A)-Cd(1)-O(1)	90.7(3)
O(2)-Cd(1)-O(4 ⁱ)	126.30(10)	O(9B)-Cd(1)-O(1)	84.3(5)
O(2)-Cd(1)-O(9A)	90.5(3)	O(2)-Cd(2)-O(2 ⁱⁱⁱ)	180.0
O(2)-Cd(1)-O(9B)	85.4(5)	O(6)-Cd(2)-O(2 ⁱⁱⁱ)	87.26(9)
O(5)-Cd(1)-O(1)	95.54(11)	O(6 ⁱⁱⁱ)-Cd(2)-O(2 ⁱⁱⁱ)	92.74(9)
O(5)-Cd(1)-O(2)	87.07(10)	O(6)-Cd(2)-O(2)	92.74(9)
O(5)-Cd(1)-O(9A)	170.1(2)	O(6 ⁱⁱⁱ)-Cd(2)-O(2)	87.26(9)
O(5)-Cd(1)-O(9B)	170.7(4)	O(6)-Cd(2)-O(6 ⁱⁱⁱ)	180.0
O(4 ⁱ)-Cd(1)-O(1)	166.15(10)	O(6)-Cd(2)-O(3 ^{iv})	89.87(13)
O(4 ⁱ)-Cd(1)-O(9A)	79.6(3)	O(6)-Cd(2)-O(3 ⁱ)	90.13(13)
O(4 ⁱ)-Cd(1)-O(9B)	85.6(4)	O(6 ⁱⁱⁱ)-Cd(2)-O(3 ⁱ)	89.87(13)
O(7 ⁱⁱ)-Cd(1)-O(1)	98.36(10)	O(6 ⁱⁱⁱ)-Cd(2)-O(3 ^{iv})	90.13(13)
O(7 ⁱⁱ)-Cd(1)-O(2)	149.61(10)	O(3 ⁱ)-Cd(2)-O(2)	74.54(10)
O(7 ⁱⁱ)-Cd(1)-O(5)	84.70(10)	O(3 ^{iv})-Cd(2)-O(2)	105.46(10)
O(7 ⁱⁱ)-Cd(1)-O(4 ⁱ)	93.33(11)	O(3 ^{iv})-Cd(2)-O(2 ⁱⁱⁱ)	74.54(10)
O(7 ⁱⁱ)-Cd(1)-O(9A)	102.0(3)	O(3 ⁱ)-Cd(2)-O(2 ⁱⁱⁱ)	105.46(10)
O(7 ⁱⁱ)-Cd(1)-O(9B)	104.5(4)	O(3 ^{iv})-Cd(2)-O(3 ⁱ)	180.00(19)
Symmetry codes: ⁱ -1+x,+y,+z; ⁱⁱ 1-x,1-y,1-z; ⁱⁱⁱ 1-x,1-y,-z; ^{iv} 2-x,1-y,-z; ^v 1+x,+y,+z			

Table 4.9 Hydrogen bond geometry (Å, °) for compound (**3**)

<i>D</i> -H... <i>A</i>	<i>D</i> -H	H... <i>A</i>	<i>D</i> ... <i>A</i>	<i>D</i> -H... <i>A</i>
Intramolecular hydrogen bonds				
C3-H3...O6 ^{vi}	0.93	2.58	3.504(7)	173
C18-H18A...O10	0.96	2.42	2.792(15)	103
Intermolecular hydrogen bonds				
C21-H21...O12 ^{viii}	0.93	2.38	3.112(16)	135
C22A-H22E...O10 ^{vii}	0.96	2.60	3.46(3)	150
Symmetry code: ^{vi} 1-x, 1-y, -z, ^{vii} 1+x, 1+y, z, ^{viii} x, 1+y, z				

4.2.9.3 Structural comparison

To the best of our knowledge of structure closely related to compound (**3**), the 3D Co(II) coordination polymer containing trinuclear SBUs [H₂N(CH₃)₂]₂[Co₃(1,3-bdc)₄].H₂O (1,3-bdcH₂=1,3-benzenedicarboxylic acid) has been reported by Luo and coworkers in 2008 [103]. This compound crystallized in the monoclinic space group *P*2₁/*c*. Each trinuclear SBUs in this structure contains two crystallographically independent Co(II) atoms as shown in Figure 4.38(a). All Co(II) atoms are in [CoO₆], octahedral geometry. The central and a side Co(II) atoms in a SBU are bridged by two carboxyl groups with the Co...Co separation of ca. 3.533 Å, while the Cd(II)...Cd(II) separation in compound (**3**) is ca. 3.756 Å. Further, all trinuclear SBUs are connected together via 1,3-bdc²⁻ bridging ligand in μ₃- and μ₄-coordination mode to give the 3D coordination framework as shown in Figure 4.38(b).

Other related coordination polymer with trinuclear SBUs containing 1,3-benzendicarboxylate derivative ligand have been published, such as [Mn₃(5-py-1,3-bdc)₂(HCOO)₂(H₂O)₂]_n where 5-py-1,3-bdcH₂ = 5-(pyridin-4-yl) isophthalic acid [104] and [Mn₃(5-ID-1,3-bdc)₃(DMA)(H₂O)₂]_n·[(H₂O)(DMA)] where (5-ID-1,3-bdcH₂=5-(1-oxoisindolin-2-yl) isophthalic acid [105]. The trinuclear SBUs and packing structure of both compounds are shown in Figures 4.39 and 4.40

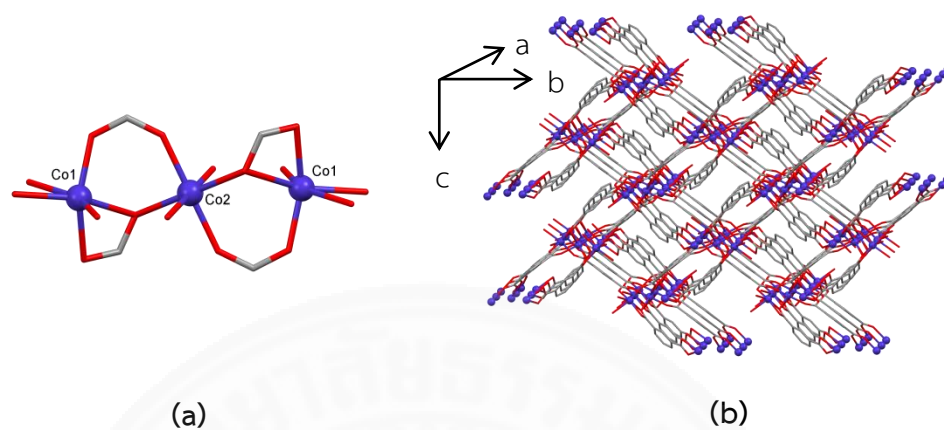


Figure 4.38 (a) Trinuclear SBUs and (b) packing structure of $[\text{H}_2\text{N}(\text{CH}_3)_2]_2[\text{Co}_3(1,3\text{-bdc})_4]\cdot\text{H}_2\text{O}$ [103]

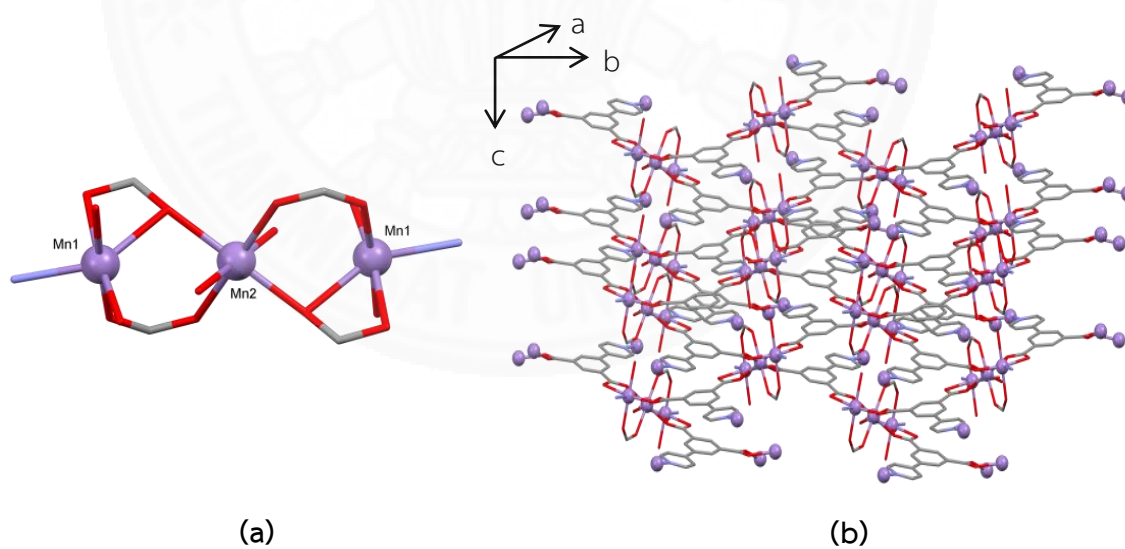


Figure 4.39 (a) Trinuclear SBUs and (b) packing structure of $[\text{Mn}_3(5\text{-py-}1,3\text{-bdc})_2(\text{HCOO})_2(\text{H}_2\text{O})_2]_n$ [104]

CHAPTER 5

CONCLUSIONS AND RECOMMENDATIONS

5.1 Conclusions

This research concerns about the design, synthesis, characterization and properties studies of novel coordination polymers by using aromatic dicarboxylate ligands. In this research, pyridine-2,6-dicarboxylic acid (2,6-dipicH₂) and benzene-1,3-dicarboxylic acid (1,3-bdcH₂) were chosen for used as bridging ligand. Three novel coordination polymers namely [Zn(2,6-dipic)]_n (**1**), {CdNa₂(1,3-bdc)₂(H₂O)₂(DMF)}_n (**2**) and {[Cd₂(1,3-bdc)₂(DMF)]·DMF·2H₂O}_n (**3**) were successfully synthesized in both of crystalline and precipitate forms by direct method. Crystal structures of all synthesized coordination polymers were carried out by using single crystal X-ray diffraction technique. In addition, compound (**1**) and (**2**) were characterized by various techniques namely Fourier transform infrared spectroscopy, elemental analysis, powder X-ray diffraction, energy dispersive X-ray spectroscopy, thermogravimetric analysis and solid-state photoluminescence spectroscopy. Moreover, catalytic properties of (**1**) and solvent sensing properties of (**2**) were investigated. According to the previous chapters, the summarization and recommendations of this study are presented.

5.1.1 A novel 2D coordination polymer [Zn(2,6-dipic)]_n (**1**)

Compound (**1**) was synthesized by the reaction of Zn(NO₃)₂·4H₂O, pyridine-2,6-dicarboxylic acid and NaOH in mixed solvent of methanol and water at 60 °C. The obtained product was characterized by FT-IR technique, in which the results showed the existence of 2,6-dipic²⁻ in this structure. The X-ray crystal structure of compound (**1**) presents interesting 2D coordination network containing three crystallographic independent Zn(II) centers which adopt octahedral, trigonal bipyramidal and tetrahedral geometries. All Zn(II) centers are linked together via 2,6-dipic²⁻ with μ₃-coordination mode. The phase purity of crystalline and powder

products of **(1)** were confirmed by PXRD technique. Thermal stability of **(1)** is highly stable at high temperature to about 450 °C. For the luminescence property, compound **(1)** presented the fluorescence enhancement and intense emission bands which observed at 417 nm, which may be attributed to ligand to metal charge transfer (LMCT) band. Finally, the catalytic activity of compound **(1)** in transesterification reaction of phenyl acetate and methanol was preliminary studied. The results showed that the optimal reaction condition is 75 °C for 48 h, with the maximum yields of methyl acetate of 53.50 %. Moreover, compound **(1)** can be reused at least 2 cycles without any significant loss of catalytic activity.

5.1.2 A novel 3D coordination polymer $\{CdNa_2(1,3-bdc)_2 \cdot (H_2O)_2(DMF)\}_n$ (**2**)

This compound was synthesized by the reaction of $Cd(NO_3)_2 \cdot 4H_2O$, benzene-1,3-dicarboxylic acid and NaOH in mixed solvent of methanol, water and DMF at 60 °C. The obtained product was characterized by FT-IR technique, in which the results showed the existence of 1,3-bdc²⁻, water and DMF in this structure. The X-ray crystal structure of compound **(2)** is 3D coordination framework. All metal centers are connected together via 1,3-bdc²⁻ in μ_5 -coordination mode. In addition, the presence of Na(I) ions in this framework was also confirmed by SEM-EDX technique. The phase purity of crystalline and powder products of **(2)** were confirmed by PXRD technique. Compound **(2)** is thermally stable up to 450 °C. The solid-state luminescence spectra of **(2)** exhibited quenching phenomenon when compared with free 1,3-bdcH₂ ligand. Finally, the luminescence sensing properties in liquid suspension of **(2)** in different small organic solvents were studied. It was observed that compound **(2)** shows interesting emission profile in presence of acetone, DMSO, EtOH, MeOH, DCM, benzene, toluene, hexane and THF solvents. Fluorescence emission of compound **(2)** suspended in ethanol solvent was observed to be efficiently and selectively quenched by acetone (LOD = 0.024 %v/v or 240 ppm) over the other common solvents. These results reveal potential application of compound **(2)** as a luminescent sensing material for acetone detection.

In addition, $\{[\text{Cd}_2(1,3\text{-bdc})_2(\text{DMF})]\cdot\text{DMF}\cdot 2\text{H}_2\text{O}\}_n$ (**3**) was received by using the same synthetic condition of compound (**2**). Unfortunately, compound (**3**) could not be reproduced. In this thesis, only the structural feature of this compound is reported. The X-ray structure of compound (**3**) is 2D coordination network constructing from trinuclear Cd(II) SBUs which are linked together by 1,3-bdc bridging ligand with μ_3^- and μ_4 -coordination modes.

5.2 Recommendations

5.2.1 The properties studies of a novel 2D coordination polymer

$[\text{Zn}(2,6\text{-dipic})]_n$ (**1**)

5.2.1.1 To further study the catalytic performance of compound (**1**) with transesterification reaction, the reaction of other substrates such as 4-nitrophenyl acetate, 4-methylphenyl acetate, phenyl benzoate and vinyl acetate should be investigated.

5.2.1.2 In order to further apply in catalytic activity, compound (**1**) should be tested in the other organic reaction such as cyanosilylation, oxidation and Henry reaction [52].

5.2.2 The properties studies of a novel 3D coordination polymer

$\{\text{CdNa}_2(1,3\text{-bdc})_2(\text{H}_2\text{O})_2(\text{DMF})\}_n$ (**2**)

5.2.2.1 To prevent the coordination of Na(I) ions with organic linkers, the suitable chelating agent such as phosphate ion should be used in the synthesis procedure.

5.2.2.2 The result of thermogravimetric analysis (TGA) indicates that compound (**2**) readily lost terminal pendant DMF and H_2O molecules in the temperature range of 25-300 °C. Therefore, the removal of terminal pendant DMF and H_2O molecules should be performed to activate compound (**2**) for further applications such as gas absorption. The porosity of activated compound (**2**) should be studied by using Brunauer–Emmett–Teller (BET) analysis. Moreover, the guest-

exchange properties of activated compound (2) should be tested by soaking in various type of organic solvents.



REFERENCES

1. Shibata, Y., *Absorption spectra of metallic-ammino complexes. II. A. Absorption spectra and conductivities of aqueous solutions of cobalt-nitro-ammines which are co-ordination polymers*. Journal of the College of Science, Imperial University of Tokyo, 1916, **37**, 1-17.
2. Bailar, J. C., *Preparative Inorganic Reactions*. Interscience Publishers, 1964, **1**, 1- 27.
3. Batten, S. R., Champness, N. R., Chen, X.-M., Martinez, J. G., Kitagawa, S., Ohrstrom, L., O’Keeffe, M., Suh, M. P. and Reedijk, J., *Terminology of metal-organic frameworks and coordination polymers (IUPAC Recommendations 2013)*. Pure and Applied Chemistry, 2013, **85**(8), 1715-1724.
4. Janiak, C., *Engineering coordination polymers towards applications*. Dalton Transactions, 2003, 2781-2804.
5. Zhang, S.-Y., Zhang, Z. and Zaworotko, M. J., *Topology, Chirality and Interpenetration in Coordination Polymers*. Chemical Communications, 2013, **49**, 9700-9703.
6. Xue, D.-X., Lin, Y.-Y., Cheng, X.-N. and Chen, X.-M., *A Tetracarboxylate-Bridged Dicopper(II) Paddle-Wheel-Based 2-D Porous Coordination Polymer with Gas Sorption Properties*. Crystal Growth & Design, 2007, **7**(7), 1332-1336.
7. Hu, S., He, K.-H., Zeng, M.-H., Zou, H.-H. and Jiang, Y.-M., *Crystalline-State Guest-Exchange and Gas-Adsorption Phenomenon for a “Soft” Supramolecular Porous Framework Stacking by a Rigid Linear Coordination Polymer*. Inorganic Chemistry, 2008, **47**, 5218-5224.
8. Qiu, Y., Deng, H., Yang, S., Mou, J., Daiguebonne, C., Kerbellec, N., Guillou, O. and Batten, S. R., *Syntheses, Crystal Structures, and Gas Storage Studies in New Three-Dimensional 5-Aminoisophthalate Praseodymium Polymeric Complexes*. Inorganic Chemistry, 2009, **48**, 3976-3981.

9. Agarwal, R. A., Aijaz, A., Sanudo, C., Xu, Q. and Bharadwaj, P. K., *Gas Adsorption and Magnetic Properties in Isostructural Ni(II), Mn(II), and Co(II) Coordination Polymer*. *Crystal Growth & Design*, 2013, **13**, 1238-1245.
10. Duan, J., Jin, W. and Krishna, R., *Natural Gas Purification Using a Porous Coordination Polymer with Water and Chemical Stability*. *Inorganic Chemistry*, 2015, **54**(9), 4279–4284.
11. Agarwal, R. A., Mukherjee, S., Sanudo, E. C., Ghosh, S. K. and Bharadwaj, P. K., *Gas Adsorption, Magnetism, and Single-Crystal to Single-Crystal Transformation Studies of a Three-Dimensional Mn(II) Porous Coordination Polymer*. *Crystal Growth & Design*, 2014, **14**, 5585-5592.
12. Liang, J.-Y., Li, G.-P., Gao, R.-C., Bai, N.-N., Tong, W.-Q., Hou, L. and Wang, Y.-Y., *Four New 3D Metal-Organic Frameworks Constructed by a V-shaped Tetracarboxylates Ligand: Selective CO₂ Sorption and Luminescent Sensing*. *Crystal Growth & Design*, **17**(12), 6733–6740.
13. Xiang, J., Chang, C., Li, M., Wu, S., Yuan, L. and Sun, J., *A Novel Coordination Polymer as Positive Electrode Material for Lithium Ion Battery*. *Crystal Growth & Design*, **8**(1), 280-282.
14. Liu, Q., Yu, L., Wang, Y., Ji, Y., Horvat, J., Cheng, M.-L., Jia, X. and Wang, G., *Manganese-Based Layered Coordination Polymer: Synthesis, Structural Characterization, Magnetic Property, and Electrochemical Performance in Lithium-Ion Batteries*. *Inorganic Chemistry*, **52**, 2817-2822.
15. Song, Y., Yu, L., Gao, Y., Shi, C., Cheng, M., Wang, X., Liu, H.-J. and Liu, Q., *One-Dimensional Zinc-Based Coordination Polymer as a Higher Capacity Anode Material for Lithium Ion Batteries*. *Inorganic Chemistry*, 2017, **56**(19), 11603–11609.
16. Yu, L., Wang, X., Cheng, M., Rong, H., Song, Y. and Liu, Qi., *A Three Dimensional Copper Coordination Polymer Constructed by 3-Methyl-1H-pyrazole-4-carboxylic Acid with Higher Capacitance for Supercapacitors*. *Crystal Growth & Design*, 2018, **18**(1), 280–285.

17. Imaz, I., Martinez, M. R., Fernandez, L. G., Garcia, F., Molina, D. R., Hernando, J., Puntesa, V. and MasPOCH, D., *Coordination polymer particles as potential drug delivery systems*. Chemical Communications, 2010, **46**, 4737–4739.
18. Wang, L., Wang, W. and Xie, Z., *Tetraphenylethylene-based fluorescent coordination polymers for drug delivery*. Journal of Materials Chemistry B, 2016, **4**, 4263–4266.
19. Wang, T., Liu, X., Zhu, Y., Cui, Z. D., Yang, X. J., Pan, H., Yeung, K.W. K. and Wu, S., *Metal Ion Coordination Polymer-Capped pH-Triggered Drug Release System on Titania Nanotubes for Enhancing Self-antibacterial Capability of Ti Implants*. ACS biomaterials science & materials, 2017, **3**(5), 816–825.
20. Zhao, J., Yang, Y., Han, X., Liang, C., Liu, J., Song, X., Ge, Z. and Liu, Z., *Redox Sensitive Nanoscale Coordination Polymers for Drug Delivery and Cancer Theranostics*. ASC Applied Materials & Interfaces, 2017, **9**(28), 23555–23563.
21. Huang, Y., Liu, T., Lin, J., Lu, J., Lin, Z. and Cao, R., *Homochiral Nickel Coordination Polymers Based on Salen(Ni) Metalloligands: Synthesis, Structure, and Catalytic Alkene Epoxidation*. Inorganic Chemistry, 2011, **50**, 2191–2198.
22. Karmakar, A., Titi, H. M. and Goldberg, I., *Coordination Polymers of 5-(2-Amino/Acetamido-4-carboxyphenoxy)-benzene-1,3-dioic Acids with Transition Metal Ions: Synthesis, Structure, and Catalytic Activity*. Crystal Growth & Design, 2011, **11**, 2621–2636.
23. Ni, T., Xing, F., Shao, M., Zhao, Y., Zhu, S. and Li, M., *Coordination Polymers of 1,3,5-Tris(triazol-1-ylmethyl)-2,4,6-trimethylbenzene: Synthesis, Structure, Reversible Hydration, Encapsulation, and Catalysis Oxidation of Diphenylcarbonohydrazide*. Crystal Growth & Design, 2011, **11**, 2999–3012.
24. Karmakar, A., Rubio, G. M. D. M., Silva, M. F. C. G., Hazra, S. and Pombeiro, A. J. L., *Solvent dependent structural variation of zinc(II) coordination polymers and their catalytic activity in the Knoevenagel condensation reaction*. Crystal Growth & Design, 2015, **15**(9), 4185–4197.

25. Srivastava, S., Kumar, V. and Gupta, R., *A Carboxylate-Rich Metalloligand and Its Heterometallic Coordination Polymers: Syntheses, Structures, Topologies, and Heterogeneous Catalysis*. *Crystal Growth & Design*, 2016, **16**(5), 2874–2886.
26. Karmakar, A., Paul, A., Rúbio, G. M. D. M., M. Silva, F. C. G. and Pombeiro, A. J. L., *Zn(II) and Cu(II) Metal Organic Frameworks Constructed from Terphenyl-4,4''-dicarboxylic Acid Derivative: Synthesis, Structure and Catalytic Application in Aldehyde Cyanosilylation*. *European Journal of Inorganic Chemistry*, 2016, **36**, 5557-5567.
27. Denga, D., Guoa, H., Jia, B., Wanga, W., Maa L. and Luob, F., *Size-selective catalysts in five functionalized porous coordination polymers with unsaturated zinc centers*. *New Journal of Chemistry*, 2017, **41**, 12611-12616.
28. Liu, B., Lin, X., Li, H., Li, K., Huang, H., Bai, L., Hu, H., Liu, Y. and Kang, Z., *Luminescent Coordination Polymers for Highly Sensitive Detection of Nitrobenzene*. *Crystal Growth & Design*, 2015, **15**(9), 4355–4362.
29. Cao, X.-M., Wei, Na., Liu, L., Li, L. and Han, Z.-B. *Luminescent lanthanide–organic polyrotaxane framework as a turn-off sensor for nitrobenzene and Fe³⁺*. *RSC Advances*, 2016, **6**, 19459–19462.
30. White, C. L. and LaDuca, R. L., *Luminescent cadmium dimethylsuccinate and dimethylglutarate coordination polymers self-assembled in the presence of flexible dipyridylamide ligands with capability for nitrobenzene detection*. *Inorganica Chimica Acta*, 2016, **441**, 169–180.
31. Shi, M., Yang, J., Liu, Y.-Y. and Ma, J.-F., *Four coordination polymers based on 1,4,8,11-tetrazacyclotetradecane-N,N',N'',N'''-tetra-methylene-benzoic acid: Syntheses, structures, and selective luminescence sensing of iron(III) ions, dichromate anions, and nitrobenzene*. *Dyes and Pigments*, 2016, **129**, 109-120.

32. Pan, Y., Wang, J., Guo, X., Liu, X., Tang, X. and Zhang, H., *A new three-dimensional zinc-based metal-organic framework as a fluorescent sensor for detection of cadmium ion and nitrobenzene*. Journal of Colloid and Interface Science, 2018, **513**, 418–426.
33. Huang, Y.-R., Gao, L.-L., Zhang, J., Wang, X.-Q., Fan, L.-M. and Hu, T.-P., *Two novel luminescent Cd(II)/Zn(II) coordination polymers based on 4,4'-(1H-1,2,4-triazol-1-yl)methylene-bis(benzonic acid) for sensing organic molecules and Fe³⁺ ion*. Inorganic Chemistry Communications, 2018, **91**, 35-38.
34. Forster, P. M., Stock, N. and Cheetham, A. K., *A High-Throughput Investigation of the Role of pH, Temperature, Concentration, and Time on the Synthesis of Hybrid Inorganic–Organic Materials*. Angewandte Chemie, 2005, **44**, 7608-7611.
35. Fromm, K. M., *Coordination polymer networks with s-block metal ions*. Coordination Chemistry Reviews, 2008, **252**, 856–885.
36. Noro, S.-I., Kitagawa, S., Akutagawa, T. and Nakamura, T., *Coordination polymers constructed from transition metal ions and organic N-containing heterocyclic ligands: Crystal structures and microporous properties*. Progress in Polymer Science, 2009, **34**, 240-279.
37. Wang, Y., Tian, Y. and Luo, J., *Two new d¹⁰ metal-directed coordination polymers based on an unsymmetrical ligand 3-pyrimidin-5-ylbenzoic acid*. Inorganic Chemistry Communications, 2011, **14**, 1258-1261.
38. Song, Y. J., Kwak, H., Lee, Y. M., Kim, S. H., Lee, S. H., Park, B. K., Jun, J. Y., Yu, S. M., Kim, C., Kim, S.-J. and Kim, Y., *Metal-directed supramolecular assembly of metal(II) benzoates (M = Co, Ni, Cu, Zn, Mn, and Cd) with 4,4'-bipyridine: Effects of metal coordination modes and novel catalytic activities*. Polyhedron, 2009, **28**, 1241–1252.
39. Murdock, C. R., Lu, Z. and Jenkins, D. M., *Effects of Solvation on the Framework of a Breathing Copper MOF Employing a Semirigid Linker*. Inorganic Chemistry, 2013, **52**, 2182–2187.

40. Kitagawa, S., Kitaura, R. and Noro, S.-I., *Functional Porous Coordination Polymers*. *Angewandte Chemie*, 2004, **43**, 2334–2375.
41. Lin, H.-Y., Luan, J., Wang, X.-L., Zhang, J.-W., Liu, G.-C. and Tian, A.-X., *Construction and properties of cobalt(II)/copper(II) coordination polymers based on N-donor ligands and polycarboxylates mixed ligands*. *RSC Advances*, 2014, **4**, 62430-62445.
42. Zheng, S.-L., Tong, M.-L., Yu, X.-L. and Chen, X.-M., *Syntheses and structures of six chain-, ladder- and grid-like co-ordination polymers constructed from μ -hexamethylenetetramine and silver salts*. *Journal of the Chemical Society, Dalton Transactions*, 2001, 586–592.
43. Liu, Y., Qi, Y., Su, Y.-H., Zhao, F.-H., Che, Y.-X. and Zheng, J.-M., *Five novel cobalt coordination polymers: effect of metal–ligand ratio and structure characteristics of flexible bis(imidazole) ligands*. *Crystal engineering communications*, 2010, **12**, 3283–3290.
44. Li, L., Wang, S., Chen, T., Sun, Z., Luo, J. and Hong, M. *Solvent-Dependent Formation of Cd(II) Coordination Polymers Based on a C₂-Symmetric Tricarboxylate Linker*. *Crystal Growth & Design*, 2012, **12**, 4109-4115.
45. Xia, Y. and Sun, W.-Y., *Influence of temperature on metal-organic frameworks*. *Chinese Chemical Letters*, 2014, **25**, 823–828.
46. Zhang, S.-M., Hu, T.-L., Du, J.-L. and Bu, X.-H., *Tuning the formation of copper(I) coordination architectures with quinoxaline-based N,S-donor ligands by varying terminal groups of ligands and reaction temperature*. *Inorganica Chimica Acta*, 2009, **362**, 3915–3924.
47. Yuan, F., Xie, J., Hu, H.-M., Yuan, C.-M., Xu, B., Yang, M.-L., Dong, F.-X. and Xue, G.-L. *Effect of pH/metal ion on the structure of metal–organic frameworks based on novel bifunctionalized ligand 4'-carboxy-4,2':6',4''-terpyridine*. *Crystal engineering communications*, 2013, **15**, 1460–1467.
48. Janicki, R., Mondry, A. and Starynowicz, P., *Carboxylates of rare earth elements*. *Coordination Chemistry Reviews*, 2017, **340**, 98-113.

49. Ye, B.-H., Tong, M.-L. and Chen, X.-M., *Metal-organic molecular architectures with 2,2'-bipyridyl-like and carboxylate ligands*. Coordination Chemistry Reviews, 2005, **249**, 545–565.
50. Zhang, P., Li, D.-S., Zhao, J., Wu, Y.-P., Li, C., Zou, K. and Lu, J. Y., *Four Zn(II)/Cd(II) coordination polymers derived from isomeric benzene dicarboxylates and 1,6-bis(triazol)hexane ligand: synthesis, crystal structure, and luminescent properties*. Journal of Coordination Chemistry, 2011, **64**, 2329–2341.
51. Cheng, P.-C., Kuo, P.-T., Liao, Y.-H., Xie, M.-Y., Hsu, W. and Chen, J.-D., *Ligand-Isomerism Controlled Structural Diversity of Zn(II) and Cd(II) Coordination Polymers from Mixed Dipyridyladipoamide and Benzenedicarboxylate Ligands*. Crystal Growth & Design, 2013, **13**(2), 623–632.
52. Chughtai, A. H., Ahmad, N., Younus, H. A., Laypkov A. and Verpoort, F., *Metal-organic frameworks: versatile heterogeneous catalysts for efficient catalytic organic transformations*. Chemical Society Reviews, 2015, **44**, 6804–6849.
53. Ma, L., Abney, C. and Lin, W., *Enantioselective catalysis with homochiral metal-organic frameworks*. Chemical Society Reviews, 2009, **38**, 1248–1256.
54. Hwang, I. H., Bae, J. M., Hwang, Y.-K., Kim, H.-Y., Kim, C., Huh, S., Kim, S.-J. and Kim, Y., *CO₂ selective dynamic two-dimensional Zn^{II} coordination polymer*. Daltons Transactions, 2013, **42**, 15645–15649.
55. Wani, M. A., Kumar, A., Pandey, M. D. and Pandey, R., *Heteroleptic 1D Coordination Polymers: 5-Coordinated Zinc(II) Polymer as an Efficient Transesterification Catalyst*. Polyhedron, 2017, **126**, 142–149.
56. Hasegawa, S., Horike, S., Matsuda, R., Furukawa, S., Mochizuki, K., Kinoshita, Y. and Kitagawa, S., *Three-Dimensional Porous Coordination Polymer Functionalized with Amide Groups Based on Tridentate Ligand: Selective Sorption and Catalysis*. The Journal of the American Chemical Society, 2007, **129**, 2607–2614.

57. Allendorf, M. D., Bauer, C. A., Bhakta, R. K. and Houk, R. J. T., *Luminescent metal-organic frameworks*. Chemical Society Reviews, 2009, **38**, 1330–1352.
58. Fang, Q., Zhu, G., Shi, X., Wu, G., Tian, G., Wang, R. and Qiu, S., *Synthesis, structure and fluorescence of a novel three-dimensional inorganic-organic hybrid polymer constructed from trimetallic clusters and mixed carboxylate ligands*. Journal of Solid State Chemistry, 2004, **177**, 1060–1066.
59. Fang, Q., Zhu, G., Xue, M., Sun, J., Tian, G., Wu, G. and Qiu, S., *Influence of organic bases on constructing 3D photoluminescent open metal-organic polymeric frameworks*. Dalton Transactions, 2004, 2202–2207.
60. Zhang, S., Wang, Z., Zhang, H., Cao, Y., Sun, Y., Chen, Y., Huang, C. and Yu, X., *Self-assembly of two fluorescent supramolecular frameworks constructed from unsymmetrical benzene tricarboxylate and bipyridine*. Inorganica Chimica Acta, 2007, **360**, 2704–2710.
61. Rachuri, Y., Parmar, B., Bisht, K. K. and Suresh, E., *Solvothermal Self-assembly of Cd²⁺ Coordination Polymers with Supramolecular Networks Involving N-donor Ligands and Aromatic Dicarboxylates: Synthesis, Crystal Structure and Photoluminescence Studies*. Dalton Transactions, 2017, **46**, 3623–3630.
62. Li, Y., Song, H., Chen, Q., Liu, K., Zhao, F.-Y., Ruan, W.-J. and Chang, Z., *Two coordination polymers with enhanced ligand centered luminescence and assembly imparted sensing ability for acetone*. Journal of Materials Chemistry A, 2014, **2**, 9469–9473.
63. Li, Y.-L., Zhao, Y., Wang, P., Kang, Y.-S., Liu, Q., Zhang, X.-D. and Sun, W.-Y., *Multifunctional Metal-Organic Frameworks with Fluorescent Sensing and Selective Adsorption Properties*. Inorganic Chemistry, 2016, **55**, 11821–11830.
64. Wen, L.-L., Dang, D.-B., Duan, C.-Y., Li, Y.-Z., Tian, Z.-F. and Meng, Q.-J., *1D Helix, 2D Brick-Wall and Herringbone, and 3D Interpenetration d¹⁰ Metal-Organic Framework Structures Assembled from Pyridine-2,6-dicarboxylic Acid N-Oxide*. Inorganic Chemistry, 2005, **44**, 7161–7170.

65. Gao, H.-L., Yi, L., Zhao, B., Zhao, X.-Q., Cheng, P., Liao, D.-Z. and Yan, S.-P., *Synthesis and Characterization of Metal-Organic Frameworks Based on 4-Hydroxypyridine-2,6-dicarboxylic Acid and Pyridine-2,6-dicarboxylic acid Ligands*. *Inorganic Chemistry*, 2006, **45**, 5980-5988.
66. Wu, H.-F., Chen, X.-D. and Du, M., *A one-dimensional Cd^{II} coordination polymer: poly[[[bis[methanolcadmium(II)]- μ_2 -aqua]-bis-(μ_3 -pyridine-2,6-dicarboxylato- $K^5 O:O,N,O':O')$]]. *Acta Crystallographica Section E*, 2007, **E63**, 126-128.*
67. Liu, H.-Y., Wu, H., Ma, J.-F., Liu, Y.-Y., Liu, B. and Yang, J., *Syntheses, Structures and Photoluminescence of Zinc(II) Coordination Polymers Based on Carboxylates and Flexible Bis-[(pyridyl)-benzimidazole] Ligands*. *Crystal Growth & Design*, 2010, **10**, 4795-4805.
68. Ma, L.-F., Li, X.-Q., Meng, Q.-L., Wang, L.-Y., Du, M. and Hou, H.-W., *Significant Positional Isomeric Effect on Structural Assemblies of Zn(II) and Cd(II) Coordination Polymers Based on Bromoisophthalic Acids and Various Dipyridyl-Type Coligands*. *Crystal Growth & Design*, 2011, **11**, 175-184.
69. Sharif, M. A. and Najafi, G. R., *Synthesis, Structure and Characterization of a Helical Seven-Coordinated Pyridine-2,6-dicarboxylate-Bridged Cadmium(II) Complex*. *Acta Chimica Slovenica*, 2013, **60**, 138-143.
70. Paraschiv, C., Cucos, A., Shova, S., Madalan, A. M., Maxim, C., Visinescu, D., Cojocaru, B., Parvulescu, V. I. and Andruh, M., *New Zn(II) Coordination Polymers Constructed from Amino-Alcohols and Aromatic Dicarboxylic Acids: Synthesis, Structure, Photocatalytic Properties, and Solid-State Conversion to ZnO*. *Crystal Growth & Design*, 2015, **15**, 799-811.
71. Wang, J., Zhao, X.-Q., Wang, N. and Li, Y.-C., *Syntheses, structures, and photoluminescence of three cadmium(II) coordination complexes based on pyridine-2,6-dicarboxylic acid and a derivative*. *Journal of Coordination Chemistry*, 2015, **68**, 904-915.

72. Tripathi, S., Sachan, K. S. and Anantharama, G., *Crystal engineering of zinc and cadmium coordination polymers via a mixed-ligand strategy regulated by aromatic rigid/flexible dicarboxylate ancillary ligands and metal ionic radii: Tuning structure, dimension and photoluminescence properties*. Polyhedron, 2016, **119**, 55-70.
73. Croitor, L., Coropceanu, E. B., Duca, G., Siminel, A. V. and Fonari, M. S., *Nine Mn(II), Zn(II) and Cd(II) mixed-ligand coordination networks with rigid dicarboxylate and pyridine-n-aldoxime ligands: Impact of the second ligand in the structures' dimensionality and solvent capacity*. Polyhedron, 2017, **129**, 9-21.
74. Wen, L., Li, Y., Lu, Z., Lin, J., Duan, C. and Meng, Q., *Syntheses and Structures of Four d^{10} Metal-Organic Frameworks Assembled with Aromatic Polycarboxylate and bix [bix=1,4-Bis(imidazol-1-ylmethyl)benzene]*. Crystal Growth & Design, 2006, **6**, 530-537.
75. He, H., Collins, D., Dai, F., Zhao, X., Zhang, G., Ma, H. and Sun, D., *Construction of Metal-Organic Frameworks with 1D Chain, 2D Grid, and 3D Porous Framework Based on a Flexible Imidazole Ligand and Rigid Benzenedicarboxylates*. Crystal Growth & Design, 2010, **10**, 895-902.
76. Zhang, K.-L., Zhang, J.-B., Jing, C.-Y., Zhang, L., Walton, R. I., Zhu, P. and Ng, S. W., *Synthesis, structures and properties of a family of four two-dimensional coordination polymers constructed from 5-hydroxy-isophthalate*. Journal of Solid State Chemistry, 2014, **211**, 8-20.
77. Zhang, C., Zhang, M., Qin, L. and Zheng, H., *Crystal Structures and Spectroscopic Properties of Metal-Organic Frameworks Based on Rigid Ligands with Flexible Functional Groups*. Crystal Growth & Design, 2014, **14**, 491-499.
78. Hu, J.-S., Yao, X.-Q., Zhang, M.-D., Qin, L., Li, Y.-Z., Guo, Z.-J., Zheng, H.-G. and Xue, Z.-L., *Syntheses, Structures, and Characteristics of Four New Metal-Organic Frameworks Based on Flexible Tetrapyridines and Aromatic Polycarboxylate Acids*. Crystal Growth & Design, 2012, **12**, 3426-3435.

79. Lin, W.-F., Wu, M.-F., Dai, S.-C., Dai, W.-L. and Zou, J.-P., *A novel (4,6)-connected 3D metal-organic framework based on chelidamic acid: Synthesis, crystal structure and photoluminescence*. Inorganic Chemistry Communications, **35**, 326–329.
80. Bruker, SMART (version 5.6), Bruker AXS Inc., Madison, WI, USA, 2000.
81. Siemens, SAINT, Version 4 Software Reference Manual, Siemens Analytical X-Ray Systems, Inc., Madison, WI, USA, 2000.
82. G.M. Sheldrick, SADABS, Program for Empirical Absorption correction of Area Detector Data, University of Go'ttingen, Go'ttingen, Germany, 2000.
83. Siemens, SHELXTL, 2000, Version 6.12 Reference Manual, Siemens Analytical X-Ray Systems, Inc., Madison, WI, USA, 2000.
84. Liu, Y., Dou, J.-M., Wang, D., Zhang, X.-X. and Zhou, L., *Diaqua(pyridine-2,6-dicarboxylato)nickel(II)*. Acta Crystallographica Section E, 2006, **E62**, 2208–2209.
85. Wang, L., Duan, L., Wang, E., Xiao, D., Li, Y., Lan, Y., Xu, L. and Hu, C., *Novel hydrogen-bonded three-dimensional network complexes containing cobalt-pyridine-2,6-dicarboxylic acid*. Transition Metal Chemistry, 2004, **29**, 212–215.
86. Liu, M.-S., Yu, Q.-Y., Cai, Y.-P., Su, C.-Y., Lin, X.-M., Zhou, X.-X. and Cai, J.-W., *One-, Two-, and Three-Dimensional Lanthanide Complexes Constructed from Pyridine-2,6-dicarboxylic Acid and Oxalic Acid Ligands*. Crystal Growth & Design, 2008, **8**, 4083-4091.
87. Kukovec, B.-M., Venter, G. A. and Oliver, C. L., *Structural and DFT Studies on the Polymorphism of a Cadmium(II) Dipicolinate Coordination Polymer*. Crystal Growth & Design, 2012, **12**, 456-465.
88. Karmakar, A., Silva, M. F. C. G. and Pombeiro, A. J. L., *Zinc metal-organic frameworks: efficient catalysts for the diastereoselective Henry reaction and transesterification*. Dalton Transactions, 2014, **43**, 7795–7810.
89. Yoo, D.-W., Han, J.-H., Nam, S. H., Kim, H. J., Kim, C. and Lee, J.-K., *Efficient transesterification by polymer-supported zinc complexes: Clean and recyclable catalysts*. Inorganic Chemistry Communications, 2006, **9**, 654-657.

90. Ryu, J. Y., Han, J. H., Lee, J. Y., Hong, S. J., Choi, S. H., Kim, C., Kim, S.-J. and Kim, Y., *Crystal structures and catalytic activities of Zn(II) compounds containing btp ligands*. *Inorganica Chimica Acta*, 2005, **358**, 3659-3670.
91. Kim, Y., Kim, S.-J., Choi, S. H., Han, J. H., Nam, S. H., Lee, J. H., Kim, H. J., Kim, C., Kim, D. W. and Jang, H. G., *Crystal structures and catalytic activities of Zn(II) compounds containing 1,3-bis(4-pyridyl)propane*. *Inorganica Chimica Acta*, 2006, **359**, 2534-2542.
92. Lee, Y. M., Hong, S. J., Kim, H. J., Lee, S. H., Kwak, H., Kim, C., Kim, S.-J. and Kim, Y., *Anion effect on construction of zinc(II) coordination polymer with a chelating ligand 2,2'-dipyridylamine (Hdpa): Novel heterogenous catalytic activities*. *Inorganic Chemistry Communications*, 2007, **10**, 287-291.
93. Gupta, A. K., Dhir, A and Pradeep, C. P., *Multifunctional Zn(II) complexes: Photophysical properties and Catalytic transesterification toward biodiesel synthesis*. *Inorganic Chemistry*, 2016, **55**, 7492-7500.
94. Bruker (2013). APEX2, SAINT and SADABS. Bruker AXS Inc., Madison, Wisconsin, USA.
95. Sheldrick, G. M., *SHELXT - Integrated space-group and crystal-structure Determination*, *Acta Crystallographica A*, 2015, **71**, 3-8.
96. Che, G.-B., Liu, C.-B., Wang, L. and Cui, Y.-C., *Solvothermal syntheses, structures, and luminescence of two heterometallic metal-organic frameworks constructed from m-BDC (m -BDC = 1,3-benzene-dicarboxylate)*. *Journal of Coordination Chemistry*, 2007, **60**, 1997-2007.
97. Du, F., Zhang, H., Tian, C. and Du, S., *Synthesis and Structure of Two Acentric Heterometallic Inorganic-Organic Hybrid Frameworks with Both Nonlinear Optical and Ferroelectric Properties*. *Crystal Growth & Design*, 2013, **13**, 1736-1742.
98. Xu, H., Wang, R. and Li, Y., *Zn₂Na₂(BDC)₃(DMF)₂(μ-H₂O)₂: rare 3D channel-structures with pendant DMF constructed by carboxyl group bridging heterometallic ions*. *Journal of Molecular Structure*, 2004, **688**, 1-3.

99. Wang, L., Shi, Z., Li, G., Fan, Y., Fu, W. and Feng, S., *Solvothermal synthesis and structural characterization of a three-dimensional metal-organic polymer [NaZn(1,2,4-BTC)] (1,2,4-BTC = 1,2,4-benzenetricarboxylate)* Solid State Sciences, 2004, **6**, 85-90.
100. Yang, Y.-t., Zhao, Q., Tu, C.-Z., Cheng, F.-X. and Wang, F., *A novel heterobimetallic Cd-Na polynuclear framework showing α -Po topology based on unprecedented $Cd_2Na(CO_2)_6$ molecular building block (MBB)*. Inorganic Chemistry Communications, 2014, **40**, 43-46.
101. Yang, W., Feng, J. and Zhang, H., *Facile and rapid fabrication of nano structured lanthanide coordination polymers as selective luminescent probes in aqueous solution*. Journal of Materials Chemistry, 2012, **22**, 6819-6823.
102. Xiao, Y., Wang, L., Cui, Y., Chen, B., Zapata, F. and Qiana, G., *Molecular sensing with lanthanide luminescence in a 3D porous metal-organic framework*. Journal of Alloys and Compounds, 2009, **484**, 601-604.
103. Luo, F., Che, Y.-X. and Zheng, J.-M., *Trinuclear Cobalt Based Porous Coordination Polymers Showing Unique Topological and Magnetic Variety upon Different Dicarboxylate-like Ligands*. Crystal Growth & Design, 2009, **9**, 1066-1071.
104. Liu, Y., Li, H., Han, Y., Lv, X., Hou, H. and Fan, Y., *Template-Assisted Synthesis of Co,Mn-MOFs with Magnetic Properties Based on Pyridinedicarboxylic Acid*. Crystal Growth & Design, 2012, **12**, 3505-3513.
105. Ye, R.-P., Zhang, X., Qin, Y.-Y. and Yao, Y.-G., *Combined influence of hydrogen bonds and π - π interactions in the assembly of five manganese coordination polymers with magnetic properties*. Crystal engineering communications, 2017, **19**, 1658-1668.

APPENDICES



APPENDIX A

THE CATALYTIC STUDY

For the optimal condition: 75 °C, 48 h with a 1:6 molar ratio of PA: methanol

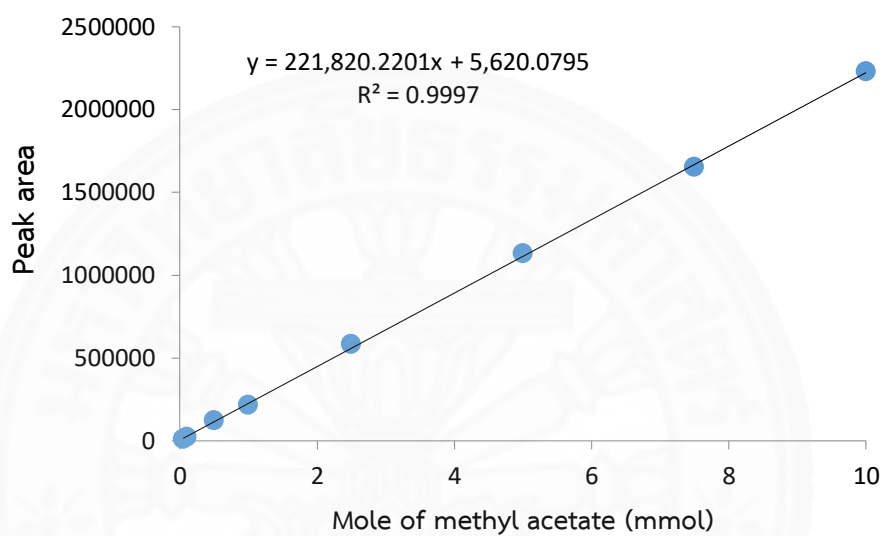


Figure S1 Calibration curve for calculating the methyl acetate yields (%)

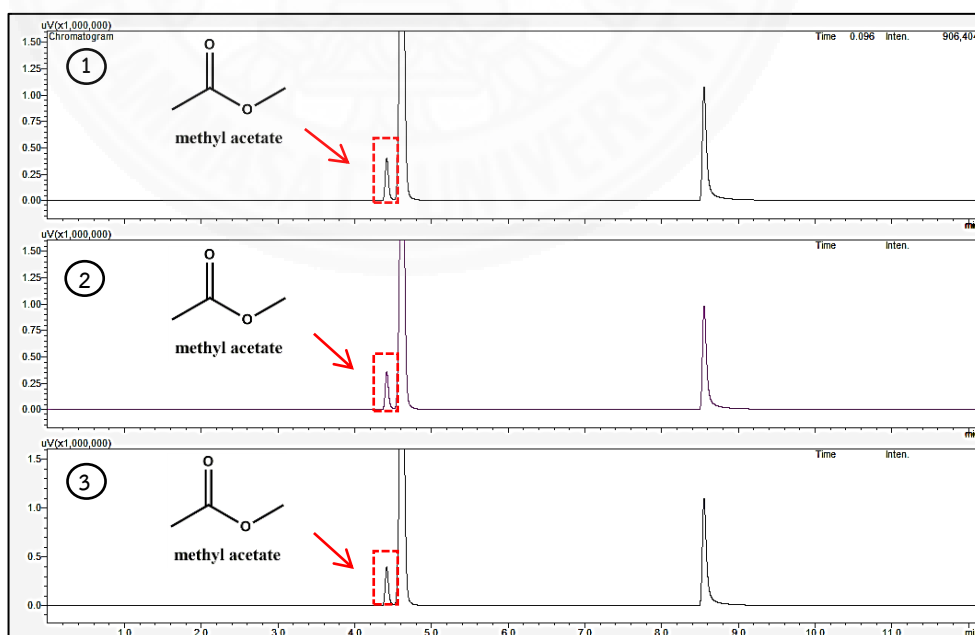


Figure S2 Gas chromatogram of product from optimal condition

- Methyl acetate yield (%) calculation

Peak area				Mole of methyl acetate produced (mmol)
1	2	3	Average	
1244955.2	1103846.5	1227463.8	1192088.5	5.35

$$\text{Methyl acetate yields (\%)} = \frac{\text{Mole of methyl acetate product}}{\text{Mole of initial phenyl acetate}} \times 100$$

$$= \frac{5.35}{10} \times 100 = 53.5 \%$$

Table S1 The optimal operating conditions for GC-FID used

Condition	
Injection volume	1 μ L
Injection mode	Split
Carrier Gas	He
Flow control mode	Velocity
Linear velocity	20.0 cm/sec
Column	Rtxwax
Column temperature program	35 $^{\circ}$ C, hold 2.0 min 20 $^{\circ}$ C/min to 55 $^{\circ}$ C 40 $^{\circ}$ C/min to 220 $^{\circ}$ C, hold 5.0 min Total program time: 12.13 min
Flame ionization detector (FID)	230 $^{\circ}$ C

APPENDIX B
THE SOLVENT SENSING STUDY

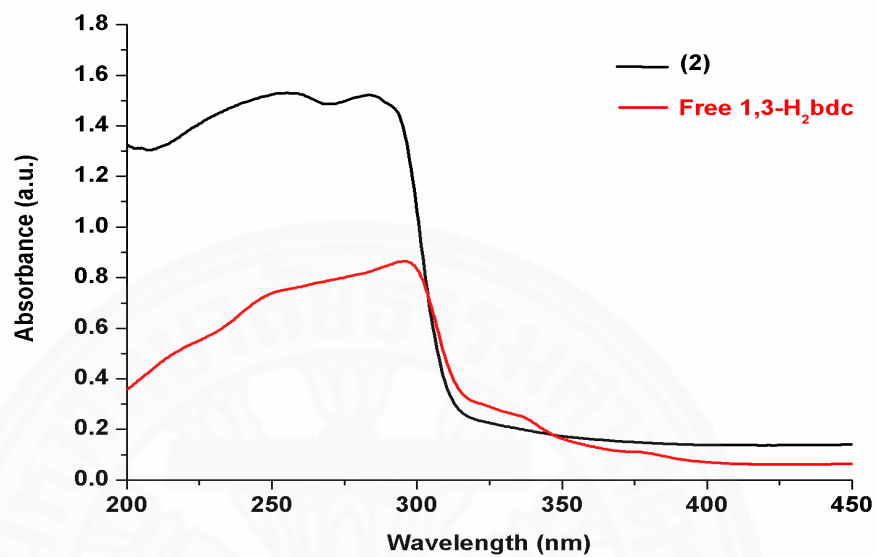


Figure S3 Solid UV-Vis spectra of 1,3-bdcH₂ and compound (2)

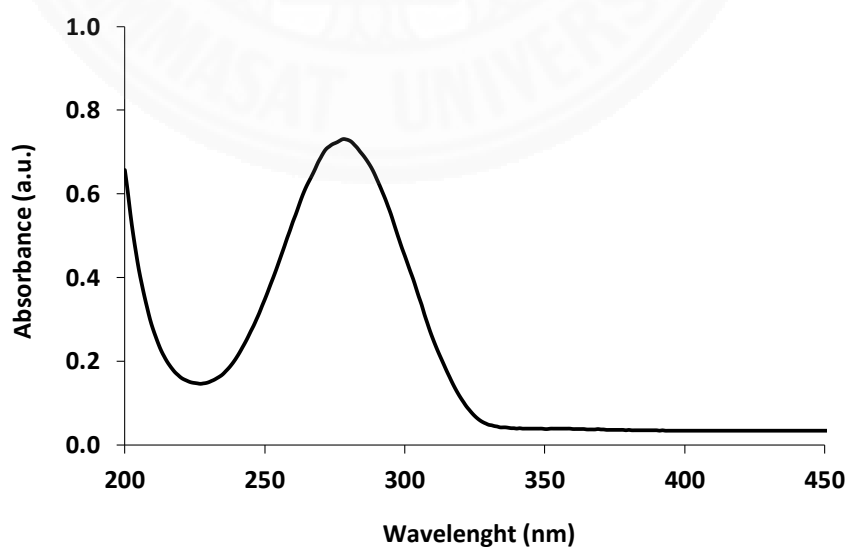


Figure S4 UV-Vis spectrum of acetone

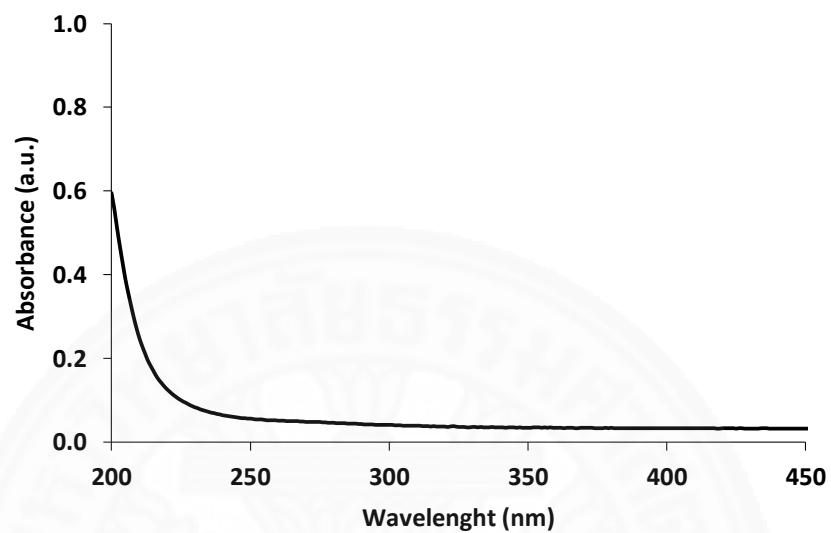


Figure S5 UV-Vis spectrum of hexane

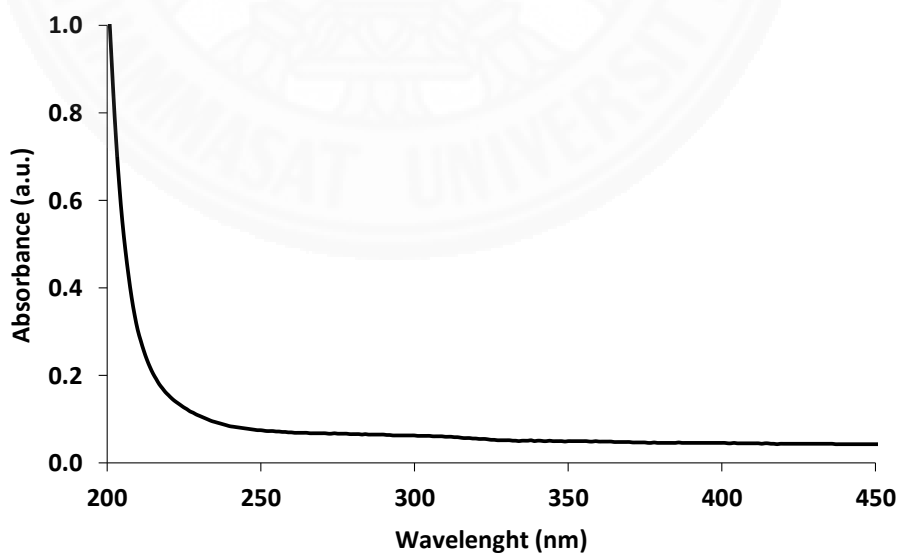


Figure S6 UV-Vis spectrum of methanol

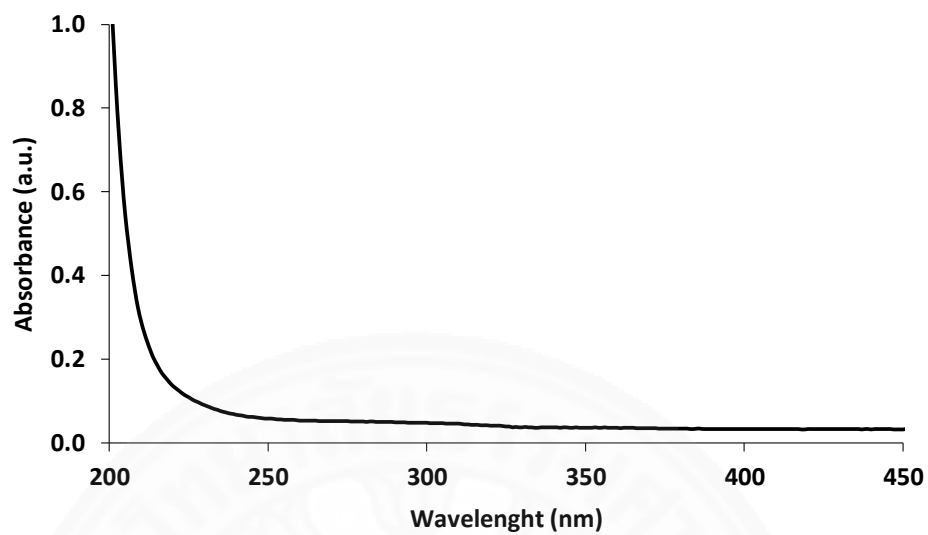


Figure S7 UV-Vis spectrum of Ethanol

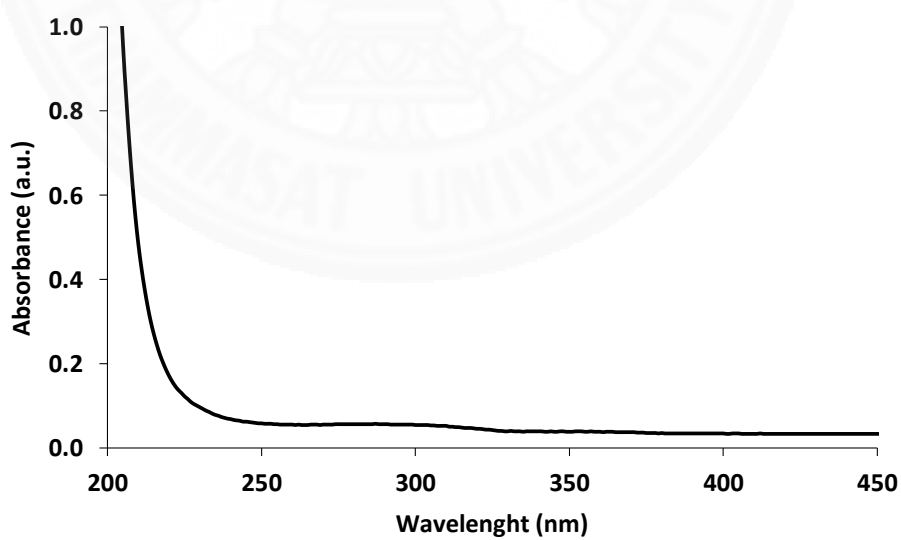


Figure S8 UV-Vis spectrum of dichloromethane

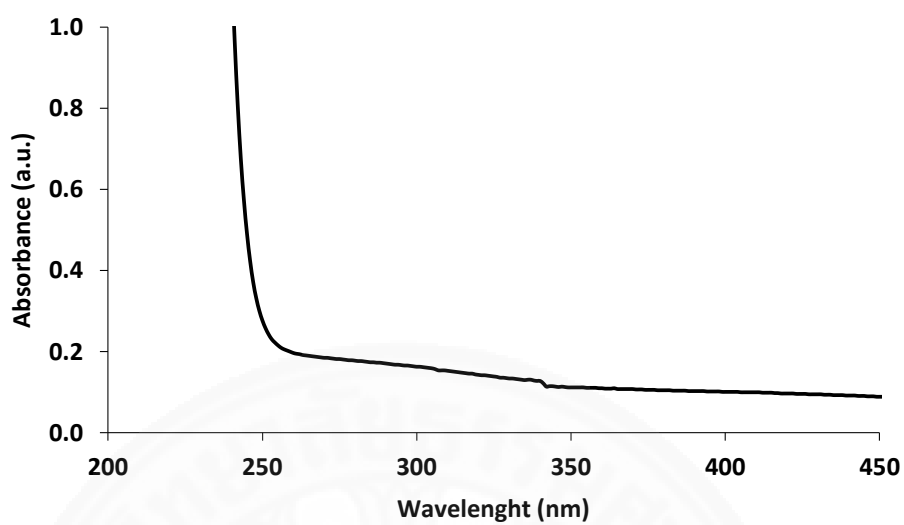


Figure S9 UV-Vis spectrum of dimethyl sulfoxide

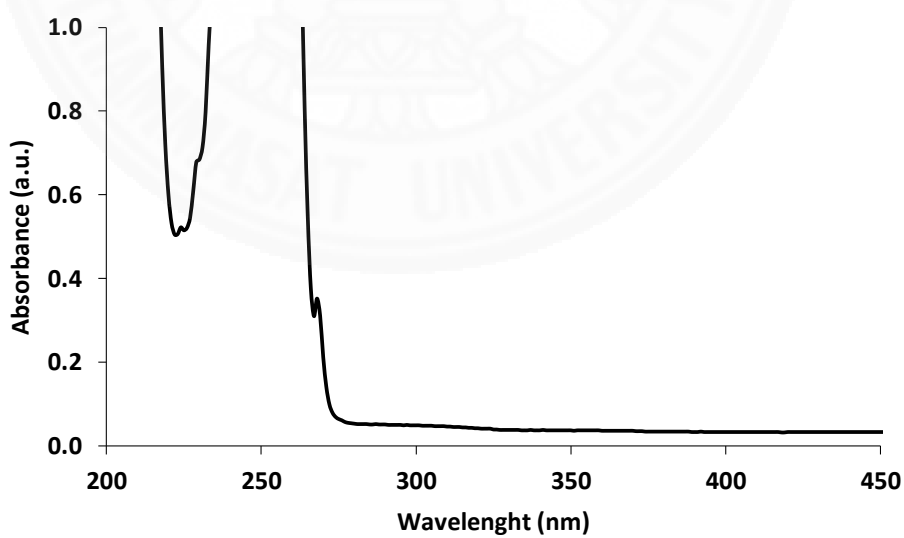


Figure S10 UV-Vis spectrum of benzene

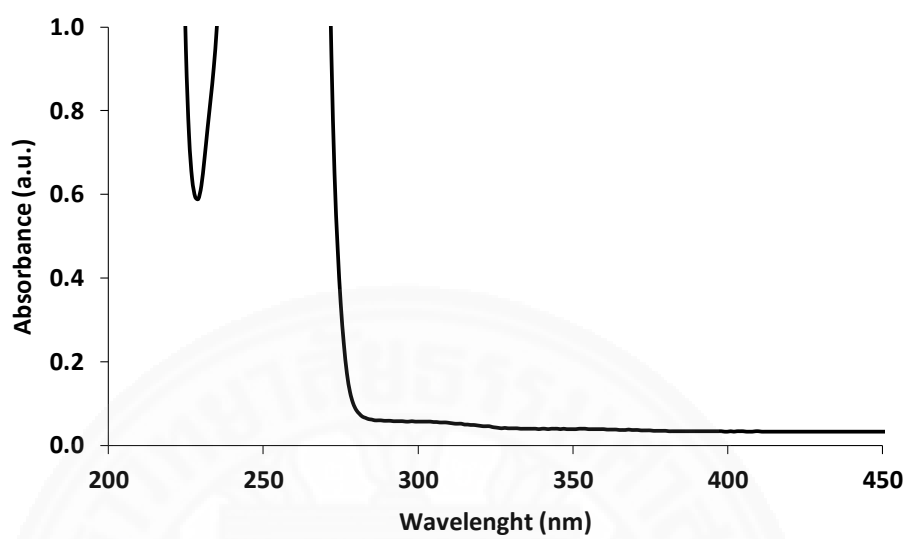


Figure S11 UV-Vis spectrum of toluene

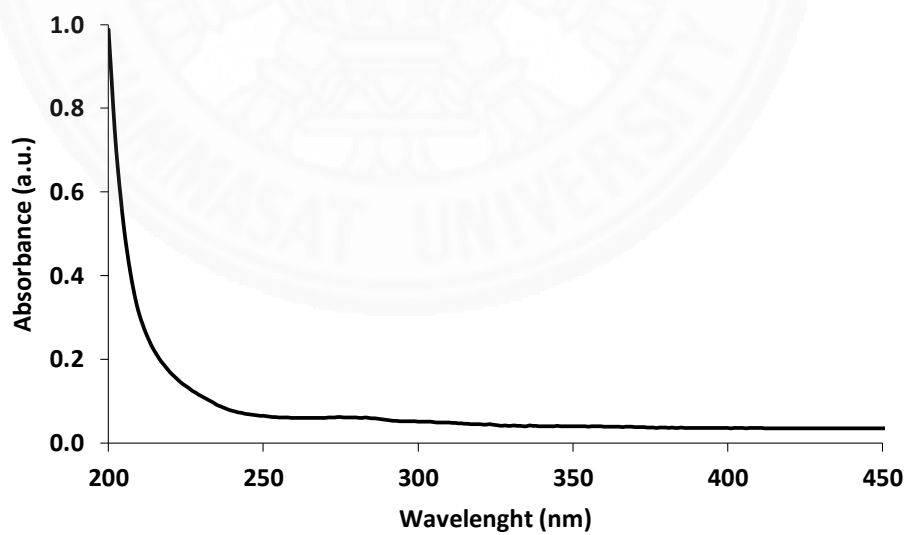


Figure S12 UV-Vis spectrum of tetrahydrofuran

APPENDIX C
PUBLICATION

electronic reprint

CRYSTALLOGRAPHIC
COMMUNICATIONSISSN: 2056-9890
journals.iucr.org/e**Crystal structure of
poly[di-aquabis(μ_5 -benzene-1,3-dicarboxylato)(*N,N*-dimethyl-
formamide)cadmium(II)disodium(I)]****Matimon Sangsawang, Kittipong Chainok and Nanthawat Wannarit***Acta Cryst.* (2017). E73, 1599–1602**IUCr Journals**

CRYSTALLOGRAPHY JOURNALS ONLINE

This open-access article is distributed under the terms of the Creative Commons Attribution Licence
<http://creativecommons.org/licenses/by/2.0/uk/legalcode>, which permits unrestricted use, distribution, and
reproduction in any medium, provided the original authors and source are cited.



CRYSTALLOGRAPHIC
COMMUNICATIONS

ISSN 2056-9890

Crystal structure of poly[di-aquabis(μ_5 -benzene-1,3-dicarboxylato)(*N,N*-dimethylformamide)-cadmium(II)disodium(I)]

Matimon Sangsawang,^a Kittipong Chainok^b and Nanthawat Wannarit^{a*}^aDepartment of Chemistry, Faculty of Science and Technology, Thammasat University, Khlong Laung, Pathumthani 12121, Thailand, and ^bMaterials and Textile Technology, Faculty of Science and Technology, Thammasat University, Khlong Laung, Pathumthani 12121, Thailand. *Correspondence e-mail: nwan0110@tu.ac.thReceived 2 September 2017
Accepted 26 September 2017

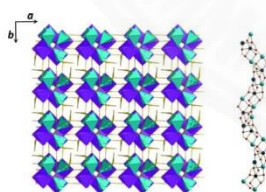
Edited by T. J. Prior, University of Hull, England

Keywords: crystal structure; Cd^{II}–Na^I bimetallic; three-dimensional framework.**CCDC reference:** 1576543**Supporting information:** this article has supporting information at journals.iucr.org/e

The title compound, [CdNa₂(C₈H₄O₄)₂(C₃H₇NO)(H₂O)₂]_n, or [CdNa₂(1,3-bdc)₂(DMF)(H₂O)₂]_n, is a new Cd^{II}–Na^I heterobimetallic coordination polymer. The asymmetric unit consists of one Cd^{II} atom, two Na^I atoms, two 1,3-bdc ligands, two coordinated water molecules and one coordinated DMF molecule. The Cd^{II} atom exhibits a seven-coordinate geometry, while the Na^I atoms can be considered to be pentacoordinate. The metal ions and their symmetry-related equivalents are connected *via* chelating–bridging carboxylate groups of the 1,3-bdc ligands to generate a three-dimensional framework. In the crystal, there are classical O–H...O hydrogen bonds involving the coordinated water molecules and the 1,3-bdc carboxylate groups and π – π stacking between the benzene rings of the 1,3-bdc ligands present within the frameworks.

1. Chemical context

Porous coordination polymers or metal–organic frameworks (MOFs) constructed from *d*¹⁰ transition metals and benzene polycarboxylate bridging ligands have been widely studied (Yaghi *et al.*, 1999; Lin *et al.*, 2008; Seco *et al.*, 2017) due to the varieties of coordination framework topologies and also potential applications in gas adsorption (Suh *et al.*, 2012), photoluminescence (Wang *et al.*, 2012) and photocatalysis (Wu *et al.*, 2017). Among the most common ligands in this class, the rigid and planar backbone of benzene dicarboxylates such as benzene-1,3-dicarboxylic acid (1,3-H₂bdc) and benzene-1,4-dicarboxylic acid (1,4-H₂bdc) are widely employed in the construction of these solids owing to their rich coordination modes. Studies incorporating alkaline metal ions into *d*¹⁰-MOFs with one type of bridging ligand to construct novel heterobimetallic *d*¹⁰-alkaline metal ion MOFs have been undertaken (Lin *et al.*, 2010*a,b*). The alkali metal ions could provide an unpredictable coordination number and pH-dependent self-assembly in the construction of coordination frameworks with various types of topology and dimensionality (Borah *et al.*, 2011; Chen *et al.*, 2011). However, the members of three-dimensional coordination framework heterobimetallic Zn^{II} or Cd^{II}/Na^I MOFs with benzenepolycarboxylate ligands are still limited; previous reports include [ZnNa(1,2,4-btc)] where 1,2,4-btc = benzene-1,2,4-tricarboxylate (Wang *et al.*, 2004), [Zn₂Na₂(1,4-bdc)₃(DMF)₂(*m*-H₂O)₂] where 1,4-bdcH₂ = benzene-1,4-dicarboxylic acid (Xu *et al.*, 2004), [[CdNa(1,3-bdc)₂].[NH₂(CH₃)₂]] where 1,3-bdcH₂ = benzene-1,3-dicarboxylic acid (Che *et al.*, 2007), [CdNa(OH-1,3-bdc)₂(H₂O)₂].2H₂O where OH-1,3-bdcH₂ = 5-hydroxy-



OPEN ACCESS

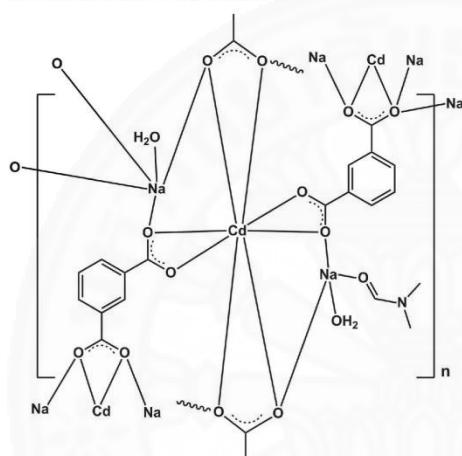
Acta Cryst. (2017). E73, 1599–1602

electronic reprint

https://doi.org/10.1107/S2056989017013871 1599

research communications

benzene-1,3-dicarboxylic acid (Du *et al.*, 2013) and $[\text{Cd}_8\text{Na}(\text{ntc})_6(\text{H}_2\text{O})_8]$ where $\text{ntcH}_3 = 5\text{-nitrobenzene-1,2,3-tricarboxylic acid}$ (Yang *et al.*, 2014). With the aim of searching for new members of this heterobimetallic MOFs system containing benzene-1,3-dicarboxylic acid (1,3-bdcH₂), we explored mixed sources of $\text{Zn}^{\text{II}}/\text{Cd}^{\text{II}}\text{-Na}^{\text{I}}$ with this ligand. The expected products are prepared by using a direct synthetic method, mixing metal nitrate salts, 1,3-bdcH₂ and NaOH (mole ratio 1:1:2) in water, methanol and DMF solvents. However, only the $\text{Cd}^{\text{II}}\text{-Na}^{\text{I}}$ MOF product has been successfully synthesized. As part of our ongoing studies on this complex, we describe here the synthesis and crystal structure of a novel three-dimensional heterobimetallic $\text{Cd}^{\text{II}}\text{-Na}^{\text{I}}$ MOF, $[\text{CdNa}_2(1,3\text{-bdc})_2(\text{DMF})(\text{H}_2\text{O})_2]_n$ (**1**).



2. Structural commentary

The title compound (**1**) crystallizes in the tetragonal crystal system with polar $P4_3$ space group. The asymmetric unit of (**1**) consists of one Cd^{II} ion, two crystallographically independent Na^{I} ions, two 1,3-bdc ligands, two coordinated water molecules and one DMF molecules, as shown in Fig. 1. Each Cd^{II} ion is coordinated by seven carboxylate oxygen atoms from four different 1,3-bdc ligands with the $\text{Cd}-\text{O}$ bond distances range between 2.301 (3) and 2.555 (3) Å (Table 1). The Na1 ion is surrounded by three carboxylate oxygen atoms of three different 1,3-bdc ligands, one oxygen atom from a water molecule, and one DMF molecule with the $\text{Na}-\text{O}$ bond distances ranging between 2.304 (7) and 2.498 (11) Å, while the Na2 ion adopts a five-coordinate $[4+1]$ coordination with four oxygen atoms from three different 1,3-bdc ligands and one oxygen atom from a water molecule. The $\text{Na}-\text{O}$ bond distances are in the range 2.275 (5) to 2.354 (8) Å. Fig. 2 shows the coordination modes of the 1,3-bdc ligand in compound (**1**). The 1,3-bdc molecule is fully deprotonated and coordinated to

Table 1
Selected geometric parameters (Å, °).

$\text{Cd1}-\text{O1}$	2.301 (3)	$\text{Na1}-\text{O4}^{\text{i}}$	2.441 (5)
$\text{Cd1}-\text{O2}$	2.555 (3)	$\text{Na1}-\text{O9}$	2.304 (7)
$\text{Cd1}-\text{O3}^{\text{i}}$	2.496 (3)	$\text{Na1}-\text{O11B}$	2.498 (11)
$\text{Cd1}-\text{O4}^{\text{i}}$	2.385 (3)	$\text{Na1}-\text{O11A}$	2.475 (18)
$\text{Cd1}-\text{O5}$	2.284 (4)	$\text{Na2}-\text{O4}^{\text{iv}}$	2.655 (5)
$\text{Cd1}-\text{O7}^{\text{ii}}$	2.396 (3)	$\text{Na2}-\text{O5}$	2.277 (5)
$\text{Cd1}-\text{O8}^{\text{ii}}$	2.472 (3)	$\text{Na2}-\text{O7}^{\text{ii}}$	2.282 (4)
$\text{Na1}-\text{O1}$	2.368 (5)	$\text{Na2}-\text{O8}^{\text{v}}$	2.275 (5)
$\text{Na1}-\text{O3}^{\text{iii}}$	2.339 (5)	$\text{Na2}-\text{O10}$	2.354 (8)
$\text{O1}-\text{Cd1}-\text{O2}$	53.12 (15)	$\text{O1}-\text{Na1}-\text{O4}^{\text{i}}$	77.84 (17)
$\text{O1}-\text{Cd1}-\text{O3}^{\text{i}}$	131.59 (15)	$\text{O1}-\text{Na1}-\text{O11B}$	104.1 (3)
$\text{O1}-\text{Cd1}-\text{O4}^{\text{i}}$	80.31 (12)	$\text{O3}^{\text{iii}}-\text{Na1}-\text{O1}$	151.1 (2)
$\text{O1}-\text{Cd1}-\text{O7}^{\text{ii}}$	125.91 (12)	$\text{O3}^{\text{iii}}-\text{Na1}-\text{O4}^{\text{i}}$	94.59 (15)
$\text{O1}-\text{Cd1}-\text{O8}^{\text{ii}}$	92.04 (13)	$\text{O3}^{\text{iii}}-\text{Na1}-\text{O11B}$	82.9 (3)
$\text{O3}^{\text{i}}-\text{Cd1}-\text{O2}$	173.00 (16)	$\text{O4}^{\text{i}}-\text{Na1}-\text{O11B}$	177.4 (3)
$\text{O4}^{\text{i}}-\text{Cd1}-\text{O2}$	132.60 (15)	$\text{O9}-\text{Na1}-\text{O1}$	95.8 (2)
$\text{O4}^{\text{i}}-\text{Cd1}-\text{O3}^{\text{i}}$	53.37 (13)	$\text{O9}-\text{Na1}-\text{O3}^{\text{iii}}$	112.0 (2)
$\text{O4}^{\text{i}}-\text{Cd1}-\text{O7}^{\text{ii}}$	122.40 (12)	$\text{O9}-\text{Na1}-\text{O4}^{\text{i}}$	88.3 (2)
$\text{O4}^{\text{i}}-\text{Cd1}-\text{O8}^{\text{ii}}$	78.81 (13)	$\text{O9}-\text{Na1}-\text{O11B}$	93.2 (4)
$\text{O5}-\text{Cd1}-\text{O1}$	125.67 (14)	$\text{O5}-\text{Na2}-\text{O4}^{\text{iv}}$	95.45 (19)
$\text{O5}-\text{Cd1}-\text{O2}$	90.36 (16)	$\text{O5}-\text{Na2}-\text{O7}^{\text{ii}}$	83.03 (18)
$\text{O5}-\text{Cd1}-\text{O3}^{\text{i}}$	82.65 (15)	$\text{O5}-\text{Na2}-\text{O10}$	104.5 (2)
$\text{O5}-\text{Cd1}-\text{O4}^{\text{i}}$	128.83 (14)	$\text{O7}^{\text{ii}}-\text{Na2}-\text{O4}^{\text{iv}}$	94.98 (14)
$\text{O5}-\text{Cd1}-\text{O7}^{\text{ii}}$	80.41 (12)	$\text{O7}^{\text{ii}}-\text{Na2}-\text{O10}$	80.5 (2)
$\text{O5}-\text{Cd1}-\text{O8}^{\text{ii}}$	133.24 (16)	$\text{O8}^{\text{v}}-\text{Na2}-\text{O4}^{\text{iv}}$	77.02 (13)
$\text{O7}^{\text{ii}}-\text{Cd1}-\text{O2}$	85.03 (15)	$\text{O8}^{\text{v}}-\text{Na2}-\text{O5}$	110.18 (16)
$\text{O7}^{\text{ii}}-\text{Cd1}-\text{O3}^{\text{i}}$	94.01 (14)	$\text{O8}^{\text{v}}-\text{Na2}-\text{O7}^{\text{ii}}$	164.93 (18)
$\text{O7}^{\text{ii}}-\text{Cd1}-\text{O8}^{\text{ii}}$	53.55 (14)	$\text{O8}^{\text{v}}-\text{Na2}-\text{O10}$	102.3 (2)
$\text{O8}^{\text{ii}}-\text{Cd1}-\text{O2}$	93.07 (11)	$\text{O10}-\text{Na2}-\text{O4}^{\text{iv}}$	158.8 (2)
$\text{O8}^{\text{ii}}-\text{Cd1}-\text{O3}^{\text{i}}$	91.92 (10)		

Symmetry codes: (i) $x, y-1, z$; (ii) $x-1, y, z$; (iii) $-y+1, x, z-\frac{1}{2}$; (iv) $y-1, -x, z+\frac{1}{2}$; (v) $y, -x+1, z+\frac{1}{2}$.

the Cd^{II} and Na^{I} ions in a μ_5 -coordination mode, creating a one-dimensional heterobimetallic chain running parallel to the c axis, Fig. 3. Adjacent chains are further connected

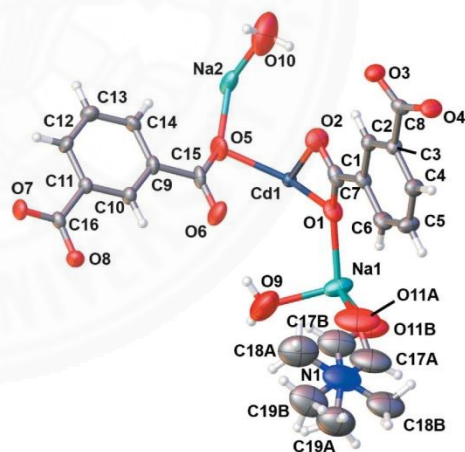


Figure 1
Asymmetric unit of (**1**) with the atomic-numbering scheme. Displacement ellipsoids are drawn at the 50% probability level.

Table 2
Hydrogen-bond geometry (Å, °).

$D-H\cdots A$	$D-H$	$H\cdots A$	$D\cdots A$	$D-H\cdots A$
$O9-H9B\cdots O6$	0.90	2.22	3.074 (8)	159
$O10-H10B\cdots O6^v$	0.86	2.29	3.073 (8)	152

Symmetry code: (v) $y, -x + 1, z + \frac{1}{2}$.

through the 1,3-bdc ligands in the a - and b -axis directions, generating a three-dimensional framework structure as shown in Fig. 4. The coordinated water and DMF molecules adopt a monodentate coordination mode and serve as a terminal pendant ligand pointing inside the channels.

3. Supramolecular features

In the crystal of (**I**), classical O—H \cdots O hydrogen bonds and aromatic π – π stacking interactions are observed and these interactions presumably help to stabilize the frameworks. All water molecules are shown to act as O—H \cdots O hydrogen-bond donors towards the carboxylate groups of the 1,3-bdc ligands (Table 2). The π – π stacking interactions are between symmetry-related aromatic rings of the 1,3-bdc ligands with a $Cg1\cdots Cg2^i$ distance of 3.588 (3) Å and a dihedral angle of 3.8 (4)° [$Cg1$ and $Cg2$ are the centroids of the C1–C6 and C9–C14 rings, respectively; symmetry code: (i) $-y, x, z - 1/4$].

4. Database survey

To the best of our knowledge of structures closely related to (**I**), only the three-dimensional coordination framework $\{[CdNa(1,3-bdc)_2]\cdot[NH_2(CH_3)_2]\}$ has been reported (Che *et al.*, 2007). This compound crystallized in the centrosymmetric space group $C2/c$. The Cd^{II} and Na^I centers are linked by a 1,3-bdc ligand in a μ_4 -coordination mode. The DMF solvent decomposes under solvothermal synthesis, with the construction of a 3D coordination framework with open channels containing $NH_2(CH_3)_2$ molecules. In comparison, compound

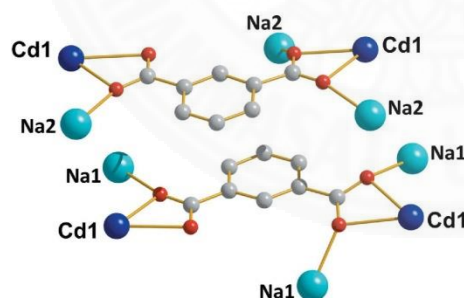


Figure 2
Coordination mode of the μ_5 -1,3-bdc bridging ligands found in (**I**). All hydrogen atoms are omitted for clarity.

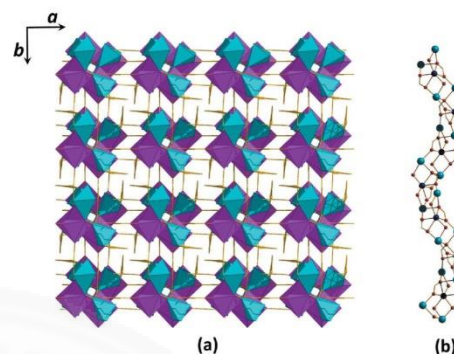


Figure 3
Perspective view along the crystallographic c axis of (a) the three-dimensional framework of (**I**) (the coordination polyhedra for Cd^{II} and Na^I are pink and green, respectively) and (b) helical chain-like structure of the Cd–Na clusters (dark blue = Cd, blue = Na and red = O).

(**I**) contains coordinated H_2O and DMF molecules projecting into the framework channels. Other related three-dimensional heterobimetallic d^{10} - Na^I coordination frameworks containing benzenepolycarboxylate ligands have been published, such as $[CdNa(OH-1,3-bdc)_2(H_2O)_2]\cdot 2H_2O$ where $OH-1,3-bdcH_2 = 5$ -hydroxy-benzene-1,3-dicarboxylic acid (Du *et al.*, 2013), $[Zn_2Na_2(1,4-bdc)_3(DMF)_2(m-H_2O)_2]$ where 1,4-bdc $H_2 =$ benzene-1,4-dicarboxylic acid (Xu *et al.*, 2004), $[ZnNa(1,2,4-btc)]$ where 1,2,4-btc = 1,2,4-benzenetricarboxylate (Wang *et al.*, 2004), and $[Cd_8Na(ntc)_6(H_2O)_8]$ where $ntcH_3 = 5$ -nitrobenzene-1,2,3-tricarboxylic acid (Yang *et al.*, 2014). The three-dimensional coordination framework topologies of these compounds are the result of the construction of different types of metal centers, geometries and carboxylate ligand derivatives. It is found that the carboxylate ligand derivatives in the structure of these related compounds exhibit a μ_4 -coordination mode.

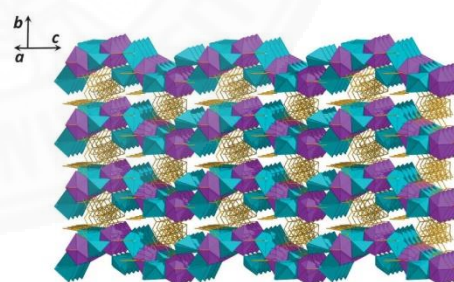


Figure 4
Perspective view of the three-dimensional framework of (**I**) (the coordination polyhedra for Cd^{II} and Na^I are pink and green, respectively). All hydrogen atoms are omitted for clarity.

research communications

Table 3
Experimental details.

Crystal data	
Chemical formula	[CdNa ₂ (C ₈ H ₄ O ₄) ₂ (C ₃ H ₇ NO)(H ₂ O) ₂]
<i>M_r</i>	595.73
Crystal system, space group	Tetragonal, <i>P</i> 4 ₃
Temperature (K)	296
<i>a</i> , <i>c</i> (Å)	10.1437 (8), 21.4664 (15)
<i>V</i> (Å ³)	2208.8 (4)
<i>Z</i>	4
Radiation type	Mo <i>K</i> α
<i>μ</i> (mm ⁻¹)	1.09
Crystal size (mm)	0.35 × 0.21 × 0.16
Data collection	
Diffractometer	Bruker APEXII D8 QUEST CMOS
Absorption correction	Multi-scan (<i>SADABS</i> , Bruker, 2013)
<i>T_{min}</i> , <i>T_{max}</i>	0.647, 0.704
No. of measured, independent and observed [<i>I</i> > 2σ(<i>I</i>)] reflections	56814, 5708, 5301
<i>R_{int}</i>	0.074
(sin θ/λ) _{max} (Å ⁻¹)	0.676
Refinement	
<i>R</i> [<i>F</i> ² > 2σ(<i>F</i> ²)], <i>wR</i> (<i>F</i> ²), <i>S</i>	0.028, 0.068, 1.03
No. of reflections	5708
No. of parameters	351
No. of restraints	160
H-atom treatment	H-atom parameters constrained
Δρ _{max} , Δρ _{min} (e Å ⁻³)	0.52, -0.45
Absolute structure	Flack <i>x</i> determined using 2427 quotients [(<i>I</i> ⁺ - <i>I</i> ⁻)] / [(<i>I</i> ⁺ + <i>I</i> ⁻)] (Parsons <i>et al.</i> , 2013)
Absolute structure parameter	0.081 (13)

Computer programs: *APEX2* and *SAINT* (Bruker, 2013), *SHELXT* (Sheldrick, 2015a), *SHELXL* (Sheldrick, 2015b) and *OLEX2* (Dolomanov *et al.*, 2009).

5. Synthesis and crystallization

A mixture solution of 1,3-bdcH₂ (1.0 mmol) and NaOH (2.0 mmol) in 10 mL of distilled water was slowly dropped to a methanolic solution (10 ml) of Cd(NO₃)₂·4H₂O (1.0 mmol). The reaction mixture was stirred at 333 K for 30 min and allowed to cool to room temperature and then filtered. The filtrate was allowed to stand to slowly evaporate at ambient temperature. Colorless block-shaped crystals suitable for single crystal X-ray diffraction were obtained after three days (76% yield based on Cd).

6. Refinement

Crystal data, data collection and structure refinement details are summarized in Table 3. All hydrogen atoms except those

of water molecules were generated geometrically and refined isotropically using a riding model, with C–H = 0.93 Å and *U*_{iso}(H) = 1.2*U*_{eq}(C). The coordinated DMF molecule was found to be disordered with two sets of sites with a refined occupancy ratio of 0.382 (10) and 0.618 (10).

Acknowledgements

The authors acknowledge the Department of Chemistry, Faculty of Science and Technology, Thammasat University, Thailand, for financial support and the Central Scientific Instrument Center (CSIC) for funds to purchase the X-ray diffractometer at the Faculty of Science and Technology, Thammasat University, Thailand.

References

- Borah, B. M., Dey, S. K. & Das, G. (2011). *Cryst. Growth Des.* **11**, 2773–2779.
- Bruker (2013). *APEX2*, *SAINT* and *SADABS*. Bruker AXS Inc., Madison, Wisconsin, USA.
- Che, G.-B., Liu, C.-B., Wang, L. & Cui, Y.-C. (2007). *J. Coord. Chem.* **60**, 1997–2007.
- Chen, Y., Zheng, L., She, S., Chen, Z., Hu, B. & Li, Y. (2011). *Dalton Trans.* **40**, 4970–4975.
- Dolomanov, O. V., Bourhis, L. J., Gildea, R. J., Howard, J. A. K. & Puschmann, H. (2009). *J. Appl. Cryst.* **42**, 339–341.
- Du, F., Zhang, H., Tian, C. & Du, S. (2013). *Cryst. Growth Des.* **13**, 1736–1742.
- Lin, J.-D., Cheng, J.-W. & Du, S.-W. (2008). *Cryst. Growth Des.* **8**, 3345–3353.
- Lin, J.-D., Long, X. F., Lin, P. & Du, S.-W. (2010). *Cryst. Growth Des.* **10**, 146–157.
- Lin, J.-D., Wu, S. T., Li, Z. H. & Du, S.-W. (2010). *Dalton Trans.* **39**, 10719–10728.
- Parsons, S., Flack, H. D. & Wagner, T. (2013). *Acta Cryst.* **B69**, 249–259.
- Seco, J. M., Pérez-Yáñez, S., Briones, D., García, J.Á., Cepeda, J. & Rodríguez-Diéguez, A. (2017). *Cryst. Growth Des.* **17**, 3893–3906.
- Sheldrick, G. M. (2015a). *Acta Cryst.* **A71**, 3–8.
- Sheldrick, G. M. (2015b). *Acta Cryst.* **C71**, 3–8.
- Suh, M. P., Park, H. J., Prasad, T. K. & Lim, D.-W. (2012). *Chem. Rev.* **112**, 782–835.
- Wang, X.-L., Mu, B., Lin, H.-Y., Yang, S., Liu, G.-C., Tian, A.-X. & Zhang, J.-W. (2012). *Dalton Trans.* **41**, 11074–11084.
- Wang, L., Shi, Z., Li, G., Fan, Y., Fu, W. & Feng, S. (2004). *Solid State Sci.* **6**, 85–90.
- Wu, Z., Yuan, X., Zhang, J., Wang, H., Jiang, L. & Zeng, G. (2017). *ChemCatChem*, **9**, 41–64.
- Xu, H., Wang, R. & Li, Y. (2004). *J. Mol. Struct.* **688**, 1–3.
- Yaghi, O. M., Li, H., Eddaoudi, M. & O'Keeffe, M. (1999). *Nature*, **402**, 276–279.
- Yang, Y.-T., Zhao, Q., Tu, C.-Z., Cheng, F. X. & Wang, F. (2014). *Inorg. Chem. Commun.* **40**, 43–46.

BIOGRAPHY

Name	Miss Matimon Sangsawang
Date of Birth	May 18, 1993
Educational Attainment	2014: Bachelor degree of science, Major of Chemistry, Thammasat University
Present status	M.Sc. student, Chemistry (Inorganic Chemistry), Thammasat University, Thailand
Scholarship	Year 2015: Teaching Assistantship (TA) supported by Thammasat University

Presentation and award

1. Poster presentation in a topic of “Synthesis, characterization, crystal structure and photoluminescent properties of Zn(II) Metal-organic framework containing pyridine-2,6-dicarboxylato bridging ligand” at 14th Conference of the Asian Crystallographic Association (ASCA 2016), Hanoi, Vietnam (4-7 December 2016)
2. Poster presentation in a topic of “Two-dimensional Zn(II) metal-organic framework containing pyridine-2,6-dicarboxylato bridging ligand: Synthesis, characterization, crystal structure, photoluminescent and catalytic properties” at Pure and Applied Chemistry International Conference 2017 (PACCON2017), Bangkok, Thailand (2-3 February 2017)
3. Poster presentation in a topic of “Synthesis, characterization and crystal structure of a novel 3D heterobimetallic coordination polymer constructed from benzene-1,3-dicarboxylato bridging ligand” at The 43rd Congress on Science and Technology of Thailand (STT 43), Bangkok, Thailand (17-19 October 2017)
4. **Award:** The Best Poster Presentation Award, Poster presented at STT 43, Bangkok, Thailand. (17-19 October 2017)

Qualification:

2015 – present M.Sc student (Chemistry), Thammasat University, Thailand

Thesis title: “Novel zinc(II) and cadmium(II) coordination polymers containing aromatic dicarboxylate bridging ligands and their applications in catalysis and photoluminescence

2011 – 2014 B.Sc. student (Chemistry), Thammasat University, Thailand

Senior project: “Development of colorimetric method for analysis of lead in water”

Publication

1. Matimon Sangsawang, Kittipong Chainok and Nanthawat Wannarit. Crystal structure of poly[di-aquabis(μ_5 -benzene-1,3-dicarboxylato)(*N,N*-dimethylformamide) cadmium(II)disodium(I)]. *Acta Cryst*, 2017(E73), pages 1599–1602.
2. Matimon Sangsawang, Chanatip Samart, Pongthipun Phuengphai, Chaveng Pakawatchai, Filip Kielar, Sujitra Youngme and Nanthawat Wannarit. *Synthesis, characterization, crystal structure, photoluminescence and catalytic properties of a novel 2D zinc(II) coordination polymer*. *Inorg Chem Commun*, 2018, manuscript preparation.

Work Experiences:

Teaching assistant in chemistry laboratory at Faculty of Science and Technology, Thammasat University

Instrument skills:

UV-Visible spectrometer, IR-spectrometer, Fluorescence spectrometer and Gas chromatography

Computational skills:

Office programs: Microsoft office and Microcal Origin

Crystallographic programs: Olex², Mercury, PLATON

Graphic program: Diamond4, Photoshop, POV-Ray

Computational Chemistry: ChemDraw

Language:

English	-Listening: Fair	-Reading: Good
	-Speaking: Fair	-Writing: Good

References:

1. Asst. Prof. Dr. Nanthawat Wannarit
Department of Chemistry,
Faculty of Science and Technology
Thammasat University, Pathum Thani, 12121
2. Asst. Prof. Dr. Kittipong Chainok
Department of Materials and Textile technology,
Faculty of Science and Technology
Thammasat University, Pathum Thani, 12121